

Electronic Thesis and Dissertation Repository

5-28-2021 10:00 AM

Expression and subcellular localization of circRNAs dysregulated ALS that are encoded in cytoskeletal protein genes

Asieh Alikhah, *The University of Western Ontario*

Supervisor: Strong, Michael J., *The University of Western Ontario*

Co-Supervisor: Rylett, Jane, *The University of Western Ontario*

A thesis submitted in partial fulfillment of the requirements for the Master of Science degree in Pathology and Laboratory Medicine

© Asieh Alikhah 2021

Follow this and additional works at: <https://ir.lib.uwo.ca/etd>



Part of the [Molecular and Cellular Neuroscience Commons](#)

Recommended Citation

Alikhah, Asieh, "Expression and subcellular localization of circRNAs dysregulated ALS that are encoded in cytoskeletal protein genes" (2021). *Electronic Thesis and Dissertation Repository*. 7816.
<https://ir.lib.uwo.ca/etd/7816>

This Dissertation/Thesis is brought to you for free and open access by Scholarship@Western. It has been accepted for inclusion in Electronic Thesis and Dissertation Repository by an authorized administrator of Scholarship@Western. For more information, please contact wlsadmin@uwo.ca.

Abstract

Amyotrophic lateral sclerosis (ALS) is a fatal and progressive neurodegenerative disorder caused by the degeneration and death of motor neurons. While alterations in the metabolism of RNA, including RNA-binding proteins (RBPs) have been linked to the pathogenesis of ALS, our understanding of the role of non-coding RNAs including circular RNAs (circRNAs) is less well developed. In this study, using a combination of fluorescence *in situ* hybridization (FISH) and immunofluorescence (IF) with markers of RNP granules, I investigated the effect of osmotic stress on the localization and expression of a selection of circRNAs whose expression is dysregulated in ALS. Alteration in the number of granules for two circRNAs was observed in HEK293T cells under osmotic stress. I also have observed that circRNAs are present in ribonucleoprotein (RNP) granules under a stress condition. This finding is consistent with the hypothesis that circRNAs might participate in the biology of RNP granules under pathological conditions such as those observed in ALS.

Keywords

Non-coding RNA, circRNA, Amyotrophic lateral sclerosis, RNP granule, transport granules, stress granule, p-bodies, paraspeckles.

Summary for Lay Audience

There is a recently discovered group of RNAs which is circular and more stable than their linear counterparts. Evidence shows that these circular RNAs are abundant in the brain and can have a regulatory function at the cellular level. Some studies have suggested that circular RNAs (circRNAs) play a role in neurodegenerative diseases. Amyotrophic Lateral Sclerosis (ALS) is a progressive nervous system disease that is caused by loss of neurons controlling motor functions such as walking, grabbing, standing, reaching etc., and eventually results in death within 3 to 5 years of diagnosis. It is shown that specific types of proteins that interact with RNA are aggregated in the neurons of ALS patients. There are also changes in the RNA expression in the spinal cord of ALS patients, supporting the idea of ALS as a disorder of altered RNA metabolism. RNA metabolism refers to different events occurring in the life cycle of RNAs such as, RNA synthesis, RNA processing and modification, RNA folding, and RNA degradation. Several studies also showed that there is a link between ALS pathogenesis and specific types of membraneless granular structures in the cells that are composed of RNAs and proteins. The formation of these granules can be affected by cellular stress which been said to play roles in ALS pathogenesis. In this study, I examined the effect of cellular stress on the expression and localization of circular RNAs for which the expression is altered in ALS. I have found that cellular stress results in colocalization of candidate circRNA within those specific membraneless granular structures.

Dedication

I would like to dedicate my thesis to the individuals and families who have had to endure the extreme challenges of ALS.

Their strength and relentless fight are a real inspiration to all the research community to find a way for living in a world free of ALS disease.

Acknowledgments

First, I would like to express my deepest appreciation to my supervisor Dr. Michael Strong. The completion of my thesis would not have been possible without his enthusiasm, encouragement, support, and continuous optimism. I thank you for never wavering in your support and encouragement.

I would particularly like to thank Dr. Danae Campos-Melo, who is a great and knowledgeable mentor to me. Without your help and wise guidance, this project would have not been the same!

I would like to thank my co-supervisor Dr. Jane Rylett and the members of my advisory committee, Dr. Caroline Schild-Poulter, Dr. Martin Duennwald, and Dr. Subrata Chakrabarti, who have offered valuable advice and guidance from the beginning of my studies. Also, I would like to thank Dr. Stephen H. Pasternak for providing valuable training, advice, and access to a software needed for my project.

I would like to express my gratitude to Crystal McLellan, Kathy Volkening, and Cristian Droppelmann for their unequivocal support in the lab. They have supported me in my research by offering me advice and helping me in troubleshooting methodological problems in my experiments.

I would like to thank all the members of the Strong lab, past and present, Zachary Hawley, Neil Donison, Alex Moszczyński, Matthew Hintermayer, Ben Withers, Hind Amzil, and Veronica Noches Gallardo for their friendship and support which helped make this period a more enjoyable experience. I greatly appreciate the fantastic scientific support that I received from Zachary Hawley. I also thank for heart-warming kindness from Neil Donison whose support and encouragement are worth more than I can express on paper.

I would like to acknowledge the people in the Pathology department, from the graduate chair Dr. Zia Khan to the administrative staff, especially Ms. Tracey Koning and Ms. Susan Underhill. They have helped me every step of the way since I joined the program.

My deep and sincere gratitude to my family for their continuous and unparalleled love, help, and support. I am grateful to my siblings, Hanieh, Mary, and Sadra and my beloved nephew, Siavash, for always being there for me as a friend. I am forever indebted to my parents for giving me the opportunities and experiences that have made me who I am. They selflessly encouraged me to

explore new directions in life and seek my destiny. This journey would not have been possible if not for them, and I dedicate this milestone to them.

I cannot forget friends who went through hard times together, cheered me on, and celebrated each accomplishment, Shokooh, Ali, and Niloufar.

Finally, I am deeply grateful to my partner, Hamid Elahi. I could not have done my master's project without you. You have been my best friend and a great companion, and your support and encouragement helped me to overcome all the immigration challenges. You made Canada a home away from home.

List of Abbreviations

18S	18S Ribosomal RNA
2-D	Two-dimensional
3'UTR	3 Prime Untranslated Region
3-D	Three-dimensional
ACM	Amyloid-converting motif
AGO2	Argonaute 2
ALS	Amyotrophic Lateral Sclerosis
ALS2	Alsin Rho Guanine Nucleotide Exchange Factor ALS2
ALS3	Amyotrophic Lateral Sclerosis 3
ANG	Angiogenin
ANK	Ankyrin repeat
<i>ANXA 1</i>	Gene encoding annexin 1 protein
ARHGEF28	Rho Guanine Nucleotide Exchange Factor 28 – gene name of RGNEF
ATXN2	Ataxin 2
C9orf72	Gene encoding Chromosome 9 open reading frame 72
CBs	Cajal bodies
CD19+	Cluster of Differentiation 19
CD34+	Cluster of Differentiation 34
CDK2	Cyclin-dependent kinase 2
cDNA	Complementary DNA
CFTR	Cystic fibrosis transmembrane conductance regulator
CHCHD10	coiled-Coil-Helix-Coiled-Coil-Helix Domain Containing 10
CHMP2B	Charged Multivesicular Body Protein 2B
CHRNA3	Cholinergic Receptor Nicotinic Alpha 3 Subunit
circRNA	circular RNA
ciRNA	circular intronic RNA
CST	Corticospinal tract
CNS	Central Nervous System

CRC	Colorectal cancer
CT	Cycle Threshold
DAO	D-Amino Acid Oxidase
DCTN1	Dynactin Subunit 1
DGCR8	DiGeorge syndrome chromosomal region 8
DICER	Dicer
DIG	Digoxigenin
DMEM	Dulbecco's Modified Eagle Media
DNA	Deoxyribonucleic Acid
EAAT2	Excitatory amino acid transporter 2
ecircRNA	exonic circRNA
EIciRNA	Exon-intron circRNAs
EIF3	Eukaryotic translation initiation factor 3
EIF3J	Eukaryotic translation initiation factor 3 subunit J
EIF4A3	Eukaryotic initiation factor 4A3
ELP3	Elongator Acetyltransferase Complex Subunit 3
ENCODE	Encyclopedia of DNA Elements Consortium
ERBB4	Erb-B2 Receptor Tyrosine Kinase 4
EWSR1	WS RNA-binding protein 1
FAK	Focal adhesion kinase
fALS	Familial Amyotrophic Lateral Sclerosis
FBS	Fetal Bovine Serum
FG	Phenylalanine-glycine
FISH	Fluorescent In Situ Hybridization
FLI1	Friend leukemia virus integration 1
FMR1	Fragile X mental retardation 1
FMRP	Fragile X Mental Retardation Protein 1
FTD	Frontotemporal Dementia
FUS	Fused in Sarcoma
G3BP	RasGAP-associated endoribonuclease
GAPDH	Glyceraldehyde 3-phosphate Dehydrogenase

GBM	Glioblastoma multiforme
GW182	Glycine-Tryptophan Protein of 182 kilodaltons
HCC	Hepatocellular carcinoma
HEK293T	Human Embryonic Kidney 293 T-antigen
HIF1A	Hypoxia Inducible Factor 1 Subunit Alpha
hnRNPA1	Heterogeneous Nuclear Ribonucleoprotein A1
hnRNPA2B1	Heterogeneous nuclear ribonucleoprotein A2/B1
HNRNPK	Heterogeneous nuclear ribonucleoprotein K
HRP	Horse Radish Peroxide
HSATIII	Highly repetitive satellite III
HUR	Hu-antigen R
ID1	Inhibitor of DNA Binding 1
IDRs	Intrinsically disordered protein regions
IF	Immunofluorescens
Iifs	Intermediate filaments
IGF2BPs	IGF2 mRNA-binding protein family
IL-10	Interleukin 10
IMP1	Insulin-like growth factor II mRNA-binding protein 1
INA	Alpha-Internexin
IP	Immunoprecipitation
iPSC	Induced Pluripotent Stem Cells
IRES	Internal ribosome entry site
Kank2	KN motif and ankyrin repeat domains 2
KIFAP3	Kinesin-associated protein 3
KIFs	Kinesin superfamily proteins
LCD	Low complexity domains
LIN28	Lin-28 Homolog A
lincRNAs	Long intergenic non-coding RNAs
LLPS	Liquid–liquid phase separation
LNA	Locked Nucleic Acid
lncRNA	Long Non-coding RNA

<i>MAPT</i>	Gene encoding microtubule-associated protein tau
MATR3	Matrin 3
MBNL1	Muscleblind-like protein 1
MBP	Myelin basic protein
MCPIP1	Monocyte Chemotactic Protein-1-induced Protein-1
miRNA	MicroRNA
MLOs	Membraneless organelles
MRE	MiRNA Recognition Element
mRNA	Messenger RNA
MSA	Multiple system atrophy
NCI	Neuronal Cytoplasmic Inclusions
ncRNA	Non-coding RNA
NEAT1_2	Nuclear Enriched Abundant Transcript 1 and 2
<i>NEFH</i>	Neurofilament Heavy (transcript)
<i>NEFL</i>	Neurofilament light (transcript)
NEK1	NIMA Related Kinase 1
NES	Nuclear export signal
NF	Neurofilament
NFH	Neurofilament Heavy (protein)
NFL	Neurofilament Light (protein)
NFM	Neurofilament Medium (protein)
NLS	Nuclear Localization Signal
NMD	Nonsense-mediated decay
NR2F6	Nuclear receptor subfamily 2 group F member 6
nSBs	Nuclear stress bodies
NURF	Nucleosome remodelling factor
OPTN	Optineurin
P54nrb	Non-POU domain-containing octamer-binding protein
PABP	Polyadenylate-binding protein
PABPN1	Poly(A) binding protein 1
P-bodies	Processing bodies

PBS	Phosphate buffered saline
PCC	Pearson's correlation coefficient
PcG bodies	Polycomb group proteins
PCR	Polymerase chain reaction
PD	Parkinson's disease
PES1	Pescadillo homologue 1
PFA	Paraformaldehyde
PFN1	Profilin 1
piRNAs	Piwi-associated RNAs
PKM2	Pyruvate kinase M2
PML	Promyelocytic leukaemia
PNPLA6	Patatin Like Phospholipase Domain Containing 6
PON1-3	Paraoxonase 1-3
PRPH	Peripherin
PTB	Polypyrimidine tract-binding protein
RBD	RNA binding domain
RBM14	RNA Binding Motif Protein 14
RG	Arginine-glycine
RGNEF	Rho Guanine Nucleotide Exchange Factor
RhoA	RAS Homolog Family Member A
RISC	RNA-induced silencing complex
RNA	Ribonucleic Acid
RNA Pol	RNA Polymerase
RNA pol II	RNA polymerase II
RNA-seq	RNA sequencing
RNP	Ribonucleoprotein
ROI	Region of interest
RRM	RNA recognition motif
rRNA	Ribosomal RNA
RT-qPCR	Reverse Transcriptase Quantitative PCR
sALS	Sporadic Amyotrophic Lateral Sclerosis

SBS	STAU1-binding site
SDS	Sodium Dodecyl Sulfate
SEM	Standard Error of the Mean
SETX	Senataxin
SFPQ	Splicing Factor Proline and Glutamine Rich
SG	Stress Granule
SH-SY5Y	Thriced sub-cloned cell derived from SK-N-SH neuroblastoma cell line
SIGMAR1	Sigma Non-Opioid Intracellular Receptor 1
siRNA	Small Interfering RNA
SIRT1	Sirtuin 1
SMA	Spinal Muscular Atrophy
smFISH	Single-molecule fluorescence in situ hybridization
SMN1	Survival Motor Neuron 1
SMN2	Survival Motor Neuron 2
SNBs	Sam68 nuclear bodies
snoRNA	Small nucleolar RNA
snRNA	Small nuclear RNA
SOD1	Superoxide Dismutase 1
SOX4	SRY-box transcription factor 4
SPG11	Spastic paraplegia 11
SQSTM1	Sequestosome 1
STAU	Staufen
STMN2	Stathmin-2
SWI/SNF	Switch/Sucrose Non-Fermentable
TAF15	TATA-box Binding Protein Associated Factor 15
TARDBP	Transactive Response DNA-binding Protein – gene name of TDP-43
TBK1	TANK Binding Kinase 1
TDP-43	Transactive Response DNA-binding Protein of 43 kilodaltons
TERT	Telomerase Reverse Transcriptase
TET1	Ten–eleven translocation 1
TFIIB	Transcription Factor II B

TIA-1	T-Cell-Restricted Intracellular Antigen-1
TIAR	TIA-1-related
trkB	Tropomyosin receptor kinase B
tRNA	Transfer RNA
TSA	Tyramide Signal Amplification
TUBA4A	Tubulin Alpha 4a
UBQLN2	Ubiquilin 2
UTR	Untranslated region
UV	Ultraviolet
VAPB	VAMP Associated Protein B and C
VCP	Vasolin-containing Protein
$\Delta\Delta CT$	Delta Delta Cycle Threshold

Table of Contents

Abstract.....	ii
Summary for Lay Audience.....	iii
Dedication.....	iv
Acknowledgments.....	v
List of Abbreviations.....	vii
Table of Contents.....	xiv
List of Tables.....	xviii
List of Figures.....	xix
Chapter 1.....	1
1 Introduction and background.....	1
1.1 Circular RNAs (circRNAs).....	1
1.1.1 NcRNAs.....	1
1.1.2 CircRNAs discovery and expression.....	5
1.1.3 Properties of circRNAs.....	5
1.1.4 Categories and biogenesis of circRNA.....	6
1.1.5 circRNA functions.....	10
1.1.5.1 MicroRNA Sponge.....	10
1.1.5.2 Protein sponge.....	10
1.1.5.3 Protein scaffolding.....	11
1.1.5.4 Template for translation.....	12
1.1.5.5 Transporting molecules and information.....	13
1.1.5.6 Generating pseudogenes.....	13
1.1.6 CircRNAs in CNS.....	16
1.1.7 CircRNA in neurodegenerative disease.....	17

1.2 Amyotrophic lateral sclerosis	19
1.2.1 Overview.....	19
1.2.2 Genetics of amyotrophic lateral sclerosis	20
1.2.3 Neuropathology of ALS.....	25
1.2.4 Altered RNA Metabolism in ALS	25
1.2.4.1 RNA splicing.....	26
1.2.4.2 mRNA stability.....	27
1.2.4.3 RNA transport	28
1.2.4.4 RNA translation.....	29
1.3 Membraneless organelles.....	31
1.3.1 Overview.....	31
1.3.2 RNP granules	34
1.3.2.1 Transport Granules	39
1.3.2.2 Stress granules	40
1.3.2.3 Processing bodies	42
1.3.2.4 Paraspeckles	43
1.4 Relevance to the current study.....	46
1.5 Hypothesis.....	48
1.6 Specific aims.....	48
Chapter 2.....	49
2 Procedures and methodology	49
2.1 circRNAs selection	49
2.2 Primer design	51
2.3 RNA extraction and RNase R exonuclease assay.....	54
2.4 Reverse-transcription and real-time PCR	55

2.5	Data analysis of real-time PCR data	56
2.6	Cell culture and stress condition	57
2.7	Expression and localization analyses with fluorescent <i>in situ</i> hybridization (FISH).....	57
2.8	Immunofluorescence.....	59
2.9	Confocal microscopy and image processing.....	63
2.10	Spot counting and analysis.....	64
Chapter 3.....		65
3	Results.....	65
3.1	Experimental set 1 – Real-time PCR shows no significant differential expression of candidate circRNAs in the spinal cord tissue of ALS versus control patients.....	65
3.1.1	Introduction.....	65
3.1.2	Results.....	66
3.1.2.1	Real-time PCR showed no significant differences in the expression of candidate circRNAs between ALS and control patients’ samples.....	66
3.2	Experimental set 2 – dysregulation of candidate circRNAs’ expression in stressed HEK293T cells.....	83
3.2.1	Introduction.....	83
3.2.2	Results.....	83
3.2.2.1	circRNAs show an altered granule formation in stressed HEK293T cells compared with unstressed cells.....	83
3.3	Experimental set three: circRNAs colocalize with the markers for RNP granules in HEK293T cells under stress.....	85
3.3.1	Introduction.....	85
3.3.2	Results.....	86
3.3.2.1	Visual evaluation in 2-D showed colocalization between circRNAs with markers of RNP granules	86
3.3.2.2	3-D analysis showed colocalization between circRNAs with markers of RNP granules	111

3.3.2.3 Quantitative and statistical evaluation of colocalization	123
Chapter 4.....	129
4 Discussion and conclusion.....	129
4.1 Overexpression of circRNAs encoded by cytoskeletal genes in ALS may affect their host gene expression or function.....	129
4.2 Downregulation of hsa_circVIM_011 and hsa_circANXA1_001 in HEK293T cells in response to osmotic stress.....	131
4.3 Potential role of candidate circRNAs in RNP granule biology	133
4.4 Future direction.....	136
Bibliography	139
Curriculum Vitae	172

List of Tables

Table 1-1: List of ncRNAs with their mean size and functions.....	4
Table 1-2: Genetics of ALS.	22
Table 1-3: Characteristics of currently known RNP granules.	38
Table 2-1: List of candidate circRNAs.	50
Table 2-2: Oligonucleotides for real-time PCR amplification.....	54
Table 2-3: Oligonucleotides for fluorescence in situ hybridization.....	58
Table 2-4: List of primary antibodies used in this study.	61
Table 2-5: List of secondary antibodies used in this study.	62
Table 3-1: Raw data for real-time PCR of CDR1as in control and ALS samples.....	79
Table 3-2: Raw data for real-time PCR of hsa_circVIM_005 in control and ALS samples.	80
Table 3-3: Raw data for real-time PCR of hsa_circVIM_011 in control and ALS samples.	81
Table 3-4: Raw data for real-time PCR of hsa_circDNM1_004 in control and ALS samples.....	82

List of Figures

Figure 1-1: Schematic illustration of human genome presented by the Encyclopedia of DNA Elements Consortium (ENCODE).....	2
Figure 1-2: Types of ncRNAs.....	3
Figure 1-3: Possible models of circRNA biogenesis and different types of circRNAs.....	8
Figure 1-4: Schematic representation of the six main functions of circRNA.....	15
Figure 1-5: Schematic illustration of liquid-liquid phase separation.....	32
Figure 2-1: CircRNAs annotated from <i>VIM</i> gene.....	52
Figure 2-2: Schematic of the design of convergent and divergent primers.	53
Figure 3-1: Amplification and melting curve plots for target circRNAs and TBP gene amplified from ALS and control samples.	72
Figure 3-2: Amplification and melting curve plots for hsa_circANXA1_001 primers used on cDNA from HEK293T.....	74
Figure 3-3: Agarose gel electrophoresis of qPCR products from ALS and control samples.	76
Figure 3-4: Real-time PCR did not show significant differences in the expression of candidate circRNAs between ALS and control patients' samples.....	78
Figure 3-5: Quantification of circRNA hsa_circVIM_011 and hsa_circANXA1_001 by RNA FISH.....	84
Figure 3-6: CDR1as colocalizes with Staufen positive stress granules under osmotic stress.	88
Figure 3-7: Hsa_circVIM_005 colocalizes with Staufen positive transport granules under osmotic stress.....	89
Figure 3-8: Hsa_circDNM1_004 colocalizes with Staufen positive transport granules under osmotic stress.....	90

Figure 3-9: Hsa_circVIM_011 does not colocalize with Staufen positive transport granules under osmotic stress.....	91
Figure 3-10: Hsa_circANXA1_001 does not colocalize with Staufen positive transport granules under osmotic stress.....	92
Figure 3-11: CDR1as colocalizes with TIA-1 positive stress granules under osmotic stress.	93
Figure 3-12: Hsa_circVIM_005 colocalizes with TIA-1 positive stress granules under osmotic stress.....	94
Figure 3-13: Hsa_circDNM1_004 colocalizes with TIA-1 positive stress granules under osmotic stress.....	95
Figure 3-14: Hsa_circVIM_011 does not colocalize with TIA-1 positive stress granules under osmotic stress.....	96
Figure 3-15: Hsa_circANXA1_001 does not colocalize with TIA-1 positive stress granules under osmotic stress.....	97
Figure 3-16: CDR1as colocalizes with Dcp1 positive P-bodies under osmotic stress.	98
Figure 3-17: Hsa_circVIM_005 colocalizes with Dcp1 positive P-bodies under osmotic stress.	99
Figure 3-18: Hsa_circDNM1_004 colocalizes with Dcp1 positive P-bodies under osmotic stress.....	100
Figure 3-19: Hsa_circVIM_011 colocalizes with Dcp1 positive P-bodies under osmotic stress.....	101
Figure 3-20: Hsa_circANXA1_001 does not colocalize with Dcp1 positive P-bodies under osmotic stress.....	102
Figure 3-21: Hsa_circDNM1_004 colocalizes with PSPC1 cytoplasmic fibrillar structures under osmotic stress.....	103

Figure 3-22: CDR1as does not colocalize with PSPC1 cytoplasmic fibrillar structures under osmotic stress.....	104
Figure 3-23: Hsa_circVIM_005 does not colocalizes with PSPC1 cytoplasmic fibrillar structures under osmotic stress.....	105
Figure 3-24: Hsa_circVIM_011 does not colocalize with PSPC1 cytoplasmic fibrillar structures under osmotic stress.....	106
Figure 3-25: Hsa_circANXA1_001 does not colocalize with PSPC1 cytoplasmic fibrillar structures under osmotic stress.	107
Figure 3-26: Hsa_circDNM1_004 colocalizes with NONO positive cytoplasmic structures under osmotic stress.....	108
Figure 3-27: Hsa_circVIM_011 colocalizes with NONO positive cytoplasmic structures under osmotic stress.....	109
Figure 3-28: Hsa_circANXA1_001 does not colocalize with NONO positive paraspeckles in the nucleus of HEK293T cells under osmotic stress.	110
Figure 3-29: CircRNAs partially colocalize with Staufen positive transport granules in HEK293T cells under osmotic stress.....	113
Figure 3-30: CircRNAs colocalize with TIA-1 positive stress granules in HEK293T cells under osmotic stress.....	115
Figure 3-31: CircRNAs colocalize with Dcp1 positive P-bodies in HEK293T cells under osmotic stress.....	117
Figure 3-32: Hsa_circDNM1_004 CircRNA colocalizes with PSPC1 and NONO in HEK293T cells under osmotic stress.....	119
Figure 3-33: Hsa_circVIM_011 CircRNA does not colocalize with Dcp1 positive P-bodies in HEK293T cells under osmotic stress.....	121

Figure 3-34: Hsa_circVIM_011 CircRNA does not colocalize with NONO positive cytoplasmic structures in HEK293T cells under osmotic stress. 122

Figure 3-35: Comparison of quantification of the percentage of circRNAs volume above established threshold colocalized with the marker of RNP granule in HEK293T cells under osmotic stress. 124

Figure 3-36: Comparison of the degree of colocalization between circRNAs and RNP granule markers in HEK293T cells under stress using PCC values in ROI volumes. 127

Figure 4-1: RNA-binding protein sites matching to circRNAs. 138

Chapter 1

1 Introduction and background

1.1 Circular RNAs (circRNAs)

1.1.1 ncRNAs

Although the most well-studied sequences in the human genome are protein-coding genes, non-protein-coding RNA occupies the majority of the human genome. The latest Human GENCODE Release 38 (GRCh38.p13), presented by the Encyclopedia of DNA Elements Consortium (ENCODE), showed that the human genome is composed of 60649 genes. Among those, 19955 are protein-coding genes, whereas the remaining two-thirds of the genome represent noncoding RNA (ncRNA) genes (17944 long ncRNA genes, 7567 small ncRNA genes, and 14773 pseudogenes) (Figure 1-1) (Genecode, 2021).

In recent years, our understanding of the roles and functions of ncRNAs has dramatically increased, leading to a more comprehensive annotation of genomic locations and features of ncRNAs as well as to a better understanding of their function in various biological processes (Mattick & Makunin, 2006). Although there are different criteria considered for the classification of non-coding RNAs, in one classification, ncRNAs are classified as either housekeeping or regulatory ncRNAs. Housekeeping ncRNAs are constitutive expressing RNAs that are required for the maintenance of several key cellular processes. Ribosomal (rRNA), transfer (tRNA), small nuclear (snRNA), and small nucleolar RNAs (snoRNAs) are categorized in this group of ncRNAs. The other group is regulatory noncoding RNAs which are generally classified into two major classes: short ncRNAs (<200 nucleotides) and long ncRNAs (lncRNAs, >200 nucleotides) (Ponting et al, 2009; Sun & Kraus, 2015; Wilusz et al, 2009). Long ncRNAs could further be categorized into two types, linear ncRNAs and circular RNAs (circRNAs) (Figure 1-2) (Amodio et al, 2013; Costa, 2010). Table 1-1 provides more detail of the size and functions of ncRNAs.

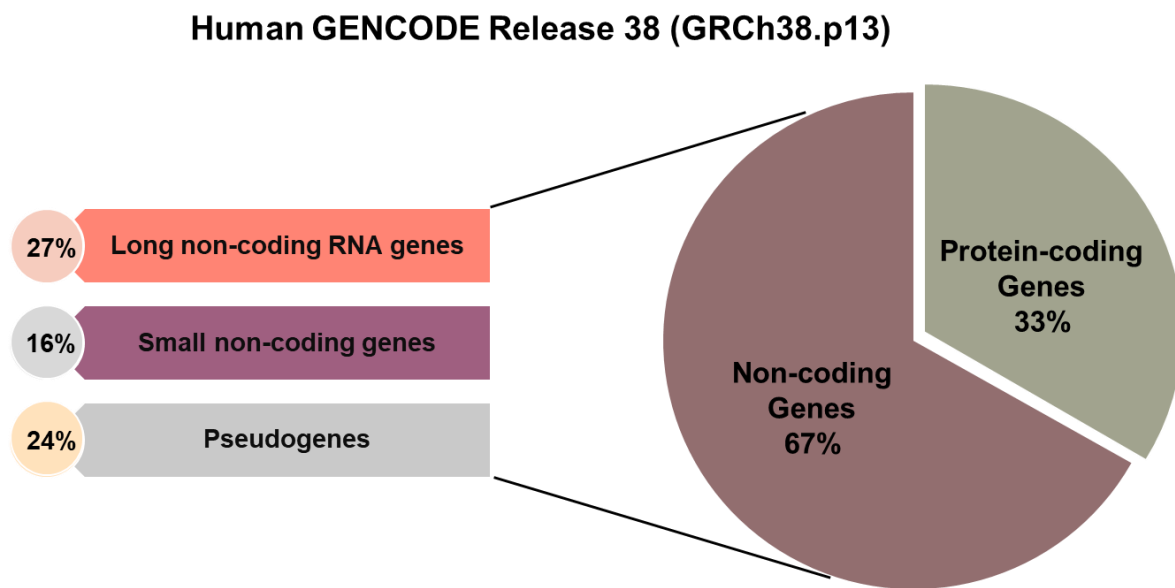


Figure 1-1: Schematic illustration of human genome presented by the Encyclopedia of DNA Elements Consortium (ENCODE).

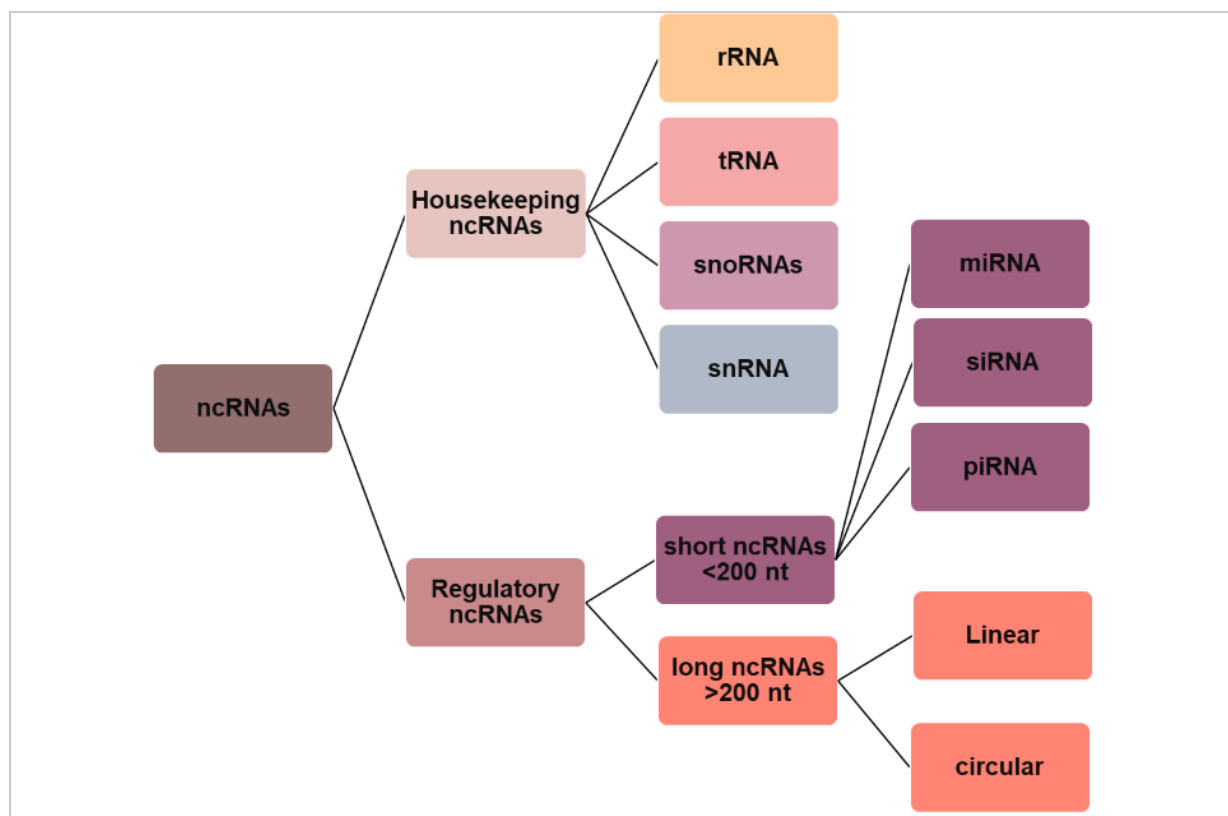


Figure 1-2: Types of ncRNAs. Noncoding RNAs are categorized into housekeeping and regulatory noncoding RNAs. Housekeeping ncRNAs include rRNA, tRNA, snRNA, and snoRNAs. Regulatory noncoding RNAs include short ncRNAs or long ncRNAs. Long ncRNAs are including linear and circular RNAs (circRNAs).

Table 1-1: List of ncRNAs with their mean size and functions.

Type	Name	Mean size	Function
Housekeeping ncRNAs	Ribosomal RNA (rRNA)	~ 1.9 kb	Protein synthesis (Dahlberg, 1989)
	Transfer RNA (tRNA)	~ 17 kb	Protein synthesis (Nishimuka, 1972)
	Small nuclear RNA (snRNA)	100-300 nt	Involved in spliceosome complex (Karijovich & Yu, 2010)
	Small nucleolar RNA (snoRNA)	60-300 nt	Methylation and pseudo uridylation of other RNAs (Bachellerie et al, 2002)
Regulatory ncRNAs	MicroRNA (miRNA)	18-21 nt	regulation of gene expression (Huang et al, 2011)
	Small interfering RNAs (siRNAs)	~ 21 nt	Defense against viruses and transposon activity, gene regulation (Buchon & Vaury, 2006)
	Piwi-associated RNAs (piRNAs)	26-31 nt	Regulation of chromatin state and transposon activity (Ernst et al, 2017; Yamanaka et al, 2014)
	long intergenic non-coding RNAs (lincRNAs)	≥ 200 nt	Involved in large ribonucleoprotein complexes [1, 2]
	long intronic non-coding RNAs	≥ 200 nt	Gene expression regulation (Heo & Sung, 2011; Louro et al, 2009; Tahira et al, 2011)
	circular RNAs (circRNAs)	≥ 200 nt	not known with certainty

1.1.2 CircRNAs discovery and expression

A less studied group of non-coding RNAs are circular RNAs (circRNAs) which have been shown to be evolutionarily conserved across mammals. To date, more than 140,000 human circRNA have been annotated according to CircBank data base (circbank). CircRNAs are long, noncoding endogenous RNA molecules with a covalently closed continuous loop without 5'–3' polarity or a polyadenylated tail and which are largely concentrated in the nucleus. CircRNAs are generally formed by covalent binding of the 5' site of an upstream exon with the 3' of the same or a downstream exon (termed 'back splicing'; discussed in detail later) (Jeck & Sharpless, 2014).

CircRNAs were first discovered in RNA viruses as viroids in early 1976 (Sanger et al, 1976). CircRNAs have now been observed in eukaryotic species although mostly at very low expression levels. Although initially considered as a by-product of spliceosome-mediated splicing errors, circRNAs are abundant in various cell lines and across different species (Chen & Yang, 2015). Advanced RNA sequencing (RNA-seq) and bioinformatics have revealed that there is a dynamic expression pattern of circRNAs in various physiological conditions and developmental stages (Li et al, 2015a; Li et al, 2015b; Zhu et al, 2017).

1.1.3 Properties of circRNAs

CircRNAs are distinguished by their covalently closed circular structures without a 5' cap or a 3' polyA tail. They are more stable than linear RNAs because of their circular structures, which makes them resistant to degradation by most RNA decay machinery. Most exonic circular RNAs exhibit a half-life of more than 48 hours, while an average half-life for mRNAs is 10 hours (Eneka et al, 2016; Jeck et al, 2013; Schwanhaussner et al, 2013). CircRNAs (except for intron-containing circRNA) are transported from the nucleus to the cytoplasm by an ATP- dependent mechanism. It has been also reported that transportation of long circRNAs from nucleus to the cytoplasm also requires helicase activity, so that the helicase depletion results in nuclear accumulation of long circRNAs (Huang et al, 2018). Nuclear retained circRNAs were found to be involved in transcriptional regulation (Jeck & Sharpless, 2014). They tend to have longer flanking introns (compared to non-circularized expressed exons) that are enriched with reverse complementary sequences, helping in their biogenesis. In some cases, circRNAs show higher

expression than their linear counterpart isoforms (Capel et al, 1993; Memczak et al, 2013; Salzman et al, 2013a; Sanger et al, 1976). CircRNAs exhibit cell and tissue type and developmental stage-specific expression (Salzman et al, 2013b). For instance, hsa-circRNA 2149 is expressed in CD19⁺ leukocytes but cannot be detected in CD34⁺ leukocytes, neutrophils, or HEK293 cells. Several nematode circRNAs are expressed in oocytes but absent in 1- or 2-cell embryos (Memczak et al, 2013).

1.1.4 Categories and biogenesis of circRNA

Four groups of circRNAs have been identified which differ in their size, function and biogenesis. These include exonic circRNAs (ecircRNA) (single exon and multiple), exon-intron circRNAs (EIciRNA), circular intronic RNAs (ciRNA), and intergenic circRNAs (Lasda & Parker, 2014; Wang & Dong, 2019). Back-splicing ligates a downstream splice donor with an upstream splice acceptor, generating a covalently closed RNA transcript. This process is an additional type of alternative splicing that needs both *cis*-regulatory elements and *trans*-acting factors for the regulation of circRNA formation (Wang & Wang, 2015). CircRNAs use the same splicing machinery for their biogenesis as canonical alternative splicing; thus it is been said that circRNA production competes with pre-mRNA splicing (Ashwal-Fluss et al, 2014). While the precise details of the mechanism of circRNAs formation remained uncertain, three different models of circRNA biogenesis have been suggested. These include exon skipping or lariat-driven circularization, intron pairing-driven circularization (Ivanov et al, 2015; Jeck et al, 2013), and resplicing-driven circularization (Kameyama et al, 2012). Each model is further discussed below (see also).

In the lariat-driven circularization model, the pre-mRNA partially folds during transcription which causes the 5' splicing site of the upstream intron to approach and attack the 3' splicing site of the downstream intron. When the middle exons are skipped during a linear alternative splicing event, the spliced-out intron lariat contains those skipped exons. This lariat precursor then can lead to the formation of circRNA when the lariat undergoes internal back-splicing (Eger et al, 2018; Kelly et al, 2015; Kristensen et al, 2018a).

Intron pairing-driven circularization is also known as the direct back-splicing mechanism. It has been proposed that looping is required for intron pairing-driven circularization. In this model, the

intron sequences flanking the downstream splice-donor site and the upstream splice-acceptor site need to be brought into close proximity to make a loop. It is hypothesized that looping can be provided by either of two mechanisms. One mechanism is the base pairing of inverted repeat elements (such as Alu elements) at both sites of circRNA which enhances looping. The other mechanism is the dimerization of RNA-binding proteins (RBP), such as the FUS (Fused in Sarcoma) protein, which binds to flanking introns (Errichelli et al, 2017). Direct back-splicing has a different molecular mechanism to the linear alternative splicing. In this model, two types of circRNAs can be produced according to whether partial intron sequences are retained, producing EcircRNAs, or circRNAs that contain both an intron and exon sequences (EIciRNAs) (Bahn et al, 2015). An example of intron pairing-driven circRNAs is Hsa-circ-POLR2A (Koh et al, 2014).

Resplicing-driven circularization has also been proposed as a model for the generation of exonic circRNAs. This model requires a two-step splicing pathway, in which canonical splice sites are removed by initial splicing and thereby cryptic splice sites on the spliced mRNAs can be used for circularization in an exon-skipping fashion (Kameyama et al, 2012).

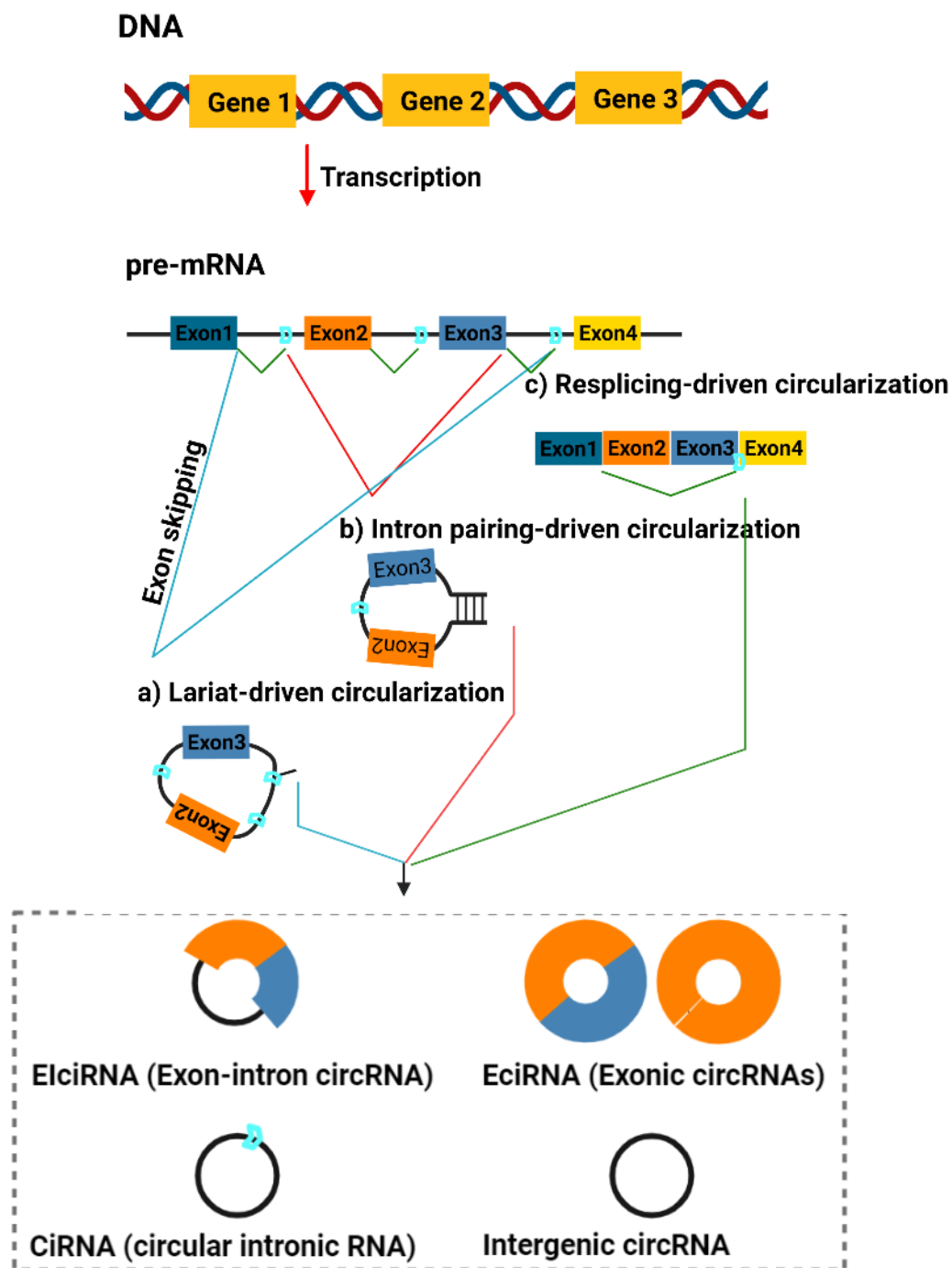


Figure 1-3: Possible models of circRNA biogenesis and different types of circRNAs. (a) Lariat-driven circularization; in this model, during a linear alternative splicing event the pre-mRNA partially folds, and the 5' splicing site of the upstream intron binds to 3' splicing site of the downstream intron results in a spliced-out intron lariat contains skipped exons. This lariat

precursor then can lead to the formation of circRNA when the lariat undergoes internal back-splicing. (b) Intron-pairing-driven circularization; In this model, the intron sequences flanking the downstream splice-donor site and the upstream splice-acceptor site need to be brought into close proximity to make a loop. This process is named looping and can be facilitated by either base pairing of inverted repeat elements at both sites of circRNA or the dimerization of RBPs that bind to flanking introns. (c) Resplicing-driven circularization; This model requires a two-step splicing pathway. The circularization can occur on the spliced mRNAs using cryptic splice sites to produce exonic circRNAs composing skipped exons. The blue arrows represent splice sites.

1.1.5 circRNA functions

1.1.5.1 MicroRNA Sponge

To date, the biological functions of only a minor proportion of the known circRNAs have been studied. However, it is generally agreed that some circRNAs can play a role as super sponges for miRNAs and thus regulate their function (Hansen et al, 2013; Militello et al, 2017).

MiRNAs are 18 to 25 nucleotides long ncRNAs. They are essential regulators of gene expression and function by binding to the 3'-untranslated regions (3' UTR) targeting mRNAs at specific miRNA recognition elements (MREs). In the majority of instances, miRNAs promote mRNA degradation or inhibit protein translation. Our lab and others have however also shown that certain miRNAs, albeit rare, can lead to mRNA stabilization (Campos-Melo et al, 2013a; Fabian et al, 2010; Jing et al, 2005). MiRNAs can regulate different physiological processes, such as hematopoiesis (Bissels et al, 2012), body development (Chen & Wang, 2012), virus defense (Grassmann & Jeang, 2008), cell proliferation, apoptosis (Hwang & Mendell, 2006), and fat metabolism (Hwang & Mendell, 2006).

Human/mouse CDR1as (also known as cirRS-7), which is the most studied circRNA, has a high expression level in the human and mouse brain and acts as a sponge/inhibitor of miR-7, thus resulting in the promotion of the stability of miR-7 target genes and indirectly regulating many processes in the cells (Hansen et al, 2013; Memczak et al, 2013). For instance, as miR-7 is closely related to the occurrence and development of tumors, it has been proposed that alteration of CDR1as expression affects tumor development and occurrence (Zhong et al, 2019).

1.1.5.2 Protein sponge

It has been proposed that circRNAs that have RBP binding motifs may also function as sponges or decoys for these proteins and indirectly regulate their functions. One example of a circRNA functioning as a protein sponge is circMbl which is encoded from the *MBNL1* gene (muscleblind-like protein 1) in humans and *mbl* in *D. melanogaster*. This circRNA, in humans and flies, harbors binding sites for mbl and MBNL1, respectively (Ashwal-Fluss et al, 2014). Another example is circPABPN which sequesters RBP Hu-antigen R (HUR) and thus suppresses the translation of nuclear poly(A) binding protein 1 (PABPN1) mRNA in HeLa cells

(Abdelmohsen et al, 2017). Also, circANRIL impairs pre-rRNA processing and ribosome biogenesis by sequestering pescadillo homologue 1 (PES1) in the macrophages and human vascular smooth muscle cells (Holdt et al, 2016).

1.1.5.3 Protein scaffolding

NcRNAs can regulate gene expression at both the transcription and post-transcriptional levels through physical interaction with RBPs or other ncRNAs (Turner et al, 2014). This role can also be generalized to circRNAs, as some studies have investigated the association of circRNAs with RBPs such as AGO2 and RNA Pol II (Jeck et al, 2013; Memczak et al, 2013). CircRNAs might have a similar role in protein interactions to mediate cellular functions. Crosslinking immunoprecipitation (IP) data sets have shown that there are multiple binding sites for many different RBPs on circRNAs sequences, supporting an interaction between them. These interactions suggest that circRNAs can also function as a protein scaffold to mediate complex formation between particular enzymes and substrates, thus enhancing protein function (Salzman, 2016). MBL (muscleblind) protein has also been shown to directly bind to circMbl. This interaction is due to the presence of functional MBL binding sites on circMbl. Moreover, the interaction between the circMbl and MBL protein was found to modulate the splicing activity of MBL and regulate the pre-mRNA splicing of the host gene by competing with the canonical splicing machinery (Ashwal-Fluss et al, 2014). Another example is circFoxo3 that was found to form a ternary complex with cell cycle proteins cyclin-dependent kinase 2 (CDK2) and cyclin-dependent kinase inhibitor 1 (p21) which blocks cell cycle progression by inhibiting CDK2 from interacting with cyclins A and E, which is required for cell cycle progression (Du et al, 2016). circFoxo3 can also interact with senescence response-associated proteins ID1, E2F1, FAK, and HIF1A and promotes cardiac senescence through these interactions (Du et al, 2017b).

Some circRNAs provide a scaffold for proteins to recruit them to a specific site of action, including a role for circRNAs in recruiting proteins such as transcription factors, DNA or histone-modifying enzymes, and chromatin remodelers to DNA. For instance, knockout of circRHOT1 prevents hepatocellular carcinoma (HCC) proliferation, migration, and invasion through recruiting a specific transcription factor to the nuclear receptor subfamily 2 group F member 6 (NR2F6) promoter and initiating transcription (Wang et al, 2019b). One example of recruiting DNA modifying enzymes to the chromatin is when circFEER1 recruits Ten-eleven

translocation methylcytosine dioxygenase 1 (TET1) to the promotor of the Friend leukemia virus integration 1 (*FLII*) gene to induce DNA demethylation (Chen et al, 2018). In addition, the nucleosome remodeling factor (NURF), which is a chromatin remodeler complex, can be recruited to the SRY-box transcription factor 4 (SOX4) promoter by circDONSON and promotes gastric cancer proliferation, migration, and invasion (Ding et al, 2019).

One of the suggested functions for circRNAs is regulation of transcription through enhancing RNA polymerase II (RNA pol II) function in the nucleus. Some of the exon-intron circRNAs (EIciRNAs) which localize in the nucleus interact with U1 snRNP and associate with RNA pol II to enhance the expression of their own host genes (Li et al, 2015c). In a study, the exon-intron circRNA EIciEIF3J was found to associate with RNA polymerase II in human cells. These nuclear-localized EIciRNAs interact with U1 snRNP and the RNA Pol II transcription complex at the promoter of its parental gene Eukaryotic translation initiation factor 3 subunit J (*EIF3J*) and enhances its expression (Li et al, 2015c). EIciPAIP2 is also another EIciRNA that regulate the expression of its parental gene by interacting with U1 snRNP and the RNA Pol II transcription complex. Depletion of these two circRNAs resulted in down regulation of their parental genes (*EIF3J* or *PAIP2* genes, respectively) (Li et al, 2015c).

1.1.5.4 Template for translation

There is emerging evidence that endogenous circRNAs can be translationally active. However, polysome profiling has shown that this is an uncommon property of circRNAs in that the majority of circRNAs show no evidence for translational activity (Guo et al, 2014a). The first evidence for the endogenous translational capacity of circRNAs in eukaryotes was obtained from the study of circ-ZNF609. Circ-ZNF609 has been shown to contain a start codon and an in-frame stop codon, which is created upon circularization. This circRNA, which participates in the regulation of myoblast proliferation and is associated with heavy polysomes, is translated to a protein through a cap-independent, splicing dependent mechanism (Legnini et al, 2017). It has also been reported that a subset of circRNAs expressed in *Drosophila* are associated with translating ribosomes, including circMbIV5, circCdiV5, and circPde8V5. Interestingly, circMbl circRNA encodes a 37.04 kDa protein which is different from those proteins produced by any of the other known *MBL* isoforms (Pamudurti et al, 2017).

Lacking polyA tail and cap structures in circRNAs makes them to undergo another type of translation mechanism called Cap-independent translation. This type of translation, requiring an internal ribosome entry site (IRES), was initially discovered in viral RNAs (Pelletier & Sonenberg, 1988) and then identified in cellular RNAs (Weingarten-Gabbay et al, 2016). Several lines of evidence indicate that the insertion of the IRES and reading frames to a synthesized circRNA could lead to their translation *in vitro* (Abe et al, 2015; Chen & Sarnow, 1995; Wang & Wang, 2015). Therefore, endogenous circRNAs derived from the protein-coding DNA sequence, for example, those with ATG translational start site, might be able to translate into functional proteins (Guo et al, 2014b; Jeck et al, 2013).

1.1.5.5 Transporting molecules and information

CircRNAs have been found in exosomes which are critical mediators in the exchange of molecules and information between cells (Li et al, 2015b). Studies show that exosomes, which are released by the majority of cell types, play roles not only in normal physiological conditions but also in pathological conditions. An alteration of circRNAs levels in exosomes has been reported in recent studies. Moreover, emerging evidence shows that certain exosomal circRNAs play critical roles in pathological conditions such as cancer (Wang et al, 2019a).

It has been suggested that exosomal circRNAs may play a role as intercellular signaling molecules to transport molecules and information. For instance, ciRS-122 which is transported inside exosomes from drug-resistant colorectal cancer (CRC) cells to sensitive ones, accelerates glycolysis and improves chemoresistance in sensitive CRC cells. This circRNA does this function through sponging miR-122 which results in upregulation of pyruvate kinase M2 (PKM2) (Hon et al, 2019; Wang et al, 2019a).

1.1.5.6 Generating pseudogenes

The computational examination of the mouse and human reference genomes has recognized several circRNA-derived pseudogenes (Dong et al, 2016; Zhang et al, 2004). This data suggested that some stabilized circRNAs can undergo reverse transcription and integration into the genome as pseudogenes. In the mouse genome, an analysis of the circRFWD2 corresponding circle locus (exon 6-exon 2) has revealed several circRFWD2-derived pseudogenes and 6 exon sequences outside of the circRFWD2-containing pseudogene. Given that most circRFWD2-related

pseudogenes do not contain poly (A) sequences, the mechanism of retrotranscription remains unknown.

The six main functions that have been proposed for circRNAs are shown in the schematic illustration (Figure 1-4).

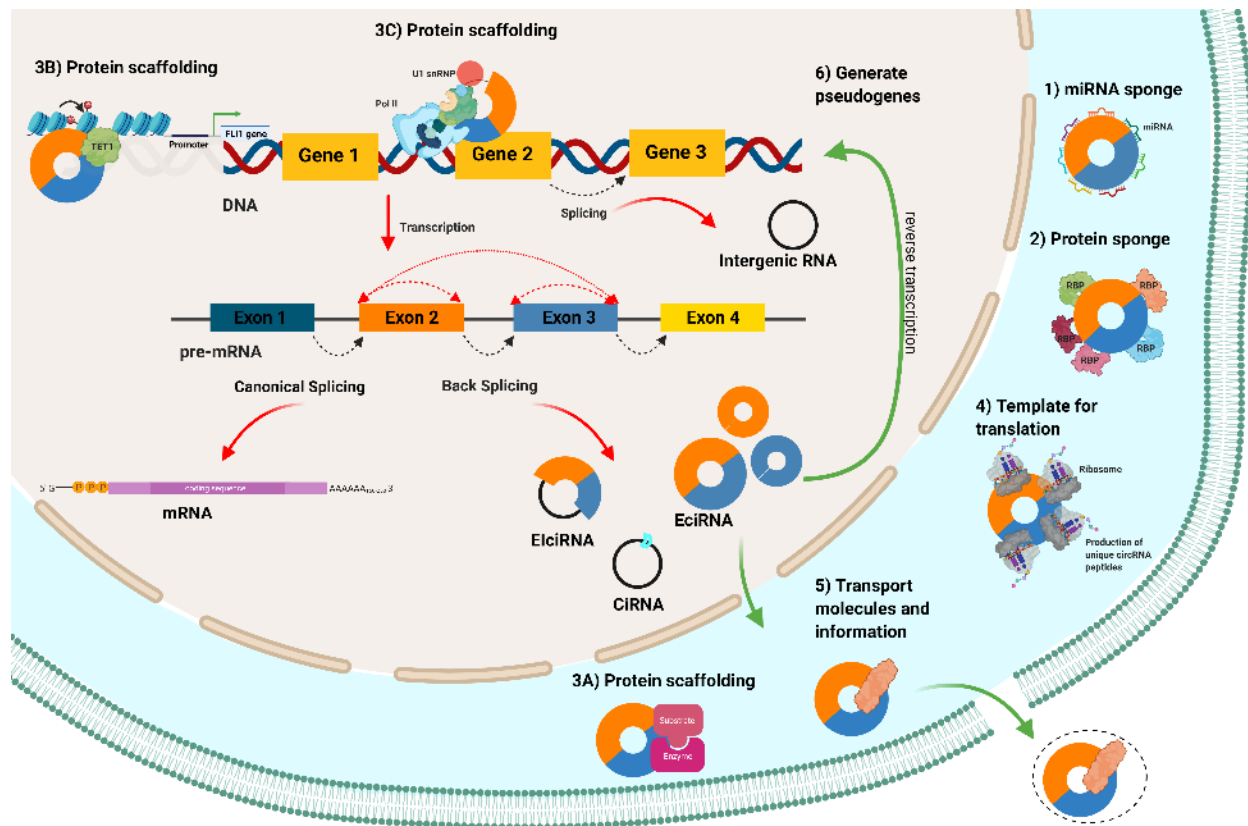


Figure 1-4: Schematic representation of the six main functions of circRNA. 1) MiRNA sponging activity: There are multiple binding sites for miRNAs on some of the circRNAs sequence which provides miRNA sponging function for circRNAs. 2) Protein sponging activity: CircRNAs can sponge RBPs and indirectly regulate their functions. 3) Protein scaffolding activity: A) Protein scaffolding activity: CircRNAs can act as scaffolds to mediate complex formation between particular enzymes and substrates. B) CircRNAs can act as scaffolds to recruit proteins such as transcription factors, DNA or histone-modifying enzymes, and chromatin remodelers to DNA. C) Nuclear circRNAs can associate with RNA polymerase II and enhance its function and regulate gene expression. 4) Translational activity: A group of circRNAs have the ability to be translated to peptides although the majority of circRNAs provide no evidence for translation. 5) Transporting molecules and information: A huge number of stable circRNAs are found in exosomes which may play a role as intercellular signaling molecules to transport substances and information. 6) Generating pseudogenes: stabilized circRNAs could undergo reverse transcription and integrate into the genome as pseudogenes.

1.1.6 CircRNAs in CNS

The expression of genes in the brain demands extreme control and regulation through the various brain developmental stages of an organism. Non-coding RNAs play a significant role in regulating different brain developmental stages as well as synaptogenesis, neurite outgrowth, neuronal maturation, synaptic plasticity. Newly discovered circRNAs that are highly expressed in the mammalian brain have emerged as novel regulatory non-coding RNAs, although their specific roles in the central nervous system are just starting to be elucidated (Ma et al, 2020; Xie et al, 2017). Almost one-fifth of the protein-coding genes in the brain generate circRNAs. Studies show that the expression pattern of circRNAs differs from one region of the brain to the other as well as in different developmental stages. For instance, circRims2, circEl2, and circDym are expressed at a high level in the cerebellum, while circPlxnd1 is enriched in the cortex. For some of these circRNAs, specific functions were found; for example, circRims2 is probably involved in neuronal differentiation and developmental processes (Venø et al, 2015a) but the functions of circEl2 and circDym remain to be elucidated (Wang et al, 2021).

CircRNAs have been found in the dendrites of neurons using fluorescent *in situ* hybridization (FISH). Several neuronal circRNAs have been shown to undergo significant up or downregulation in response to homeostatic changes related to neuronal activity. An alteration in circRNAs expression also occurs during synaptogenesis, suggesting their potential role in the regulation of synaptic function (You et al, 2015).

Interestingly, the expression level of circRNAs does not always correspond to the expression level of their linear counterparts. For example, circMyst4, circKlhl2, and circAagab significantly overexpress during synaptogenesis while their linear cognates show downregulation (Hanan et al, 2017). There is also evidence that on average that the ratio of circRNA abundance to the relative transcript abundance is higher in the brain when a host gene is expressed in the brain as well as other tissue(s) (You et al, 2015). This suggests that certain circRNAs might also play biological roles independent from their linear host genes. CircRNAs are not only more abundantly and diversely expressed in the brain, but they are also differentially expressed in the different regions and cell types of the brain (Jeck et al, 2013; Venø et al, 2015b). Although the function of circRNAs in the brain is the subject of considerable interest, little is known. So far, suggested physiological functions include potential regulatory roles through miRNA sponging,

regulation of transcriptional activities in neurons, and protein and RNA transport within the cells. For example, knock-out study of CDR1as in the murine brain showed a downregulation in the expression of miR-7 and miR-671 that directly interact with CDR1as. Subsequently, the expression of target genes of these miRNAs was altered in the brain of mutant mouse which affected neuropsychiatric-like behavior of CDR1as knock-out mice. Moreover, CDR1as knock-out mice have dysfunctional synaptic transmission in excitatory neurons suggesting a role of CDR1as in regulating synaptic transmission (Piwecka et al, 2017).

1.1.7 CircRNA in neurodegenerative disease

Although the role of circRNAs in the pathogenesis of neurodegenerative disorders is just beginning to be elucidated, several studies have proposed a strong connection between circRNAs and nervous system diseases. Some of the important circRNAs linked to nervous system diseases are circzip-2 in Parkinson's disease (Kumar et al, 2018); CDR1as/ciRS-7 in Alzheimer's disease (Lukiw, 2013); IQCK, MAP4K3, EFCAB11, DTNA, and MCTP1 circRNAs in multiple system atrophy (MSA) (Chen et al, 2016a); circDLGAP4 in cerebrovascular diseases (Bai et al, 2018); and circ-TTBK2, cZNF292, and circ-FBXW7 in glioblastoma multiforme (GBM) (Yang et al, 2016; Yang et al, 2018; Zheng et al, 2017).

The high expression of circRNAs in the mammalian nervous system would provide novel insight into the studies of the pathogenesis of neurodegenerative disease. For example, miR-7 regulates aggregation and inhibition of α -synuclein, a protein involved in Parkinson's disease. ciRS-7/CDR1as is an inhibitor of miR-7, which may point towards the participation of ciRS-7/CDR1as in Parkinson's disease (Asikainen et al, 2010; Doxakis, 2010; Miñones-Moyano et al, 2011). In addition, one interaction study revealed that circzip-2 possibly sponges miR-60 towards asserting an important role in various processes associated with PD (Kumar et al, 2018). ciRS-7/CDR1as, which is a super sponge and inhibitor of miR-7, is reported to be downregulated in Alzheimer's disease, while miR-7 is upregulated. This ciRS-7/miR-7 axis can alter the expression of proteins associated with Alzheimer's disease such as ubiquitin-linked protein ligase A (Lukiw, 2013). Age-related overexpression of circRNAs in CNS tissues is observed across different species suggesting their potential role in aging and age-related diseases in the central nervous system such as ALS. Interestingly, this age accumulation of circRNAs is independent to

the mRNA expression of their parental genes (Cai et al, 2019). There is also increasing use of circRNAs as an indicator of aging (Westholm et al, 2014).

Although the participation of circRNAs in neurodegenerative diseases is starting to be elucidated, the broader picture lacks clarity as more experimental studies are required to identify their targets and the mechanism of regulation. So far, very little is known about the participation of circRNAs in ALS pathogenesis. A study characterized several circRNAs that are affected by the knock-out of FUS and by FUS mutations associated with familial forms of ALS. This study revealed that FUS could bind to circularizing exon-intron junctions of circRNAs and regulate their back-splicing (Errichelli et al, 2017). In addition, another study presented the first circRNA differential expression analysis in PBMCs samples from patients with amyotrophic lateral sclerosis. Microarray-based circRNA expression profiling in this study on a subset of samples from ALS patients compared to controls revealed 274 upregulated and 151 downregulated circRNAs. This study suggests that circRNAs have the potential of being blood biomarkers for ALS diagnosis (Dolinar et al, 2019).

1.2 Amyotrophic lateral sclerosis

1.2.1 Overview

Amyotrophic lateral sclerosis (ALS) is a fatal and progressive neurodegenerative disorder. ALS is also known as Charcot disease in honor of the first person who described the disease in 1869, Jean-Martin Charcot. The progression of ALS is rapid and results in progressive paralysis because of loss of the upper and lower motor neurons in the spinal cord and brain (Strong et al, 2005). Respiratory failure is the main cause of death in ALS patients although heart failure and pulmonary embolism cause death in a minority of patients (Corcia et al, 2008). Male sex (until menopausal age for women when rates become equal), aging, a family history of ALS, and smoking are considered risk factors of ALS. The mean age of onset of ALS varies across populations and across historical cohorts; however, it is reported that it is usually from 50 to 65 years with 5% of the cases having an onset <30 years of age (Byrne et al, 2013; Zarei et al, 2015).

While the classical concept of ALS is that of a pure motor neuron disorder, ALS is now considered to be a multisystem degenerative process in which frontotemporal dysfunction can be prominent, including cognitive and behavioral disruptions similar to those observed in frontotemporal dementia (FTD) (Burke et al, 2017). There are also pathological and genetic overlaps between these two disorders that support the concept of a disease spectrum that includes both ALS and FTD (De Silva et al, 2016).

ALS is classified into three variants: sporadic (90-95%), familial (5-10%), and a previously hyperendemic Western Pacific variant (Garruto, 1991). Familial ALS (fALS) has prominent genetically inherited components although almost all of the genetic mutations associated with fALS have also been found in sporadic ALS (sALS) (Andersen & Al-Chalabi, 2011). The combination of upper and lower motor neuron degeneration causes various signs and symptoms that are the clinical hallmark of ALS. Weakness, muscle atrophy, and fasciculations are designated as lower motor neuron signs, whereas hyperreflexia and hypertonia are consistent with upper motor neuron involvement. For the diagnosis of ALS, clinicians consider criteria that support both upper and lower motor neuron impairment with involvement of at least three

regions of the body; the bulbar region and at least two spinal regions or in three spinal regions (de Carvalho et al, 2008; Li et al, 2017a; Traynor et al, 2000).

Unfortunately, because the pathophysiology of ALS remains poorly understood, a cure has not been discovered yet. However, there are lots of effective treatments for ALS such as Riluzole and Edaravone which are currently the only FDA-approved drug treatments that are associated with an increase in disease duration (Miller et al, 2003; Rothstein, 2017).

Given that the molecular mechanisms underlying motor neuron degeneration in ALS are not yet fully understood, illuminating the role of alterations in gene expression can provide expanding strategies for more effective treatments. To now, several hypotheses have been suggested for the pathogenesis of ALS. Structural and functional abnormalities of mitochondria, glutamate excitotoxicity, oxidative stress, and impaired axonal structure are the most frequently studied amongst these (Rothstein, 2009).

1.2.2 Genetics of amyotrophic lateral sclerosis

Although sALS accounts for more than 90 % of ALS cases, 5-10 % of cases are associated with a family history. A clear Mendelian inheritance pattern, which is primarily autosomal dominant, has led to the identification of a specific and broad array of genetic mutations in fALS (Taylor et al, 2016). Several of the gene mutations found in fALS have been also observed in sALS cases (Al-Chalabi & Hardiman, 2013). Over 25 genes have been found to be associate with ALS with several being considered to be causative (Andersen & Al-Chalabi, 2011). Among these latter genes, mutations in four are responsible for the majority of fALS cases, including superoxidase dismutase 1 (*SOD1*) (Rosen et al, 1993), TAR DNA-binding protein 43 (*TARDBP*) (Sreedharan et al, 2008), fused in sarcoma (*FUS*) (Deng et al, 2010) and Chromosome 9 open reading frame 72 (*C9orf72*) (DeJesus-Hernandez et al, 2011).

The first gene associated with fALS was *SOD1*, which encodes for copper/zinc ion-binding SOD1. A significant difference has been observed regarding the frequency of *SOD1* mutations in ALS between different populations. For example, *SOD1* mutations account for 14.8% of cases of fALS and 1.2% of sALS in the European population, while in Asian populations, *SOD1* mutations account for 30.0% of cases of fALS and 1.5% of sALS (Zou et al, 2017). So far,

several mechanisms have been proposed for mutated SOD1 toxicity in ALS (Gaudette, 2000; Guareschi et al, 2012; Higgins et al, 2003; Nagai et al, 2007). Most however suggest that these mutations are responsible for structural instability of SOD1 that causes protein misfolding which results in its aggregation in motor neurons (Rosen et al, 1993; Rotunno & Bosco, 2013).

Mutations in *TARDBP* that encodes TAR DNA-binding protein 43 (TDP-43) are responsible for the cytoplasmic mislocalization and aggregation of TDP-43 in the brain and spinal cord of ALS patients (Braak et al, 2013). *FUS*, which codes for Fused in sarcoma/translated in liposarcoma (FUS/TLS or FUS), is a nuclear RNA-binding protein that is mutated in a small percentage of fALS cases and is mislocalized from the nucleus to the cytoplasm where it accumulates as protein inclusions (Gal et al, 2011). Most genetic mutations involved in ALS are missense substitutions, although *C9orf72* is mutated to have enormous expansions of an intronic hexanucleotide repeat. These expansions were first characterized in patients with FTD, then in ALS (DeJesus-Hernandez et al, 2011; Renton et al, 2011).

The majority of these mutations are inherited in an autosomal-dominant manner. ALS-associated genetic mutations can be categorized into subsets by similar proposed mechanisms such as disruption in RNA metabolism, protein trafficking, and degradation, cytoskeletal and axonal dynamics (Brown & Al-Chalabi, 2017; Ling et al, 2013; Strong, 2010). A list of genes with mutations that are implicated in the pathogenesis of ALS is shown in Table 1-2.

Table 1-2: Genetics of ALS.

ALS-associated gene	Location	Protein	Proportion of ALS		Disease causative	Protein function
			Familial	Sporadic		
RNA metabolism						
<i>TARDBP</i>	1p36.22	TDP-43	5%	<1%	Yes	RNA-binding protein (Blokhuys et al, 2013; Davidson et al, 2016; Sreedharan et al, 2008)
<i>FUS</i>	16p11.2	Fused in sarcoma	5%	<1%	Yes	RNA-binding protein (Buchan et al, 2013; Deng et al, 2010)
<i>ANG</i>	14q11	Angiogenin	<1%	<1%		Ribonuclease (Greenway et al, 2006)
<i>SETX</i>	9q34.13	Senataxin			Yes	DNA/RNA metabolism and helicase activity (Chen et al, 2004)
<i>ATXN2</i>	12q24.12	Ataxin2				RNA processing (Elden et al, 2010; Sproviero et al, 2017)
<i>TAF15</i>	17q12	TATA-binding protein associated factor 2N				Initiation of transcription (Couthouis et al, 2012)
<i>MATR3</i>	5q31.2	Matrin 3	<1%	<1%		RNA-binding protein (Johnson et al, 2010)
<i>EWSR1</i>	22q12.2	EWS RNA-binding protein 1				RNA splicing, mRNA processing (Johnson et al, 2014)
<i>ELP3</i>	8p21.1	Elongator complex protein 3				Maturation of projection neurons (Simpson et al, 2009)
<i>ARHGEF28</i>	5q13.2	RGNEF				RNA-binding protein (Droppelmann et al, 2013b)
<i>hnRNPA1</i>	12q13.1	Heterogeneous nuclear ribonucleoprotein in A1	<1%	<1%	Yes	RNA-binding protein (Kim et al, 2013; Liu et al, 2016)
<i>hnRNPA2B1</i>	7p15.2	Heterogeneous nuclear ribonucleoprotein in A2/B1				RNA splicing, mRNA processing (Kim et al, 2013)
Protein trafficking and degradation						

<i>C9ORF72</i>	9p21-22	Guanin nucleotid exchange C9orf72	10%	25%	Yes	Possible guanine nucleotide exchange factor, endosomal trafficking, autophagy (DeJesus-Hernandez et al, 2011; Renton et al, 2011)
<i>ALS2</i>	2q33.1	Alsin				Endosomal dynamics and trafficking (Hadano et al, 2001)
<i>VAPB</i>	20q13.32	Vesicle-associated membrane				Vesicle trafficking (Lee & Brown, 2012)
<i>CHMP2B</i>	3p11.2	Charged multivesicular body protein 2b				Protein trafficking to lysosomes (Parkinson et al, 2006)
<i>SQSTM1</i>	5q35	Sequwstosome-1	<1%	<1%		Autophagy adaptor (Fecto et al, 2011; Teyssou et al, 2013)
<i>OPTN</i>	10p15-p14	Optineurin	4%	<1%	Yes	Autophagy adaptor (Maruyama et al, 2010)
<i>SIGMAR1</i>	9p13.3	Signa non-opoid intracellular receptor 1	<1%	<1%		Lipid transport from ER, mitochondrial axonal transport (Luty et al, 2010)
<i>UBQLN2</i>	Xp11.23-Xp13.1	Ubiquilin-2	<1%	<1%	Yes	Autophagy adaptor (Deng et al, 2011)
<i>FIG4</i>	6q21	Poly phospho-inositide phosphate				Autophagy regulation, endosomal trafficking to Golgi network (Chow et al, 2009)
<i>VCP</i>	9p13.3	Valosin Containing Protein	1–2%	<1%		Ubiquitin segregase (Johnson et al, 2010)
<i>TBK1</i>	12q14.1	Tank Binding Kinase 1	10 %	?		autophagy and activation of innate immunity (Freischmidt et al, 2015; Li et al, 2018a; Oakes et al, 2017)
Cytoskeletal and axonal dynamics						
<i>PFN1</i>	17p13.2	Profilin 1	<1%	<1%		Actin-binding protein (Wu et al, 2012)

<i>SPG11</i>	15q15–21.1	Spatascin				Cytoskeletal stability (Orlacchio et al, 2010)
<i>PRPH</i>	12q13.12	Peripherin				Cytoskeletal protein (Gros-Louis et al, 2004)
<i>NEFH</i>	22q12.2	Neurofilament heavy polypeptide				maintenance of neuronal caliber)Figlewicz et al, 1994(
<i>NEK1</i>	4q33	NIMA (Never In Mitosis Gene A)-Related Kinase 1				DNA damage response, neuronal morphology (Brenner et al, 2016)
<i>TUBA4A</i>	2q36.1	Tubulin α -4A chain	<1%	<1%		Microtubule subunit (Smith et al, 2014)
<i>DCTN1</i>	2p13.1	Dynactin subunit 1				Microtubule anchoring, vesicle transport, axonogenesis (Münch et al, 2004)
Enzymatic activity						
<i>SOD1</i>	21q22.1	Cu–Zn superoxide dismutase	20%	2%	Yes	Superoxide dismutase (Rosen et al, 1993)
Other						
<i>ERBB4</i>	2q34	Receptor tyrosine-protein kinase erbB-4				Neuronal differentiation (Takahashi et al, 2013)
<i>CHCHD10</i>	22q11.23	Coiled-Coil Helix Domain Containing 10	<1%	<1%		Mitochondrial protein, oxidative phosphorylation (Bannwarth et al, 2014)
<i>SS18L1</i>	20q13	Calcium-responsive transactivator				Chromatin remodeling (Teyssou et al, 2014)
<i>PNPLA6</i>	19p13.2	Neuropathy target esterase				Regulation of neuronal membrane composition (Rainier et al, 2008)
<i>PON1-3</i>	7q21.3	Paraoxonase 1-3				Enzymatic breakdown of nerve toxins (Saeed et al, 2006)
<i>DAO</i>	12q24	D-amino-acid-oxidase				Regulate D-serin level (Mitchell et al, 2010)
<i>CHRNA3</i>	15q25.1	Neuronal acetylcholine receptor				Cholinergic Neurotransmission (Sabatelli et al, 2009)
<i>ALS3</i>	18q21	ALS3	<1%	<1%		Disulfide redox protein (Hand et al, 2002)

*The empty cells indicate unknown values.

1.2.3 Neuropathology of ALS

The classic pathology of ALS is characterized by the loss of descending supraspinal motor neurons, both spinal and bulbar lower motor neurons and the associated corticospinal tract (CST) and motor nerves. Reactive gliosis, an inflammatory response to the degeneration of the neighboring motor neurons, is also observed (Leigh et al, 1988; Schiffer et al, 1996). A hallmark of ALS is the presence of neuronal cytoplasmic inclusions (NCI) that are categorized by their morphology, reaction with various histologic stains, and by immuno-reactivity for associated proteins (Saber et al, 2015). At the protein aggregate level, these pathological intracellular protein aggregates are multiple forms of inclusion bodies that have been described for ALS in the motor neurons, including Bunina bodies, which are ubiquitin-negative inclusions; basophilic inclusions; and ubiquitinated inclusions such as round bodies, skein-like inclusions, and hyaline inclusions (Bäumer et al, 2010). Skein-like inclusions, which are TDP-43 positive inclusions, are the most common inclusions observed and are present in approximately 90% of ALS patients (Saber et al, 2015).

1.2.4 Altered RNA Metabolism in ALS

Dynamic regulation of events occurring from genes to proteins must be strictly controlled. This regulation happens during the transcriptional and post-transcriptional events of mRNA, including pre-mRNA splicing, mRNA processing, editing, transport, stabilization and translation, and degradation. The disruption of normal RNA transport and metabolism has been proposed to be the functional consequence of several of the genetic mutations linked to ALS. Several genetic mutations associated with ALS exist in RBPs coding genes such as *TARDBP*, *FUS/TLS*, *TAF15*, and *ARHGEF28* which are involved in gene transcription, RNA stability, RNA transport, RNA translation, and ribonucleoprotein (RNP) granule formation Table 1-2: Genetics of ALS.. These RBPs have been shown to be present in NCIs in motor neurons. RNA transcripts resulting from the hexanucleotide repeat expansion of the *C9orf72* gene have been shown to form RNA foci that could sequester RBPs and disrupt their normal functions (DeJesus-Hernandez et al, 2011). In addition, extensive alterations in the expression of coding and non-coding RNAs have been reported in ALS, which supports the idea of ALS as a disorder of RNA metabolism (Bergeron et al, 1994; Lin et al, 1998; Mu et al, 1996; Roberts et al, 2014; Strong, 2010).

MRNAs have different half-lives, ranging from those short-lived mRNA involved in signaling pathways to long-lived mRNAs, which are translating to housekeeping proteins. The regulation of mRNA turnover is crucial because it affects transcriptional rates (Bolognani & Perrone-Bizzozero, 2008; Hargrove & Schmidt, 1989). There is a growing body of evidence that in the majority of ALS cases, alterations in the metabolism of RNA underpins the disease process. In the next section, I will address aspects of RNA metabolism that are dysregulated in ALS.

1.2.4.1 RNA splicing

Motor neurons have been shown to be susceptible to defects in RNA metabolism. For example, in spinal muscular atrophy (SMA) in which lower motor neurons progressively degenerate, the causative gene, survival motor neuron (*SMN*), encodes for a RBP with known roles in splicing. Two highly homologous *SMN* variants have been found, including *SMN1* which is responsible for the production of the majority of functional SMN protein, and *SMN2* which is responsible for the production of less protein. SMA occurs when the *SMN1* gene is lost and the presence of *SMN2* cannot compensate for the deficit in SMN protein levels. SMN protein complex interacts with specific spliceosome proteins and plays a role in the biogenesis of spliceosomal small nuclear ribonucleoproteins as well as the assembly, metabolism, and transport of several ribonucleoproteins (Kolb et al, 2007; Mourelatos et al, 2001). A higher level of SMN protein is required for the normal function of motor neurons than other types of cells (Burghes & Beattie, 2009). It is reported that lower *SMN2* copy numbers and lower levels of estimated SMN protein increase susceptibility to and severity of ALS (Veldink et al, 2005).

Several RBPs associated with ALS are involved in mRNA splicing, such as TDP-43, FUS, heterogeneous nuclear ribonucleoprotein A1 (hnRNP1), heterogeneous nuclear ribonucleoprotein A2/B1 (hnRNPA2B1), and valosin-containing protein (VCP). Therefore mis-splicing of mRNA is a common consequence of dysregulation of ALS-related RBPs. For example, TDP-43 participates in dysregulation of mRNA splicing of several genes including *hnRNPA1*, human cystic fibrosis transmembrane conductance regulator (*CFTR*), *SMN2*, and *STMN2*. TDP-43 plays a role in the regulation of alternative splicing of hnRNPA1 by binding to *HNRNPA1* pre-mRNA and modulate its splicing. Thus, TDP-43 mislocalization may contribute to altered *HNRNPA1* pre-mRNA splicing in ALS (Deshaies et al, 2018). TDP-43 also participates in the promotion of exon skipping in *CFTR* mRNA (Buratti et al, 2001) and exon inclusion of *SMN2* pre-mRNA

(Bose et al, 2008). Klim et al. showed that the expression of *STMN2* which encodes a mediator of neuronal growth and axonal regeneration is decreased by mislocalization or knock-down of TDP-43 within iPSC (Induced Pluripotent Stem Cells)-derived motor neurons. They showed that TDP-43 mislocalization or depletion causes the production of a cryptic exon in *STMN2* mRNA which prevents protein production through early termination of translation (Klim et al, 2019).

Regulation of splicing of several transcripts by FUS has been also reported to occur in the central nervous system. FUS interacts with the spliceosome and the splicing factors then directly binds to target pre-mRNAs and regulates their splicing. Thus, mislocalization of FUS to the cytoplasm and pathological mutations of its gene in ALS might result in aberrant alternative splicing of its target genes (Orozco & Edbauer, 2013). An example of endogenous neuronal splicing targets for FUS is microtubule-associated protein tau (*MAPT* encoding tau protein) (Orozco et al, 2012). Tau is one of the most studied proteins in neurodegenerative disease such as ALS. FUS depletion in rat neurons results in an aberrant alternative splicing of tau transcripts. It is also reported that FUS interact with tau transcripts in brain (Orozco et al, 2012).

ALS-linked mutations in the *VCP* gene have been shown to cause intron retention in a nuclear protein named Splicing Factor Proline and Glutamine rich (*SFPQ*) transcript through aberrant splicing (Luisier et al, 2018). This intron retention results in nuclear depletion and cytoplasmic aggregation of SFPQ protein in the motor neuron of ALS patients.

Another example of dysregulated RNA splicing in ALS occurs when the *PRPH* (*peripherin*) gene, which is one of the ALS-associated genes, is transcribing. The *Per 28* isoform is a toxic splice variant of *peripherin* that is associated with NCIs in spinal motor neurons in ALS (Corbo & Hays, 1992). This type of dysregulation has been also observed in the case of the excitatory amino acid transporter 2 (*EAAT2*) gene for which abnormal mRNA splice variants are observed in the brain of ALS patients (Lin et al, 1998).

1.2.4.2 mRNA stability

Neurofilaments, peripherin (PRPH), and α -internexin (INA) are neuronal intermediate filaments (IFs) that are essential components providing neuronal structures. There are three types of neurofilaments that are defined by their molecular weight, including neurofilament light (NFL),

medium (NFM), and heavy (NFH). Several of these IFs form pathological NCI in motor neurons of ALS patients (Hirano et al, 1984; Strong et al, 2005).

TDP-43, Rho guanine nucleotide exchange factor (RGNEF), SOD1, and 14-3-3 protein have been shown to regulate mRNA stability of several ALS-related proteins, such as *NEFL* through binding to 3' UTR region of their transcripts (Droppelmann et al, 2013a; Ge et al, 2007; Ge et al, 2005; Strong et al, 2007; Volkening et al, 2009). Interestingly, the aggregation of neurofilament proteins in ALS is associated with alterations in *NEFL* mRNA stability with quantitative *in situ* hybridization of *NEFL* transcript demonstrating a significant decrease in its expression in ALS spinal motor neurons compared to control patients (Bergeron et al, 1994; Wong et al, 2000).

RNA stability also can be affected by miRNAs, which are highly abundant and conserved small non-coding RNAs derived from endogenous genes. MiRNAs are single-stranded RNAs that control RNA expression and stability (Fabian et al, 2010). They are increasingly recognized to play a crucial role in the regulation of neuronal development and function and participate in neuronal degeneration (Davis et al, 2015). Previously our lab described the miRNA expression profile in the spinal cord of ALS patients compared to controls (Campos-Melo et al, 2013a). This study showed significant differential expression of a large group of miRNAs, which is another sign of altered RNA metabolism in ALS. This study also examined the effect of those population of miRNAs which have MREs within the human *NEFL* mRNA 3' UTR on *NEFL* mRNA expression. Among these miRNAs, there is a group (miR-146a*, 524-5p, and 582-3p) that directly downregulates the *NEFL* mRNA, suggesting an involvement in the altered stability of the *NEFL* mRNA in the spinal motor neurons in ALS (Campos-Melo et al, 2013b). Further research in our lab also has described the role of miR-105 and miR-9 in the regulation of *NEFL* expression and which are down-regulated within the spinal cord of ALS patients (Hawley et al, 2019).

1.2.4.3 RNA transport

Dyneins and the kinesin superfamily proteins (KIFs) are known to participate in the transportation of RNP granules along dendrites and axons. Dynein is a microtubule minus end-directed motor that is required for retrograde axonal transport. Dynein also plays roles in mRNA localization and neurofilament transport. Mutation in dynein heavy chain which has a function in

the microtubule motor dynein complex formation has been found in a progressive motor neuronopathy and severe impairments in retrograde signaling. Dynein plays its role in retrograde signaling in association with a protein complex named dynactin that has been found to have mutations in some cases of ALS (Hafezparast et al, 2003; Münch et al, 2005; Puls et al, 2003). Although no mutations related to disrupting RNA transport in kinesin superfamily proteins have been yet reported, one study showed that downregulation of the kinesin-associated protein 3 (KIFAP3) is associated with enhanced survival in sALS (Landers et al, 2009).

Insulin-like growth factor II mRNA-binding protein 1 (IMP1), associated with FUS protein, is involved in the recruitment and transportation of target mRNAs to cytoplasmic complexes in neurons. This protein is found in FUS-positive cytoplasmic inclusions when *FUS* is mutated, suggesting that *FUS* mutations might alter the transportation of mRNA targets of IMP (Kamelgarn et al, 2016). In addition, the localization of the discoidin domain tyrosine kinase receptor 2 (*DDR2*) and KN motif and ankyrin repeat domains 2 (*Kank2*) transcripts can be influenced by *FUS* mutations (Yasuda et al, 2017).

In addition, dysregulation of nuclear pore complexes occurs in ALS which causes the disruption of nucleocytoplasmic transport. Whereas insoluble TDP-43 interacts with nuclear pore complexes, ALS-related mutations in the *TARDBP* gene in mouse models and iPSC-derived motor neuron models showed the disruption of nucleocytoplasmic transport of polyadenylated transcripts (Chou et al, 2018). A similar effect has also been observed when *MATR3* and *C9ORF72* were mutated (Boehringer et al, 2017; Zhang et al, 2015).

1.2.4.4 RNA translation

There is evidence suggesting a relationship between RNA translation and ALS pathogenesis. Several mutations that are known to be causative in ALS affect RNA translation, including *FUS* and TDP-43 (Coyne et al, 2017).

Neuronal activities depend on the localization of synaptic proteins such as signaling molecules and neurotransmitters (Krichevsky & Kosik, 2001). Neuronal RNP granules (also known as transport granules) are responsible for transporting ribosomes and temporary translationally arrested mRNAs in response to synaptic stimuli. Several RBPs associated with ALS play a

pivotal role in the assembly and regulation of these transport granules. Dysfunctional neuronal transport granules have been reported to be associated with ALS (Elvira et al, 2006; Kanai et al, 2004). TDP-43 is present in neuronal transport granules and collaborates with other RBPs to repress the translation initiation. Mutations in TDP-43 observed in ALS affect neuronal transport granule trafficking and hence RNA translation (Alami et al, 2014).

Substantial evidence implicates cellular stress as an important mechanism for motor neuron death. For instance, mutations in SOD1 affect the oxidative stress mechanisms in motor neurons and thus might cause neurodegeneration (Abe et al, 1995; Beal et al, 1997). Moreover, ALS patients show markers of oxidative damage in their spinal cord fluid (Bogdanov et al, 2000). Many RBPs associated with ALS are localized in stress granules (SGs) which are a type of RNP granules formed in response to stress. Therefore ALS-related mutations in these RBPs can dysregulate SGs assembly and disassembly. As non-translated mRNA is a key component of SGs, dysregulation of SGs formation and dynamics might cause disruption in translation (Anderson & Kedersha, 2009).

1.3 Membraneless organelles

1.3.1 Overview

Advanced visualization technologies have revealed that in addition to membrane-bounded compartments, the nucleus and cytosol of eukaryotic cells contain non-membrane bounded macromolecular assemblies named membraneless organelles (MLOs). These biological assemblies are also termed biomolecular condensates. Recently discovered MLOs are highly dynamic macromolecular assemblies that often show liquid-like physical properties that range in size from nanometers to micrometers (Mitrea & Kriwacki, 2016). Despite numerous studies on these macromolecular assemblies, the exact functions and mechanisms underlying their formation are yet to be fully understood.

A wide range of membraneless structures, from RNP granules to centrosomes and clusters of signaling molecules on membranes, are formed via a process called liquid-liquid phase separation (LLPS) (Banjade & Rosen, 2014; Li et al, 2018b; Molliex et al, 2015). The basic principles of phase separation of organic polymers in the solution can be described by Flory-Huggins solution theory which delineates the free energy of a polymer-solvent mixture, where polymers are considered as simplified arrays of modules that represent their repetitive segments (Flory, 1941; Huggins, 1942). When a critical concentration or temperature threshold is crossed, solutions of macromolecules undergo LLPS and condense into a dense phase that coexists with a dilute phase (Figure 1-5). The driving force underlying this process is the exchange of macromolecule/water interactions for macromolecule/macromolecule and water/water interactions in which the polymer becomes a better solvent for itself than the solution it is dissolved in. LLPS enables cells to compartmentalize spatiotemporally within a boundary which allows dynamic trafficking of biomolecules into and out of the compartment. Moreover, the concentration of certain molecules within macromolecular assemblies can be increased by phase separation. This probably accelerates reaction rates and biochemical activities inside membraneless organelles (Zhou et al, 2018).

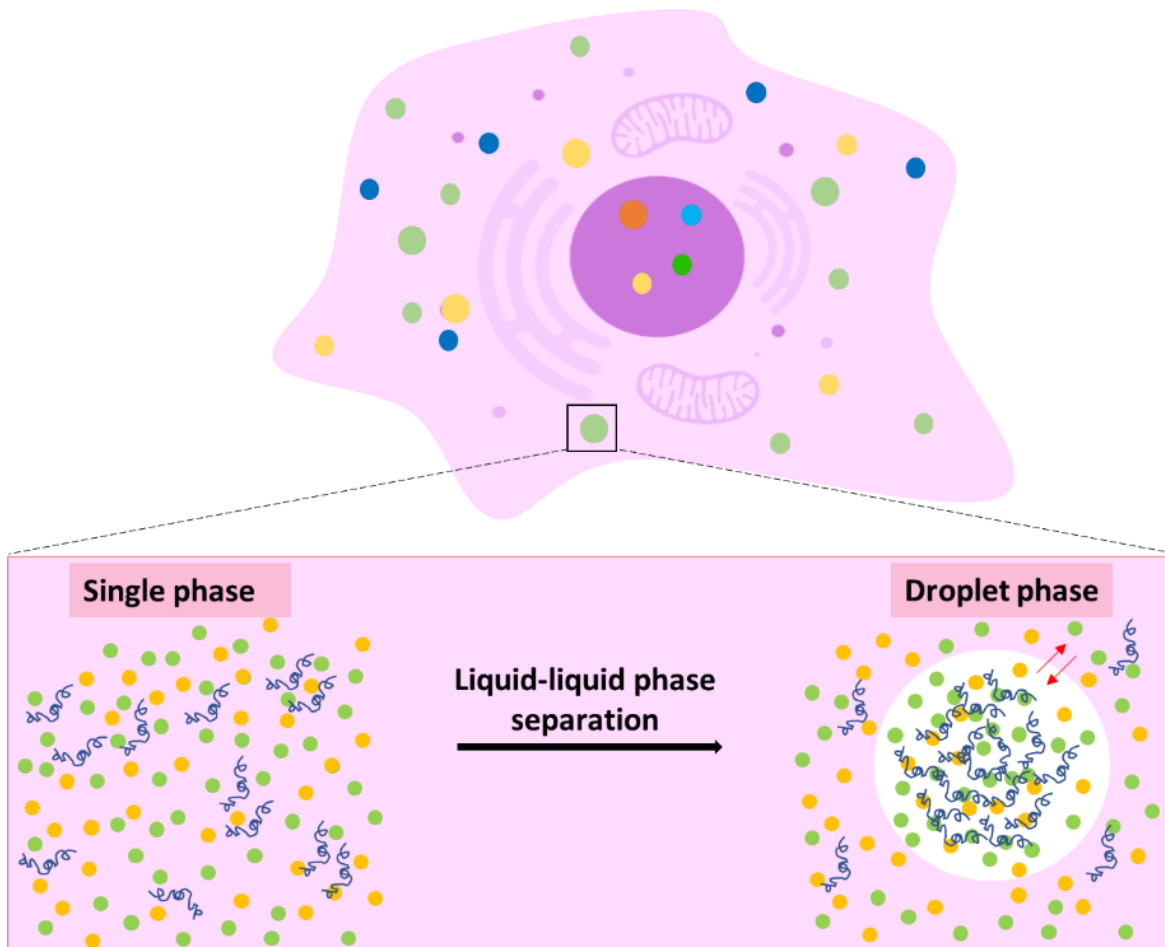


Figure 1-5: Schematic illustration of liquid-liquid phase separation. In cells, LLPS occurs when solutions of macromolecules such as proteins and/or nucleic acids condense into a dense phase that coexists with a dilute phase. This process can result in the formation of liquid droplets and membraneless organelles.

Phase separation can occur for many proteins *in vitro*, although not all do so under physiological conditions. It has been observed that proteins associated with these assemblies often contain two types of domains: folded domains that acquire stable secondary and tertiary structures, and intrinsically disordered protein regions (IDRs) that do not adopt stable secondary and tertiary structures. A subset of disordered protein regions is termed low complexity domains (LCD) in that they contain amino acid composition with little diversity. Interestingly, some proteins within membrane-less organelles are entirely disordered (called intrinsically disordered proteins or IDPs). It is proposed that the high degree of conformational flexibility and dynamics of membrane-less organelles arises from the over-presentation of low-complexity sequences and disordered regions in their protein composition. Multivalency which is achieved through the repetitive presence of folded domains and LCDs in proteins that are associated with phase separation is likely to contribute to the liquid and dynamic properties of membrane-less organelles. However, one of these two types of multivalent interactions is sufficient for protein phase separation. In other words, both folded domains and disordered/low complexity regions can initiate phase separation (Uversky, 2017; 2019).

In addition to proteins, RNA self-assembly/condensation has been proposed to have an important role in formation of MLOs that contain RNA. Several lines of evidence have suggested the role of intermolecular RNA–RNA interactions in RNP granule formation. For instance, the high concentration of local RNA is a driving factor for the formation of many RNP granules like paraspeckles and histone locus bodies (Yamazaki et al, 2019). In addition, decreasing translation initiation or inhibiting RNA degradation which results in an increased level of untranslated mRNA causes higher SG and P-bodies formation, respectively (Bounedjah et al, 2014; Mahadevan et al, 2013)

Biological phase separation carries an entropic cost which is counteracted by numerous weak interactions. This type of interaction maintains membraneless organelles in phase (Brangwynne et al, 2015). These important weak interactions include π – π stacking, cation- π interactions, charge-charge interactions, and transient cross- β -contacts. π – π stacking refers to attractive, noncovalent interactions between aromatic rings since they contain π bonds. π bonds happen where two lobes of an orbital on two atoms laterally overlap two lobes of an orbital on another atom. Electrons that are involved in π bonds are referred to π electrons (Matsuo & Hayakawa,

2018). These interactions are involved in both RNA and protein stacking. For example, aromatic amino acids contain delocalized π electrons which are involved in π - π interactions in proteins associated with LLPS (Vernon et al, 2018). Cation- π interaction is a noncovalent molecular interaction between the face of an electron-rich π system (e.g., electron-rich aromatic groups) and an adjacent cation (e.g., the positively-charged amino acids). An example of cation- π interaction is between FG (phenylalanine-glycine) and RG (arginine-glycine) regions of Ddx4 RNA helicase that drives this protein into phase separation in vitro and in vivo. Moreover, multiple π - π interactions and cation- π interactions have the ability to disrupt the internal π - π interaction of nucleic acid duplexes and drive them to phase separation (Nott et al, 2016; Nott et al, 2015). Charge neutralization refers to a state in which the net electrical charge of polymers in an aqueous solution has been counteracted by the adsorption of an equal number of opposite charges. This charge neutralization is an important driver for phase separation and has been observed for mixtures of RNA and cationic peptides as well as proteins both in vitro and in vivo (Aumiller & Keating, 2016; Pak et al, 2016).

A wide range of membraneless organelles exists in eukaryotic cells. Membraneless organelles within nuclei are also called nuclear bodies and examples of them include the nucleolus, paraspeckles, nuclear speckles, Cajal bodies, and PML (promyelocytic leukemia) bodies. Cytosolic membrane-less organelles include transport granules, SGs, processing bodies (P-bodies), and germ granules. The majority of membraneless organelles are RNP granules (also called RNA granules) that consist of RBPs and RNA assembled via LLPS (Uversky, 2017). However, there are different types of MLOs that do not contain RNAs (e.g., SUMO-1 nuclear bodies, Cleavage bodies, chromatin, Insulator bodies) (Uversky, 2017).

1.3.2 RNP granules

RNP granules are self-assembled ribonucleoprotein complexes in nuclear and/or cytoplasmic structures that are not defined by membranes. These types of membraneless organelles require the coding and/or non-coding RNAs for their formation. Besides RNAs, RNP granules are composed of the proteins involving in the regulation of localized RNA translation, silencing, or decay (Kiebler & Bassell, 2006). RNP granules are categorized into nuclear and cytoplasmic RNP granules base on their cellular localization (Table 1-3 is modified from a table in Uversky's paper (Uversky, 2017)). RNP granules in the nucleus regulate various steps of RNA and RNP

processing while cytoplasmic granules regulate RNA translation, RNA degradation, signaling pathways, and stress responses (Kedersha et al, 2013; Trinkle-Mulcahy & Sleeman, 2017). RNA transport and localized translation can be regulated by RNP transport granules in neurons and myogranules in skeletal muscle (Kiebler & Bassell, 2006; Vogler et al, 2018).

RNP granule proteomes have been studied using different approaches. Initially, locally concentrated proteins in RNP granules have been identified using immunofluorescence techniques. Mass spectroscopy of RNP granules extracted by differential centrifugation or by particle sorting has provided a more complete identification of the protein composition of RNP granules (Hubstenberger et al, 2017; Jain et al, 2016). Recently, more advanced methods like Bio-ID or APEX labeling have been used to characterize the RNP granule proteome (Markmiller et al, 2018; Wheeler et al, 2016). Taken together, these approaches have revealed that RNP granules contain three types of RBPs. Some RBPs provide protein-based assembly and play roles in the formation of a specific granule; this type of RBPs can be only found in that specific granule. Other RBPs are carried to RNP granules by interacting with RNAs and therefore can be in common between different types of RNP granules. The last types are RBPs that promote RNA-RNA interactions by binding to the RNA embedded within RNP granules and thus can be found in more than one type of RNP granule (Boundedjah et al, 2014; Tauber et al, 2020). Other types of proteins also can be found in RNP granules. For example, proteins involved in cellular signaling pathways and metabolism have been found in SGs, providing evidence of the influence of SGs in cell signaling and metabolism (Tauber et al, 2020). The nucleolus is another example of RNP - that contain a vast variety of proteins besides RBPs (Boisvert et al, 2007).

Whereas RNP granules regulate different aspects of RNA metabolism, other RNA species are also involved in the assembly and integrity of RNP granules. All the mRNAs contained in RNP granules are translationally suppressed (Bregues et al, 2005). The RNA composition of RNP granules is generally related to granule function. For instance, snRNAs localized to paraspeckles, where they are organized into snRNPs, and ribosomal RNAs localize to the nucleolus, where they are assembled into ribosomal subunits (Fox & Lamond, 2010; Savino et al, 2001). Specific types of RNAs are present in specific type of RNP granules, so the individual RNA constituents might be considered as the principal determinants of organelle identity. Interestingly, RNAs can have intermolecular interactions and thus induce their self-assemble into condensates in vitro. In

addition, environmental factors such as higher salt concentration can promote trans RNA-RNA interactions which enhance RNA condensation (Yamazaki et al, 2019).

There are three different approaches to identifying the RNA composition of RNP granules. The FISH technique can be used to characterize RNA composition in RNP granules. Purification of RNP granules from the cells and sequencing the RNAs that are purified is another approach (Hubstenberger et al, 2013; Khong et al, 2017). The third approach is to identify those RNAs that have interactions with the main RBPs of a specific RNP granule. This method will be usually followed by FISH to validate the data (Lee et al, 2020).

RNAs and proteins within RNP granules are assembled through multivalent interactions, including protein-protein, RNA-RNA, and protein-RNA interactions. Both well-folded domains and IDRs of proteins can contribute to multivalent protein-protein interactions in RNP granules. Interestingly, RNP granules share RNAs and RBPs that can be exchanged through dynamic interactions between them (Buchan & Parker, 2009; Kedersha et al, 2005). Previously, the transcripts that comprise different types of RNP granules have remained undetermined due to a lack of effective purification methods for RNP granules. In recent years, various purification strategies have been devised to sequence the RNAs that localize to different cytosolic RNP granules based on differential centrifugation, differential centrifugation followed by immunoprecipitation or particle sorting or differential migration through sucrose gradients (El Fatimy et al, 2016; Jain et al, 2016; Khong et al, 2017; Namkoong et al, 2018). Next, RNA-seq is used to identify the transcriptome of RNP granules (Khong et al, 2018).

In neurons, RNP granules can be found in distinct subcellular compartments, such as the soma, dendrites, axons, and synapses. In this manner, RNP granules can control the subcellular proteome and thus can facilitate the neurons' ability to respond to stress. Alterations in this process can lead to diverse pathological events in the neurons. It has been proposed that synaptic localization of mRNAs is a mechanism for synaptic plasticity and thus learning and memory (Costa-Mattioli et al, 2009). Moreover, mRNA targeting, and local protein synthesis can influence axon guidance and nerve regeneration. Therefore, RNP granules are crucial structures for neuronal functions (Krichevsky & Kosik, 2001). RBPs associated with ALS had been reported to be present in the formation and function of RNP granules. Regarding the essential

functions and components of RNP granules, they have been considered to play critical roles in RNA metabolism and potentially as the precursor for NCIs in ALS (Ling et al, 2013; Wolozin, 2012a). Neurons have different types of RNP granules, including transport granules, SGs, P-bodies, and activity-dependent granules in the cytoplasm, and paraspeckles and nuclear bodies in the nucleus (Ingelfinger et al, 2002; Kedersha et al, 2000; Martin & Ephrussi, 2009; Shelkovernikova et al, 2014; Sleeman & Trinkle-Mulcahy, 2014; Wolozin & Ivanov, 2019).

Table 1-3: Characteristics of currently known RNP granules.

Name (abbreviation)	Function	Cellular location	Quantity (foci/cell)	Size (nm)
Sam68 nuclear bodies (SNBs)	mRNA trafficking through the nucleus	nucleus	10–30	300–1000
Nuclear stress bodies (nSBs)	response to stress	nucleus	4–6	2000–2500
Oct1/PTF/transcription domains (OPT domains)	response to replication stress	nucleus	One or few	1000–3000
Polycomb group proteins (PcG bodies)	gene expression regulation	nucleus	5–30	250–500
Nucleolus	site of ribosome synthesis and assembly	nucleus	1	1000–10,000
Nuclear speckles	pre-mRNA splicing	nucleus	25–50	500–1000
Promyelocytic leukemia (PML) nucleic bodies	control cellular senescence and stem cell self-renewal	nucleus	5–30	250–500
Cajal bodies (CBs)	involve in snRNP biogenesis	nucleus	1–5	100–2000
Paraspeckles	Regulation of gene expression through nuclear retention of RNA	nucleus	5–20	500–1000
Transport granules	Protein synthesis in response to exogenous stimuli	Cytoplasm of neurons	10–50	150–1000
Stress granules (SGs)	Response to stress	Cytoplasm	10–100	100–200
Processing bodies (P-bodies)	Response to stress, mRNA decay	Cytoplasm	2–20	100–300
Germ cell granules	Regulation of germ cell development and function	Cytoplasm of embryonic cells	10–200	Continually growing and shrinking

*Table is adapted from Uversky's paper (Uversky, 2017). This reference did not specify the type of cells that have been chosen for defining the characteristics of RNP granules.

1.3.2.1 Transport Granules

In situ hybridization (ISH) had previously revealed the steady-state distribution of specific mRNAs to subcellular domains of polarized cells such as neurons. A study in live oligodendrocytes using fluorescently labeled and microinjected mRNA of myelin basic protein (MBP) showed this mRNA is involved in RNP granules formation, which transports along microtubules (Kiebler & Bassell, 2006). These granules were characterized as persistent, oscillatory, or immobile RNPs that were heterogeneous in size and were later named “RNA transport particles” by Wilhelm and Vale (Wilhelm & Vale, 1993). These are now called transport granules. They are crucial for normal cellular functioning and can be found throughout the cell under physiological conditions.

Transport granules contain translational subunits such as elongation factors, ribosomal proteins, and clusters of ribosomes supporting the idea of the involvement of transport granules in the initiation of translation at their final destination (Knowles et al, 1996). Transport granules have been found to be localized along microtubules in neurons, suggesting an important role in RNA transport and a function in supporting synaptogenesis, synapse pruning, synaptic plasticity, axon guidance, and axonal regeneration through regulation of mRNA localization and subsequent local protein synthesis (Knowles et al, 1996). Staufen (STAU), a double-stranded RBP, is a core component of transport granules. Staufen interacts with the 3' UTR of mRNA targets through binding to the STAU1-binding site (SBS). This interaction occurs when SBS forms a double-stranded RNA structure through the base pairing of 3' UTR sequences either with themselves or ncRNAs (Park & Maquat, 2013). These RNA secondary structures are required for recruiting Staufen to mRNA and the formation of transport granules. Evidence suggests that Staufen is responsible for the formation of transport granules and plays an important role in transporting specific mRNAs to the growing dendrite along microtubules in developing neurons.

Differentiated neurons might take advantage of Staufen's functioning in transporting specific mRNAs to the synapse, which provide synaptic microenvironments through local protein synthesis (Roegiers & Jan, 2000).

Deficits in neuronal transport contribute to the pathogenesis of multiple nervous system diseases. Loss of the FMRP (Fragile X Mental Retardation Protein 1) protein, encoded by the *FMRI* (fragile X mental retardation 1) gene on chromosome X, is a component of transport RNP

granules. FMRP is an RNA-binding protein expressed in most tissues but found predominantly in the brain, testes, and ovaries (Ashley et al, 1993; O'Donnell & Warren, 2002). FMRP contains a nuclear localization signal (NLS) and a nuclear export signal (NES), which provide shuttling property between the nucleus and cytoplasm of a cell (Imbert et al, 1998). FMRP is known as a neuronal RBP associated with polyribosomes, which plays a role in RNA translation and localization. (Ascano et al, 2012; Devys et al, 1993). Loss of the FMRP protein that is a component of transport RNA granules and expresses from the fragile X mental retardation gene leads to fragile X mental retardation syndrome (Tosar et al, 2012). Moreover, loss of full-length SMN protein that is also a component of RNP granules transported along neurites, results in the autosomal recessive motor neuron disease SMA. SMN deficiency causes the changes in β -actin mRNA localization in the growth cones of developing neurons, which leads to reduced neurite outgrowth (Rossoll et al, 2003). There is evidence showing TDP-43 is one of the components of neuronal RNP granules (transport granules) (Alami et al, 2014). In fact, TDP-43 is physically associated with Staufen and FMRP to form a functional complex and regulate the expression of important genes such as *Sirtuin 1 (SIRT1)* (Yu et al, 2012). Moreover, it is reported that ALS-linked mutant TDP-43 can impair RNA trafficking through neuronal transport granules which might elaborate the role of TDP-43 in RNA trafficking (Alami et al, 2014). Recently, Staufen was found in NCIs related to SGs containing TDP-43, FUS/TLS, and FMRP, suggesting the involvement of neuronal transport granules in ALS pathology (Tosar et al, 2012).

1.3.2.2 Stress granules

Stress granules are cytoplasmic phase-dense structures that are formed in response to environmental stress (e.g., heat, oxidative conditions, UV irradiation, and hypoxia). SGs recruit polyadenylated mRNA transcripts, specific RBPs, and other proteins, including several initiation factors and small ribosomal subunits (Kedersha et al, 2000). Eukaryotic cells that are exposed to stress reprogram mRNA metabolism to repair stress-induced damages and adapt to changed conditions. Therefore, the SGs formation seems to be a protective mechanism in response to cellular stress. This concept is supported by the observation that inhibitors of SG assembly decrease cell survival of some specific cell lines under stress conditions (Eisinger-Mathason et al, 2008). Eukaryotic cells under stress limit the translation of a broad array of mRNAs and shift RNA transcription and translation to only the essential proteins required for survival (Holcik &

Sonenberg, 2005; Pearce & Humphrey, 2001). This switch is achieved by collecting unnecessary mRNAs and their associated proteins, as well as factors involved in translational repression and mRNA decay into SGs. A vast variety of proteins exist in SGs, including RNA-binding proteins, non- RNA-binding proteins (such as post-translation modification enzymes, metabolic enzymes, and protein or RNA remodeling complexes), and key components of signaling pathways (Khong et al, 2017).

Interestingly, many RBPs involved in SG formation harbor IDRs, which provide the ability of self-assembly for proteins. This domain enables proteins to form reversible self-templating amyloid fibrils, which usually results in a decrease in the protein's function (Protter & Parker, 2016). Assembly and disassembly of SGs are mediated by various post-translational modifications as well as numerous RNP remodeling complexes. Protein-protein interactions in SGs can be modified by phosphorylation, methylation, and glycosylation, which influence SG assembly (Wheeler et al, 2016). SG assembly is initiated by the self-aggregation of the RBP T-Cell-Restricted Intracellular Antigen-1 (TIA-1), TIA-1-related (TIAR), and Ras-GTPase-Activating Protein SH3-Domain-Binding Protein (G3BP). TIA-1 is a key component and marker of SGs, rapidly and continuously shuttling in and out of SGs, suggesting that the assembly of SGs is a highly dynamic process (Kedersha et al, 2000). RBPs possessing IDRs can recruit target mRNAs with their RNA recognition motifs (RRM) into RNP granules. As aggregates formed by IDRs are reversible, SGs can be rapidly dissociated upon the stress dissipation, liberating the arrested mRNAs and translation machinery to resume their normal functions (Gilks et al, 2004). There is a negative correlation between SGs formation and stability of translating polysomes because polysome stabilization prevents SGs assembly, and disturbance of polysomes promotes SGs formation (Mollet et al, 2008).

Many SG-associated RNA-binding proteins contain a glycine-rich IDR (Gilks et al, 2004). This specific domain has the potential to make the protein form insoluble aggregates which can be pathological. Therefore, many studies have started to investigate the role of SGs in the pathology of different diseases, specifically neurodegenerative disorders (King et al, 2012). Recently, many studies have been suggesting a correlation between SG formation and protein aggregate formation in ALS. This might be because of the contribution of ALS-related RNA-binding proteins in SGs formation. Indeed, subsets of NCIs containing TDP-43 in ALS patients can be

labeled for SG markers such as TIA-1, eIF3 (eukaryotic translation initiation factor 3), and PABP (Polyadenylate-binding protein) (Dormann et al, 2010; Liu-Yesucevitz et al, 2010b; McGurk et al, 2014; Volkening et al, 2009). Moreover, FUS and TDP-43 have both been reported to colocalize with TIA-1 positive stress granules (Liu-Yesucevitz et al, 2010b; Sama et al, 2013). In response to cellular stress, the untranslated mRNAs enriched in some RNP granules including SGs. RNA-RNA interactions have been shown to have important role in SGs formation (Van Treeck et al, 2018).

1.3.2.3 Processing bodies

Like SGs, processing bodies (P-bodies) are also RNP granules that play crucial roles in mRNA metabolism. P-bodies are thought to participate in mRNA storage and degradation. These RNP granules play significant roles in controlling gene expression through the regulation of mRNA turnover (Decker & Parker, 1993). P-bodies were first discovered when cells that were stained for XRN1 exhibited an unusual punctate staining pattern (Bashkirov et al, 1997). P-bodies contain many other components of mRNA silencing and degradation, including RNA decapping machinery (Dcp1/Dcp2 decapping enzyme complex), decapping activators, exonucleases, mRNA deadenylases, translation repressor, nonsense-mediated decay (NMD) factors, and miRNA silencing complex (AGO2, RISC, GW182 (Glycine-Tryptophan Protein of 182 kilodaltons)) (Li et al, 2013).

P-bodies are constitutively expressed in the cells; however, translational repression induced by specific stressors may increase the number of these types of RNP granules. The classification of RNAs and RNA-binding proteins to RNP granules in cells is regulated in different manners, depending on various sources of cellular stress. Interestingly, although SGs and P-bodies are distinct foci of RNP localization, they share certain RNA-binding proteins potentially because of the ability of SG and P-bodies to physically interact with each other (Kedersha et al, 2005). Thousands of different RNAs were found to be significantly enriched in P-bodies (Hubstenberger et al, 2017). MRNAs were found to be the most abundant type of RNA in this type of RNP granules, although some long non-coding RNAs and other types of non-coding RNAs were also identified. Interestingly, P-bodies contain less RNA than SGs, which is consistent with P-bodies being much smaller than SGs (Hubstenberger et al, 2017).

The involvement of P-bodies in ALS pathogenesis has yet to be determined. However, like SGs, many RBPs in P-bodies contain low complexity domains that have the potential to form irreversible aggregates within the cytoplasm. In addition, the presence of ALS-associated RBPs such as TDP-43 and FUS in P-bodies has been reported (Volkening et al, 2009).

1.3.2.4 Paraspeckles

Paraspeckles are RNP granules located in the nucleus. To date, more than 40 RBPs have been identified to be present in paraspeckles; however, only seven of them are essential for paraspeckle formation. Essential RBPs for paraspeckle formation include SFPQ, non-POU domain-containing octamer-binding protein (NONO or P54nrb), heterogeneous nuclear ribonucleoprotein K (HNRNPK), FUS, Switch/Sucrose Non-Fermentable (SWI/SNF) chromatin remodeling complexes, RNA Binding Motif Protein 14 (RBM14), DAZ-associated protein 1, and heterogeneous nuclear ribonucleoprotein H3 (HNRNPH3) (Pisani & Baron, 2019). Besides these RBPs, paraspeckles are composed of the lncRNA Nuclear Enriched Abundant Transcript 1 (*NEATI*). *NEATI* acts as a scaffold for paraspeckle formation. This lncRNA has two transcript variants, *NEATI_1* and *NEATI_2*, with different sizes that both are present in the nuclear paraspeckles. *NEATI_2* is the longer and essential transcript for paraspeckle formation and regulation, while the function of *NEATI_1* in paraspeckles has remained unclear (Bond & Fox, 2009).

Previously, nuclear paraspeckles were considered non-essential because *NEATI* knock-out mice seemed to be healthy (Nakagawa et al, 2011). However, later studies have identified multiple functions for paraspeckles, including gene regulation through nuclear retention of RNAs and proteins, and miRNA formation (Fox & Lamond, 2010). Retention of specific RNAs in the nucleus by paraspeckles can help the cells to translate those RNAs only under specific conditions such as stress. Paraspeckles also sequester several nuclear proteins to modulate their functions, although, this sequestration does not always result in loss of function (Prasanth et al, 2005). In fact, the sequestered proteins preserve the ability to interact with promoter regions and influence gene expression (Prasanth et al, 2005). The other function that has been reported for paraspeckles is involvement in miRNA biogenesis. Under specific conditions, DiGeorge syndrome chromosomal region 8 (DGCR8), which is a subunit of the microprocessor complex involved in miRNA biogenesis, is localized into paraspeckles (Shiohama et al, 2007). It is found that about

two-thirds of the pri-miRNAs expressed in HeLa cells bound to both NONO and PSF (Jiang et al, 2017). Moreover, *NEATI* can facilitate the interaction between the microprocessor and miRNA through the formation of hairpin loops. This evidence might indicate the influence of paraspeckles in miRNA biogenesis (Krol, 2017).

The exact role of paraspeckle structures in both normal and diseases condition is unknown. However, several studies have examined the participation of paraspeckles in various pathologies such as cancer, viral infection, and neurodegenerative disease. Studies demonstrate the overexpression of *NEATI* in several cancers including non-small lung cancer (Jen et al, 2017; Sun et al, 2017), hepatocellular carcinoma (Fang et al, 2017), ovarian cancer (Chen et al, 2016b; Ding et al, 2017), breast cancer (Ke et al, 2016; Lo et al, 2016), and prostate cancer (Li et al, 2018c; Xiong et al, 2018), to name but a few. In viral infection sequestration of SFPQ, a repressor of IL-8, in paraspeckles by *NEATI* results in the transcription of IL-8 and immune response stimulation (Hirose et al, 2014).

The contribution of paraspeckles to neurodegenerative diseases has been discussed in numerous studies. For instance, one study showed the overexpression of *NEATI* in post-mortem brains of Huntington's disease patients (Sunwoo et al, 2017). Studies have also reported the overexpression of *NEATI* in models of Parkinson's disease (PD) (Liu & Lu, 2018; Pickrell & Youle, 2015). The upregulation of *NEATI* has also been reported in the serum of patients with multiple sclerosis (MS) (Santoro et al, 2016).

The role of paraspeckles in the pathology of ALS has been of recent interest. Seven of the 40 RBPs involved in paraspeckle formation and function are encoded by genes mutated in familial forms of ALS, including *TARDBP* and *FUS* (Hennig et al, 2015). ALS patients with *FUS* mutation (ALS-FUS) showed hyper-assembly of paraspeckles in their spinal neurons (An et al, 2019). In addition, ALS-FUS patients have been shown to have a pathological accumulation of NONO in their spinal cord neurons. This evidence is in line with the observation of NONO aggregation in cellular and mouse models of ALS-FUS (Shelkovnikova et al, 2014).

Interestingly, RNA-FISH using DIG-labeled *NEATI_2* probe in the motor neuron of ALS and control patients showed that *NEATI_2*, which is an essential component for paraspeckle formation, is not normally expressed in most motor neurons of control patients. However, it is

expressed in the early stages of ALS neurodegeneration and induces paraspeckles formation in the motor neurons of ALS patients (Nishimoto et al, 2013). Whereas, FUS is one of the essential components of paraspeckles, the loss of FUS from the nucleus can alter the stability of paraspeckles by mis-regulating *NEAT1* steady-state levels or even loss of paraspeckles, which might impact the cell response to the stress (Shelkovernikova et al, 2014). It is also shown in a mouse model of FUSopathy, the mis-localized FUS sequestered other essential paraspeckle proteins into NCIs. ALS-related mutation in FUS also results in colocalization of FUS and other essential paraspeckle proteins into cytoplasmic protein inclusions in cultured cells. Therefore, pathological FUS mutations might affect paraspeckle function in ALS. Despite these findings, the physiological significance of the formation of paraspeckles during ALS pathogenesis remains to be elucidated (Shelkovernikova et al, 2014).

1.4 Relevance to the current study

Despite considerable research efforts, the biological basis of ALS has remained unclear. Several studies have revealed the role of cellular stress in the pathogenesis of ALS. Eukaryotic cells use a variety of strategies to preserve themselves against a barrage of cellular stresses, such as chemical exposures, oxidative stress, heat shock, and even aging. Under stress, the top priority of cells is survival and recovery; therefore, they conserve resources through limiting translation and producing just the essential proteins required for survival (Lindquist, 1981). Stressed cells keep non-translating mRNAs and their associated RBPs in RNP granules such as SGs and P-bodies (Anderson & Kedersha, 2008). Interestingly, many RBPs associated with ALS, such as FUS and TDP-43, colocalize with several SG markers in cultured cells and primary neurons under stress. Moreover, colocalization of cytoplasmic inclusion of FUS and TDP-43 with SGs marker has been observed in post-mortem samples from ALS and FTD patients (Liu-Yesucevitz et al, 2010a; Wolozin, 2012b). Therefore, it is suggested that cytoplasmic localization of ALS-associated RBPs to SGs could serve as a critical pathway for ALS.

The study of transcriptome of RNP granules has shown that, besides RBPs, non-translating mRNAs and some non-coding RNAs are present in RNP granules (Tian et al, 2020). Thus, the study of the RNA component of RNP granules might help to better understand the role of cellular stress and RNP granules in ALS pathogenesis. In addition, massive dysregulation in the expression of coding and non-coding RNAs has been reported in ALS. Therefore, the study of the presence of these dysregulated RNAs in RNP granules or their participation in RNP granule formation and function might shed further light on the pathogenesis of ALS.

Non-coding RNAs have been recognized to be abundantly expressed in the mammalian central nervous system and to play important roles in neurodegenerative disorders (ABDULLA & CAMPBELL, 1997). CircRNAs are covalently closed lncRNAs whose participation in neurodegeneration has been started to be elucidated. Eukaryotic circRNAs have been shown to have dynamic expression patterns in various physiological conditions and developmental stages. CircRNAs potentially can regulate the cellular response to stress through various mechanisms. For example, circRNAs can regulate the function of miRNAs involved in hemostasis and stress pathways (Fischer & Leung, 2017). Interestingly, the study of circRNAs expression profile in *Arabidopsis* in response to heat stress showed a massive alteration in the expression of

circRNAs, the number of circularized exons, and alternative circularization events (Pan et al, 2018). A study of circRNAs in Parkinson's disease showed that one dysregulated circRNA in this disease, named circSLC8A, potentially has a role in oxidative stress-related Parkinsonism (Hanan et al, 2020).

Previously, whole transcriptome RNA-seq (Illumina) of libraries prepared from ribosome-depleted RNA from human spinal cord tissues was performed in our lab to investigate the alteration of circRNAs in sporadic ALS patients compared to matched controls (Campos-Melo, data not shown). In-silico analysis indicated that 25.7% of circRNAs were dysregulated in sALS patients compared to controls. Further bioinformatic analysis of these dysregulated circRNAs using CircInteractome revealed that some of the highly dysregulated circRNAs potentially have interactions with important RBPs involved in the RNA metabolism and in ALS pathogenesis. As the involvement of cytoskeletal defects in neurodegenerative disorders is becoming increasingly evident, I selected a group of candidate circRNAs encoded in genes of cytoskeletal proteins vimentin, annexin A1, and Dynamin.

Vimentin is a developmental IF protein that is broadly expressed in embryos and is often later replaced by the other major classes of IFs in cells during differentiation. Vascular endothelial cells and certain subpopulations of glial cells are the only cells in the healthy adult brain that still express vimentin. However, it has been reported that vimentin is re-expressed in both protoplasmic and fibrous astrocytes in the brain of Alzheimer's disease patients (Levin et al, 2009). Annexin A1 and dynamin 1 are cytoskeletal proteins that directly interact with actin which has been implicated in motor neuron degeneration in ALS (Alkam et al, 2017; D'Ambrosi et al, 2014; Gu et al, 2010; Hayes et al, 2004; Hensel & Claus, 2018; McGough et al, 1994). As some circRNAs regulate the expression and splicing of their linear cognate transcripts, studying the relationship between them could shed further light on the pathogenesis of neurodegeneration (Conn et al, 2017).

In this study, I examined the subcellular localization of a group of dysregulated circRNAs in ALS including hsa_circVIM_011 and hsa_circVIM_005 (encoded by *VIM* gene), hsa_circANXA1_001 (encoded by *ANXA1* gene), and hsa_circDNM1_004 (encoded by *DNM1* gene) in HEK293T cells in response to stress. I also examined the subcellular localization of

CDR1as, as a highly expressed circRNA in the mammalian nervous system, in stressed HEK293T cells.

1.5 Hypothesis

Considering the preceding evidence, the hypothesis underlying this thesis is that:

“Cellular stress affects the subcellular localization of circRNAs dysregulated in ALS”

1.6 Specific aims

Aim 1: To analyze the expression level of circRNAs in spinal cord tissue of ALS patients.

Aim 2: To study the expression and subcellular localization of candidate circRNAs under cellular stress in vitro.

Sub-aim 2.1: To compare the expression of circRNAs using FISH in HEK293T cells under stress and baseline condition.

Sub-aim 2.2: To study the subcellular localization of candidate circRNAs using FISH/IF under cellular stress in vitro.

Chapter 2

2 Procedures and methodology

2.1 circRNAs selection

Previously in our lab, Dr. Danae Campos-Melo, a research associate in the lab, had evaluated the expression levels of circRNAs within ALS (n=6) and control (neurologically and neuropathologically normal; n = 4) lumbar spinal cord using whole transcriptome RNA-seq (Illumina) of libraries prepared from ribosome-depleted RNA. Using Partek Flow software, a pool of differentially expressed circRNAs was identified (data not showed). Among the top 100 dysregulated circRNAs in ALS according to RNA-seq data, I selected a group of 4 circRNAs that showed a dysregulation in ALS ≥ 2.5 fold and whose host genes encoded for the cytoskeletal proteins: vimentin, annexin A1, and dynamin 1. Next, I used the CircInteractome database (circInteractome) to retrieve mature circRNA sequences and map RBP binding sites on the selected circRNAs. All these circRNAs are exonic and including multiple exons. Interestingly, all the candidate circRNAs which are expressed from cytoskeletal genes are multiple exonic and have multiple isoforms. Figure 2-1 shows all the circRNAs that are expressed from *VIM* gene as an example. Further *in silico* analysis using CircInteractome for the candidate circRNAs indicated that they potentially have multiple binding sites for the RBPs that are known to be involved in varying aspects of RNA metabolism within RNP granules. I also used Circbank database (circbank) to rename candidate circRNAs based on their host genes. Characteristics of selected circRNAs are shown in Table 2-1.

Table 2-1: List of candidate circRNAs.

CircBase Id	CircBank Id	Strand	Position	Length	Gene Symbol
hsa_circ_0001946	CDR1as	-	chrX:139865340 139866824	1485	CDR1
hsa_circ_0017869	hsa_circVIM_005	+	chr10:17271274-17279592	1870	VIM
hsa_circ_0017872	hsa_circVIM_011	+	chr10:17275585-17278378	735	VIM
hsa_circ_0087210	hsa_circANXA1_001	+	chr9:75772569-7578247	1743	ANXA1
hsa_circ_0138049	hsa_circDNM1_004	+	chr9:130982266-130996386	833	DNM1

2.2 Primer design

Because the candidate circRNAs for this study are multiple exonic, they have sequence overlap with their linear RNA counterpart. There is thus a chance of linear RNA amplification when undertaking PCR reactions for circRNAs. To solve this problem, three different strategies have been suggested to date. The first strategy is to digest linear RNAs using the RNase R enzyme (discussed in more detail later in section 2.3). The remaining two strategies employ divergent primers that either flank the back-splice junction (BSJ) or primers that bind to the BSJ, which is the unique sequence element of circRNAs. Divergent primers are “tail-to-tail”-oriented compared with the “convergent primers,” which are “head-to-head”-oriented. Of note, if “convergent primers” are located within circRNA-producing exons, they would detect both circular and linear RNAs (Figure 2-2).

In the present study, I took advantage of all three strategies by designing divergent primers (Table 2-2) that bind to the BSJ of candidate circRNAs and by applying reverse-transcription and qPCR reaction on RNase R treated RNA samples.

In order to check whether or not the primer pairs designed for circRNAs were unique, the specificity of primers was checked in the NCBI primer blast (NCBI). Using the NCBI primer blast, I did not observe any known sequences that would be detected by my primer sets. Also, to minimize potential dimerization and secondary structures of primers, I evaluated primer sets using the OligoAnalyzer tool (Integrated DNA Technologies, IDTDNA) (IDTDNA). The OligoAnalyzer tool is an analytical tool for determining the oligo sequences’ properties including length, GC content, and the Gibbs free energy (ΔG) values. ΔG values indicate the strength of the secondary structures such as dimers and hairpins. I checked ΔG values of self and hetero dimers as well as hairpins for every primer set; all were within the recommended range (for example IDTDNA recommends ΔG value be more than -9 for self and heterodimers).

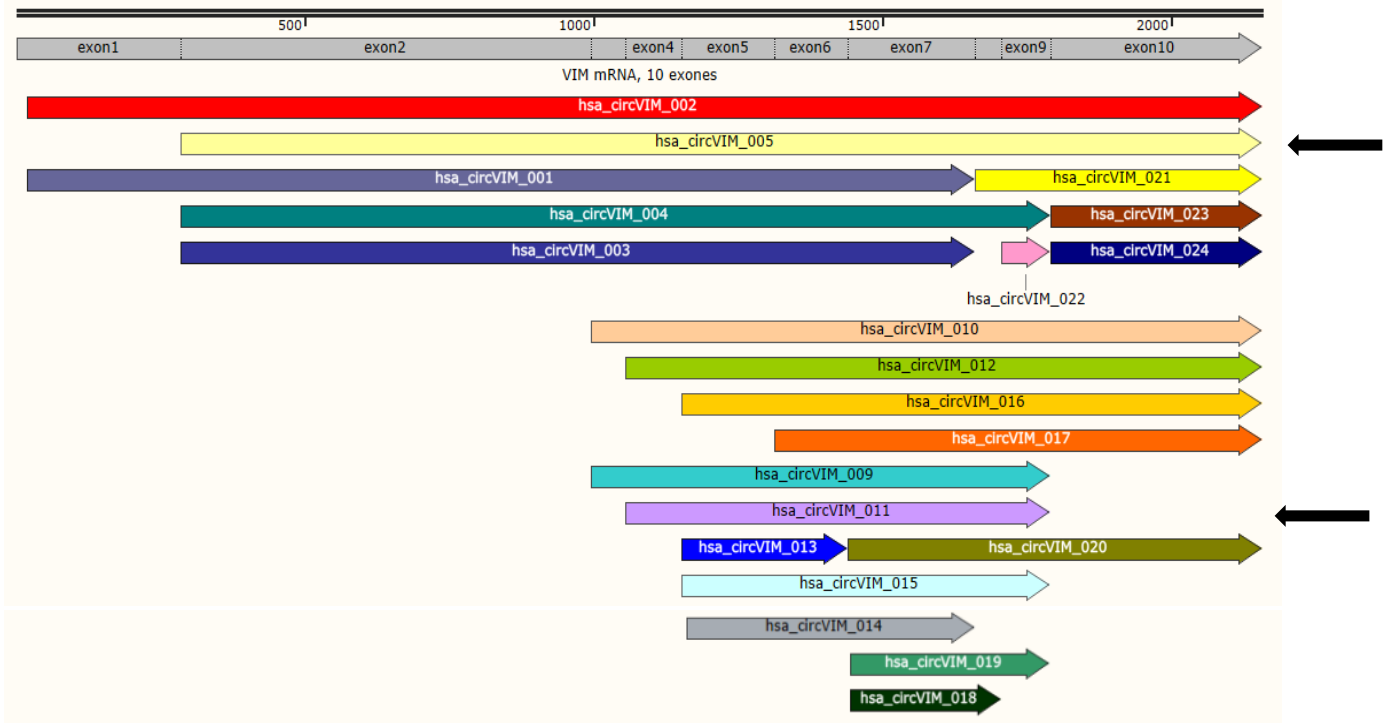


Figure 2-1: CircRNAs annotated from *VIM* gene. There are 24 circRNAs that have been annotated to be expressed from *VIM* gene. All this circRNAs are exonic including single and multiple exons. Black arrows show the candidate circRNAs, hsa_circVIM_005 and hsa_circVIM_011, which are including 9 (exon 2-10) and 5 (exon 4-8) exons, respectively.

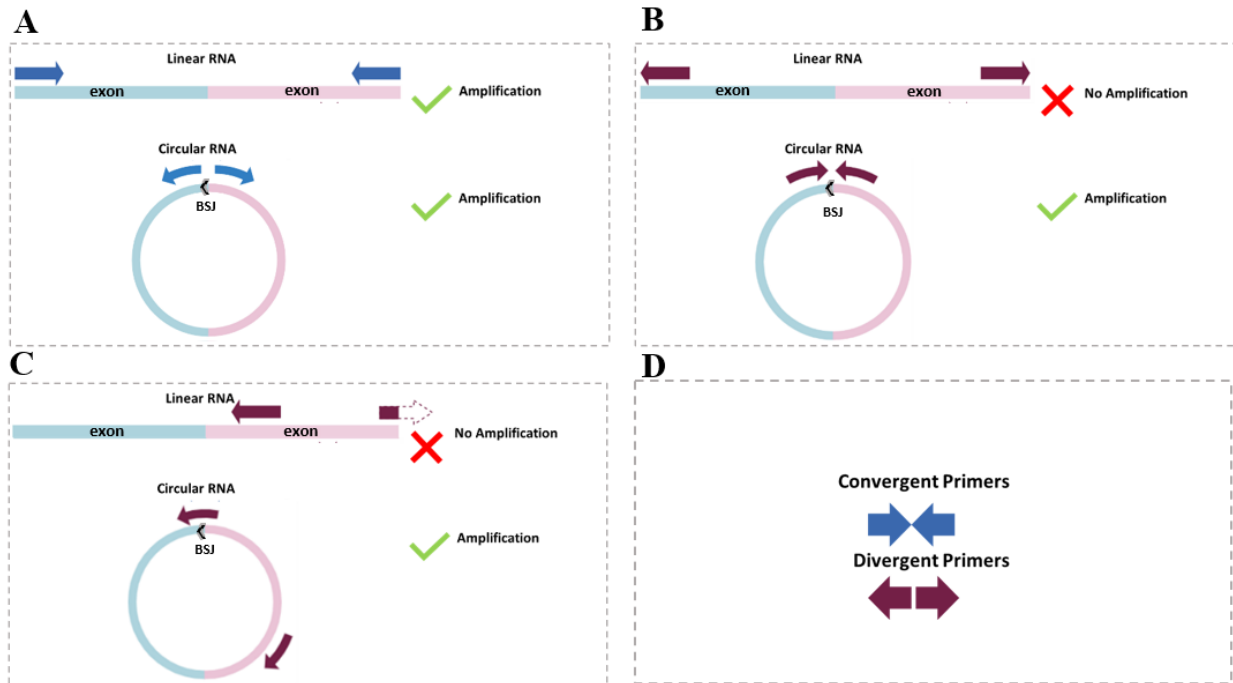


Figure 2-2: Schematic of the design of convergent and divergent primers. A) Convergent primers are able to amplify both linear RNA and circRNAs. B) Divergent primers are only able to amplify circRNAs. C) Divergent primers detecting BSJ are only able to amplify circRNAs. D) Convergent primers are shown as blue arrows and divergent primers are shown as purple arrows.

Table 2-2: Oligonucleotides for real-time PCR amplification.

Oligonucleotide	Sequence 5' to 3'	Amplicon size
CDR1as forward primer	AACTACCCAGTCTCCATCAACTGGCT	158 bp
CDR1as reverse primer	TCGCTGGAAGACCCGGAGTTGTTG	
hsa_circVIM_005 forward primer	AATCTTTGGAAAACTCTCCTCTGCCACTCTC	168 bp
hsa_circVIM_005 reverse primer	GCGGTAGGAGGACGAGGACACGGAC	
hsa_circVIM_011 forward primer	GAAACTAGAGATGGACAGGATGTTGAC	123 bp
hsa_circVIM_011 reverse primer	CTGGATTCCTCTTCGTGGAGTTTC	
hsa_circANXA1_001 forward primer	CATGAACAAAGTTCTGGACCTGGAG	124 bp
hsa_circANXA1_001 reverse primer	TTTTTCATGGCTTGATGAAGCTTCTC	
hsa_circDNM1_004 forward primer	GCACTAAGGAGCAGGCCAGCGCAC	127 bp
hsa_circDNM1_004 reverse primer	CACTCCAATGTAGCCTCTGCGCAGG	
TBP forward primer	TGTGTCCACGGTGAATCTTG	182 bp
TBP reverse primer	GTTCTCGCTTTTTGCTCCT	

2.3 RNA extraction and RNase R exonuclease assay

In order to minimize the amount of linear RNAs, I performed an RNase R exonuclease digest on all RNA samples. This enriches the ratio of circRNAs to total RNA in the samples which increases the chance of detection by primers designed for circRNAs. To optimize the RNase R exonuclease digest, I used RNA samples derived from HEK 293T cells. Total RNA from HEK293T cells was purified using TRIzol™ reagent (Life Technologies Inc., Ambion, Carlsbad, CA, USA). To do this, cells were washed gently with cold 1X PBS then were lysed by adding 400µl of TRIzol™ reagent and incubating for 5 minutes on ice. Next, 80µl of chloroform (ThermoFisher Scientific) was added to the lysate, gently mixed, and incubated for 2 minutes at room temperature and centrifuged for 15 minutes at 12,000g, 4°C. The aqueous phase was transferred into a fresh tube, RNA was precipitated by adding 200µl of isopropanol, incubating

for 10 minutes at room temperature, and centrifuging for 10 minutes at 12,000g, 4°C. 400µl 75% ethanol was used for washing the pelleted RNA and after centrifuging for 5 minutes at 7,500g, 4°C the RNA pellet was air dried. Finally, the pellet was resuspended in 20µl UltraPure RNase-free distilled water (Invitrogen, ThermoFisher Scientific) and incubated for 15 minutes at 60°C. RNA concentration and purity were measured using spectrophotometry (Nanodrop, ThermoFisher Scientific, Burlington, ON, Canada). To determine the optimal conditions for digestion of linear RNA with RNase R, I used different units of RNase R (from 2 to 20 units). The digestion of linear RNAs were optimized using 15 unit of RNase R. Based on this optimization, I performed RNase R digestion by incubating 3-5 µg of RNA from cells or previously extracted RNA from human lumbar spinal cord tissue with 15 U of RNase R (Epicentre Biotechnologies) at 37°C for 30 minutes (Suzuki et al, 2006). RNase R- treated RNA was subsequently column purified using the RNeasy Mini Kit (Qiagen Cat. # 74106).

2.4 Reverse-transcription and real-time PCR

Real-time PCR was conducted using the same ALS and control spinal cord RNA samples that were used for the original RNA-seq performed on human lumbar spinal cord tissue by Dr. Danae Campos-Melo. Reverse-transcription and real-time PCR had been standardized in RNase R-treated RNA samples from HEK293T cells. In summary, 2 µg of RNase R- treated RNA from each sample was treated with DNase I (Amplification grade, ThermoFisher scientist) for 15 minutes at room temperature to digest genomic DNA pulled down in the RNA purification. The reaction was ended by adding Ethylenediaminetetraacetic acid (EDTA) (Thermo Fisher Scientific) and incubating at 65°C for 10 minutes. The concentration of RNA samples then was quantified using spectrophotometry (Nanodrop, ThermoFisher Scientific, Burlington, ON, Canada) and 0.5 µg of each RNA sample was used for cDNA synthesis. Reverse transcription was performed using SuperScript VILO (Invitrogen) incubating at 25°C for 10 minutes, following by 42°C for 120 minutes, and 80°C for 15 minutes in a total volume of 20 µl. The product of reverse transcription was used immediately or stored at -80°C.

Each real-time PCR reaction contained 0.5 µl of cDNA, 1 µM of each primer set, and 5 µl PowerUp SYBR Green PCR master mix (Thermo Fisher Scientific), in a total volume for each reaction of 10 µl. All real-time PCR assays were carried out using only three technical replicates for each sample because of the limitation in amount of RNA samples from control patients.

Relative quantification of gene transcription was performed using TBP (TATA box binding protein) as the reference gene. Real-time PCR was performed on a ViiA7 real-time PCR machine (Applied Biosystems).

2.5 Data analysis of real-time PCR data

In order to examine the relative expression of circRNAs using data that was produced by real-time PCR, I took advantage of the $2^{-\Delta\Delta Ct}$ method (Livak & Schmittgen, 2001). The Ct (cycle threshold) is the number of cycles required for the fluorescent signal to exceeds background level (threshold). In a real-time PCR assay, a positive reaction is detected by accumulation of a fluorescent signal. QPCR was performed in triplicate for each sample, so I averaged three Cts per sample to obtain a Ct mean. Then to normalized gene expression to the reference gene, which is TBP in this study, I calculated delta Ct (ΔCt) for each sample by using the following formula:

$$\Delta Ct = Ct \text{ mean (circRNA)} - Ct \text{ mean (TBP)} \quad (2-1)$$

In order to then calculate relative gene expression, I averaged the ΔCt values of the control group to create a control ΔCt which is named ΔCt (control average)

The $\Delta\Delta Ct$ values for each sample were then calculated as:

$$\Delta\Delta Ct = \Delta Ct \text{ (ALS)} - \Delta Ct \text{ (control average)} \quad (2-2)$$

Finally, to examine the fold gene expression, I calculated 2 to the power of negative $\Delta\Delta Ct$. The formula for this is as follows:

$$\text{Fold change expression} = 2^{-\Delta\Delta Ct} \quad (2-3)$$

I have used this process for determining fold change expression for every circRNA of interest for each ALS case. In order to determine the significance of any observed differences, I checked the normality of data by Shapiro-Wilk test, then an independent t-test or Mann–Whitney U test was applied using GraphPad Prism 9.0.0 (GraphPad Software, Inc., San Diego, CA, USA). Data are represented as mean fold change of ALS samples ($n=6$) \pm SEM. In these statistical tests the mean fold change values of ALS samples for every candidate circRNAs were compared to 1 as a mean fold change for control samples. A p-value \leq of 0.05 was considered statistically significant.

2.6 Cell culture and stress condition

Human embryonic kidney (HEK293T) cells were cultured at 37°C and 5% CO₂ in Dulbecco's modified eagle medium (DMEM; ThermoFisher) supplemented with 10% fetal bovine serum (FBS; ThermoFisher) and 0.5% penicillin-streptomycin antibiotic (ThermoFisher). 24 hours before each experiment 600,000 cells per well were seeded in a 6-well plate on a 22 x 22 mm coverslip coated with attachment factor (Cascade Biologics Attachment factor, Gibco). Then, cells were exposed to osmotic stress using 400 mM D-sorbitol for 4 hours (in DMEM with 10% FBS). Post stress, cells were washed once with 1X PBS and then fixed in a 4% paraformaldehyde-1X PBS solution for 10 minutes.

2.7 Expression and localization analyses with fluorescent *in situ* hybridization (FISH)

Fluorescent *in situ* hybridization (FISH) with tyramine signal amplification was used to characterize the expression pattern and localization of the circRNAs in stressed HEK293T cells compared with non-stressed cells. LNA double DIG-labeled 48-mers probes (Qiagen, USA) were designed to target the BSJ of circRNAs, which is the unique sequence element of circRNAs (Table 2-3).

Table 2-3: Oligonucleotides for fluorescence in situ hybridization.

Oligonucleotide	Sequence 5' to 3'	Hybridization temperature (°C)
CDR1as	GAAACTAGAGATGGACAGGATGTTGAC	62
hsa_circVIM_005	AATCTTTGGAAAACTCTCCTGCCACTCTC	62
hsa_circVIM_011	GAAACTAGAGATGGACAGGATGTTGAC	62
hsa_circANXA1_001	CATGAACAAAGTTCTGGACCTGGAG	62
hsa_circDNM1_004	GCACTAAGGAGCAGGCCAGCGCAC	62

In summary, fixed cells were permeabilized using 0.2% Triton X-100 in 1X PBS solution for 10 minutes. Then, cells were incubated with pre-hybridization buffer (3% BSA in 4X SSC) in a humid chamber for 20 minutes at 22–25 °C below the predicted T_m value of each LNA oligonucleotide probe (hybridization temperature, T_H). Probes were denatured at 90 °C for 5 minutes and quickly moved to ice before they were diluted with pre-warmed hybridization buffer (20X SSC, 25% dextran sulfate, and DEPC-treated water). Coverslips were then incubated in 100-300 μ l of the diluted probe and hybridized for 1 hour at T_H . After hybridization, coverslips were washed three times, for five minutes each, in washing buffer I (20X SSC, 0.1% Tween-20 and DEPC-treated water) with agitation at 5 °C higher than T_H . Then, three washes were done in washing buffer II and buffer III (20X SSC, DEPC-treated water) for 5 minutes each at T_H . and one wash with 1X PBS for 5 minutes at room temperature. Coverslips were then incubated with freshly made hydrogen peroxide solution (3% (vol/vol) H₂O₂/1× PBS) for 20 minutes at room temperature to quench endogenous peroxidase activity before applying HRP-conjugated antibodies. Following three washes with TN buffer (1 M Tris-HCl pH 7.5, 1.5 M NaCl in DEPC-treated water), coverslips were incubated in TNB blocking buffer (0.5% (wt/vol) blocking reagent /TN buffer) for 30 minutes at room temperature. Anti-DIG/HRP secondary antibody (Roche, Indianapolis, IN, USA) diluted 1:100 in blocking solution was applied on cells for 30 minutes at room temperature. Cells were then washed three times with TNT buffer (0.5% (vol/vol) Triton X-100) /TN buffer) and incubated with Tyramide Signal Amplification tagged with a Cyanine 3 fluorophore (TSA Cy3; 1:50, PerkinElmer, Waltham, MA, USA) for 10 minutes at room temperature. Coverslips were then washed three times for 5 minutes each with TNT buffer and one time with 1X PBS. Nuclear staining was performed using 4',6-diamidino-2-phenylindole (DAPI, Abcam, #ab228549). DAPI staining solution (0.05 mM DAPI solution in 0.2% BSA/1×PBS) was used on coverslips for 5 minutes, and coverslips were then washed three times (5 minutes each) with 1X PBS and left to dry overnight. Coverslips were mounted to frosted glass microscope slides using fluorescent mounting media (Dako Canada Inc., Burlington, Ontario). All the steps after adding TSA Cy3 were performed in the dark.

2.8 Immunofluorescence

In order to observe whether circRNAs colocalize with RNP granule markers under stress, immunofluorescence was performed following FISH and before nuclear staining. Coverslips

were incubated with the blocking solution (4% BSA in 1X PBS; Fisher Scientific Company, Ottawa, Ontario) for 1 hour at room temperature to reduce non-specific antibody interactions. Each primary antibody was diluted in BSA solution (2% BSA in 1X PBS), at the titers specified in Table 2-4 and coverslips were incubated overnight at 4°C. Coverslips were then washed three times with 1X PBS and incubated for 1 hour at room temperature with secondary AlexaFluor antibodies (Life Technologies) diluted in BSA solution (2% BSA in 1X PBS), as specified in Table 2-5. Nuclear staining and mounting were performed as described in the previous section.

Table 2-4: List of primary antibodies used in this study.

Antibody target	Species	Dilution	Company (catalog #)
TIA-1	Goat	1:100	Santa Cruz (sc-1751)
Dcp-1	Mouse	1:250	Abnova (H00055802-A01)
Staufen	Rabbit	1:250	Millipore (AB5781MI)
Pspc1	Mouse	1:250	Sigma (SAB4200503)
	Rabbit	1:250	Abcam (ab10421238)
NONO	Mouse	1:250	BD Biosciences (611279)
FUS	Rabbit	1:250	Protein Tech (11570-1-AP)
TDP-43	Mouse	1:250	Protein Tech (60019-2-Ig)

Table 2-5: List of secondary antibodies used in this study.

Antibody target	Species	Dilution	Catalog # from Life Technologies
anti-goat Alexa 488	Donkey	1:1000	A-11055
anti-rabbit Alexa 488	Goat	1:1000	A-11008
anti-mouse Alexa 488	Goat	1:1000	A-11029
anti-goat Alexa 555	Donkey	1:1000	A-21432
anti-mouse Alexa 555	Rabbit	1:1000	A-27028
anti-rabbit Alexa 555	Goat	1:1000	A-27039

2.9 Confocal microscopy and image processing

Following FISH and IF, stressed and non-stressed cells were imaged using a laser scanning multi-photon confocal microscope (Leica TSC SP8, Germany) with a 63×/1.40 oil objective. Images were acquired using 488 nm (green channel) and 552 nm (red channel) laser lines for markers of RNP granules and circRNAs, respectively. The DAPI-stained nucleus was visualized using a 405 nm (blue channel) laser line.

I also acquired sequential z-sections of stained samples and used these to reconstruct a three-dimensional (3-D) image volume on which overlapping regions were determined by colocalization visualized by LASX (Leica Application Suite X (LAS X) and quantified by Imaris (Bitplane, Inc., Zürich, Switzerland) software.

Before performing quantification of colocalization, a threshold for brightness intensity was defined for every channel in the images. In digital image processing, thresholding is a type of image segmentation that separates object pixels from background pixels to make the image easier to analyze. The threshold in this system is the minimum intensity of the color channel that will be calculated for the colocalization quantification. This adjustment of brightness intensity threshold is required for colocalization analysis to identify positive pixels that are relatively unaffected by the method of image acquisition and fluorophore brightness, and the level of molecule expression.

In Imaris software, I first adjusted the threshold to identify the brightest 2% of pixels for each red and green channel to calculate circRNA and RNP granule marker colocalization statistics for the 3-D volume. For this, I used the strategy previously described by Hutcheon et al (Hutcheon et al, 2000) and also discussed in two other studies (Holmes et al, 2006; Hutcheon et al, 2004). In this method threshold is adjusted based on a fixed percentage of the brightest pixels in a channel. After adjusting thresholds for each channel, the colocalized pixels which are indicated in white was built for further quantifications. Colocalization quantification was acquired from 3-5 z-series images captured for the candidate circRNA and RNP granule markers.

2.10 Spot counting and analysis

The expression analysis of two circRNAs (hsa_circVIM_011 and hsa_circANXA1_001) whose transcripts were able to be detected as a single spot was performed by quantifying the number of circRNA spots per cell obtained from confocal microscope images. Other circRNAs showed signal accumulation (i.e., several spots located within small regions that could not be resolved by the microscope because of limitation in resolution) and for this reason they could not be quantified. For spot quantification, I automatically counted the number of fluorescent spots for an average of 20 cells per slide across six slides of both stressed and unstressed HEK293T cells using FIJI/ImageJ software, as previously described (Lee et al, 2016; Schindelin et al, 2012). The normality of data was checked by the Shapiro-Wilk test, then an independent t-test or Mann-Whitney U test was applied to assess the differences in the expression levels of circRNAs between stress and baseline condition (mean \pm SEM). All statistical analyses were performed by GraphPad Prism 9.0.0 (GraphPad Software, Inc., San Diego, CA, USA).

Chapter 3

3 Results

3.1 Experimental set 1 – Real-time PCR shows no significant differential expression of candidate circRNAs in the spinal cord tissue of ALS versus control patients

3.1.1 Introduction

In recent years, large-scale transcriptome sequencing has provided the opportunity of studying the potential alteration of coding and non-coding RNAs in various diseases including neurodegenerative disorders. Emerging evidence has implicated alterations of circRNAs expression in a wide range of complicated diseases including cancers and neurodegenerative disorders. Previously, the alteration of circRNAs in blood samples of sporadic ALS patients has been reported (Dolinar et al, 2019). Moreover, circRNAs expression was dysregulated in murine embryonic stem cell-derived motor neurons containing ALS-related mutations in FUS (Errichelli et al, 2017). Our lab had undertaken whole transcriptome RNA-seq of ribosome-depleted RNA from human lumbar spinal cord tissues and observed an alteration of circRNAs expression in sporadic ALS patients compared to matched controls (Campos-Melo, unpublished data). Using Partek Flow software a pool of differentially expressed circRNAs was identified. This data showed that 25.7% of circRNAs were dysregulated in in the human spinal cord of sALS patients versus control patients. Among the top 100 dysregulated circRNAs in ALS according to this RNA-seq data, I selected 4 circRNAs that were expressed from host genes encoding cytoskeletal proteins and were upregulated by ≥ 2.5 fold change. Then I used real-time PCR to examine the relative expression of candidate circRNAs in the same RNA sample group that was used for RNA-seq.

3.1.2 Results

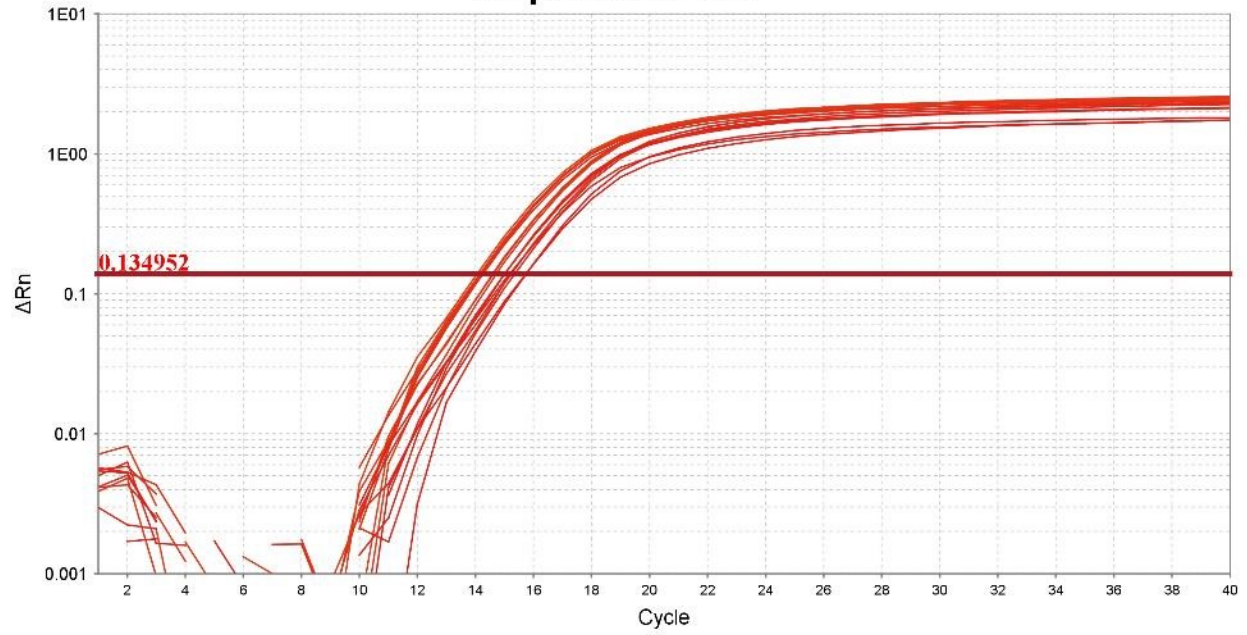
3.1.2.1 Real-time PCR showed no significant differences in the expression of candidate circRNAs between ALS and control patients' samples

As described, for the selective amplification of circRNAs I designed specific divergent primers detecting the BSJ of circRNAs and then treated RNA samples with the RNase R enzyme to decrease the amount of linear RNAs. Melting curve plots showed one single peak for every set of primers designed for circRNAs of interest except for circANXA1-001 (Figure 3-1). An analysis of the mature sequence of circANXA1-001 showed an A-rich sequence (ARS) in the BSJ, which made primer designing problematic. I used two different primer sets for the BSJ of circANXA1-001. Although optimization experiments using RNA samples from HEK293T cells showed normal amplification and melting curve plots (Figure 3-2), this result could not be reproduced in RNA samples from ALS and control patients.

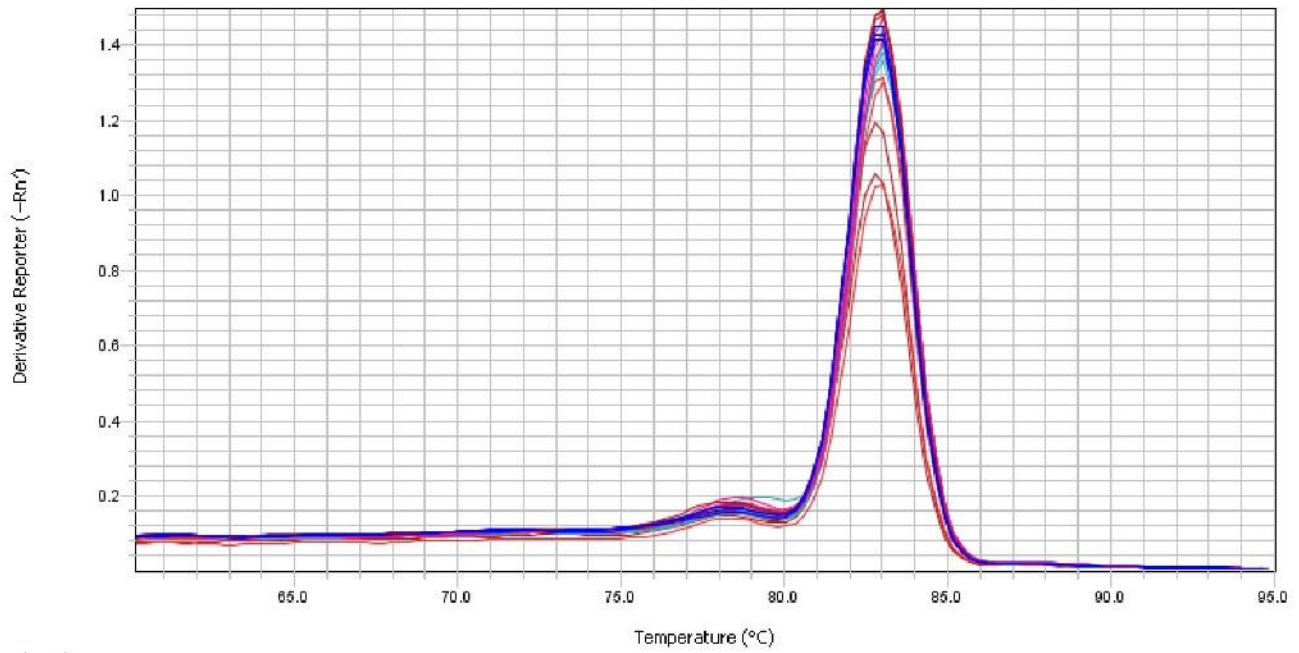
When I next analyzed the 10 μ l of the sample from qPCR on 1.5% agarose gel, I observed more than one band for circRNAs hsa_circDNM1_004 and hsa_circVIM_005 (Figure 3-3). Moreover, the qPCR sample from the primer set for hsa_circANXA1_001 did not yield any band on the agarose gel. It is possible that because of the difficulty in primers' design we could not detect this circRNA. Another possibility is that hsa_circANXA1_001 is present at very low levels in human spinal cord tissue samples. One approach that can be applied in future studies would be to increase the amount of cDNA per well in real-time PCR. However, due to limitations imposed by the current pandemic, this could not be carried out.

CDR1as

Amplification Plot

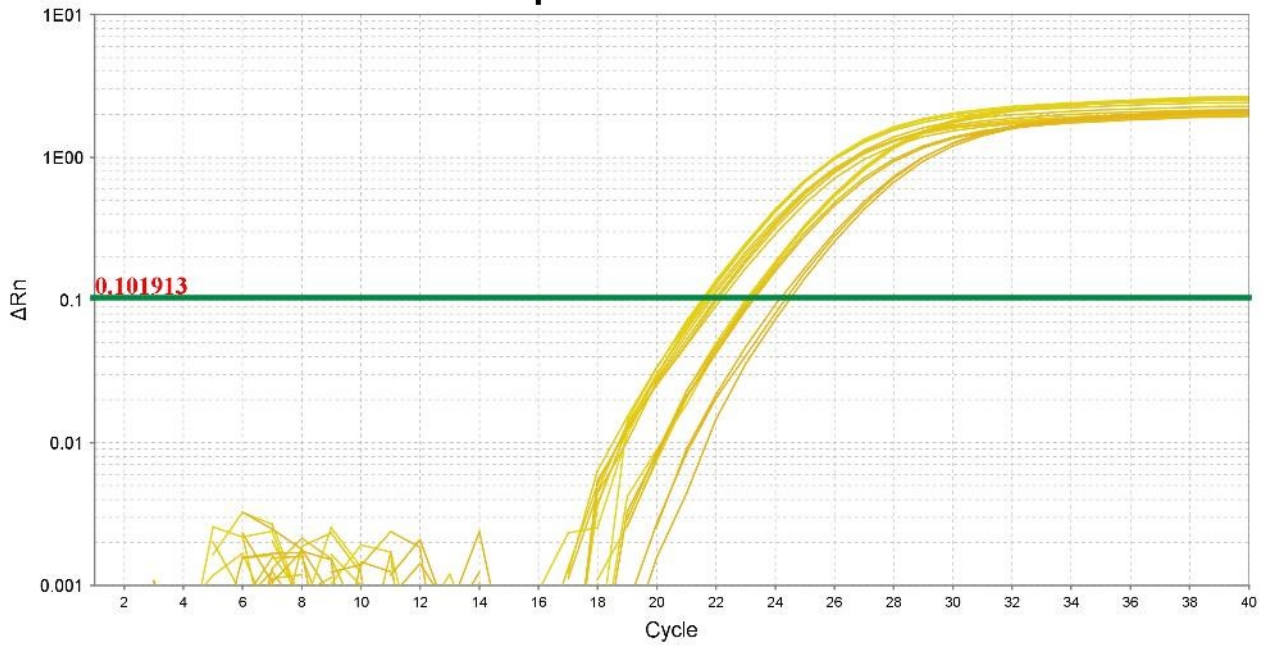


Melt Curve Plot

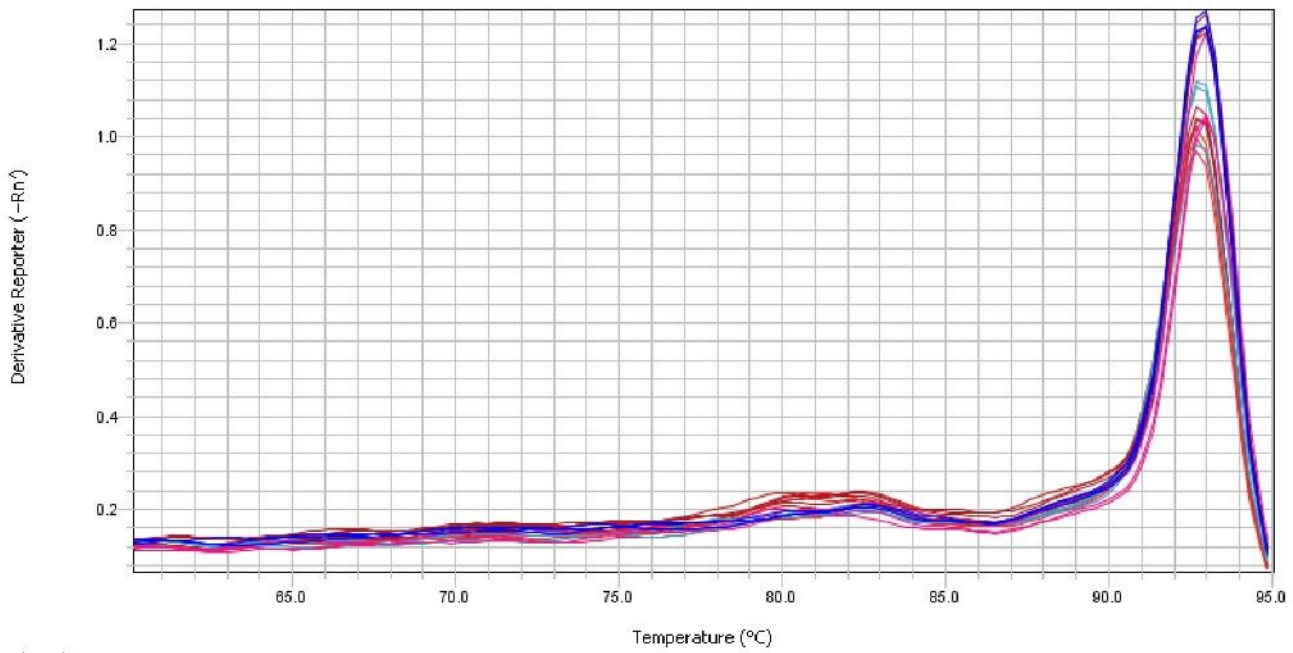


Hsa_circVIM_005

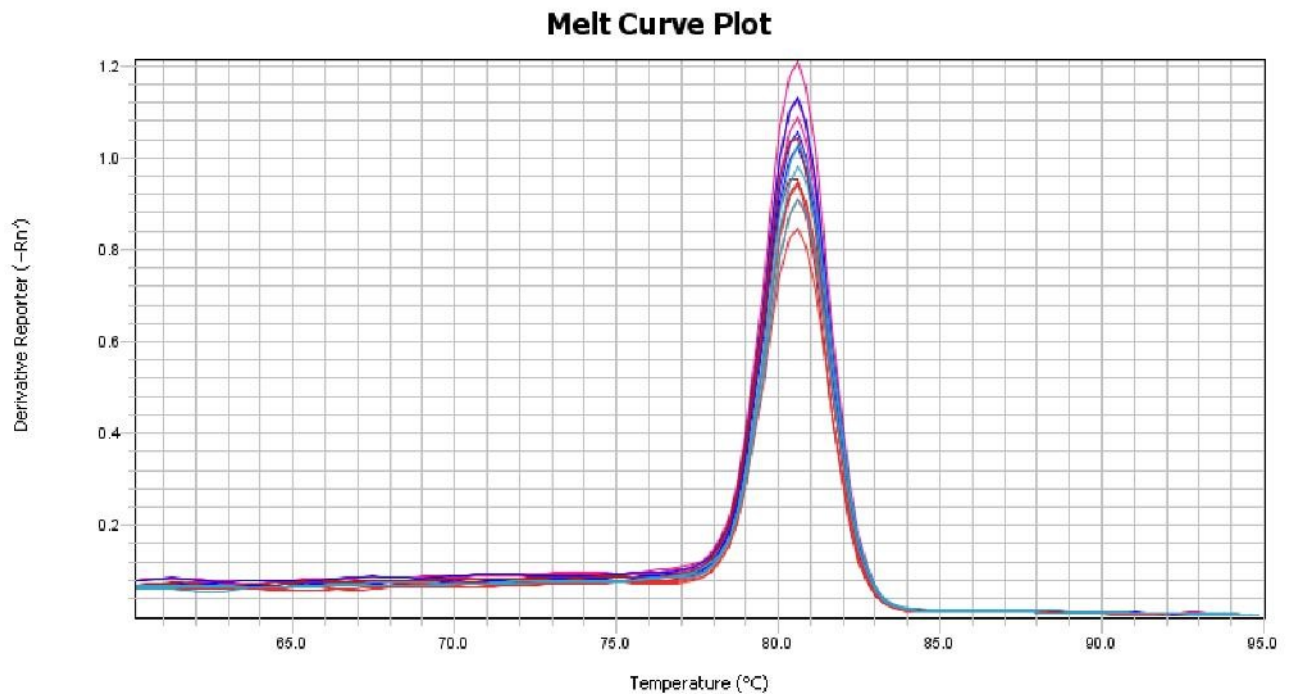
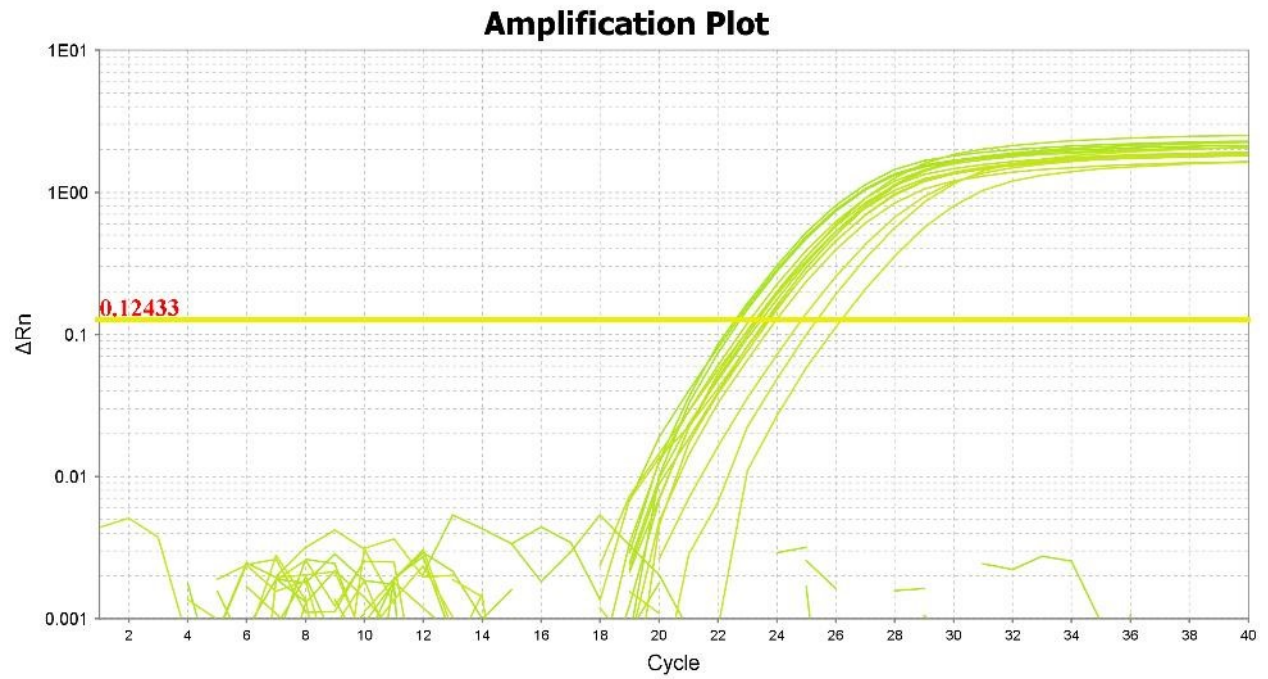
Amplification Plot



Melt Curve Plot

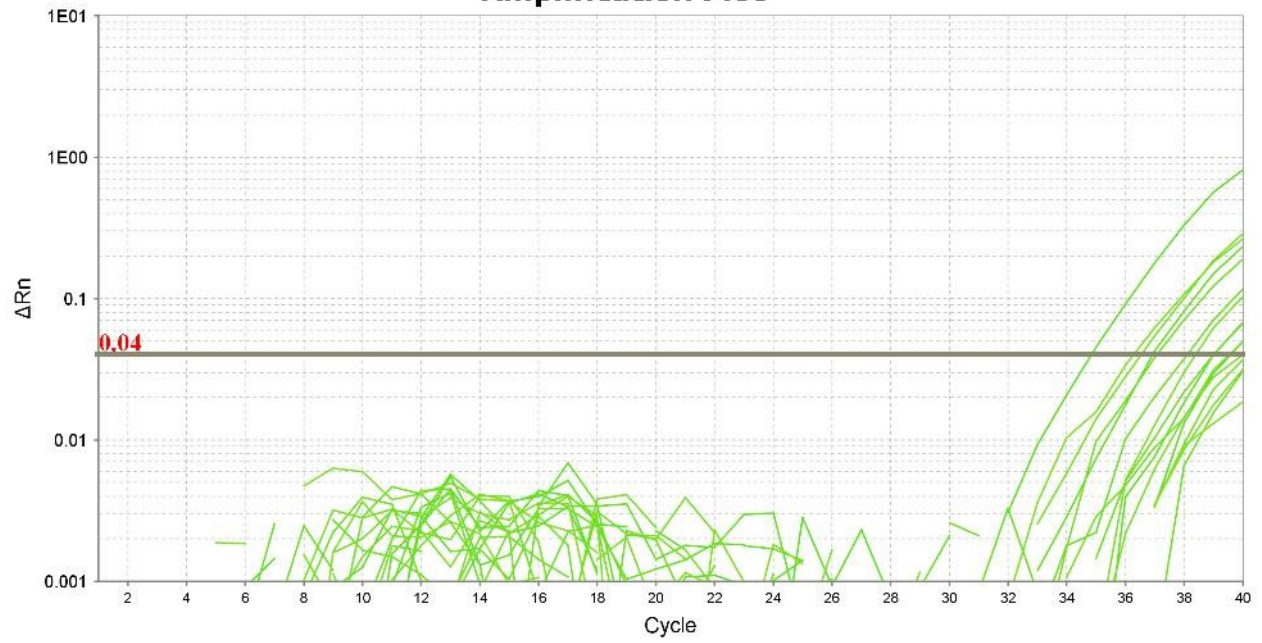


Hsa_circVIM_011

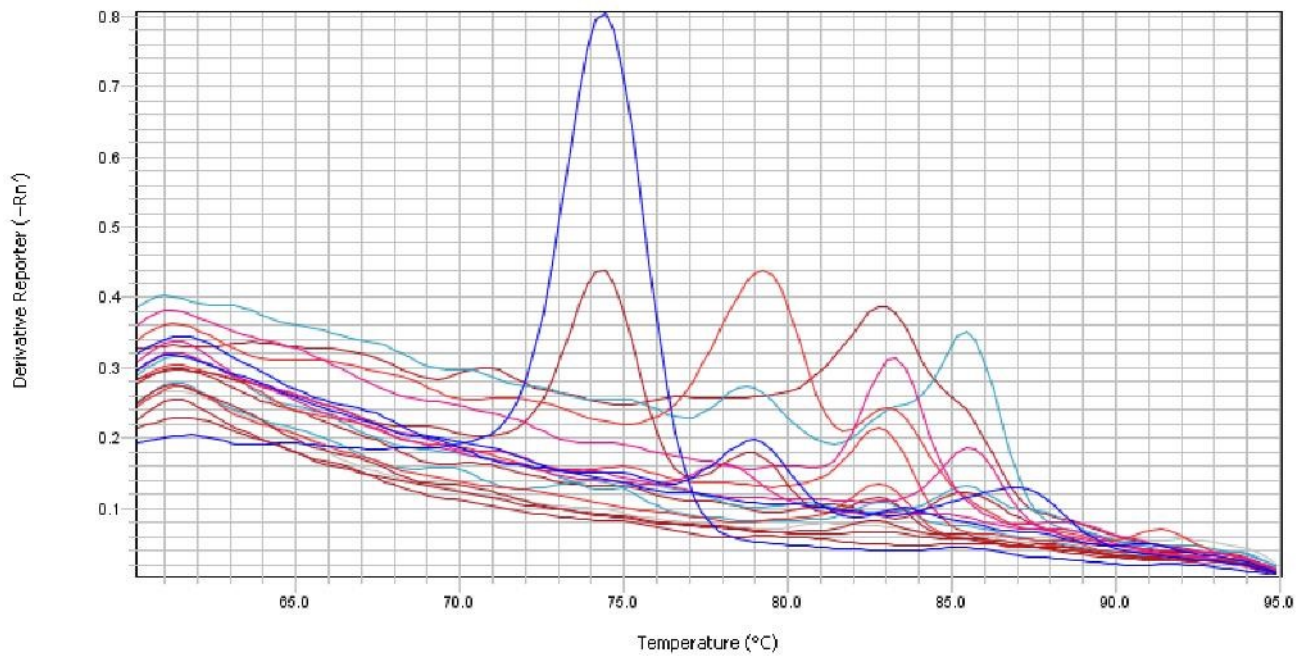


Hsa_circANXA1_001

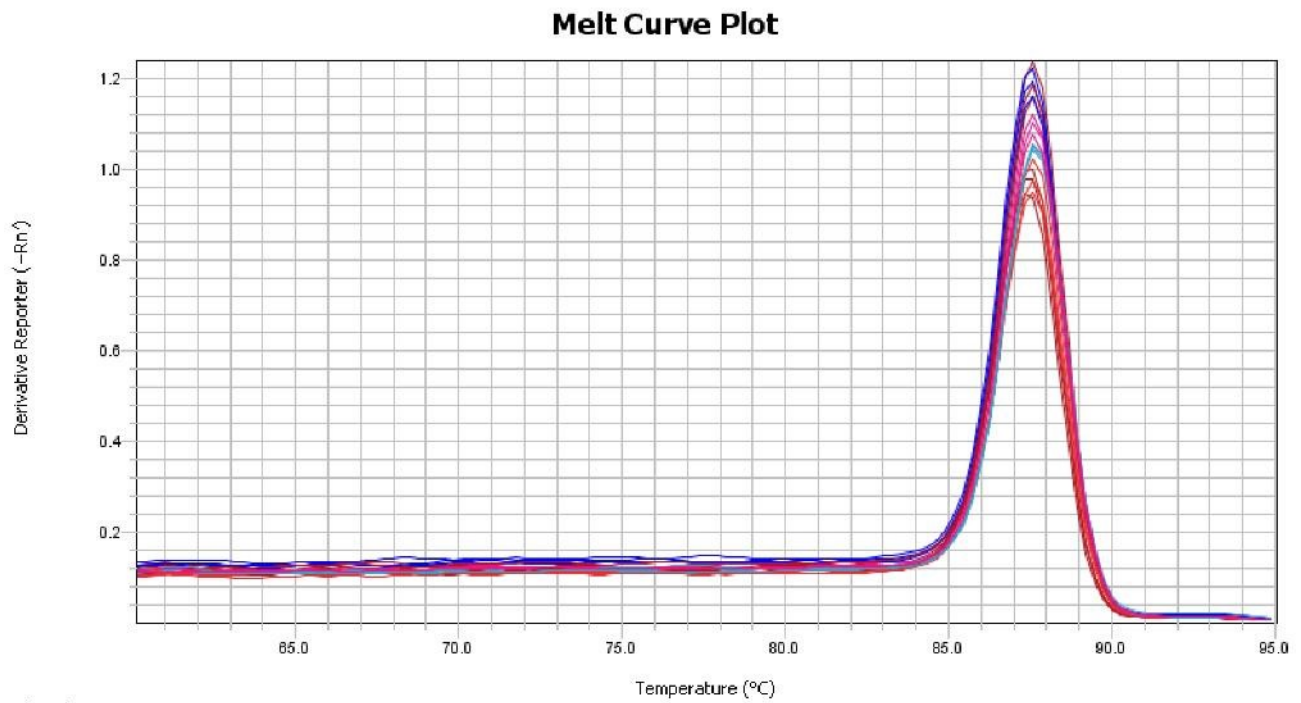
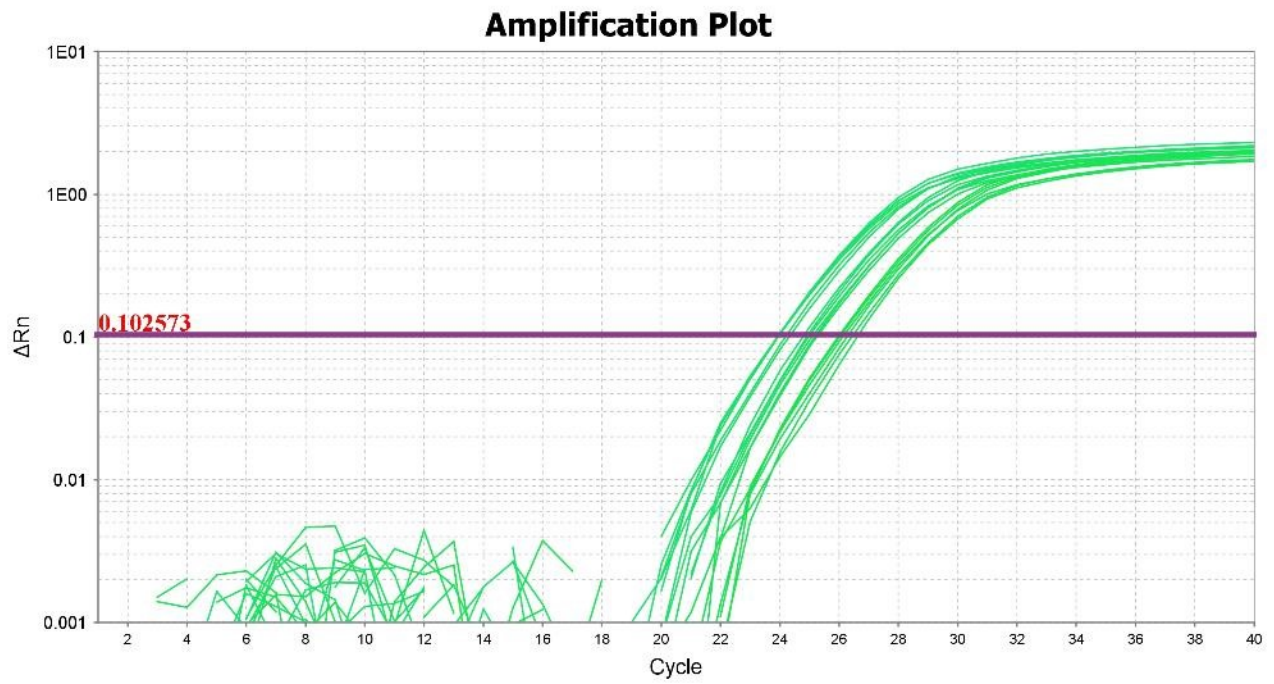
Amplification Plot



Melt Curve Plot



Hsa_circDNM1_004



TBP

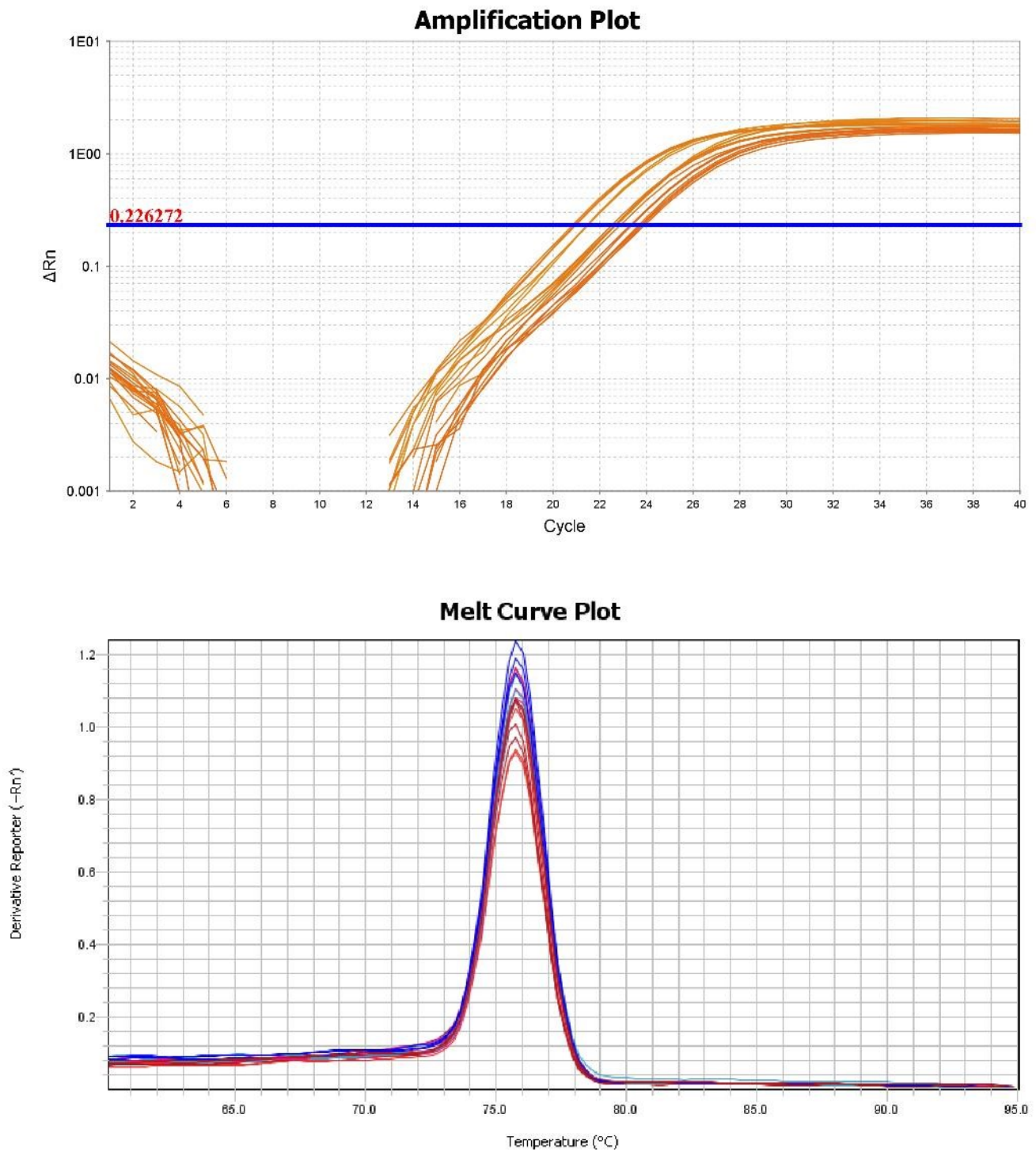


Figure 3-1: Amplification and melting curve plots for target circRNAs and TBP gene amplified from ALS and control samples. Amplification and melting curve plots showed

optimal curves for all the candidate circRNAs except for hsa_circANXA1_001.

Hsa_circANXA1_001 showed suboptimal amplification and melting curve plots which indicated a suboptimal amplification efficiency for the primer set designed for this circRNA. Left plots are showing amplification plots (Y-axis: normalized fluorescent signal (ΔR_n), X-axis: cycle number). Right plots are showing melting curves (Y-axis: difference in fluorescence/difference in temperature, X-axis: melting temperature in $^{\circ}\text{C}$).

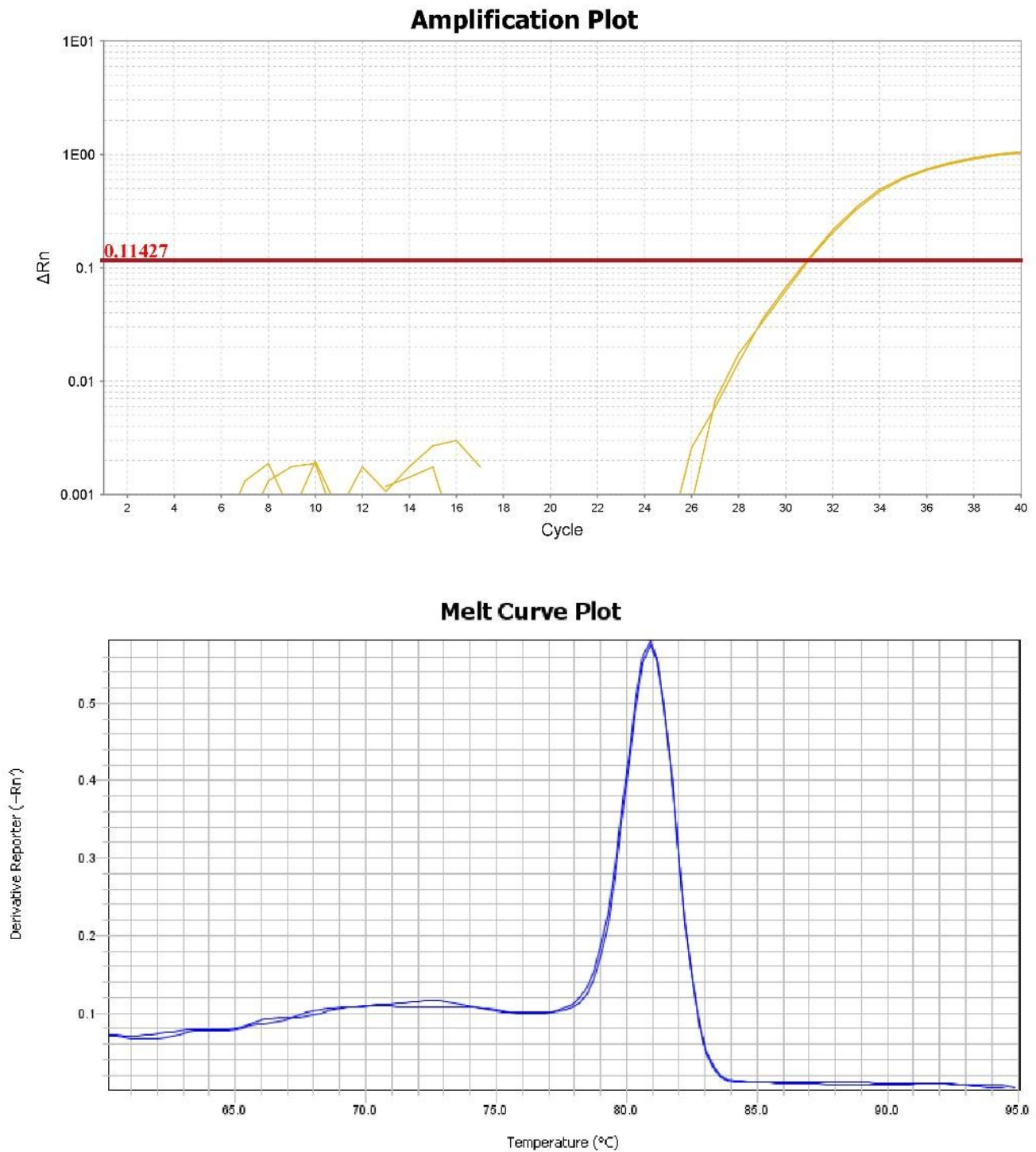
Hsa_circANXA1_001

Figure 3-2: Amplification and melting curve plots for hsa_circANXA1_001 primers used on cDNA from HEK293T. Left plot is showing amplification plot (Y-axis: normalized

fluorescent signal (ΔR_n), X-axis: cycle number). Right plot is showing melting curve (Y-axis: difference in Fluorescence/difference in temperature, X-axis: melting temperature in $^{\circ}\text{C}$).

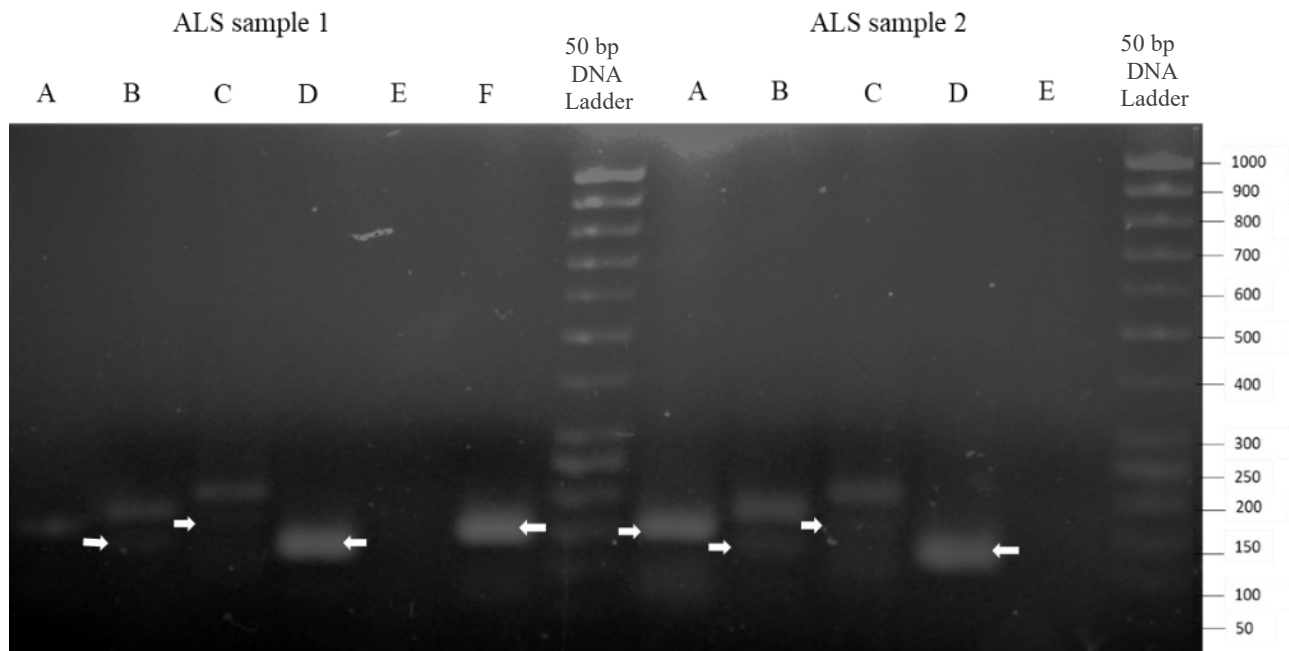


Figure 3-3: Agarose gel electrophoresis of qPCR products from ALS and control samples.

A) CDR1as. B) Hsa_circDNM1_004. C) Hsa_circVIM_005. D) Hsa_circVIM_011. E) Hsa_circANXA1_001. F) TBP. There is more than one band for circRNAs hsa_circDNM1_004 (B) and hsa_circVIM_005 (C) on the gel. We did not observe a PCR product from the primer set for hsa_circANXA1_001. Arrows are indicating the expected bands for each set of primers.

In the present study, I did not observe an alteration in the expression levels between ALS and control cases for the candidate circRNAs chosen for this analysis similar to RNA-seq data (Figure 3-4). The raw data for real-time PCR for candidate circRNAs are presented in Table 3-1 to Table 3-4.

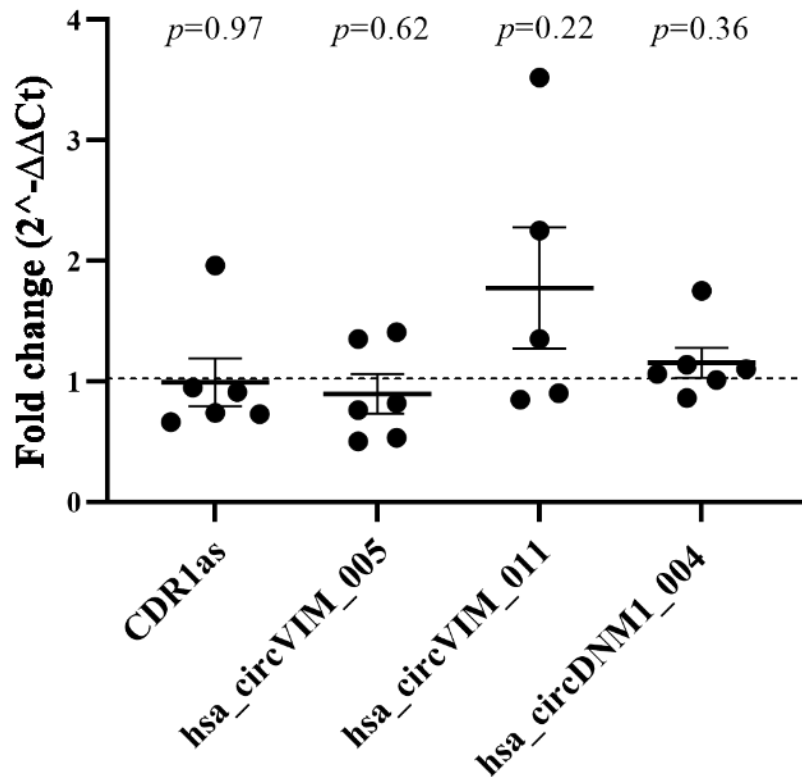


Figure 3-4: Real-time PCR did not show significant differences in the expression of candidate circRNAs between ALS and control patients' samples. Expression levels were normalized to TBP as a reference gene. Each dot represents circRNA fold change (ALS/Control) obtained from one patient sample and the bar represents mean (n=6) fold-change ($2^{-\Delta\Delta CT}$) \pm SEM. The significance of data was determined using Student's t-test (for hsa_circVIM_005 and hsa_circVIM_011) and Mann-Whitney U test (for CDR1as and hsa_circDNM1_004). A $p > 0.05$ is considered statistically non-significant (ns).

Table 3-1: Raw data for real-time PCR of CDR1as in control and ALS samples.

Sample	CDR1as Average Ct	TBP Average Ct	Δ Ct	$\Delta\Delta$ Ct	$2^{-\Delta\Delta$ Ct}
Control 1	14.7134	25.2873	-10.57		
Control 2	14.7727	25.0598	-10.29		
Control 3	14.9439	25.9463	-11.00		
Control 4	13.9811	23.9968	-10.02		
ALS 1	15.6796	26.0741	-10.39	0.08	0.95
ALS 2	15.0174	26.4587	-11.44	-0.97	1.96
ALS 3	15.2220	25.2300	-10.01	0.46	0.73
ALS 4	14.1546	24.1884	-10.03	0.44	0.74
ALS 5	14.6017	24.9281	-10.33	0.14	0.91
ALS 6	14.0794	23.9553	-9.88	0.59	0.66

Table 3-2: Raw data for real-time PCR of hsa_circVIM_005 in control and ALS samples

Sample	hsa_circVIM_005 Average Ct	TBP Average Ct	ΔCt	$\Delta\Delta Ct$	$2^{-\Delta\Delta Ct}$
Control 1	23.8487	25.2873	-1.44		
Control 2	21.1583	25.0598	-3.90		
Control 3	22.7733	25.9463	-3.17		
Control 4	21.5996	23.9968	-2.40		
ALS 1	24.3404	26.0741	-1.73	1.00	0.50
ALS 2	23.2341	26.4587	-3.22	-0.49	1.41
ALS 3	22.0718	25.2300	-3.16	-0.43	1.35
ALS 4	21.7383	24.1884	-2.45	0.28	0.82
ALS 5	23.1101	24.9281	-1.82	0.91	0.53
ALS 6	21.6253	23.9553	-2.33	0.40	0.76

Table 3-3: Raw data for real-time PCR of hsa_circVIM_011 in control and ALS samples.

Sample	hsa_circVIM_011 Average Ct	TBP Average Ct	Δ Ct	$\Delta\Delta$ Ct	$2^{\Delta\Delta$ Ct
Control 1	24.8482	25.2873	-0.44		
Control 2	22.8115	25.0598	-2.25		
Control 3	25.0141	25.9463	-0.93		
Control 4	24.1103	23.9968	0.11		
ALS 1	25.4227	26.0741	-0.65	0.23	0.85
ALS 2	23.7641	26.4587	-2.69	-1.81	3.52
ALS 3	23.1774	25.2300	-2.05	-1.17	2.25
ALS 4	23.4532	24.1884	-0.74	0.14	0.90
ALS 6	22.6445	23.9553	-1.31	-0.43	1.35

Table 3-4: Raw data for real-time PCR of hsa_circDNM1_004 in control and ALS samples.

Sample	hsa_circDNM1_004 Average Ct	TBP Average Ct	Δ Ct	$\Delta\Delta$ Ct	$2^{\Delta\Delta$ Ct}
Control 1	23.0906	25.2873	-2.20		
Control 2	21.8764	25.0598	-3.18		
Control 3	23.1907	25.9463	-2.76		
Control 4	22.0078	23.9968	-1.99		
ALS 1	23.4062	26.0741	-2.67	-0.14	1.10
ALS 2	23.7346	26.4587	-2.72	-0.19	1.14
ALS 3	22.6201	25.2300	-2.61	-0.08	1.06
ALS 4	20.8476	24.1884	-3.34	-0.81	1.75
ALS 5	22.6127	24.9281	-2.32	0.21	0.86
ALS 6	21.4068	23.9553	-2.55	-0.02	1.01

3.2 Experimental set 2 – dysregulation of candidate circRNAs' expression in stressed HEK293T cells

3.2.1 Introduction

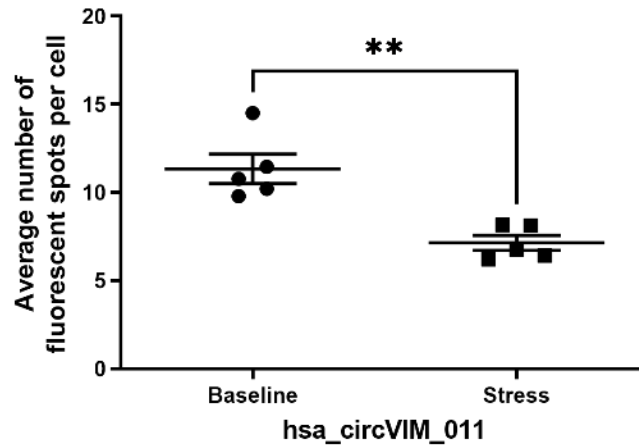
As discussed, cellular stress has been implicated in the pathogenesis of ALS. Several studies have examined the effect of cellular stress on the expression of non-coding RNAs. For example, oxidative stress has been shown to be associated with dysregulated expression of several lncRNAs (Bianchessi et al, 2015; Guo et al, 2019; Luo et al, 2019; Zhang et al, 2019). Besides, the participation of non-coding RNAs including both miRNAs and lncRNAs in the oxidative stress process have been recently revealed (Guo et al, 2017; Tang et al, 2015). Therefore, regulating the expression of non-coding RNAs can be a feasible route for the modulation of cellular stress response. In this study, I examined the expression of candidate circRNAs in stressed HEK293T cells compared to unstressed cells using FISH.

3.2.2 Results

3.2.2.1 circRNAs show an altered granule formation in stressed HEK293T cells compared with unstressed cells.

FISH allows quantification of RNA transcript abundance through both the including quantification of fluorescent signal intensity and the number of fluorescent spots. In the present study, the expression analysis of the circRNA candidates was performed quantifying the number of circRNA spots per cell obtained from confocal microscope images. Candidate circRNAs were visualized by FISH, using a DIG-labeled back-splicing junction-spanning oligonucleotide. For spot quantification, I used ImageJ (Fiji) software as previously described (Lee et al, 2016; Schindelin et al, 2012). This data showed that the number of fluorescent spots for circRNA hsa_circANXA1_001 and hsa_circVIM_011 significantly decreased in HEK293T cells in response to stress (Figure 3-5 a and b, respectively). The spot quantification was not applicable for other candidate circRNAs using this method as they showed fluorescent signal accumulation that precluded the analysis of discrete spots. The comparison of the size of fluorescent spots for these two circRNAs in stressed versus unstressed cells did not showed any significant difference (data not shown).

A



B

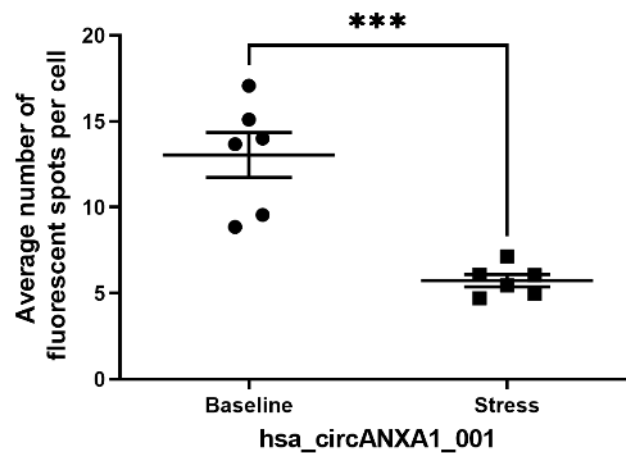


Figure 3-5: Quantification of circRNA hsa_circVIM_011 and hsa_circANXA1_001 by RNA FISH. (A) The number of fluorescent spots was significantly decreased for circRNA hsa_circVIM_011 in HEK293T cells in response to osmotic stress. (B) The number of fluorescent spots was significantly decreased for circRNA hsa_circANXA1_001 in HEK293T cells in response to stress. Fluorescent spots in 20 cells per every sample slide (n=6) were automatically counted. The bar represents the mean (n=6) average number of spots per cell (n=18) ± SEM. The significance of data was determined using a Student's t-test (** p ≤ 0.01, ***p ≤ 0.001).

3.3 Experimental set three: circRNAs colocalize with the markers for RNP granules in HEK293T cells under stress.

3.3.1 Introduction.

In fluorescence microscopy, colocalization analysis is used to determine whether two molecules colocalize with each other or with the same structures (for example, to determine whether a circRNA colocalize with an RNP granule). Of note, an overlap in fluorescence signals does not absolutely define colocalization. Every colocalization consists of two components: co-occurrence (the simple spatial overlap of two probes) and correlation (when two probes not only overlap but also co-distribute in proportion). Colocalization in fluorescence microscope images may be evaluated visually, quantitatively, and statistically (Dunn et al, 2011).

Although modern fluorescence microscopy produces detailed three-dimensional (3D) datasets, colocalization analysis and region of interest (ROI) selection is most commonly performed two-dimensionally (2D) using maximum intensity projections (MIP). However, these 2D projections exclude much of the available data. Furthermore, 2D ROI selections cannot adequately select complex 3D structures which may inadvertently lead to either the exclusion of relevant or the inclusion of irrelevant data points, consequently affecting the accuracy of the colocalization analysis.

The most common method of determining colocalization using fluorescence microscopy is to show the image of two fluorophores in the red and green channels of an RGB two-dimensional (2-D) image and consider yellow pixels in the overlay channel as a colocalization. The selection of region of interest (ROI) in 2-D excludes much of the available data because of inability in adequately selection of complex 3-D structures. Moreover, 2-D colocalization might increase the probability of false positive colocalization. This is because the observation of the merged yellow pixels depends on the relative intensities of red and green fluorophores and when the intensity levels of fluorophores are similar, even they are in different location, results in the perception of colocalization because of the restricted ability of eyes to perceive and interpret colors.

Fortunately, modern fluorescence microscopy provides a chance to acquire the z-stacks consisting of multiple 2-D images, which can be reconstructed to 3-D images using direct-volume rendering. (Bolte & Cordelières, 2006; Dunn et al, 2011).

These visual techniques are helpful to provide a spatial sense of colocalization and recognize the regions where molecules colocalize. However, the visual evaluation of colocalization is not able to determine the degree of colocalization and if this degree exceeds random coincidence (Pompey et al, 2013). Therefore, in the present study, first I used a qualitative method to identify the colocalization between candidate circRNAs and markers of RNP granules. Then I quantified the observed colocalization.

3.3.2 Results

3.3.2.1 Visual evaluation in 2-D showed colocalization between circRNAs with markers of RNP granules

Two-dimensional colocalization studies using single-molecule FISH for circRNAs and IF for RNP granules' markers showed that three of the candidate circRNAs for this study colocalize with RNP granules' markers.

The analysis of colocalization of circRNAs with Staufen positive transport granules showed that CDR1as, hsa_circVIM_005 and hsa_circDNM1_004 colocalize in Staufen positive transport granules in stressed HEK293T cells (Figure 3-36, Figure 3-7, and Figure 3-8, respectively). Hsa_circVIM_011 and hsa_circANXA1_001 did not show colocalization with this marker of transport granules (Figure 3-9 and Figure 3-10, respectively).

A study of colocalization of circRNAs with TIA-1 positive transport granules showed that CDR1as, hsa_circVIM_005, and hsa_circDNM1_004 colocalize in TIA-1 positive stress granules in stressed HEK293T cells (Figure 3-11, Figure 3-12, and Figure 3-13, respectively). Hsa_circVIM_011 and hsa_circANXA1_001 did not show colocalization with this marker of stress granules (Figure 3-14 and Figure 3-15, respectively).

The study of colocalization of circRNAs with Dcp1 positive P-bodies showed that CDR1as, hsa_circVIM_005, hsa_circDNM1_004, and hsa_circVIM_011 colocalize with Dcp1 positive P-bodies in stressed HEK293T cells (Figure 3-16, Figure 3-17, Figure 3-18, and Figure 3-19, respectively). However, hsa_circANXA1_001 did not show any colocalization with the marker of P-bodies (Figure 3-20).

A study of colocalization of circRNAs with PSPC1 showed that hsa_circDNM1_004 and colocalize with PSPC1 fibril structures (Figure 3-21). CDR1as, hsa_circVIM_005, hsa_circVIM_011, and hsa_circANXA1_001 did not show any colocalization with PSPC1 fibril structures (Figure 3-22, Figure 3-23, Figure 3-24, and Figure 3-25, respectively).

I also studied the colocalization of a random selection of candidate circRNAs with NONO as another marker for paraspeckles. The result showed that hsa_circDNM1_004 and hsa_circVIM_011 colocalize with NONO in stressed HEK293T cells (Figure 3-26 and Figure 3-27, respectively). Hsa_circANXA1_001 did not show any colocalization with this protein (Figure 3-28).

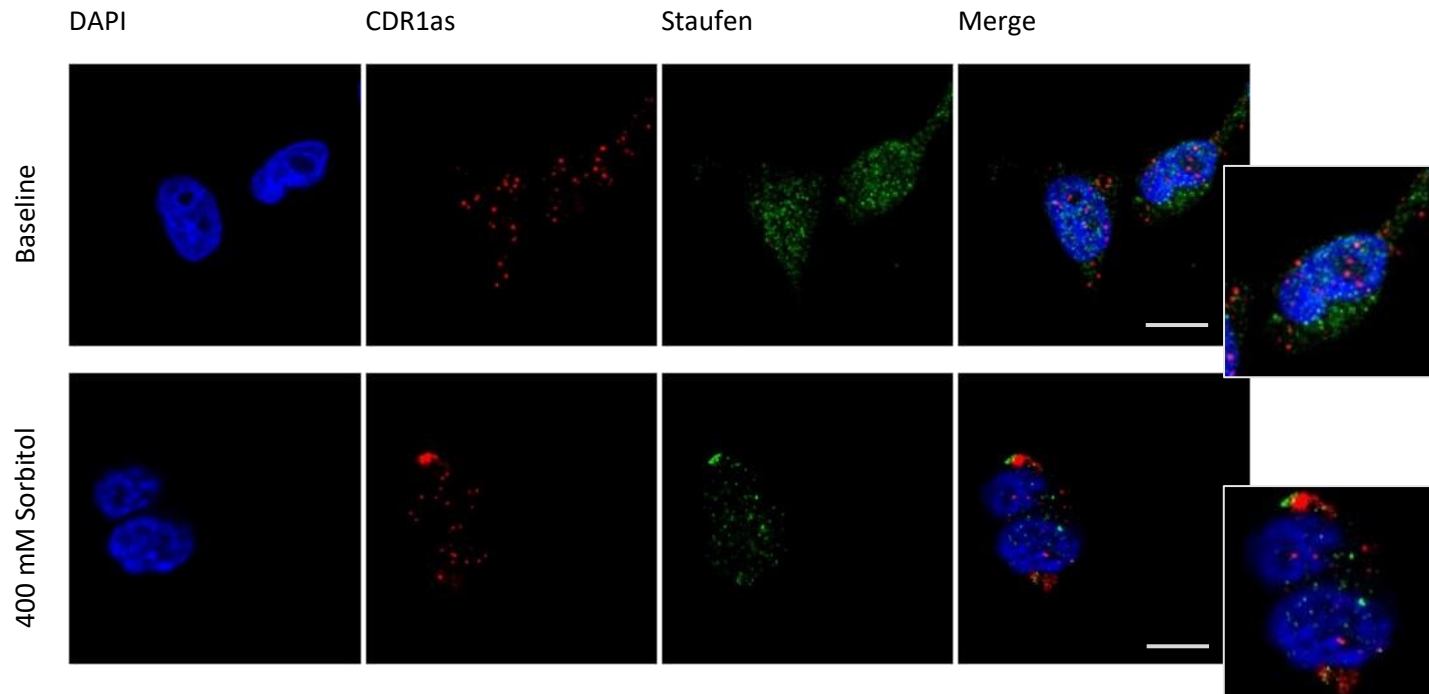


Figure 3-6: CDR1as colocalizes with Staufen positive stress granules under osmotic stress.

The upper panel shows unstressed HEK293T cells, and the lower panel shows stressed HEK293T cells (400 mM sorbitol for 4 hours). Scale bars represent 10 μm .

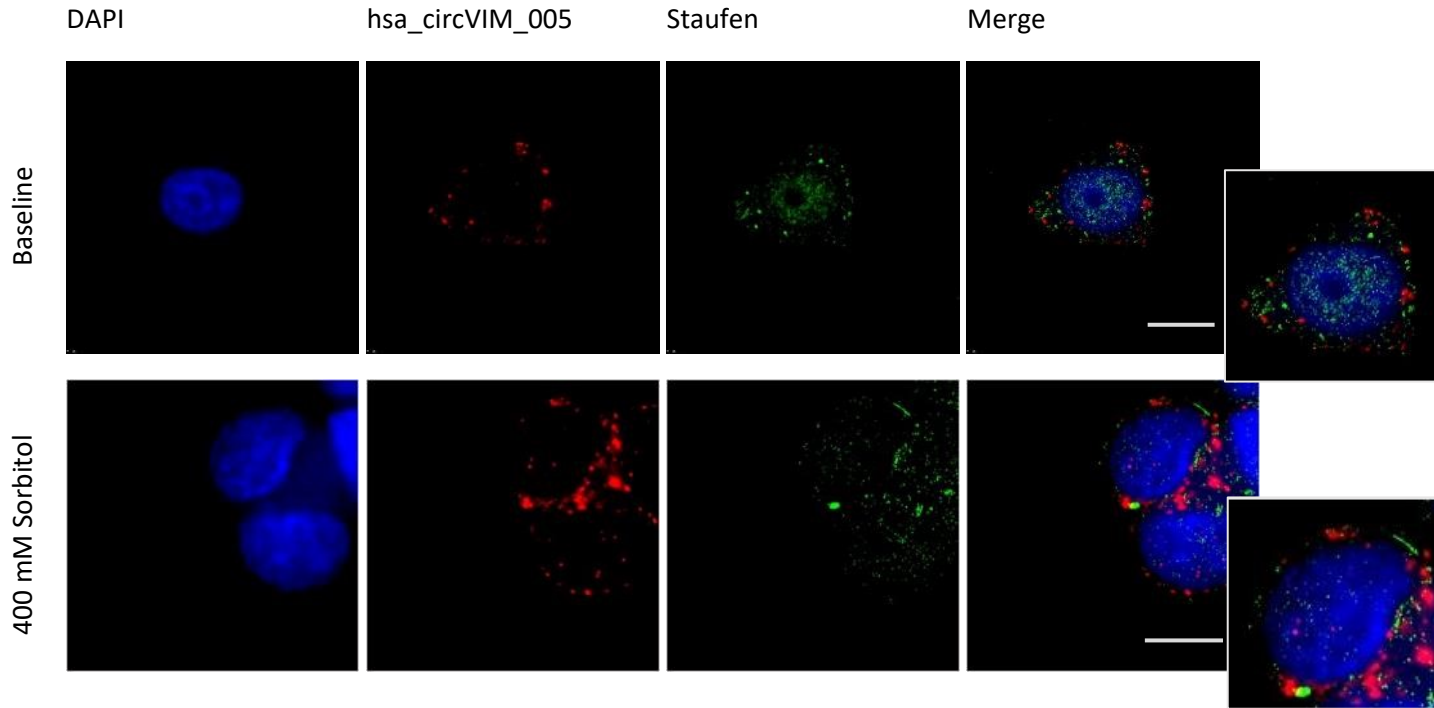


Figure 3-7: Hsa_circVIM_005 colocalizes with Staufen positive transport granules under osmotic stress. The upper panel shows unstressed HEK293T cells, and the lower panel shows stressed HEK293T cells (400 mM sorbitol for 4 hours). Scale bars represent 10 μm .

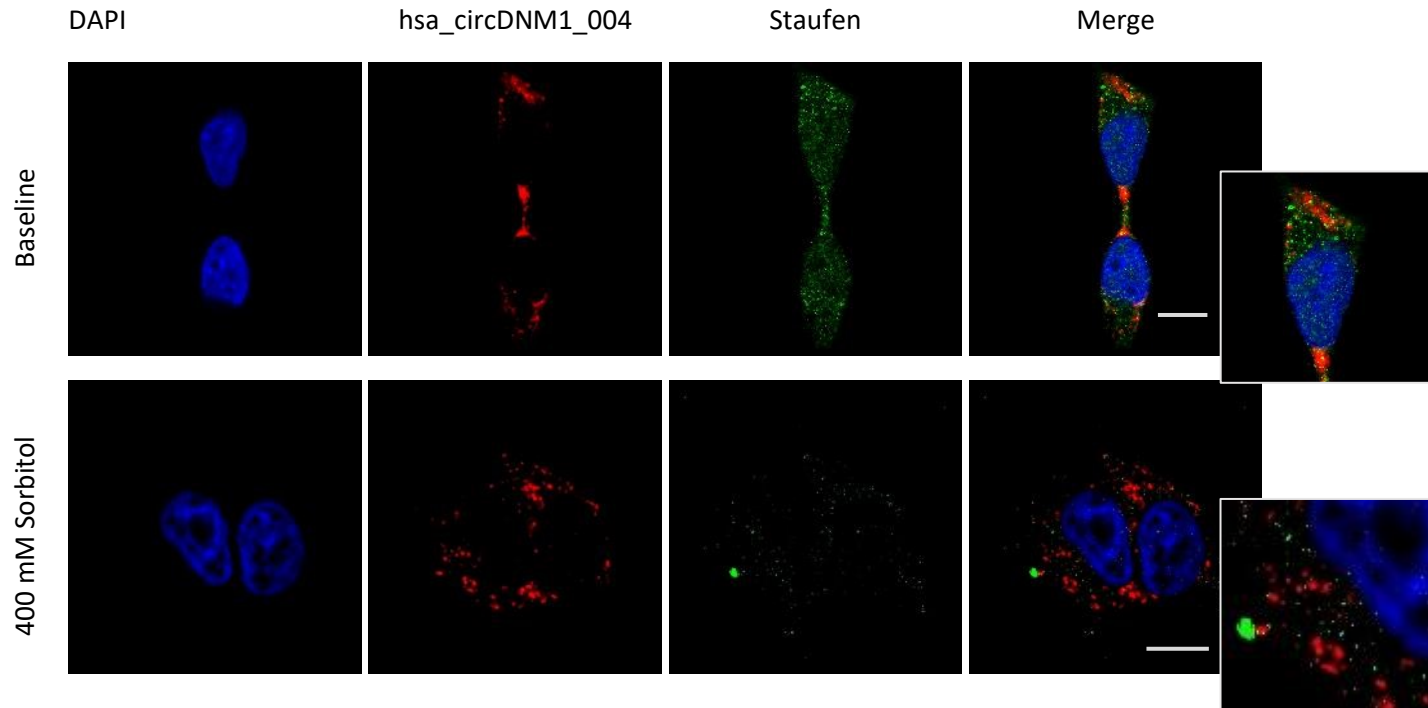


Figure 3-8: Hsa_circDNM1_004 colocalizes with Staufen positive transport granules under osmotic stress. The upper panel shows unstressed HEK293T cells, and the lower panel shows stressed HEK293T cells (400 mM sorbitol for 4 hours). Scale bars represent 10 μm .

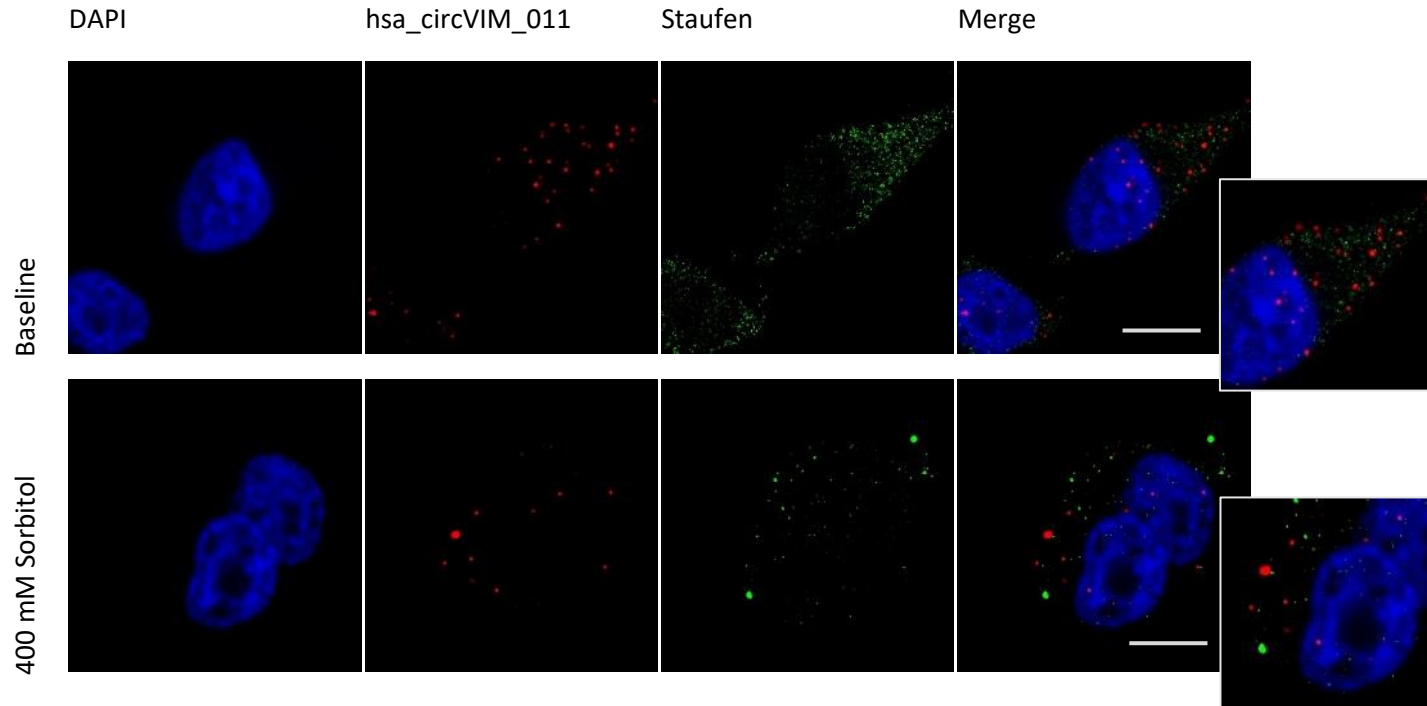


Figure 3-9: Hsa_circVIM_011 does not colocalize with Staufen positive transport granules under osmotic stress. The upper panel shows unstressed HEK293T cells, and the lower panel shows stressed HEK293T cells (400 mM sorbitol for 4 hours). Scale bars represent 10 μm .

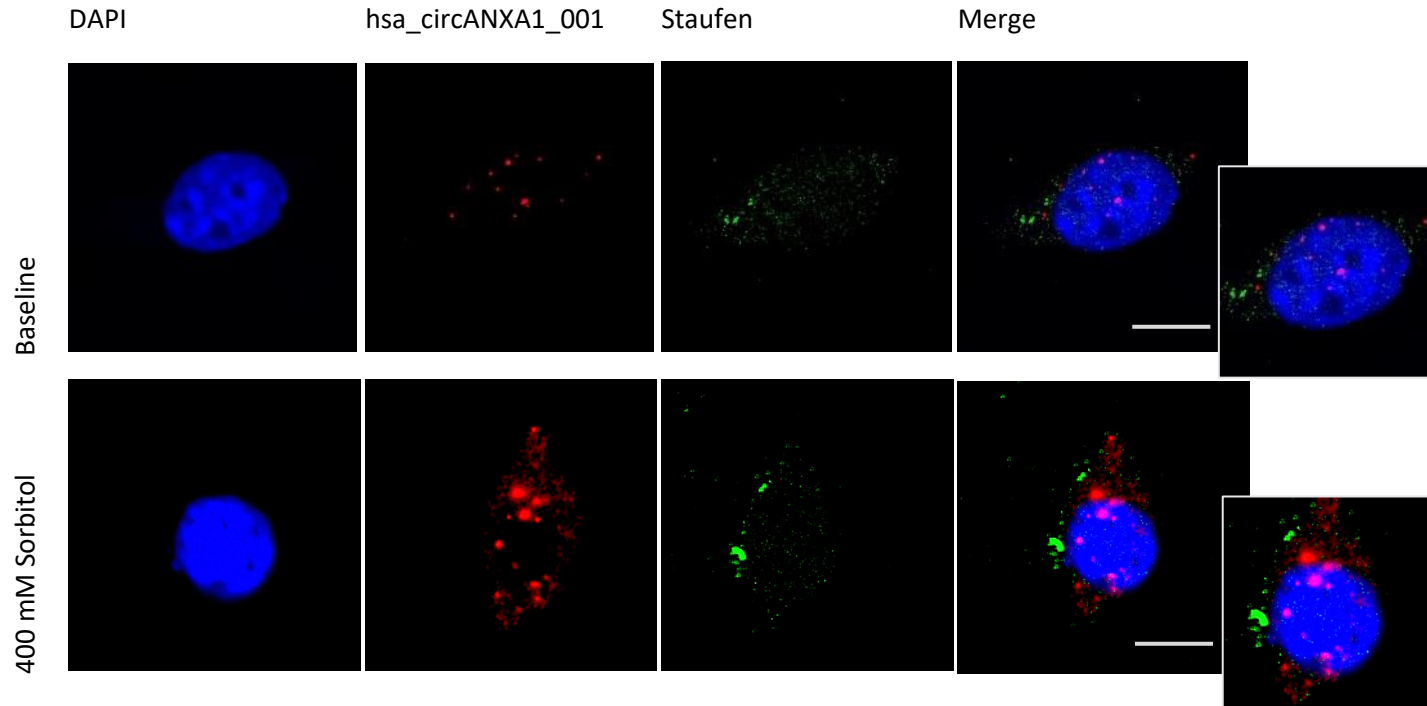


Figure 3-10: Hsa_circANXA1_001 does not colocalize with Staufen positive transport granules under osmotic stress. The upper panel shows unstressed HEK293T cells, and the lower panel shows stressed HEK293T cells (400 mM sorbitol for 4 hours). Scale bars represent 10 μm .

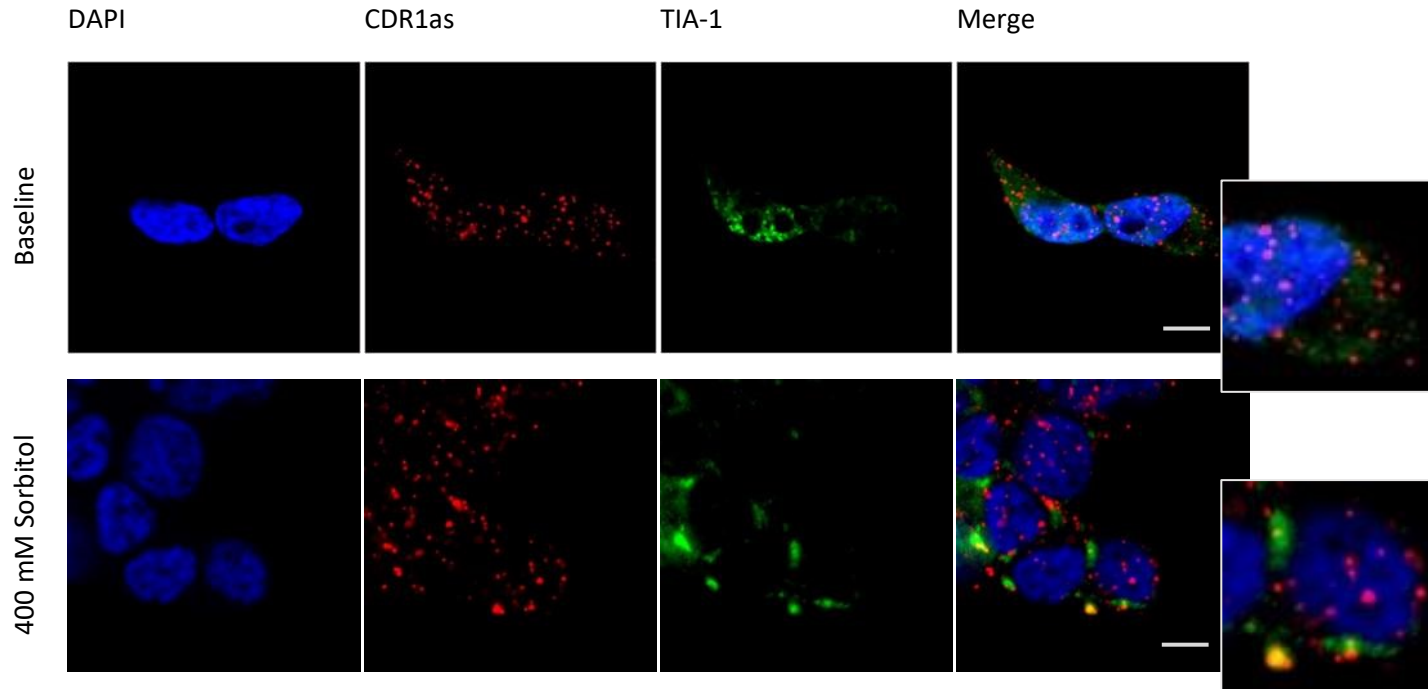


Figure 3-11: CDR1as colocalizes with TIA-1 positive stress granules under osmotic stress.

The upper panel shows unstressed HEK293T cells, and the lower panel shows stressed HEK293T cells (400 mM sorbitol for 4 hours). Scale bars represent 10 μm .

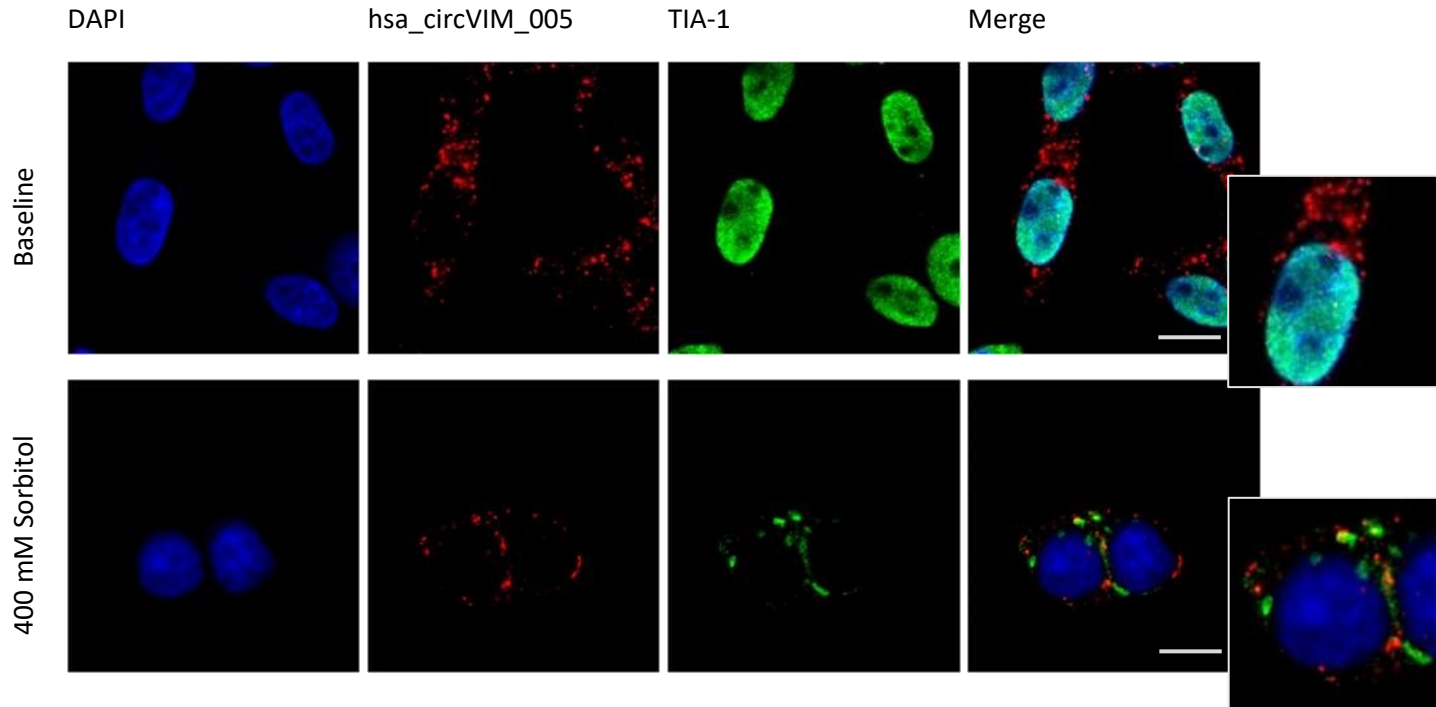


Figure 3-12: Hsa_circVIM_005 colocalizes with TIA-1 positive stress granules under osmotic stress. The upper panel shows unstressed HEK293T cells, and the lower panel shows stressed HEK293T cells (400 mM sorbitol for 4 hours). Scale bars represent 10 μ m.

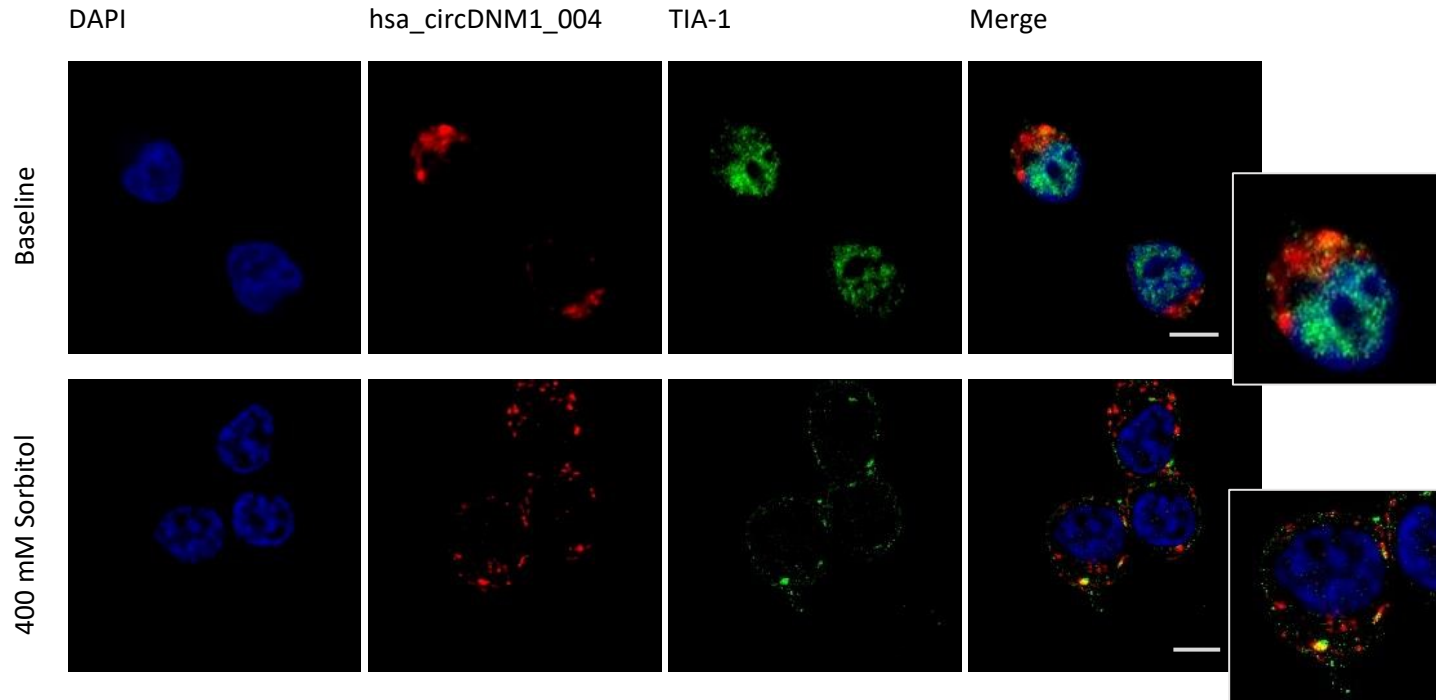


Figure 3-13: Hsa_circDNM1_004 colocalizes with TIA-1 positive stress granules under osmotic stress. The upper panel shows unstressed HEK293T cells, and the lower panel shows stressed HEK293T cells (400 mM sorbitol for 4 hours). Scale bars represent 10 μ m.

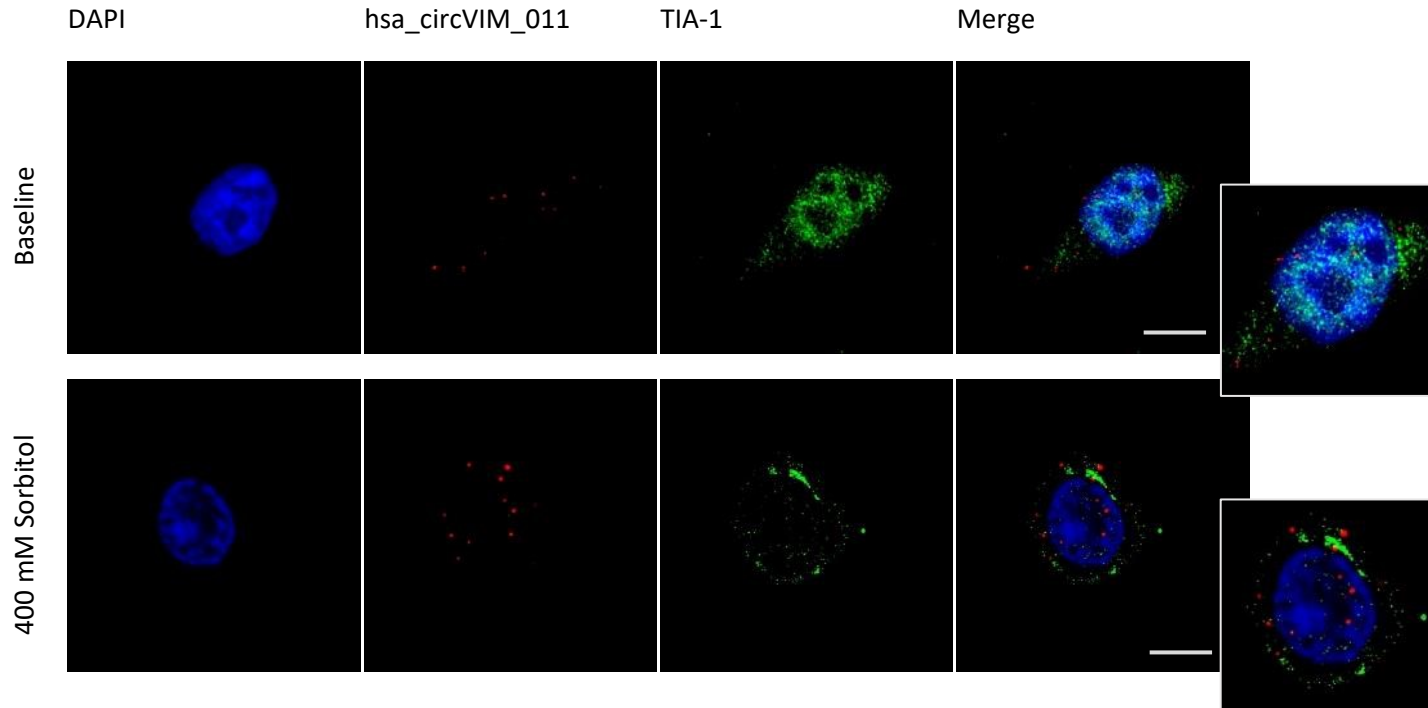


Figure 3-14: Hsa_circVIM_011 does not colocalize with TIA-1 positive stress granules under osmotic stress. The upper panel shows unstressed HEK293T cells, and the lower panel shows stressed HEK293T cells (400 mM sorbitol for 4 hours). Scale bars represent 10 μm .

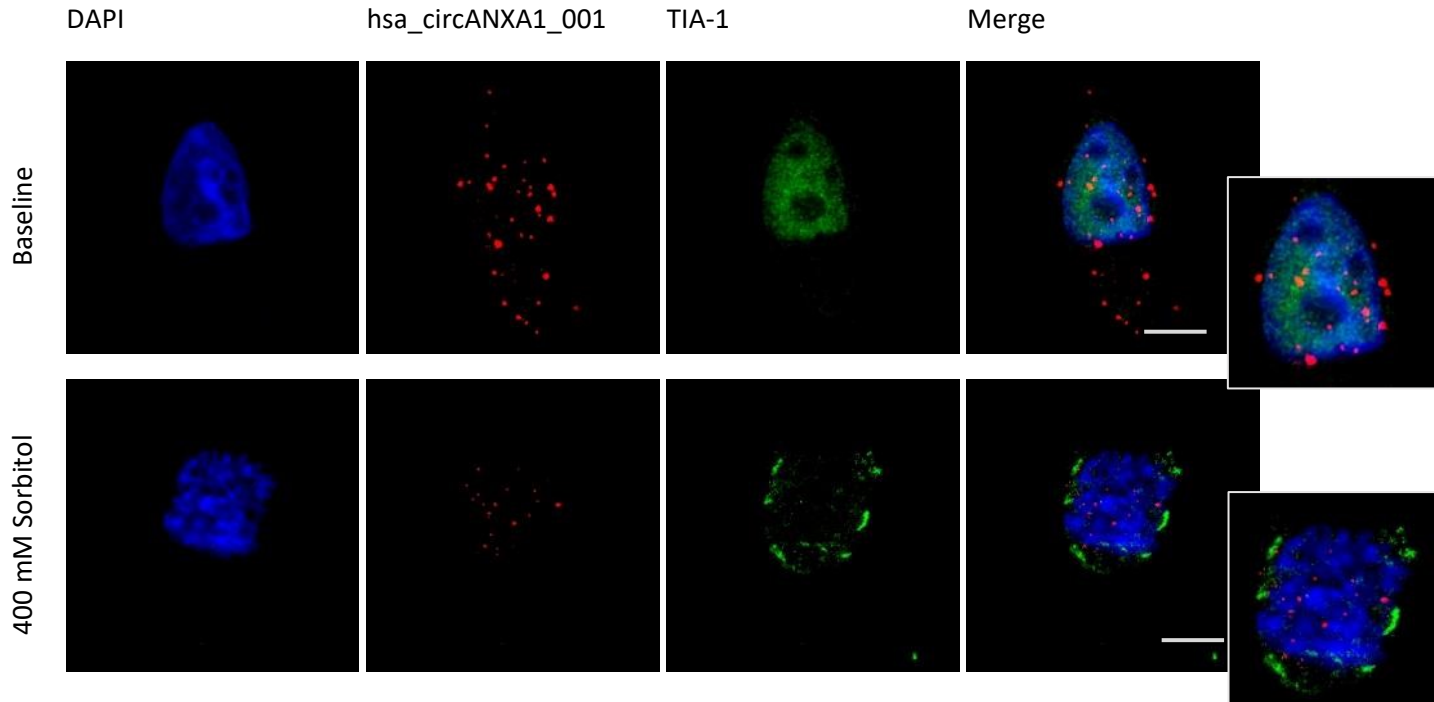


Figure 3-15: Hsa_circANXA1_001 does not colocalize with TIA-1 positive stress granules under osmotic stress. The upper panel shows unstressed HEK293T cells, and the lower panel shows stressed HEK293T cells (400 mM sorbitol for 4 hours). Scale bars represent 10 μm .

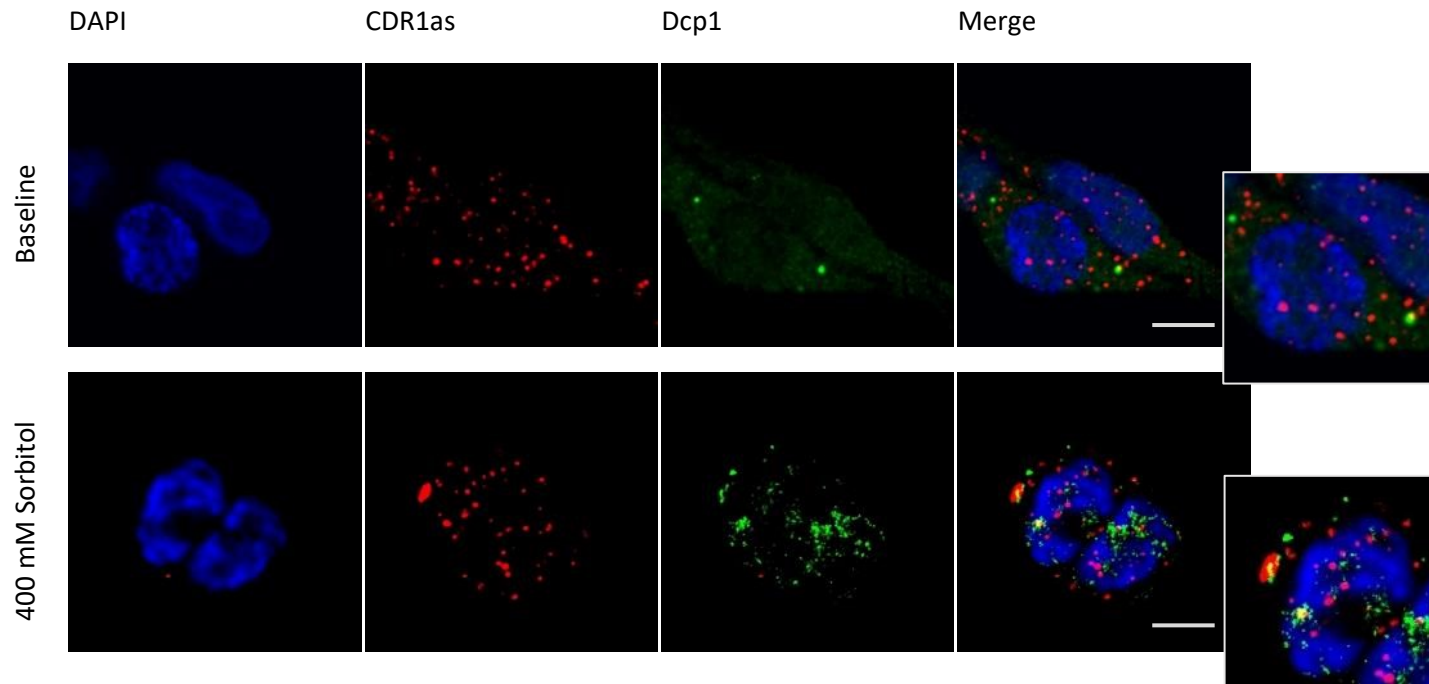


Figure 3-16: CDR1as colocalizes with Dcp1 positive P-bodies under osmotic stress. The upper panel shows unstressed HEK293T cells, and the lower panel shows stressed HEK293T cells (400 mM sorbitol for 4 hours). Scale bars represent 10 μm .

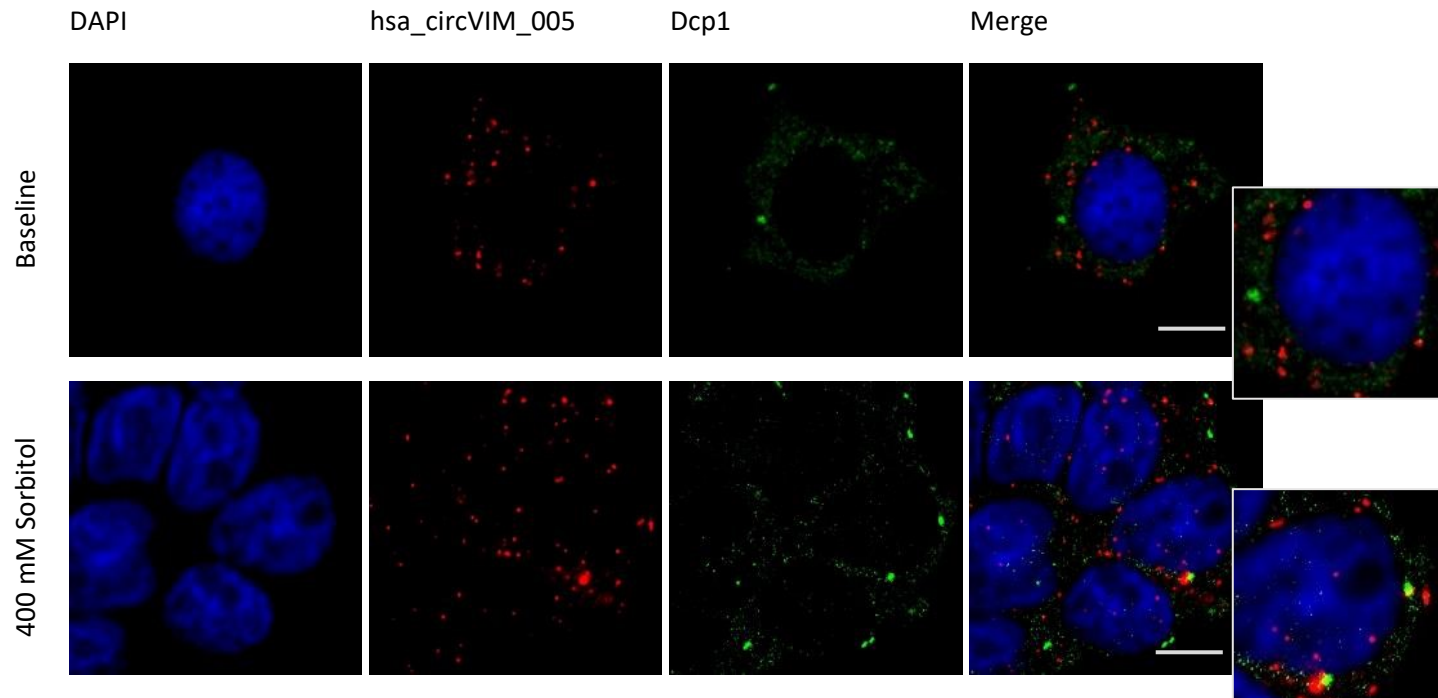


Figure 3-17: Hsa_circVIM_005 colocalizes with Dcp1 positive P-bodies under osmotic stress. The upper panel shows unstressed HEK293T cells, and the lower panel shows stressed HEK293T cells (400 mM sorbitol for 4 hours). Scale bars represent 10 μm .

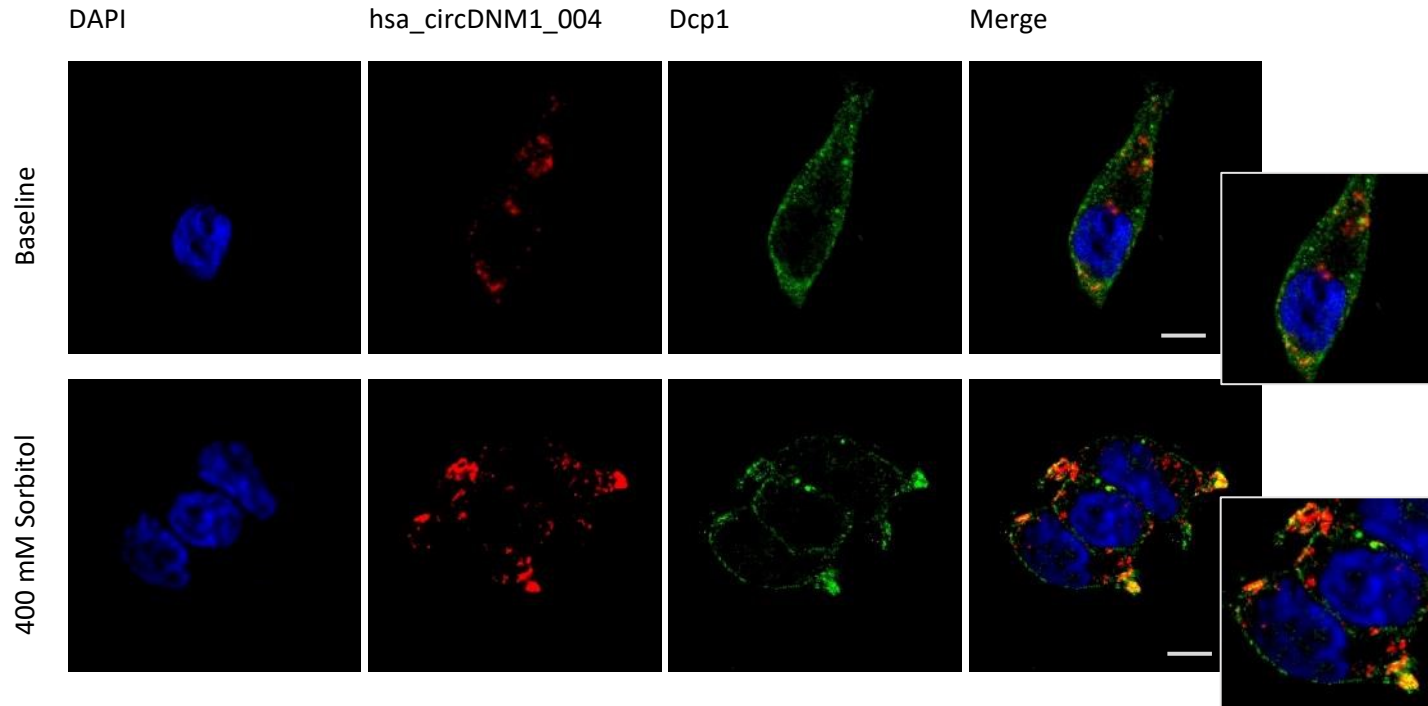


Figure 3-18: Hsa_circDNM1_004 colocalizes with Dcp1 positive P-bodies under osmotic stress. The upper panel shows unstressed HEK293T cells, and the lower panel shows stressed HEK293T cells (400 mM sorbitol for 4 hours). Scale bars represent 10 μm .

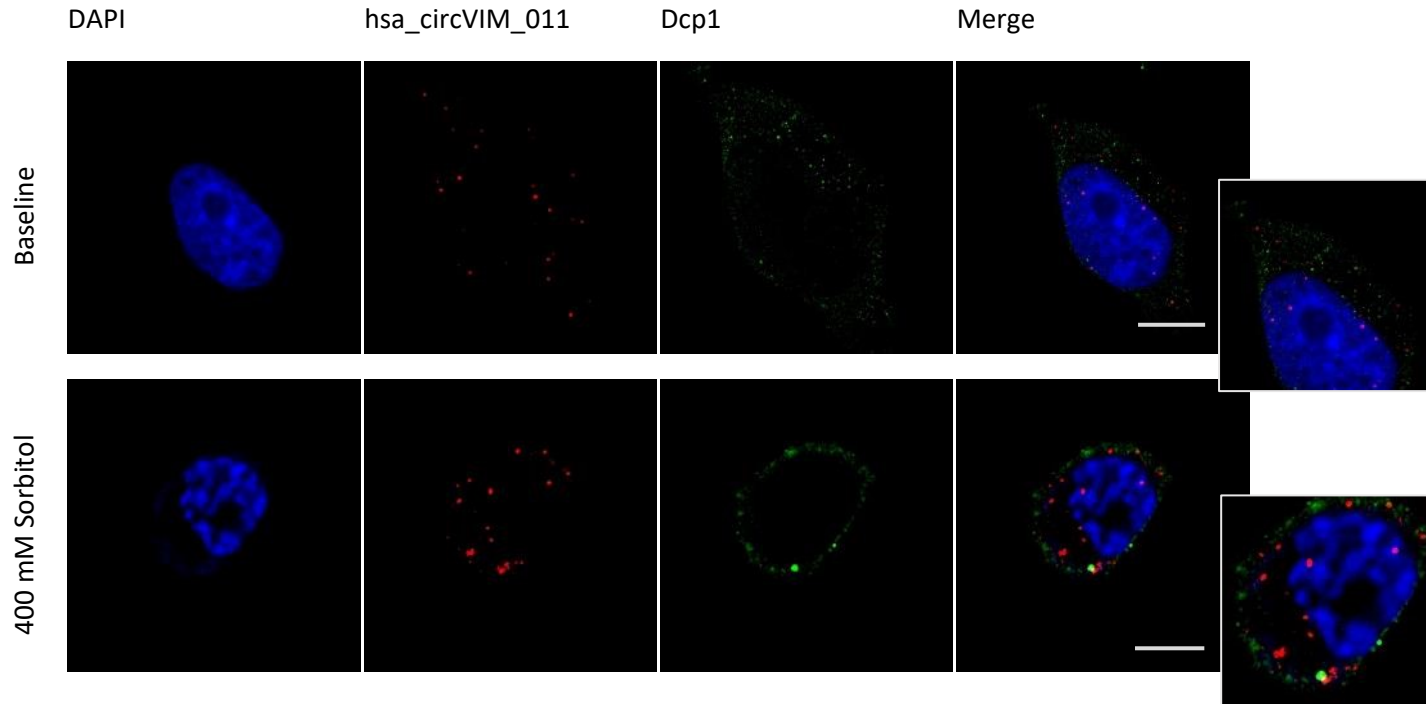


Figure 3-19: Hsa_circVIM_011 colocalizes with Dcp1 positive P-bodies under osmotic stress. The upper panel shows unstressed HEK293T cells, and the lower panel shows stressed HEK293T cells (400 mM sorbitol for 4 hours). Scale bars represent 10 μm .

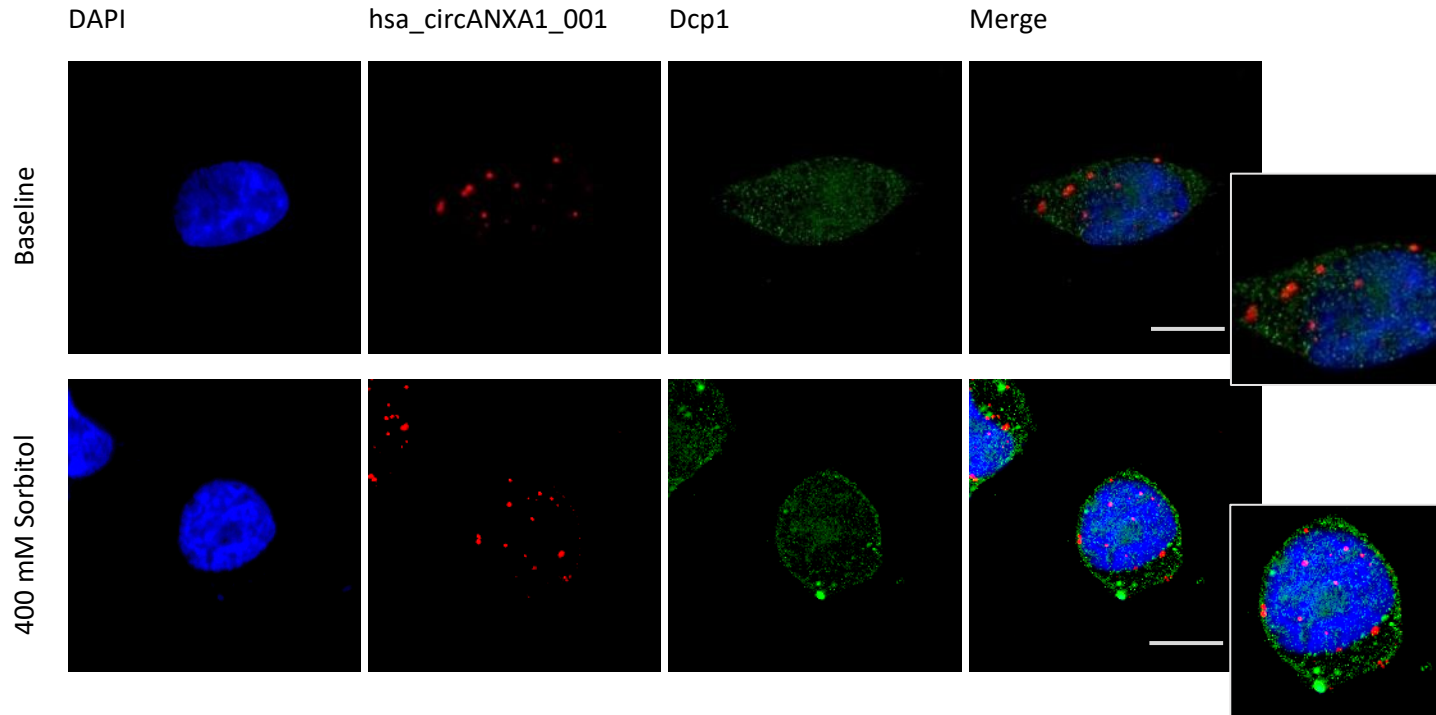


Figure 3-20: Hsa_circANXA1_001 does not colocalize with Dcp1 positive P-bodies under osmotic stress. The upper panel shows unstressed HEK293T cells, and the lower panel shows stressed HEK293T cells (400 mM sorbitol for 4 hours). Scale bars represent 10 μ m.

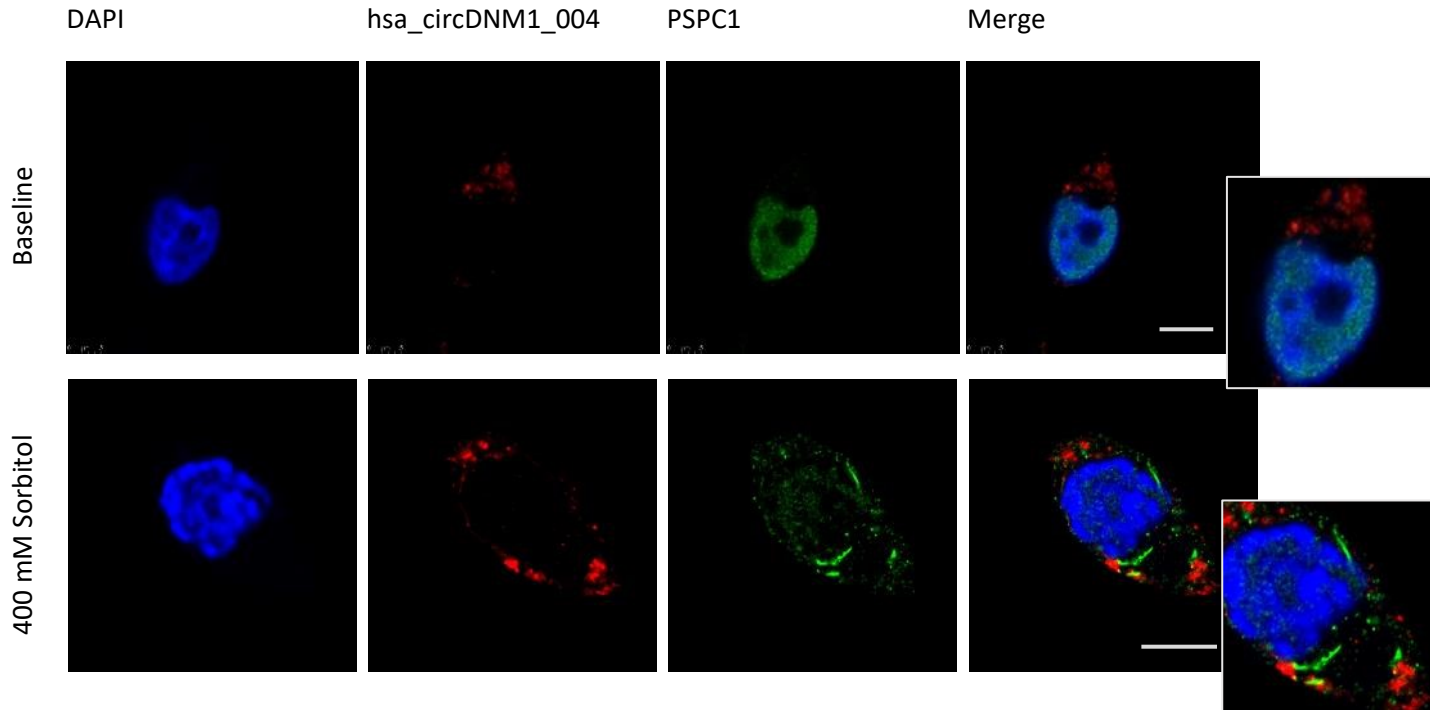


Figure 3-21: Hsa_circDNM1_004 colocalizes with PSPC1 cytoplasmic fibrillar structures under osmotic stress. The upper panel shows unstressed HEK293T cells, and the lower panel shows stressed HEK293T cells (400 mM sorbitol for 4 hours). Scale bars represent 10 μm .

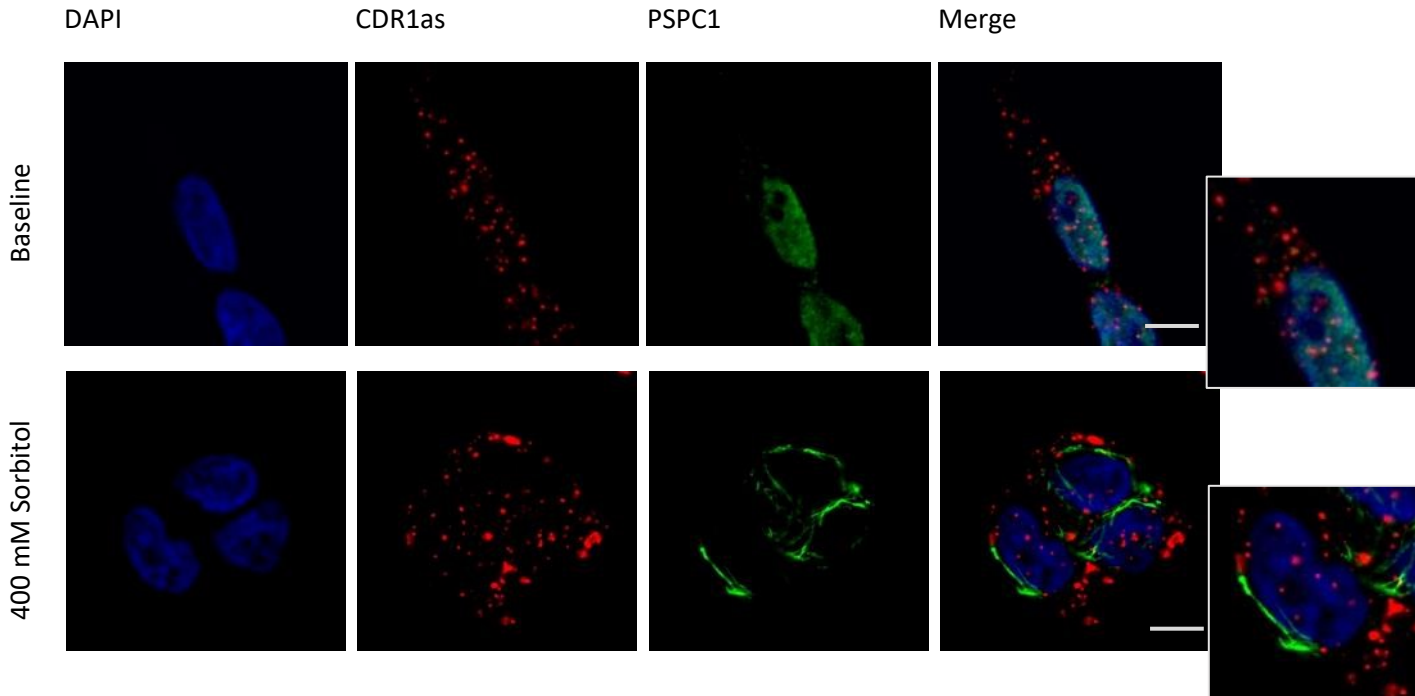


Figure 3-22: CDR1as does not colocalize with PSPC1 cytoplasmic fibrillar structures under osmotic stress. The upper panel shows unstressed HEK293T cells, and the lower panel shows stressed HEK293T cells (400 mM sorbitol for 4 hours). Scale bars represent 10 μ m.

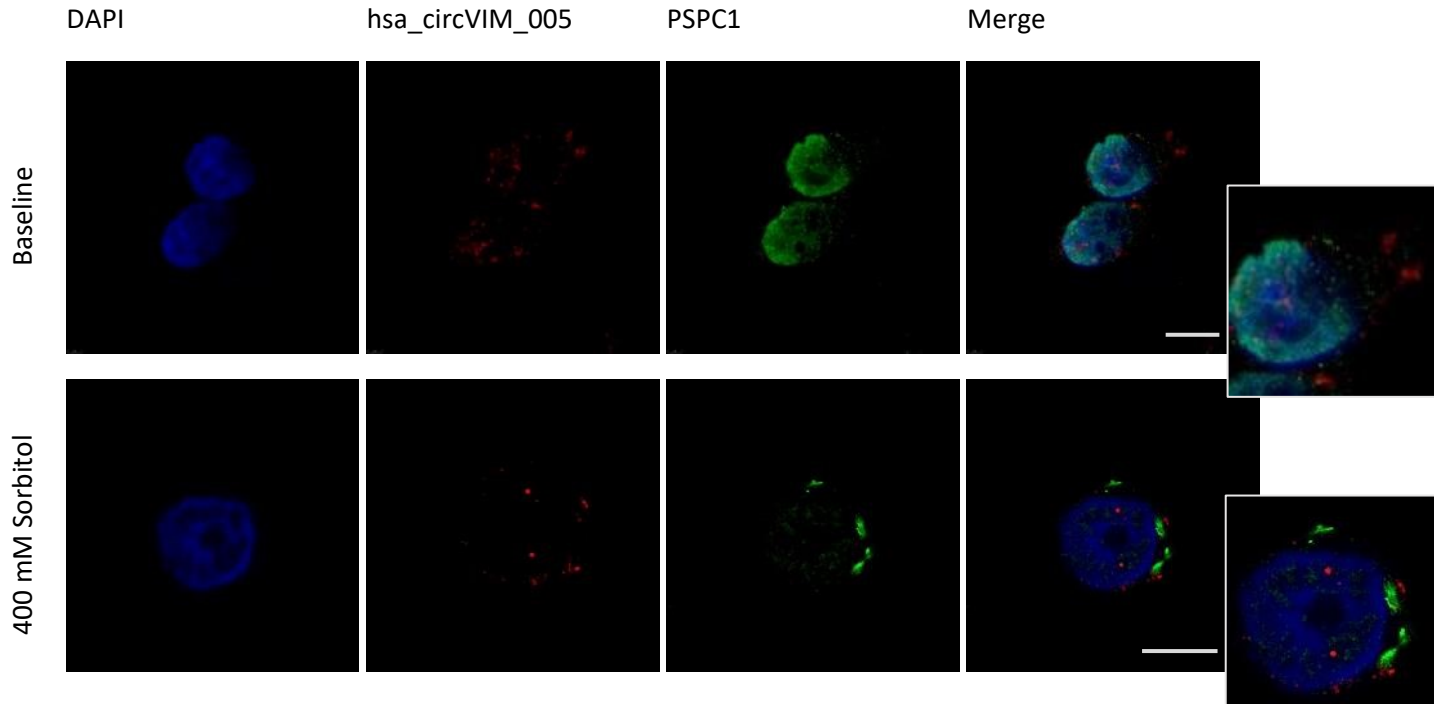


Figure 3-23: Hsa_circVIM_005 does not colocalizes with PSPC1 cytoplasmic fibrillar structures under osmotic stress. The upper panel shows unstressed HEK293T cells, and the lower panel shows stressed HEK293T cells (400 mM sorbitol for 4 hours). Scale bars represent 10 μm .

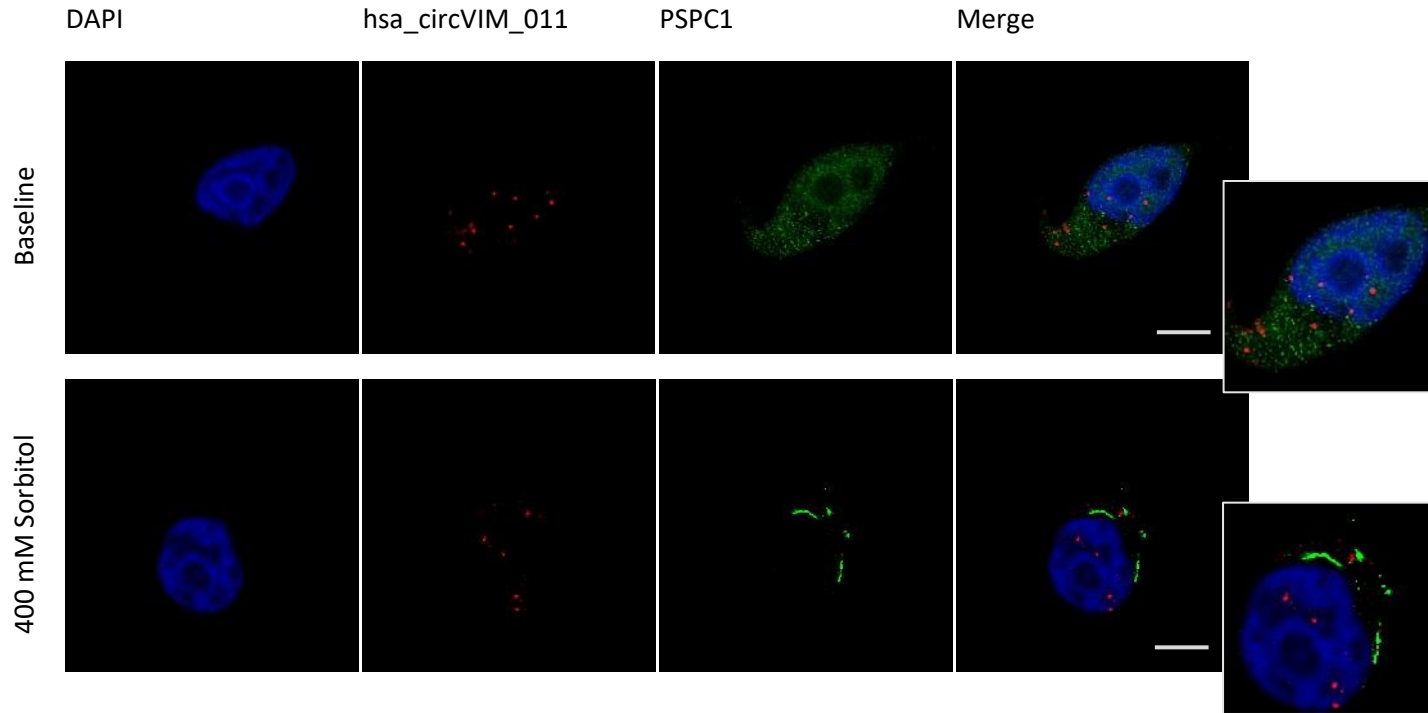


Figure 3-24: Hsa_circVIM_011 does not colocalize with PSPC1 cytoplasmic fibrillar structures under osmotic stress. The upper panel shows unstressed HEK293T cells, and the lower panel shows stressed HEK293T cells (400 mM sorbitol for 4 hours). Scale bars represent 10 μm .

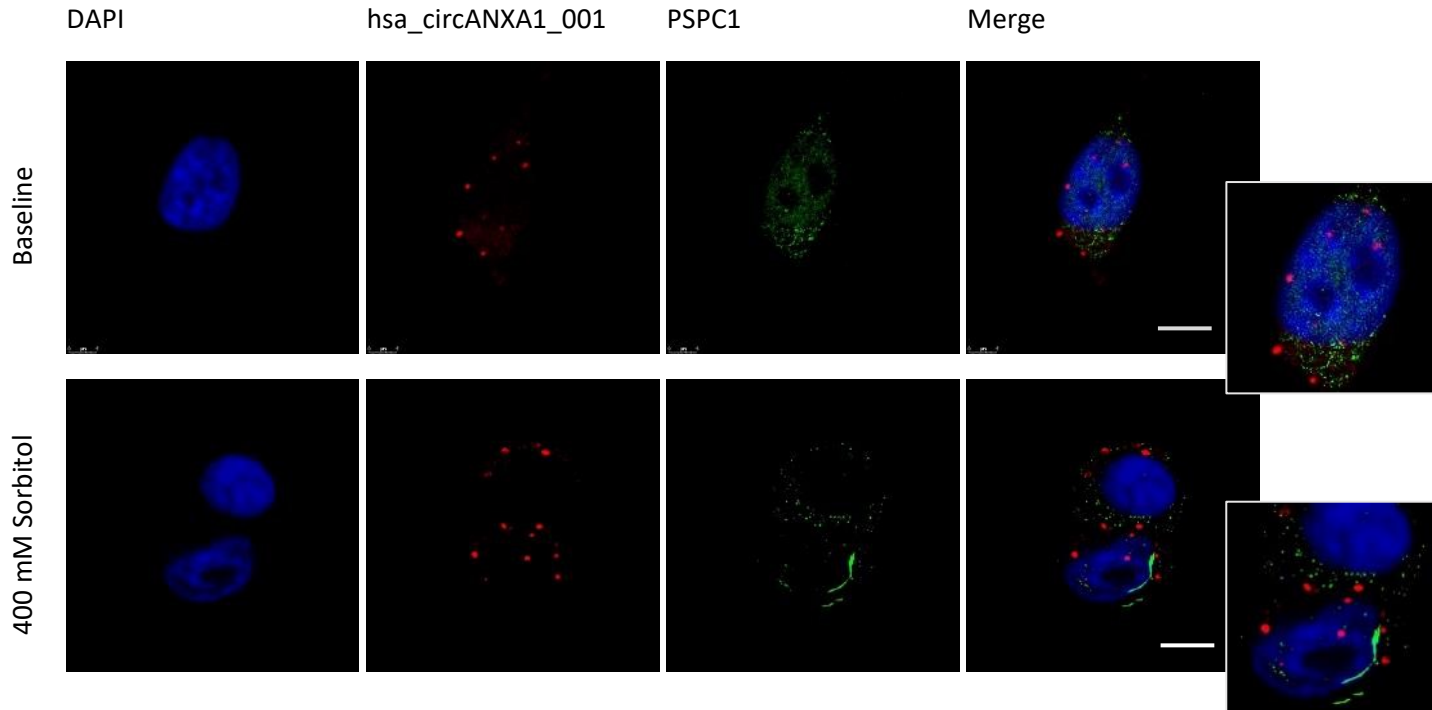


Figure 3-25: Hsa_circANXA1_001 does not colocalize with PSPC1 cytoplasmic fibrillar structures under osmotic stress. The upper panel shows unstressed HEK293T cells, and the lower panel shows stressed HEK293T cells (400 mM sorbitol for 4 hours). Scale bars represent 10 μm .

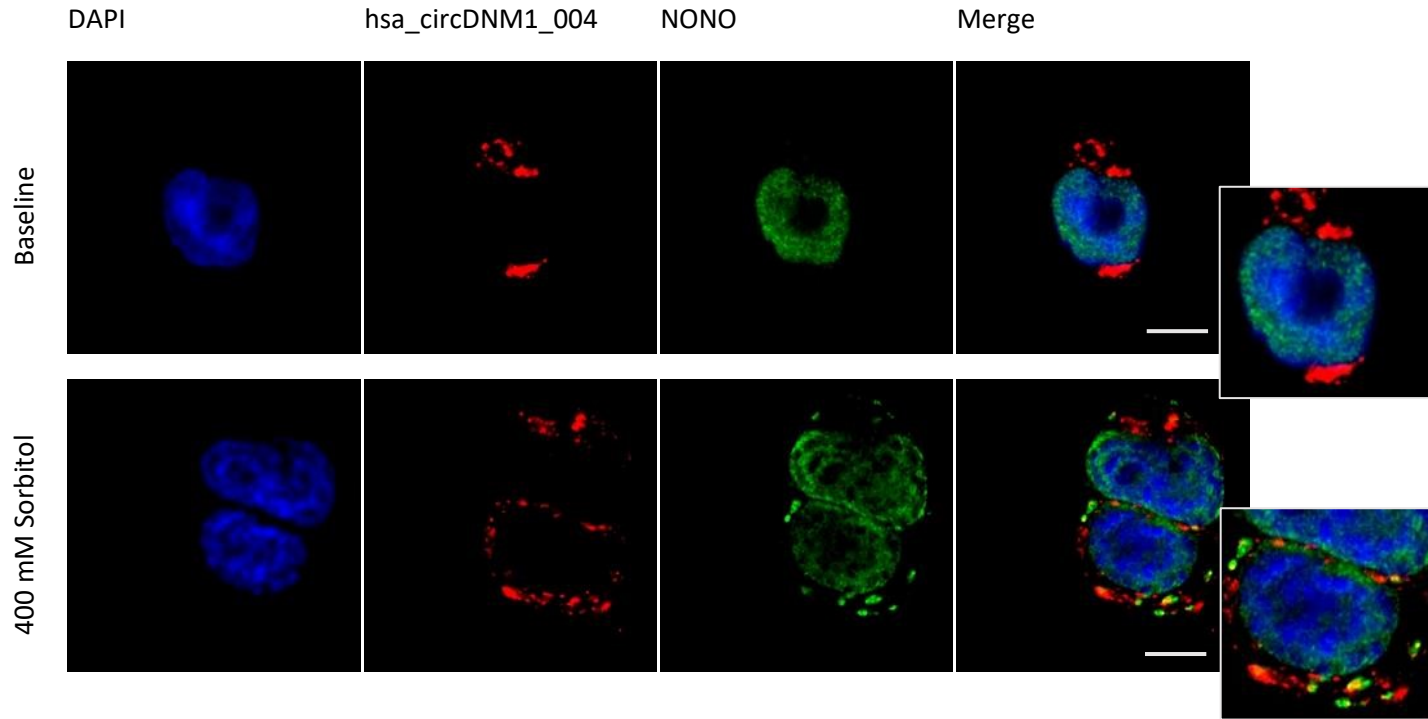


Figure 3-26: Hsa_circDNM1_004 colocalizes with NONO positive cytoplasmic structures under osmotic stress. The upper panel shows unstressed HEK293T cells, and the lower panel shows stressed HEK293T cells (400 mM sorbitol for 4 hours). Scale bars represent 10 μm .

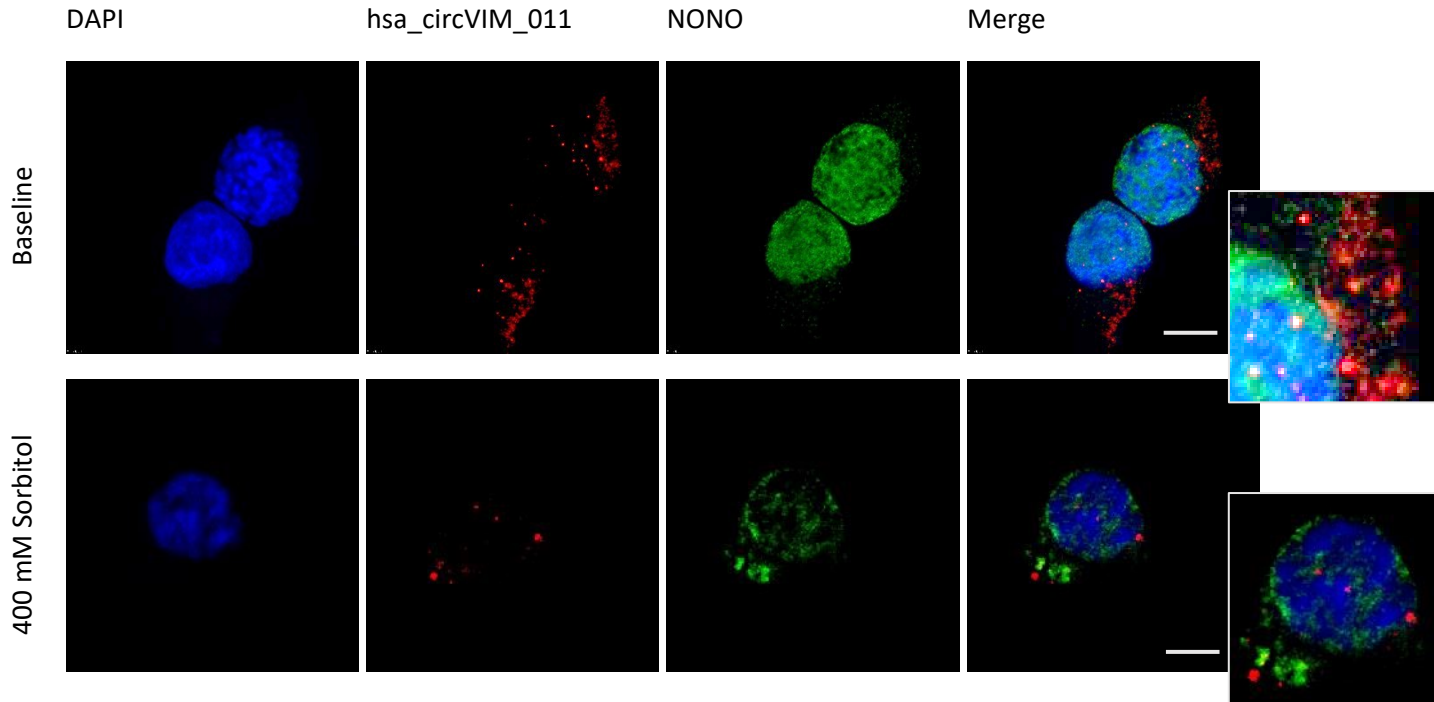


Figure 3-27: Hsa_circVIM_011 colocalizes with NONO positive cytoplasmic structures under osmotic stress. The upper panel shows unstressed HEK293T cells, and the lower panel shows stressed HEK293T cells (400 mM sorbitol for 4 hours). Scale bars represent 10 μm .

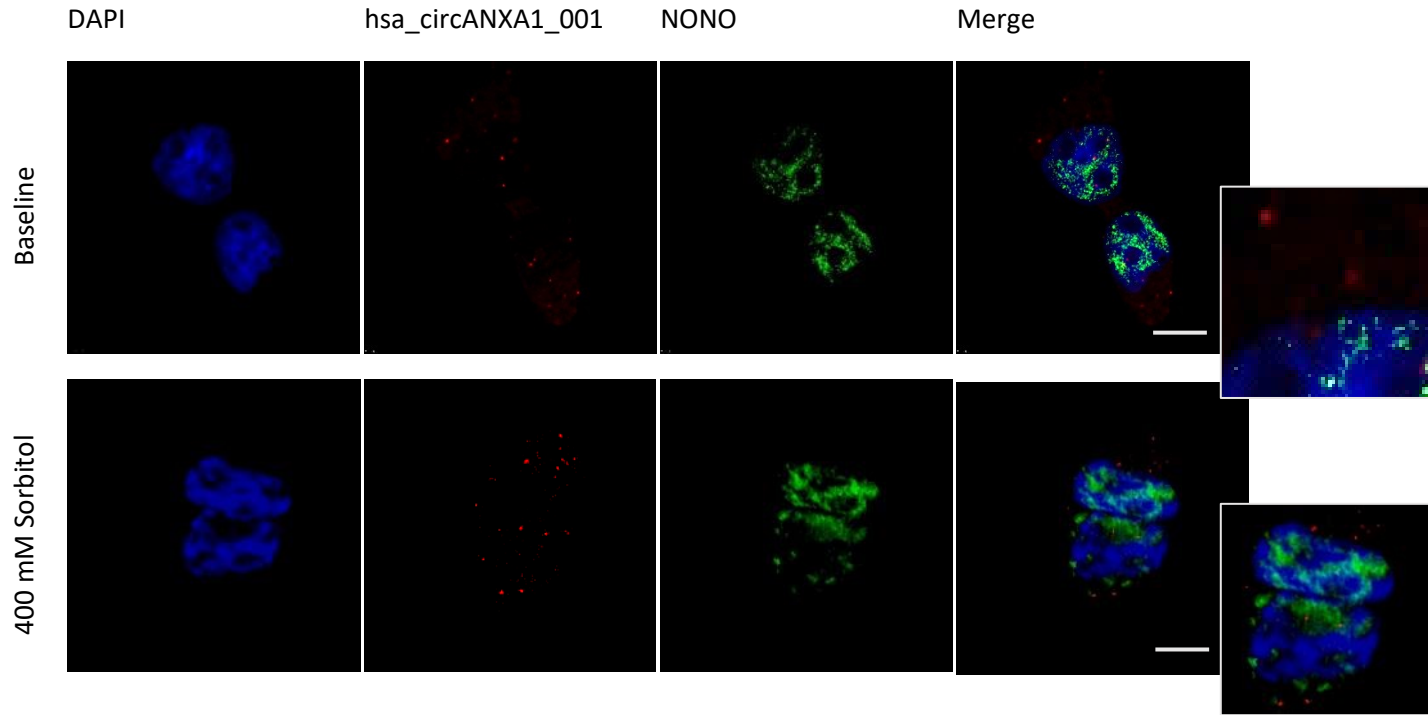


Figure 3-28: Hsa_circANXA1_001 does not colocalize with NONO positive paraspeckles in the nucleus of HEK293T cells under osmotic stress. The upper panel shows unstressed HEK293T cells, and the lower panel shows stressed HEK293T cells (400 mM sorbitol for 4 hours). Scale bars represent 10 μm .

3.3.2.2 3-D analysis showed colocalization between circRNAs with markers of RNP granules

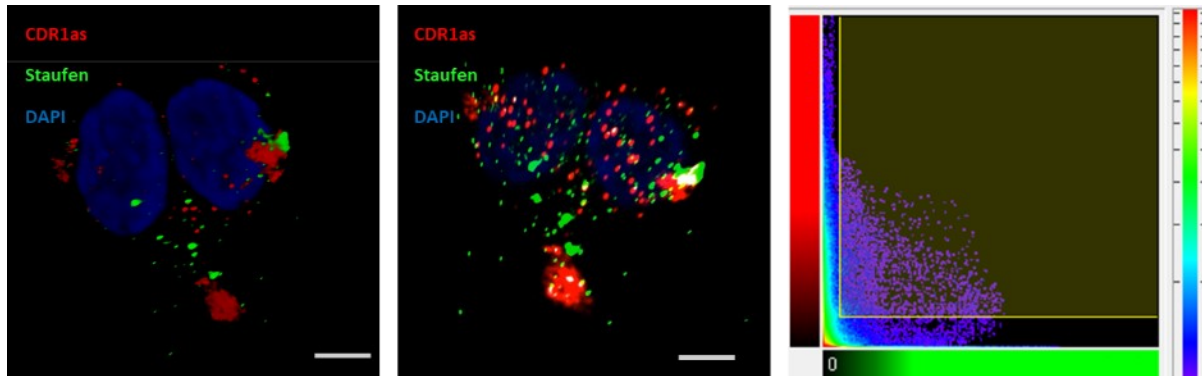
In the previous section, I showed colocalization of circRNAs with specific markers of RNP granules using 2-D merge images following FISH and IF. But that visual evaluation did not define the degree of colocalization. Therefore, I used z-series imaging to reconstruct 3-D images using LASX software. I also used Imaris software to acquire a colocalization channel which is indicated by white colour. Three-dimensional colocalization studies for circRNAs and RNP granule markers could not confirm all the colocalizations which were observed in 2-D images. As previously discussed, 2-D imaging is not as accurate as 3-D imaging because of limitation of 2-D imaging in distinguishing a true colocalization from the overlapping of signals with similar intensity which are not colocalized in the same position.

3-D imaging showed that CDR1as, hsa_circVIM_005, and hsa_circDNM1_004 circRNAs colocalize with Staufen, TIA-1, and Dcp1 as markers of transport granules, stress granules, and P-bodies, respectively. CircRNA hsa_circDNM1_004 also colocalized with PSPC1 and NONO which are markers of paraspeckles. Figure 3-29 to Figure 3-32 are showing examples of 3-D images for candidate circRNAs acquired by LASX software (left panel) and Imaris software (middle panel). However, 3-D imaging using LAS X software could not confirm colocalization observed for hsa_circVIM_011 and Dcp1 and NONO in 2-D images (Figure 3-33 and Figure 3-34, respectively).

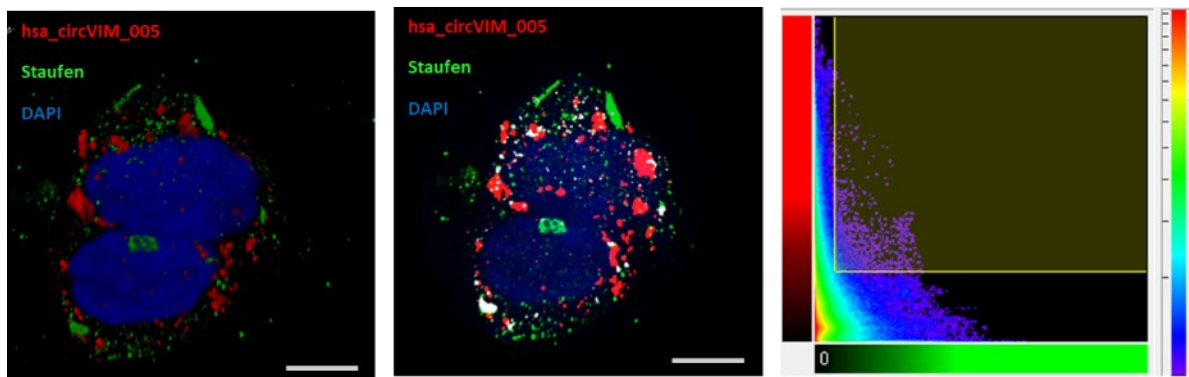
The qualitative indication of the degree of colocalizations is represented graphically in scatterplots (also called cytofluorogram) (Demandolx & Davoust, 1996). In these scatterplots, the intensity of the red color is plotted against the intensity of the green color for each voxel. Voxel is a basic picture element for composing 3D images. Every voxel in the image is plotted in the scatterplots based on its intensity level from each channel. This diagram reflects the distribution of pairs of voxel intensities occurring in the two selected channels. In this analysis, red intensity is shown on the x-axis and represents circRNA and green intensity is shown on the y-axis and represents RNP granule's marker. The density (frequency) of the voxels is visualized as a heat map-like coloring in the scatterplot. The highest number of voxels are visualized by red points and the lowest number of voxels are visualized by purple points. The hatched region with bolded yellow lines is indicating established thresholds. The bolded yellow lines define the

intensity threshold for the red and green channels. Only voxels with an intensity value above the established threshold can be considered for the colocalization analysis. Analyzing scatterplots showed that the points of any of the scatterplots did not cluster around a straight line, whose slope reflects the ratio of the fluorescence of the two colors. The pattern of the distribution of points in the scatterplots showed only a low number of voxels from each channel correlate to each other which means partial colocalization for every pair of circRNAs and marker of RNP granules (Figure 3-29 to Figure 3-32, right panels).

A



B



C

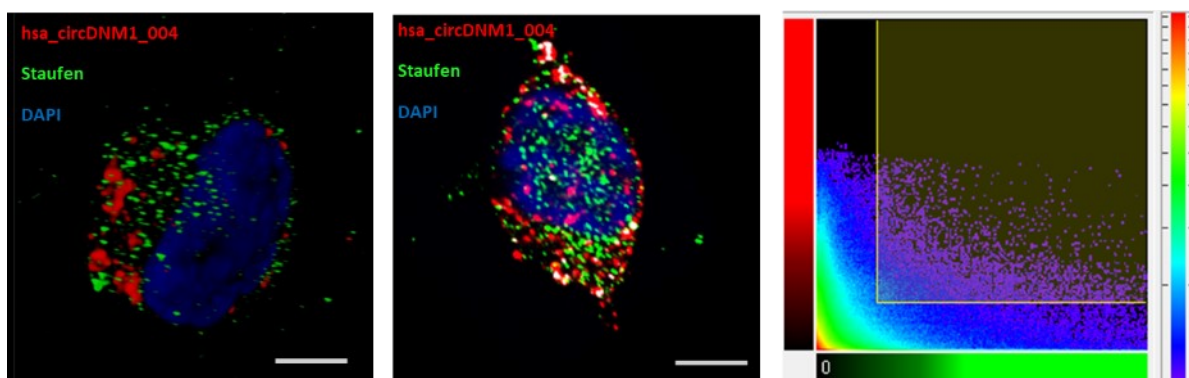
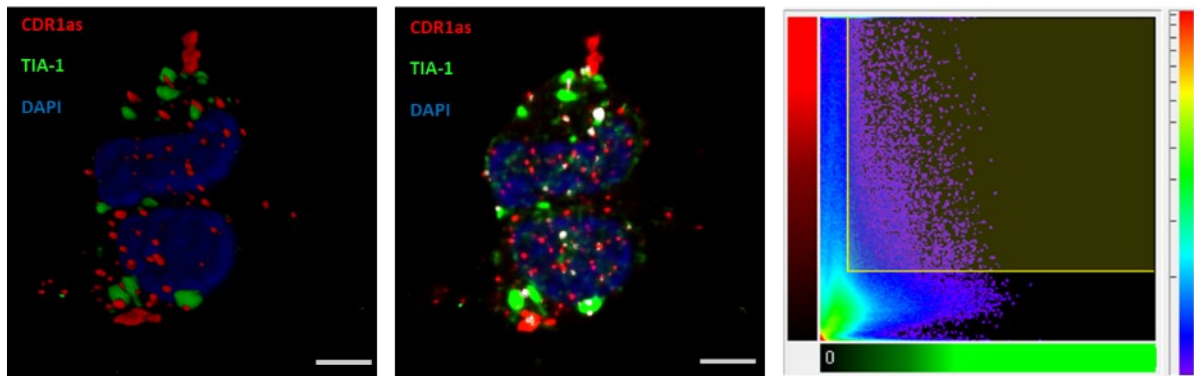


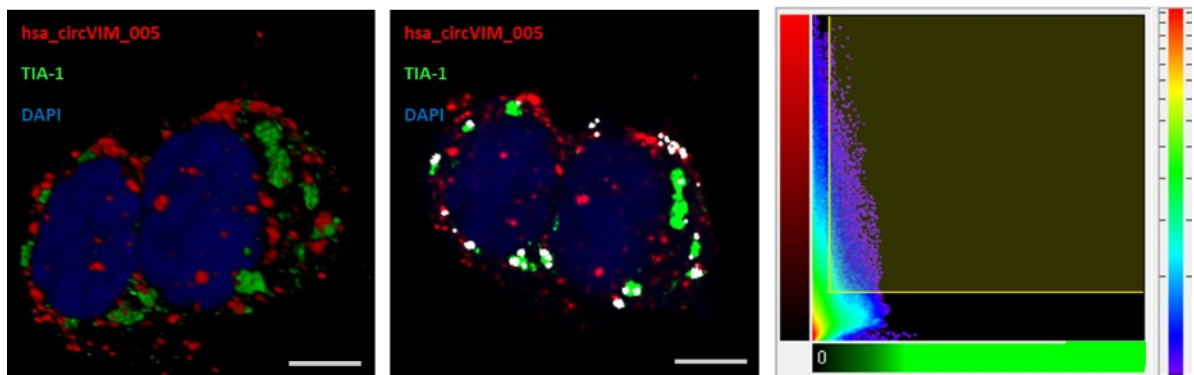
Figure 3-29: CircRNAs partially colocalize with Staufen positive transport granules in HEK293T cells under osmotic stress. Panel (A), (B), and (C) are showing colocalization of CDR1as, hsa_circVIM_005, and hsa_circDNM1_004 with Staufen positive transport granules, respectively. In each panel, the left image is showing one example of 3-D images acquired by LASX software for every candidate circRNA. The middle image is showing one example of 3-D

images acquired by Imaris software for every candidate circRNA which is indicating partial colocalization by white color. The right images are showing the intensity scatterplots. The hatched region with bolded yellow lines in the upper right quadrant defines the intensity threshold for the red and green channels. This region represents colocalized voxels. The pattern of the distribution of points and their color (red indicating the highest frequency of colocalized voxels; purple indicating the lowest frequency of colocalized voxels) in the scatterplots showed only a low number of voxels from each channel correlate to each other which means partial colocalization. All cells were imaged following stress (400 mM sorbitol for 4 hours, as previously described). Scale bars represent 5 μm .

A



B



C

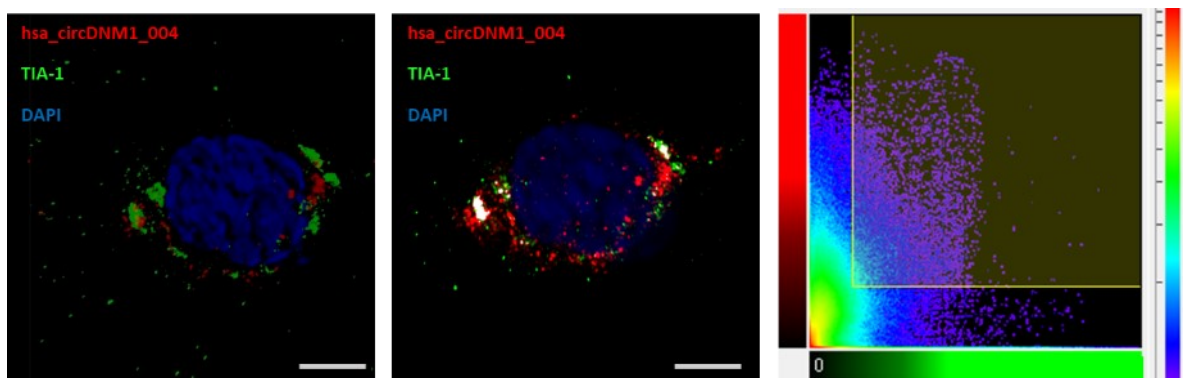
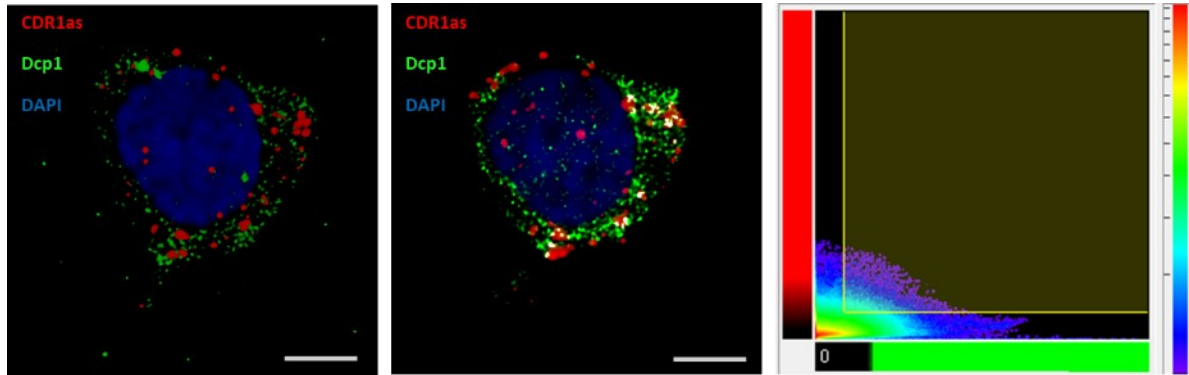


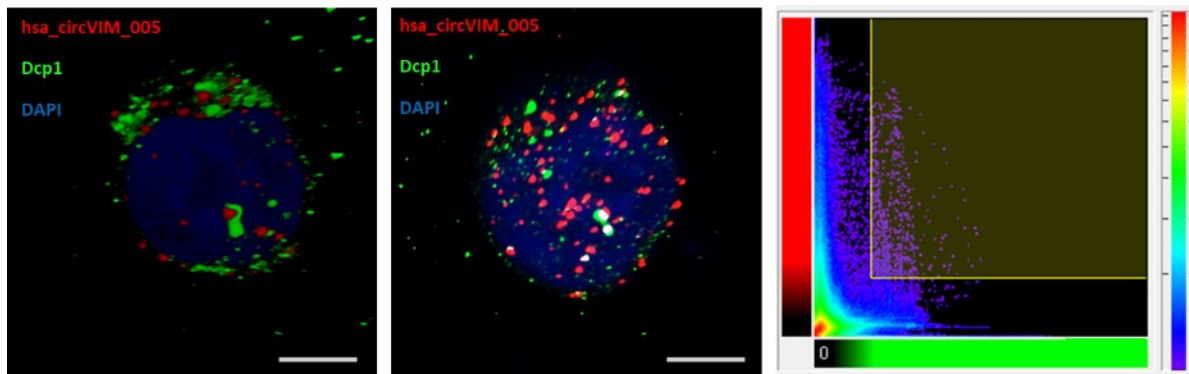
Figure 3-30: CircRNAs colocalize with TIA-1 positive stress granules in HEK293T cells under osmotic stress. Panel (A), (B), and (C) are showing colocalization of CDR1as, hsa_circVIM_005, and hsa_circDNM1_004 with TIA-1 positive stress granules, respectively. In each panel, the left image is showing one example of 3-D images acquired by LASX software for every candidate circRNA. The middle image is showing one example of 3-D images acquired

by Imaris software for every candidate circRNA which is indicating partial colocalization by white color. The right images are showing the intensity scatterplots. The hatched region with bolded yellow lines in the upper right quadrant defines the intensity threshold for the red and green channels. This region represents colocalized voxels. The pattern of the distribution of points and their color (red indicating the highest frequency of colocalized voxels; purple indicating the lowest frequency of colocalized voxels) in the scatterplots showed only a low number of voxels from each channel correlate to each other which means partial colocalization. All cells were imaged following stress (400 mM sorbitol for 4 hours, as previously described). Scale bars represent 5 μm .

A



B



C

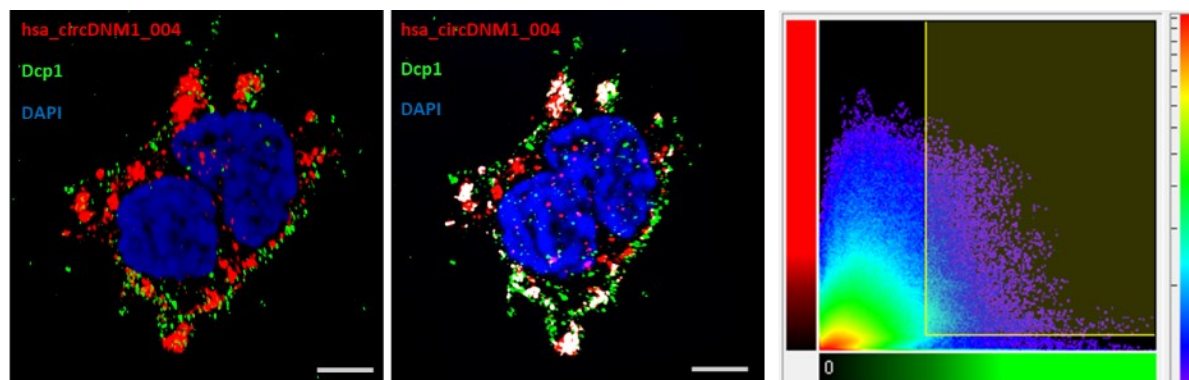
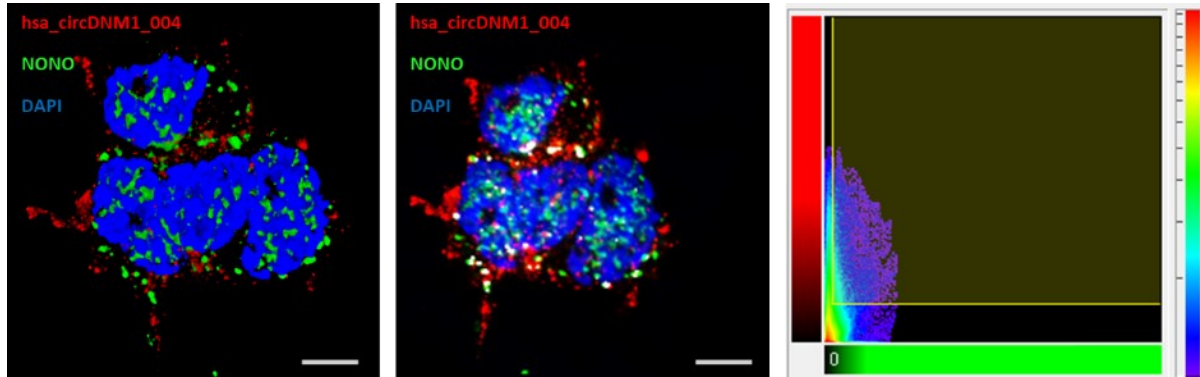


Figure 3-31: CircRNAs colocalize with Dcp1 positive P-bodies in HEK293T cells under osmotic stress. Panel (A), (B), and (C) are showing colocalization of CDR1as, hsa_circVIM_005, and hsa_circDNM1_004 with Dcp1 positive P-bodies, respectively. In each panel, the left image is showing one example of 3-D images acquired by LASX software for every candidate circRNA. The middle image is showing one example of 3-D images acquired by

Imaris software for every candidate circRNA which is indicating partial colocalization by white color. The right images are showing the intensity scatterplots. The hatched region with bolded yellow lines in the upper right quadrant defines the intensity threshold for the red and green channels. This region represents colocalized voxels. The pattern of the distribution of points and their color (red indicating the highest frequency of colocalized voxels; purple indicating the lowest frequency of colocalized voxels) in the scatterplots showed only a low number of voxels from each channel correlate to each other which means partial colocalization. All cells were imaged following stress (400 mM sorbitol for 4 hours, as previously described). Scale bars represent 5 μm .

A



B

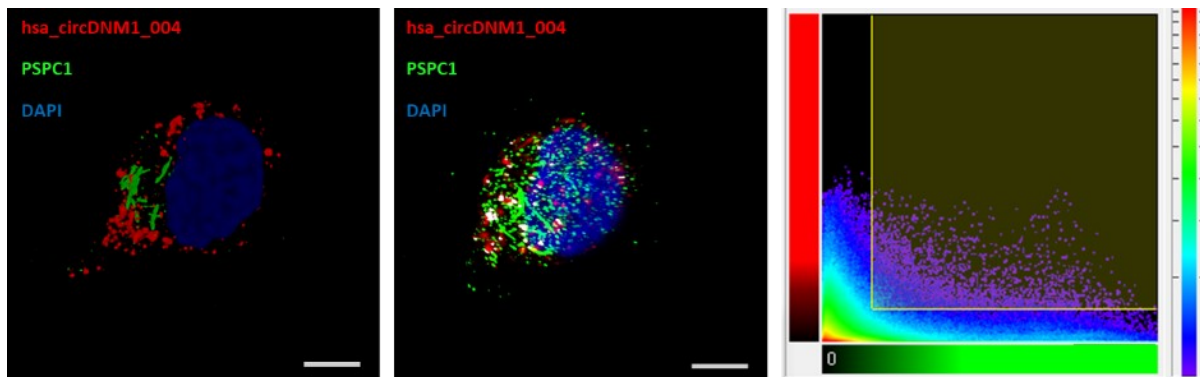


Figure 3-32: Hsa_circDNM1_004 CircRNA colocalizes with PSPC1 and NONO in HEK293T cells under osmotic stress. Panel (A) and (B) are showing colocalization of hsa_circDNM1_004 with PSPC1 and NONO as the markers for nuclear paraspeckles, respectively. However, both markers showed nuclear and cytoplasmic distribution in response to stress. PSPC1 makes fibrillar structures and NONO makes granular structures in the cytoplasm which show partial colocalization with hsa_circDNM1_004. In each panel, the left image is showing one example of 3-D images acquired by LASX software for every candidate circRNA. The middle image is showing one example of 3-D images acquired by Imaris software for every candidate circRNA which is indicating partial colocalization by white color. The right images are showing the intensity scatterplots. The hatched region with bolded yellow lines in the upper right quadrant defines the intensity threshold for the red and green channels. This region represents colocalized voxels. The pattern of the distribution of points and their color (red indicating the highest frequency of colocalized voxels; purple indicating the lowest frequency of colocalized voxels) in the scatterplots showed only a low number of voxels from each channel correlate to

each other which means partial colocalization. All cells were imaged following stress (400 mM sorbitol for 4 hours, as previously described). Scale bars represent 5 μm .

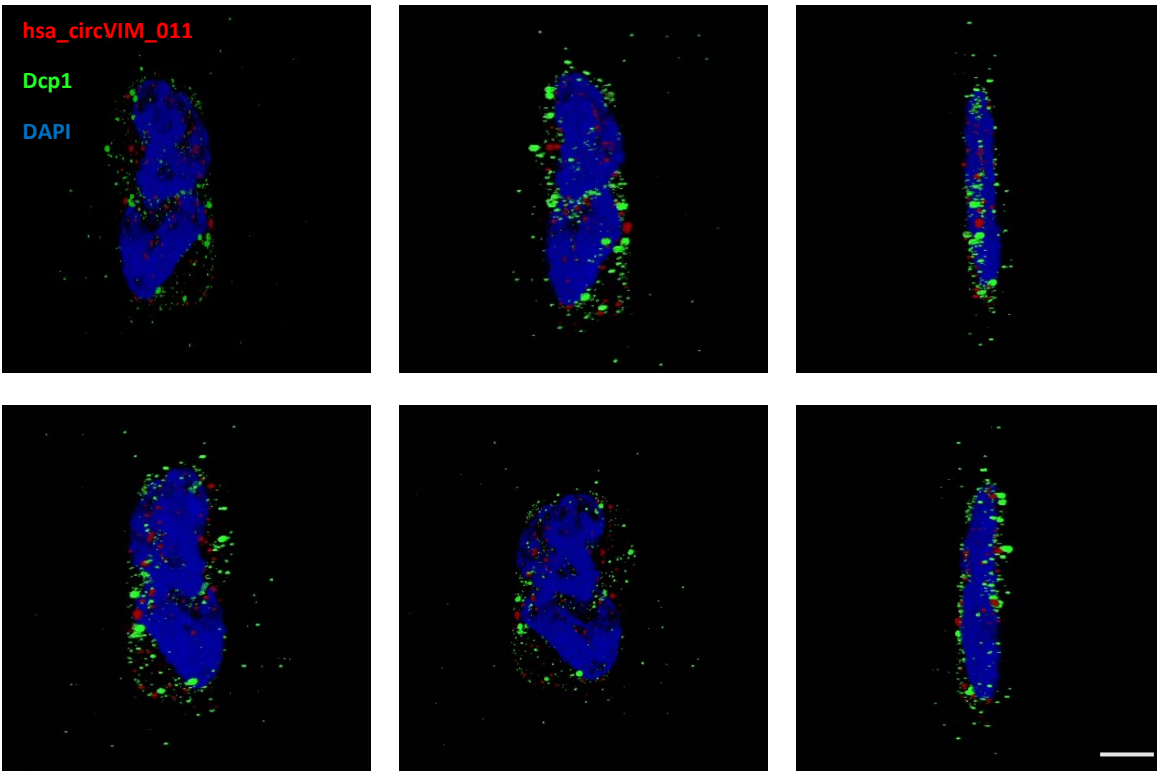


Figure 3-33: Hsa_circVIM_011 CircRNA does not colocalize with Dcp1 positive P-bodies in HEK293T cells under osmotic stress. In order to show this 3-D image in 2-D, I present different angle of the cells in separate images. Z-stack images were acquired using Leica TSC SP8 confocal microscope and 3-D image were rendered using LAS X software. The cells were imaged following stress (400 mM sorbitol for 4 hours, as previously described). Scale bar represents 10 μm .

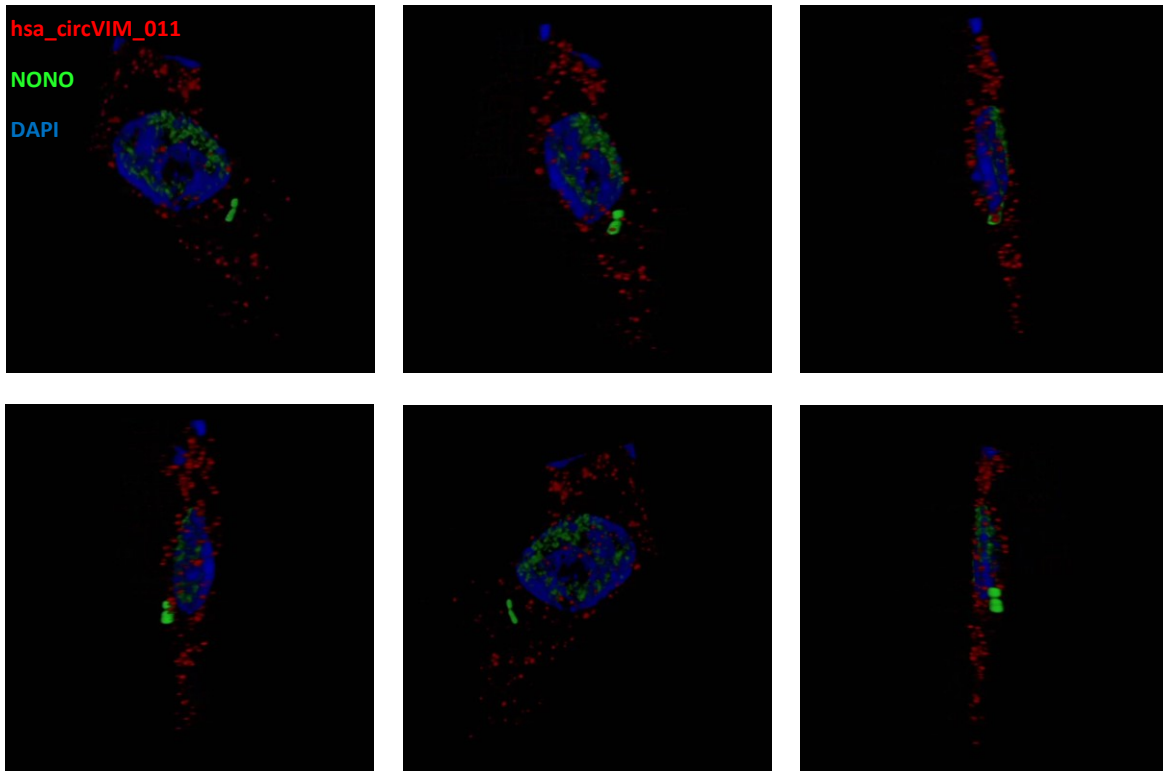


Figure 3-34: Hsa_circVIM_011 CircRNA does not colocalize with NONO positive cytoplasmic structures in HEK293T cells under osmotic stress. In order to show this 3-D image in 2-D, I present different angles of the cells in separate images. Z-stack images were acquired using Leica TSC SP8 confocal microscope and 3-D image were rendered using LAS X software. The cells were imaged following stress (400 mM sorbitol for 4 hours, as previously described). Scale bar represents 10 μm .

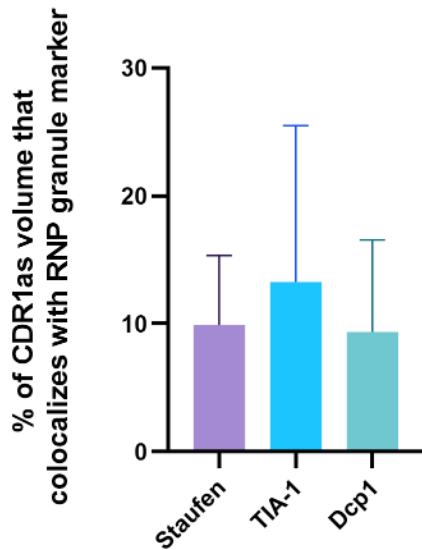
3.3.2.3 Quantitative and statistical evaluation of colocalization

To quantify the level of colocalization observed visually, I used the “coloc option” in the Imaris software. I selected the intensity-based correlation method which is one of the quantitative approaches for colocalization analysis.

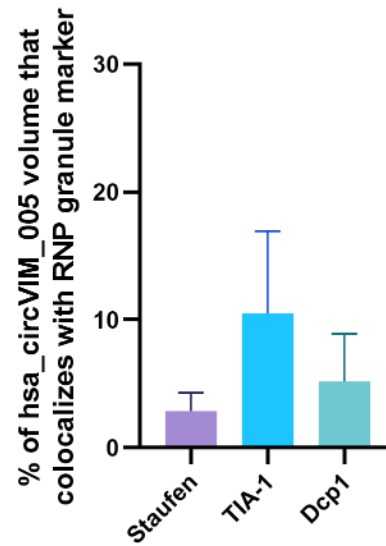
To quantify the extent of circRNA colocalization with each individual marker of RNP granule, I used the statistics provided by Imaris for the colocalized channel. This statistic shows the percentage of circRNA volume that is colocalized with the marker of RNP granules. This value is calculated by dividing the total count of colocalized voxels by the total count of red channel voxels (representing circRNA) multiply by 100. In this statistic, only voxels with intensity above the established threshold were counted. This data showed that the distribution of circRNAs varies in different RNP granules. I also used this method to quantify the percentage volume of CDR1as colocalized with FUS and TDP-43 positive aggregates. The percentage of each circRNA volume which colocalized with each marker of RNP granules is presented in the bar chart classified based on circRNAs (Figure 3-35).

Different percentages of CDR1, hsa_circVIM_005, and hsa_circDNM1_004 volumes above established threshold colocalized with different markers of RNP granules. The highest percentage of CDR1as and hsa_circVIM_005 volume above threshold (13.26 ± 12.22 and 10.49 ± 6.45 , respectively) colocalized with TIA-1 positive stress granules in HEK293T cells in response to osmotic stress (Figure 3-35 A and B, respectively). A large percentage (19.62 ± 8.75) of hsa_circDNM1_004 volumes above threshold colocalized with Dcp-1 positive P-bodies and only a small percentage (less than 10%) of hsa_circDNM1_004 volumes above threshold colocalized with PCPC1 fibrillar structure in HEK293T cells under osmotic stress (Figure 3-35 C). Some of candidate circRNAs seems to also colocalize with marker of RNP granules in baseline condition which was not analyzed in this study and needs to be addressed in the future.

A



B



C

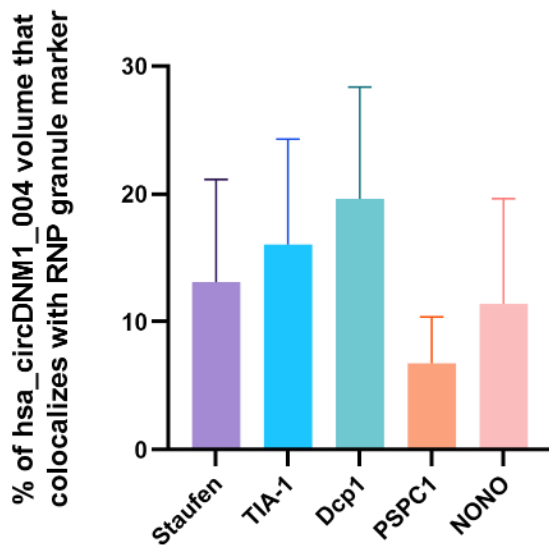


Figure 3-35: Comparison of quantification of the percentage of circRNAs volume above established threshold colocalized with the marker of RNP granule in HEK293T cells under osmotic stress. A) Different percentages of CDR1as volume above threshold colocalize with Staufen, TIA-1, and Dcp1. It seems CDR1as tends to colocalize more with TIA-1 positive stress granules than other RNP granules in HEK293T cells under stress. B) A larger percentage of hsa_circVIM_005 volume colocalize with TIA-1 positive stress granule than other markers of

RNP granules. C) A larger percentage of hsa_circDNM1_004 colocalize with Dcp1 positive P-bodies than other RNP granules. Quantifications were performed on 3 to 5 z-series images. The bar represents mean (n=3-5) \pm SD.

In order to determine whether the observed co-occurrence or correlation is just a random coincidence or a true colocalization, I used the Pearson's correlation coefficient (PCC) in ROI (region of interest) volume provided by channel statistics in coloc tool in Imaris software. PCC is a statistic for quantifying the degree of colocalization. Here PCC gives a measure of the co-distribution of fluorescence signals for circRNAs and marker of RNP granules within an image. The formula for PCC in this study is given below:

$$\text{PCC} = \frac{\sum_i (R_i - \bar{R}) \times (G_i - \bar{G})}{\sqrt{\sum_i (R_i - \bar{R})^2 \times \sum_i (G_i - \bar{G})^2}} \quad (3-1)$$

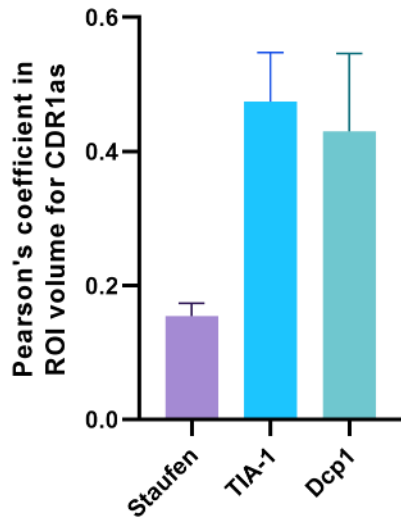
R_i and G_i refer to the intensity values of the red and green channels, respectively, of pixel i , and \bar{R} and \bar{G} refer to the mean intensities of the red and green channels, respectively, across the entire image. The PCC values range between 1 and -1. A value of 1 represents perfect correlation, 0 no colocalization, and -1 perfect inverse colocalization (Zhang et al, 2014). In the other words, PCC=1 is describing a perfectly linear relation between the intensities of two fluorophores, whereas PCC=-1 means the intensities of two fluorophores are related inversely. PCC= 0 indicates a total absence of structured relation between the intensities of two fluorophores. Mid-range PCC are more difficult to interpret but are a good trend for comparing the colocalization (Dunn et al, 2011).

Analyzing PCC values in ROI volumes of every pair of candidates circRNA and marker of RNP granule showed mid-range values (between 0 and 1) not extreme values (1 and -1) which is indicating partial colocalization. This data also showed that the degree of colocalization of circRNAs in the same RNP granule differs from each other. The PCC values in ROI volumes of every pair of circRNAs and RNP granule markers are shown in graphs A, B, and C of Figure 3-36. The information in this graph shows that the distribution of selected circRNAs varies in a different type of candidate RNP granules.

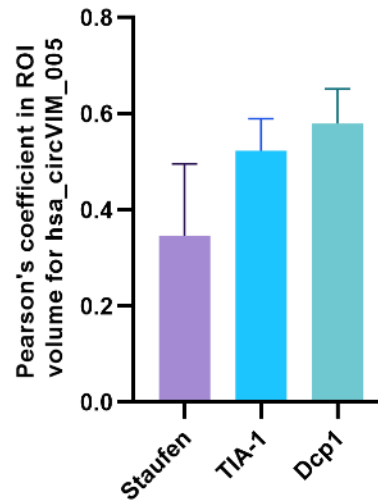
Altogether, this data showed that hsa_circDNM1_004 has a higher colocalization degree with all the candidate markers of RNP granules under stress conditions. This observation as well as 3-D colocalization analysis which showed partial colocalization for candidate circRNAs with the

marker of RNP granules under stress condition, might indicate the participation of these circRNAs in the biology of RNP granule.

A



B



C

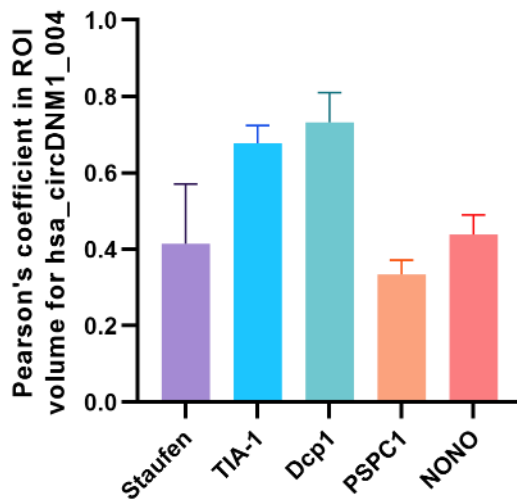


Figure 3-36: Comparison of the degree of colocalization between circRNAs and RNP granule markers in HEK293T cells under stress using PCC values in ROI volumes. A) Quantification of the degree of colocalization between CDR1as and Staufen, TIA-1, and Dcp1 showed a higher Pearson coefficient for colocalized voxels for CDR1as with TIA-1 and Dcp1

than Staufen. B) Quantification of the degree of colocalization between hsa_circVIM_005 and Staufen, TIA-1, and Dcp1 showed a higher Pearson coefficient for colocalized voxels for hsa_circVIM_005 with TIA-1 and Dcp1 than Staufen. C) Quantification of the degree of colocalization between hsa_circDNM1_004 and Staufen, TIA-1, Dcp1, PSPC1, and NONO showed a higher Pearson coefficient for colocalized voxels for hsa_circDNM1_004 with TIA-1 and Dcp1 than other markers.

Chapter 4

4 Discussion and conclusion

4.1 Overexpression of circRNAs encoded by cytoskeletal genes in ALS may affect their host gene expression or function

The observations of altered expression of both coding and non-coding RNAs in ALS has been taken to support the proposal that ALS is a disorder of RNA metabolism (Droppelmann et al, 2014; Strong, 2010). Such evidence includes spinal cord mRNA profiling by microarray which demonstrated a differential gene expression in spinal cord tissues of ALS patients compared to controls (Dangond et al, 2004; Offen et al, 2009). More recently, RNA-Seq studies have also revealed differential gene expression in ALS versus controls (Brohawn et al, 2016; D'Erchia et al, 2017; Prudencio et al, 2015). Moreover, a previous study from our lab has reported a massive dysregulation in miRNA expression in ALS (Campos-Melo et al, 2013a).

Previously, Dr. Danae Campos-Melo from our lab had conducted a whole transcriptome RNA-seq on ribosomal RNA-depleted RNA samples from ALS and the control lumbar spinal cord (unpublished observations). Using Partek Flow software, Dr Campos-Melo identified a pool of differentially expressed coding and non-coding RNAs in ALS that includes differentially expressed circRNAs. From this analysis, I selected a group of 4 circRNAs that were upregulated in ALS (≥ 2.5 fold change) and that are expressed from genes encoding cytoskeletal proteins: vimentin, annexin A1, and dynamin 1. Mature circRNA sequences and potential binding sites for RBPs were defined using the CircInteractome database (circInteractome). *In silico* analysis using this database for the candidate circRNAs indicated that they potentially have multiple binding sites for the RBPs that are known to be involved in varying aspects of RNA metabolism within RNP granules.

It is of note that when using real-time PCR with specific divergent primers detecting the back-splice junction of circRNAs on RNase R-depleted RNA from the same ALS and control samples, I did not reproduce the same results as RNA-seq with respect to the previously observed differential expression. Because RNA-seq quantifies individual sequence reads aligned to a reference sequence, it produces absolute rather than relative expression values which enable the detection of subtle changes in expression, down to 10%. This might explain the difference

between RNA-seq and real-time PCR. Moreover, multiple circRNAs can be processed from a single gene locus with different numbers of exons included through a process named alternative circularization (Zhang et al, 2014). Interestingly, all the candidate circRNAs which are expressed from cytoskeletal genes are multiple exonic and have multiple isoforms (for example, 26 different circRNA isoforms have been detected to be expressed from the DNMT1 gene).

The observation of multiple bands on agarose gels for at least two of the candidate circRNA used in this study made me speculate about the detection of multiple circRNA isoforms. However, the analysis of all the isoforms annotated for the candidate circRNAs did not show overlaps in junction sequences.

In order to understand the observed overexpression of circRNAs from cytoskeletal genes in spinal cord tissue of ALS patients from RNA-seq data, it might be helpful to review the studies about the expression and function of circRNAs in the mammalian nervous system. CircRNAs are abundant, conserved, and dynamically expressed lncRNAs in the mammalian nervous system (Hanan et al, 2017; Rybak-Wolf et al, 2015). Interestingly, several genes that encode circRNAs are exclusively expressed in the central nervous system. circRNAs abundance is also remarkably higher in the brain than in other tissues (You et al, 2015). Generally, circRNAs are overexpressed during neuronal differentiation and this differential expression is often independent of their linear counterparts (Kristensen et al, 2018b). Age-related overexpression of circRNAs in brain tissues is found across different species suggesting their possible involvement in aging and age-related diseases in the central nervous system such as ALS. Interestingly, this age accumulation of circRNAs is not largely relevant to the mRNA expression of their host genes (Cai et al, 2019). In the mammalian brain, circRNAs can be expressed from approximately 20% of protein-coding genes at the expense of their linear cognates. Thus, the production of circRNA could be an important regulator for mRNA synthesis in the central nervous system (Rybak-Wolf et al, 2015). Observed overexpression of circRNAs encoded by cytoskeletal genes might be a regulatory process for the expression of their host genes in response to cytoskeletal defects that occurred in ALS pathogenesis (Julien et al, 2005).

It has been discussed that generally there is no simple correlation between expression levels of circRNAs with the expression of their linear counterparts (Salzman et al, 2013b). It has also been

reported that most of the discovered circRNAs contain complete exons and are expressing from protein coding host genes. *In vitro* experiments demonstrate that spliceosome and RNA polymerase II (RNA pol II) mediate circRNAs expression through the back-splicing process (Braun et al, 1996; Pasmán et al, 1996). Typically, those exons that undergo back splicing cannot be alternatively spliced. circRNAs production can compete with pre-mRNA alternative splicing suggesting the role of circRNAs in the regulation of mRNA expression (Salzman et al, 2012). Ashwal-Fluss et al. conducted a comprehensive study of circRNA biogenesis and showed that linear splicing can strongly compete with circRNA biogenesis and reduce circRNA levels. Thus, linear splicing and circRNA biogenesis mutually regulate each other through competing for splice sites (Ashwal-Fluss et al, 2014).

4.2 Downregulation of hsa_circVIM_011 and hsa_circANXA1_001 in HEK293T cells in response to osmotic stress

Both unicellular organisms and cells in multicellular organisms constantly experience exposure to environmental challenges such as oxidative stress, nutrient supply deprivation, pH alteration, temperature changes, and imbalances in osmolarity. Stress exposure to cells modulates several cellular pathways to maximize cell survival through proper adaptation. The alteration of gene expression is an essential component of the response to stresses. Immediately after stress exposure, the transcriptional pattern of the cell changes remarkably. The type of genes which undergo alteration depends on the type of organisms or cells and the type of stress and its strength. Several of those stress-responsive genes are stress-essential genes that are required for adaptation to specific stresses. Stress-induced genes encode the proteins that are responsible for almost all general cell features including RNA metabolism, metabolic adjustment, cell differentiation, cellular transport, and cytoskeletal organization (Auesukaree et al, 2009; Giaever et al, 2002; Ruiz-Roig et al, 2010; Zapater et al, 2007). Moreover, a variety of lncRNAs that play key roles in normal physiological conditions have been shown to also participate in the stress responses (Valadkhan & Valencia-Hipólito, 2015).

There is substantial evidence implicating cellular stress in the pathogenesis of ALS (Barber & Shaw, 2010). Thus, I decided to examine the role of cellular stress on the expression and subcellular localization of candidate circRNAs which were upregulated in ALS patients compared to control patients. In the present study, I observed that the number of fluorescent spots of two candidate circRNAs, hsa_circVIM_011, and hsa_circANXA1_001, is decreased in HEK293T cells in response to osmotic stress (400 mM D-sorbitol). The comparison of the size of this spot in stressed and unstressed cells did not show any significant difference. This data might indicate the decrease in expression of these circRNAs. However, the fluorescence intensity of these spots, as well as the total fluorescence per cell must be also quantified to have a precise examination of the circRNAs' expression using FISH. If I consider this significant decrease in the number of fluorescent spots as an indicator of downregulation of these two candidate circRNAs under stress condition, this contradicts the overexpression of candidate circRNAs observed in ALS. To explain this, it should be mentioned that, although HEK293T cells have some neuronal characteristics, they are not neuronal cells, thus stress-induced circRNAs alterations in this cell line might be different from neuronal cells. Importantly, osmotic stress induced by sorbitol is not able to emulate exactly what is happening in spinal cord tissue in ALS (Hock et al, 2018)

Hsa_circVIM_011, and hsa_circANXA1_001 are transcribed from genes that encode the cytoskeletal related proteins vimentin and annexin A1 that directly interact with actin whose participation in ALS has been discussed in some studies (Esue et al, 2006; Gerke & Moss, 1997; Hensel & Claus, 2018).

Eukaryotic cells construct a dynamic filamentous network using cytoskeletal proteins that provide mechanical stability of the cells. Cytoskeletal proteins also participate in transport mechanisms and cell movement in the cytoplasm. They are also involved in controlling signaling pathways by providing a surface for signaling molecules (Janmey, 1998). Vimentin is a developmental IF protein that is highly conserved with a significant degree of sequence homology among species (Ferrari et al, 1986; Franke et al, 1979b; Satelli & Li, 2011). Vimentin is broadly expressed in embryos and is often later replaced by the other major classes of IFs in cells during differentiation. While vascular endothelial cells and certain subpopulations of glial cells are the only cells in the healthy adult brain that still express vimentin (Bignami et al, 1982;

Franke et al, 1979a; Izmiryman et al, 2009), vimentin is re-expressed in both protoplasmic and fibrous astrocytes in the brain of Alzheimer's disease patients (Levin et al, 2009). Annexin A1 (also known as annexin 1) is a Ca^{2+} and phospholipid-binding protein that belongs to the annexins protein multigene family which is evolutionary conserved. Annexin A1 binds to F-actin and is involved in the regulation of membrane-cytoskeleton dynamics. This protein also interacts with profilin which regulates actin polymerization through interaction with G-actin. Association of annexin A1 and profilin modifies actin polymerization (Alvarez-Martinez et al, 1997; Gerke & Moss, 1997).

Cytoskeletal rearrangement is one of the essential coping mechanisms for cells for adaptation in response to osmotic stress (Cornet et al, 1993). It has been observed that hyperosmolarity increases the speed of polymerization of F-actin and induces remodeling of the actin cytoskeleton (Bustamante et al, 2003; Di Ciano et al, 2002; Yamamoto et al, 2006). The exact mechanisms by which the cytoskeleton plays roles in osmoregulation remains unclear (Eggermont, 2003). However, it has been suggested that the cytoskeleton may involve volume rearrangement, mechanical protection against excessive shrinkage, and signal transmission from molecules sensing hyperosmolarity to the molecules responding to it. Moreover, it has been shown that osmotic stress modulates cytoskeletal protein expression. Vimentin and annexin A1 are among the cytoskeleton proteins and cytoskeleton-associated proteins that overexpress in response to osmotic stress in medullary renal cells named, thick ascending limb of Henle's loop (TALH cells) (Dihazi et al, 2005). In conclusion, the potential downregulation of hsa_circVIM_011 and hsa_circANXA1_001 might be because of overexpression of vimentin and annexin A1 in the cells in response to stress as a strategy for preservation of cell structures in response to osmotic stress. Further studies of the expression and function of circRNAs from cytoskeletal genes may shed further light on the pathogenesis of ALS (Conn et al, 2017).

4.3 Potential role of candidate circRNAs in RNP granule biology

Ribonucleoprotein (RNP) granules are large membraneless RNA–protein assemblies involved in many aspects of RNA metabolism. There are a variety of RNP granules in both the nucleus and cytoplasm of eukaryotic cells. An example of nucleic RNP granules is the paraspeckle. Transport (neuronal) granules, SGs, and P-bodies are described as cytoplasmic RNP granules. The formation of RNP granules requires protein-protein, RNA–RNA, and protein-RNA interactions.

Both coding and non-coding RNAs has been discovered in RNP granules with an essential role in the formation of these kinds of assemblies. For example, NEAT1 lncRNA is an essential component for paraspeckles assemblies in the nucleus which provides a scaffold for assemblies of other proteins and RBPs (Chen & Carmichael, 2009; Clemson et al, 2009; Sunwoo et al, 2009). SGs, P-bodies, and transport granules also contain a combination of proteins, RBPs and nontranslating mRNAs. Although the presence of non-coding RNAs has been reported in RNP granules, no study has examined the presence of circRNAs in this kind of membraneless organelles.

Here, I showed that three of the candidate circRNAs, CDR1as, hsa_circVIM_005, and hsa_circDNM1_004, colocalize with the markers of RNP granules: Staufen (a marker of transport granules), TIA-1 (a marker of SGs), and Dcp1 (a marker of P-bodies). I also observed hsa_circDNM1_004 colocalizes with PSPC1 and NONO, two important paraspeckles proteins. Quantification of the Pearson's correlation coefficients between candidate circRNAs and marker of RNP granules using Imaris software support the observation of partial colocalization between these components in that not all observed circRNAs were found to be associated with RNP granules. I hypothesize that circRNAs may play role in the RNP granule formation by providing a scaffold for the interaction of other components of RNP granules.

In support of this hypothesis, several studies have demonstrated that specific lncRNAs can act as essential architectural scaffolds for the construction of RNP granules in a variety of eukaryotes, including humans, mice, *Drosophila*, and yeast (Chujo & Hirose, 2017; Chujo et al, 2017; Yamazaki & Hirose, 2015). As mentioned before, NEAT1 lncRNA is an essential scaffold for paraspeckles proteins (Chen & Carmichael, 2009; Clemson et al, 2009; Sunwoo et al, 2009). In primates, highly repetitive satellite III (HSATIII) lncRNAs induce the formation of nuclear stress bodies (nSBs) in response to cellular stress (Aly et al, 2019; Jolly et al, 1999; Ninomiya et al, 2020). Ribosomal intergenic noncoding RNA (rIGSRNA) can induce the formation of amyloid-like solid structures termed amyloid bodies by interacting with the amyloid-converting motif (ACM) in targeting proteins (Audas et al, 2016).

It has been reported that circRNAs can bind to some RBPs and modulated their function (Li et al, 2017b). It has been proposed that circRNAs may interact, store, and sequester proteins to

specific subcellular locations and provide dynamic scaffolds for the assembly of proteins and modulate their functions (Du et al, 2017c). The sequence examination of candidate circRNAs using CircInteractome database showed multiple potential binding sites for RBPs that are reported to be included in RNP granules (Figure 4-1). For instance, AGO2 that have multiple binding sites on CDR1as (43), hsa_circVIM_005 (17), and hsa_circDNM1_004 (3) have been shown to present in RNP granules (Gallois-Montbrun et al, 2007; Goodier et al, 2007). FUS also have multiple potential binding sites on CDR1as (26), hsa_circVIM_005 (2), and hsa_circDNM1_004 (3) and is included in RNP granules (Qamar et al, 2018). The involvement of IGF2 mRNA-binding protein family (IGF2BPs) that have three members (IGF2BP1, IGF2BP2, and IGF2BP3) in RNP granule formation have been reported in several studies (Guzikowski et al, 2019; Vijayakumar, 2018; Wächter et al, 2013; Zeng et al, 2019). All the members of this protein family have multiple potential binding sites on CDR1as and hsa_circVIM_005. The other example of RBP that have multiple potential binding sites on hsa_circVIM_005 (6) and hsa_circDNM1_004 (2) is Polypyrimidine tract-binding protein (PTB also known as hnRNP1). PTB also contributes in RNP granule formation through interaction with RNAs (Guil et al, 2006; Li et al, 2012; Lin et al, 2015). Altogether the localization in RNP granules of circRNAs that have multiple potential binding sites for RBPs involved in RNP granule formation might indicate the potential role of these circRNAs in RNP granule biology.

It has also been proposed that interactions between circRNAs and RBPs might not be only sequence-dependent but that they might also be driven by the tertiary structures of circRNAs (Du et al, 2017c). Moreover, their specific covalently closed structures result in a distinct tertiary conformation of circRNAs that is different from their linear counterparts (Jeck & Sharpless, 2014). It has been proposed that different tertiary structures for circRNAs in certain tissues, cells, and even different cellular environments might account for alterations in the preference for binding to specific RBPs. Therefore, these circRNAs can play different roles in different tissues, cell types, and cellular conditions through the interaction with different RBPs (Du et al, 2017a). It is possible that cellular stress might alter the tertiary structure of the candidate circRNAs whose colocalized with RNP granule markers and in doing so, augment their ability to interact with components of RNP granules. In addition, the circular nature of circRNAs without free ends makes them exceptionally stable, with the median half-life of at least 2.5 times longer than that of their linear RNA isoforms. These properties make circRNAs attractive candidates as scaffolds

for the formation of RNP granules. Thus, circRNAs can be considered as a potential candidate for nucleating RNP granules and providing a scaffold for their formation.

4.4 Future direction

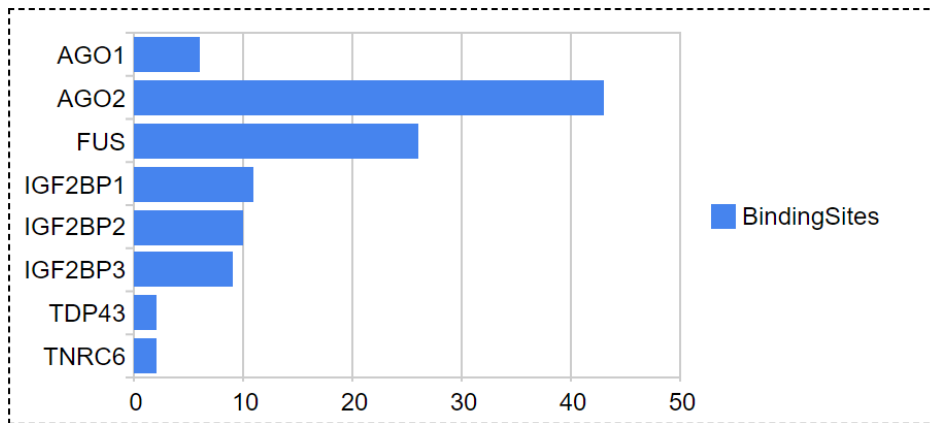
In order to proof that designed primers for candidate circRNAs are detecting expected sequences, and also to characterize the multiple bands for circRNAs hsa_circDNM1_004 and hsa_circVIM_005 from the qPCR, first I need to optimize the qPCR using different annealing temperatures and concentrations of DMSO. After the optimization, if I still detect excessive bands for circRNAs, I need to clone those bands into a pGEMT-easy vector for further sequencing. I also need to design a new set of primers for hsa_circANXA1_001 as the other two sets of primers did not work properly.

While I observed the colocalization of a selected group of candidate circRNAs with the markers of RNP granules under osmotic stress condition in HEK293T cells, additional experiments analyzing the effect of other kinds of cellular stress, such as oxidative and metabolic stresses will provide a more complete understanding of the mechanisms behind the observed colocalizations and whether such a response is a generic one independent of the nature of the cellular stress. The study of the stress-induced subcellular localization of candidate circRNAs in neuronal cell lines or patient-derived induced pluripotent stem cells (iPSCs) will provide more evidence of the potential role of circRNAs in ALS pathogenesis. As I have selected the candidate circRNAs from upregulated circRNAs in spinal cord tissue of ALS patients, the study of the expression and subcellular localization of candidate circRNAs in motor neurons of spinal cord tissues of ALS patients using the FISH technique will help to understand the potential function of candidate circRNA in ALS pathogenesis.

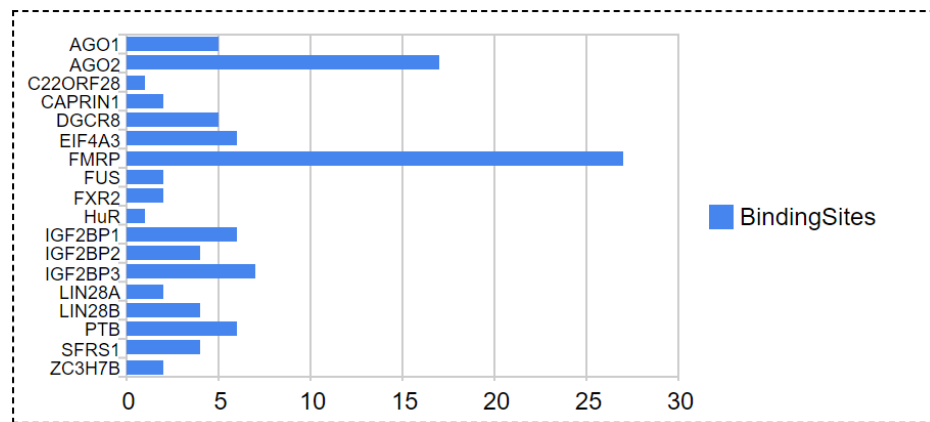
A major future direction for this work is to determine whether candidate circRNAs contribute to RNP granule formation in response to stress. Does reduction or loss of CDR1as, hsa_circVIM_005, and hsa_circDNM1_004 result in reduced RNP granule formation under stress? Does reduction or loss of CDR1as, hsa_circVIM_005, and hsa_circDNM1_004 result in reducing cell viability in response to stress? Do CDR1as, hsa_circVIM_005, and hsa_circDNM1_004 interact with RBP components of RNP granules? The answer to these questions, it will be necessary to understand the participation of these circRNAs in RNP granule

formation. Therefore, further analyzing the candidate circRNAs in these studies and whether loss of these circRNAs via knockdown or knockout models could contribute to altered RNP granule formation upon stress will help us to understand their contribution to the pathogenesis of ALS. In addition, I need to acquire 3-D images of unstressed cells and quantify potential colocalization of candidate circRNAs with marker of RNP granules to get a better comparison of stress and baseline condition.

A



B



C

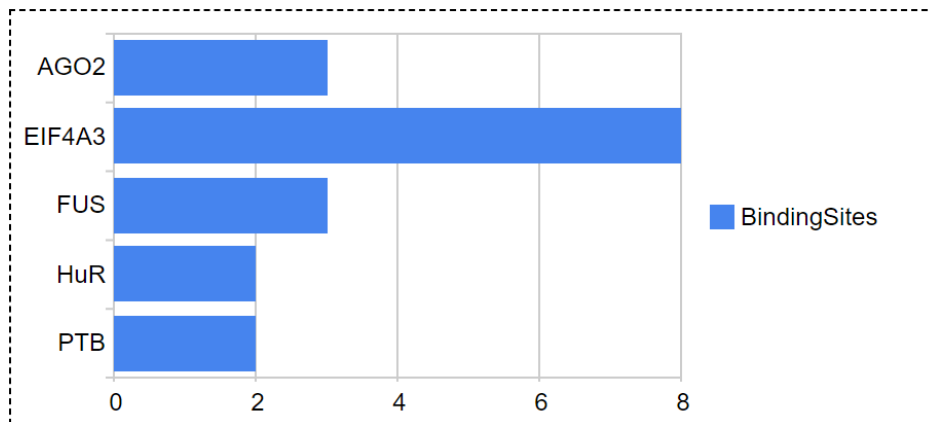


Figure 4-1: RNA-binding protein sites matching to circRNAs. A) CDR1as. B) hsa_circVIM_005. C) hsa_circDNM1_004.

Bibliography

- Abdelmohsen, K., Panda, A. C., Munk, R., Grammatikakis, I., Dudekula, D. B., De, S., Kim, J., Noh, J. H., Kim, K. M. & Martindale, J. L. (2017) Identification of HuR target circular RNAs uncovers suppression of PABPN1 translation by CircPABPN1. *RNA biology*, 14(3), 361-369.
- ABDULLA, E. M. & CAMPBELL, I. C. (1997) Studies of neurotoxicity in cellular models, *In Vitro Methods in Pharmaceutical Research* Elsevier, 155-180.
- Abe, K., Pan, L.-H., Watanabe, M., Kato, T. & Itoyama, Y. (1995) Induction of nitrotyrosine-like immunoreactivity in the lower motor neuron of amyotrophic lateral sclerosis. *Neuroscience letters*, 199(2), 152-154.
- Abe, N., Matsumoto, K., Nishihara, M., Nakano, Y., Shibata, A., Maruyama, H., Shuto, S., Matsuda, A., Yoshida, M. & Ito, Y. (2015) Rolling circle translation of circular RNA in living human cells. *Scientific reports*, 5, 16435.
- Al-Chalabi, A. & Hardiman, O. (2013) The epidemiology of ALS: a conspiracy of genes, environment and time. *Nature Reviews Neurology*, 9(11), 617.
- Alami, N. H., Smith, R. B., Carrasco, M. A., Williams, L. A., Winborn, C. S., Han, S. S., Kiskinis, E., Winborn, B., Freibaum, B. D. & Kanagaraj, A. (2014) Axonal transport of TDP-43 mRNA granules is impaired by ALS-causing mutations. *Neuron*, 81(3), 536-543.
- Alkam, D., Feldman, E. Z., Singh, A. & Kiaei, M. (2017) Profilin1 biology and its mutation, actin (g) in disease. *Cellular and molecular life sciences*, 74(6), 967-981.
- Alvarez-Martinez, M.-T., Porte, F., Liautard, J. P. & Widada, J. S. (1997) Effects of profilin-annexin I association on some properties of both profilin and annexin I: Modification of the inhibitory activity of profilin on actin polymerization and inhibition of the self-association of annexin I and its interactions with liposomes. *Biochimica et Biophysica Acta (BBA)-Protein Structure and Molecular Enzymology*, 1339(2), 331-340.
- Aly, M. K., Ninomiya, K., Adachi, S., Natsume, T. & Hirose, T. (2019) Two distinct nuclear stress bodies containing different sets of RNA-binding proteins are formed with HSATIII architectural noncoding RNAs upon thermal stress exposure. *Biochemical and biophysical research communications*, 516(2), 419-423.
- Amodio, N., Di Martino, M. T., Neri, A., Tagliaferri, P. & Tassone, P. (2013) Non-coding RNA: a novel opportunity for the personalized treatment of multiple myeloma. *Expert opinion on biological therapy*, 13(sup1), S125-S137.
- An, H., Skelt, L., Notaro, A., Highley, J. R., Fox, A. H., La Bella, V., Buchman, V. L. & Shelkovich, T. A. (2019) ALS-linked FUS mutations confer loss and gain of function in the nucleus by promoting excessive formation of dysfunctional paraspeckles. *Acta neuropathologica communications*, 7(1), 1-14.

- Andersen, P. M. & Al-Chalabi, A. (2011) Clinical genetics of amyotrophic lateral sclerosis: what do we really know? *Nature Reviews Neurology*, 7(11), 603-615.
- Anderson, P. & Kedersha, N. (2008) Stress granules: the Tao of RNA triage. *Trends in biochemical sciences*, 33(3), 141-150.
- Anderson, P. & Kedersha, N. (2009) RNA granules: post-transcriptional and epigenetic modulators of gene expression. *Nature reviews Molecular cell biology*, 10(6), 430-436.
- Ascano, M., Mukherjee, N., Bandaru, P., Miller, J. B., Nusbaum, J. D., Corcoran, D. L., Langlois, C., Munschauer, M., Dewell, S. & Hafner, M. (2012) FMRP targets distinct mRNA sequence elements to regulate protein expression. *Nature*, 492(7429), 382-386.
- Ashley, C. T., Sutcliffe, J. S., Kunst, C. B., Leiner, H. A., Eichler, E. E., Nelson, D. L. & Warren, S. T. (1993) Human and murine FMR-1: alternative splicing and translational initiation downstream of the CGG-repeat. *Nature genetics*, 4(3), 244-251.
- Ashwal-Fluss, R., Meyer, M., Pamudurti, N. R., Ivanov, A., Bartok, O., Hanan, M., Evantal, N., Memczak, S., Rajewsky, N. & Kadener, S. (2014) circRNA biogenesis competes with pre-mRNA splicing. *Molecular cell*, 56(1), 55-66.
- Asikainen, S., Rudgalvyte, M., Heikkinen, L., Louhiranta, K., Lakso, M., Wong, G. & Nass, R. (2010) Global microRNA expression profiling of *Caenorhabditis elegans* Parkinson's disease models. *Journal of Molecular Neuroscience*, 41(1), 210-218.
- Audas, T. E., Audas, D. E., Jacob, M. D., Ho, J. D., Khacho, M., Wang, M., Perera, J. K., Gardiner, C., Bennett, C. A. & Head, T. (2016) Adaptation to stressors by systemic protein amyloidogenesis. *Developmental cell*, 39(2), 155-168.
- Auesukaree, C., Damnernsawad, A., Kruatrachue, M., Pokethitiyook, P., Boonchird, C., Kaneko, Y. & Harashima, S. (2009) Genome-wide identification of genes involved in tolerance to various environmental stresses in *Saccharomyces cerevisiae*. *Journal of applied genetics*, 50(3), 301-310.
- Aumiller, W. M. & Keating, C. D. (2016) Phosphorylation-mediated RNA/peptide complex coacervation as a model for intracellular liquid organelles. *Nature chemistry*, 8(2), 129-137.
- Bachellerie, J.-P., Cavaillé, J. & Hüttenhofer, A. (2002) The expanding snoRNA world. *Biochimie*, 84(8), 775-790.
- Bahn, J. H., Zhang, Q., Li, F., Chan, T.-M., Lin, X., Kim, Y., Wong, D. T. & Xiao, X. (2015) The landscape of microRNA, Piwi-interacting RNA, and circular RNA in human saliva. *Clinical chemistry*, 61(1), 221-230.
- Bai, Y., Zhang, Y., Han, B., Yang, L., Chen, X., Huang, R., Wu, F., Chao, J., Liu, P. & Hu, G. (2018) Circular RNA DLGAP4 ameliorates ischemic stroke outcomes by targeting miR-143 to regulate endothelial-mesenchymal transition associated with blood-brain barrier integrity. *Journal of Neuroscience*, 38(1), 32-50.

- Banjade, S. & Rosen, M. K. (2014) Phase transitions of multivalent proteins can promote clustering of membrane receptors. *Elife*, 3, e04123.
- Bannwarth, S., Ait-El-Mkadem, S., Chausseot, A., Genin, E. C., Lacas-Gervais, S., Fragaki, K., Berg-Alonso, L., Kageyama, Y., Serre, V. & Moore, D. G. (2014) A mitochondrial origin for frontotemporal dementia and amyotrophic lateral sclerosis through CHCHD10 involvement. *Brain*, 137(8), 2329-2345.
- Barber, S. C. & Shaw, P. J. (2010) Oxidative stress in ALS: key role in motor neuron injury and therapeutic target. *Free Radical Biology and Medicine*, 48(5), 629-641.
- Bashkirov, V. I., Scherthan, H., Solinger, J. A., Buerstedde, J.-M. & Heyer, W.-D. (1997) A mouse cytoplasmic exoribonuclease (mXRN1p) with preference for G4 tetraplex substrates. *The Journal of cell biology*, 136(4), 761-773.
- Bäumer, D., Hilton, D., Paine, S., Turner, M., Lowe, J., Talbot, K. & Ansorge, O. (2010) Juvenile ALS with basophilic inclusions is a FUS proteinopathy with FUS mutations. *Neurology*, 75(7), 611-618.
- Beal, M. F., Ferrante, R. J., Browne, S. E., Matthews, R. T., Kowall, N. W. & Brown Jr, R. H. (1997) Increased 3-nitrotyrosine in both sporadic and familial amyotrophic lateral sclerosis. *Annals of Neurology: Official Journal of the American Neurological Association and the Child Neurology Society*, 42(4), 644-654.
- Bergeron, C., Beric-Maskarel, K., Muntasser, S., Weyer, L., Somerville, M. J. & Percy, M. E. (1994) Neurofilament light and polyadenylated mRNA levels are decreased in amyotrophic lateral sclerosis motor neurons. *Journal of neuropathology and experimental neurology*, 53(3), 221-230.
- Bianchessi, V., Badi, I., Bertolotti, M., Nigro, P., D'Alessandra, Y., Capogrossi, M. C., Zanobini, M., Pompilio, G., Raucci, A. & Lauri, A. (2015) The mitochondrial lncRNA ASncmtRNA-2 is induced in aging and replicative senescence in Endothelial Cells. *Journal of molecular and cellular cardiology*, 81, 62-70.
- Bignami, A., Raju, T. & Dahl, D. (1982) Localization of vimentin, the nonspecific intermediate filament protein, in embryonal glia and in early differentiating neurons: In vivo and in vitro immunofluorescence study of the rat embryo with vimentin and neurofilament antisera. *Developmental biology*, 91(2), 286-295.
- Bissels, U., Bosio, A. & Wagner, W. (2012) MicroRNAs are shaping the hematopoietic landscape. *Haematologica*, 97(2), 160.
- Blokhuis, A. M., Groen, E. J., Koppers, M., van den Berg, L. H. & Pasterkamp, R. J. (2013) Protein aggregation in amyotrophic lateral sclerosis. *Acta neuropathologica*, 125(6), 777-794.
- Boehringer, A., Garcia-Mansfield, K., Singh, G., Bakkar, N., Pirrotte, P. & Bowser, R. (2017) ALS associated mutations in Matrin 3 alter protein-protein interactions and impede mRNA nuclear export. *Scientific reports*, 7(1), 1-14.

- Bogdanov, M., Brown Jr, R. H., Matson, W., Smart, R., Hayden, D., O'Donnell, H., Beal, M. F. & Cudkovicz, M. (2000) Increased oxidative damage to DNA in ALS patients. *Free Radical Biology and Medicine*, 29(7), 652-658.
- Boisvert, F.-M., van Koningsbruggen, S., Navascués, J. & Lamond, A. I. (2007) The multifunctional nucleolus. *Nature reviews Molecular cell biology*, 8(7), 574-585.
- Bolognani, F. & Perrone-Bizzozero, N. I. (2008) RNA–protein interactions and control of mRNA stability in neurons. *Journal of neuroscience research*, 86(3), 481-489.
- Bolte, S. & Cordelières, F. P. (2006) A guided tour into subcellular colocalization analysis in light microscopy. *Journal of microscopy*, 224(3), 213-232.
- Bond, C. S. & Fox, A. H. (2009) Paraspeckles: nuclear bodies built on long noncoding RNA. *Journal of Cell Biology*, 186(5), 637-644.
- Bose, J. K., Wang, I.-F., Hung, L., Tarn, W.-Y. & Shen, C.-K. J. (2008) TDP-43 overexpression enhances exon 7 inclusion during the survival of motor neuron pre-mRNA splicing. *Journal of Biological Chemistry*, 283(43), 28852-28859.
- Boundedjah, O., Desforges, B., Wu, T.-D., Pioche-Durieu, C., Marco, S., Hamon, L., Curmi, P. A., Guerin-Kern, J.-L., Piétrement, O. & Pastré, D. (2014) Free mRNA in excess upon polysome dissociation is a scaffold for protein multimerization to form stress granules. *Nucleic acids research*, 42(13), 8678-8691.
- Braak, H., Brettschneider, J., Ludolph, A. C., Lee, V. M., Trojanowski, J. Q. & Del Tredici, K. (2013) Amyotrophic lateral sclerosis—a model of corticofugal axonal spread. *Nature Reviews Neurology*, 9(12), 708-714.
- Brangwynne, C. P., Tompa, P. & Pappu, R. V. (2015) Polymer physics of intracellular phase transitions. *Nature Physics*, 11(11), 899-904.
- Braun, S., Domdey, H. & Wiebauer, K. (1996) Inverse splicing of a discontinuous pre-mRNA intron generates a circular exon in a HeLa cell nuclear extract. *Nucleic acids research*, 24(21), 4152-4157.
- Bregues, M., Teixeira, D. & Parker, R. (2005) Movement of eukaryotic mRNAs between polysomes and cytoplasmic processing bodies. *Science*, 310(5747), 486-489.
- Brenner, D., Müller, K., Wieland, T., Weydt, P., Böhm, S., Lulé, D., Hübers, A., Neuwirth, C., Weber, M. & Borck, G. (2016) NEK1 mutations in familial amyotrophic lateral sclerosis. *Brain*, 139(5), e28-e28.
- Brohawn, D. G., O'Brien, L. C. & Bennett Jr, J. P. (2016) RNAseq analyses identify tumor necrosis factor-mediated inflammation as a major abnormality in ALS spinal cord. *PloS one*, 11(8), e0160520.

- Brown, R. H. & Al-Chalabi, A. (2017) Amyotrophic lateral sclerosis. *New England Journal of Medicine*, 377(2), 162-172.
- Buchan, J. R., Kolaitis, R.-M., Taylor, J. P. & Parker, R. (2013) Eukaryotic stress granules are cleared by autophagy and Cdc48/VCP function. *Cell*, 153(7), 1461-1474.
- Buchan, J. R. & Parker, R. (2009) Eukaryotic stress granules: the ins and outs of translation. *Molecular cell*, 36(6), 932-941.
- Buchon, N. & Vaury, C. (2006) RNAi: a defensive RNA-silencing against viruses and transposable elements. *Heredity*, 96(2), 195-202.
- Buratti, E., Dörk, T., Zuccato, E., Pagani, F., Romano, M. & Baralle, F. E. (2001) Nuclear factor TDP-43 and SR proteins promote in vitro and in vivo CFTR exon 9 skipping. *The EMBO journal*, 20(7), 1774-1784.
- Burghes, A. H. & Beattie, C. E. (2009) Spinal muscular atrophy: why do low levels of survival motor neuron protein make motor neurons sick? *Nature Reviews Neuroscience*, 10(8), 597-609.
- Burke, T., Pinto-Grau, M., Lonergan, K., Bede, P., O'Sullivan, M., Heverin, M., Vajda, A., McLaughlin, R. L., Pender, N. & Hardiman, O. (2017) A cross-sectional population-based investigation into behavioral change in amyotrophic lateral sclerosis: Subphenotypes, staging, cognitive predictors, and survival. *Annals of clinical and translational neurology*, 4(5), 305-317.
- Bustamante, M., Roger, F., Bochaton-Piallat, M.-L., Gabbiani, G., Martin, P.-Y. & Féraille, E. (2003) Regulatory volume increase is associated with p38 kinase-dependent actin cytoskeleton remodeling in rat kidney MTAL. *American Journal of Physiology-Renal Physiology*, 285(2), F336-F347.
- Byrne, S., Jordan, I., Elamin, M. & Hardiman, O. (2013) Age at onset of amyotrophic lateral sclerosis is proportional to life expectancy. *Amyotrophic Lateral Sclerosis and Frontotemporal Degeneration*, 14(7-8), 604-607.
- Cai, H., Li, Y., Niringiyumukiza, J. D., Su, P. & Xiang, W. (2019) Circular RNA involvement in aging: an emerging player with great potential. *Mechanisms of ageing and development*, 178, 16-24.
- Campos-Melo, D., Droppelmann, C. A., He, Z., Volkening, K. & Strong, M. J. (2013a) Altered microRNA expression profile in amyotrophic lateral sclerosis: a role in the regulation of NFL mRNA levels. *Molecular brain*, 6(1), 1-13.
- Campos-Melo, D., Droppelmann, C. A., He, Z., Volkening, K. & Strong, M. J. (2013b) Altered microRNA expression profile in amyotrophic lateral sclerosis: a role in the regulation of NFL mRNA levels. *Molecular brain*, 6(1), 26.
- Capel, B., Swain, A., Nicolis, S., Hacker, A., Walter, M., Koopman, P., Goodfellow, P. & Lovell-Badge, R. (1993) Circular transcripts of the testis-determining gene Sry in adult mouse testis. *Cell*, 73(5), 1019-1030.

- Chen, B. J., Mills, J. D., Takenaka, K., Bliim, N., Halliday, G. M. & Janitz, M. (2016a) Characterization of circular RNA s landscape in multiple system atrophy brain. *Journal of neurochemistry*, 139(3), 485-496.
- Chen, C.-y. & Sarnow, P. (1995) Initiation of protein synthesis by the eukaryotic translational apparatus on circular RNAs. *Science*, 268(5209), 415-417.
- Chen, J. & Wang, D.-Z. (2012) microRNAs in cardiovascular development. *Journal of molecular and cellular cardiology*, 52(5), 949-957.
- Chen, L.-L. & Carmichael, G. G. (2009) Altered nuclear retention of mRNAs containing inverted repeats in human embryonic stem cells: functional role of a nuclear noncoding RNA. *Molecular cell*, 35(4), 467-478.
- Chen, L.-L. & Yang, L. (2015) Regulation of circRNA biogenesis. *RNA biology*, 12(4), 381-388.
- Chen, N., Zhao, G., Yan, X., Lv, Z., Yin, H., Zhang, S., Song, W., Li, X., Li, L. & Du, Z. (2018) A novel FLII exonic circular RNA promotes metastasis in breast cancer by coordinately regulating TET1 and DNMT1. *Genome biology*, 19(1), 1-14.
- Chen, Y.-Z., Bennett, C. L., Huynh, H. M., Blair, I. P., Puls, I., Irobi, J., Dierick, I., Abel, A., Kennerson, M. L. & Rabin, B. A. (2004) DNA/RNA helicase gene mutations in a form of juvenile amyotrophic lateral sclerosis (ALS4). *The American Journal of Human Genetics*, 74(6), 1128-1135.
- Chen, Z., Zhang, Z., Xie, B. & Zhang, H. (2016b) Clinical significance of up-regulated lncRNA NEAT1 in prognosis of ovarian cancer. *Eur Rev Med Pharmacol Sci*, 20(16), 3373-3377.
- Chou, C.-C., Zhang, Y., Umoh, M. E., Vaughan, S. W., Lorenzini, I., Liu, F., Sayegh, M., Donlin-Asp, P. G., Chen, Y. H. & Duong, D. M. (2018) TDP-43 pathology disrupts nuclear pore complexes and nucleocytoplasmic transport in ALS/FTD. *Nature neuroscience*, 21(2), 228-239.
- Chow, C. Y., Landers, J. E., Bergren, S. K., Sapp, P. C., Grant, A. E., Jones, J. M., Everett, L., Lenk, G. M., McKenna-Yasek, D. M. & Weisman, L. S. (2009) Deleterious variants of FIG4, a phosphoinositide phosphatase, in patients with ALS. *The American Journal of Human Genetics*, 84(1), 85-88.
- Chujo, T. & Hirose, T. (2017) Nuclear bodies built on architectural long noncoding RNAs: unifying principles of their construction and function. *Molecules and cells*, 40(12), 889.
- Chujo, T., Yamazaki, T., Kawaguchi, T., Kurosaka, S., Takumi, T., Nakagawa, S. & Hirose, T. (2017) Unusual semi-extractability as a hallmark of nuclear body-associated architectural noncoding RNA s. *The EMBO journal*, 36(10), 1447-1462.

circbank *circbank* Available online: <http://www.circbank.cn/index.html> [Accessed].

circInteractom *circInteractom* Available online: <https://circinteractome.nia.nih.gov/> [Accessed].

- Clemson, C. M., Hutchinson, J. N., Sara, S. A., Ensminger, A. W., Fox, A. H., Chess, A. & Lawrence, J. B. (2009) An architectural role for a nuclear noncoding RNA: NEAT1 RNA is essential for the structure of paraspeckles. *Molecular cell*, 33(6), 717-726.
- Conn, V. M., Hugouvieux, V., Nayak, A., Conos, S. A., Capovilla, G., Cildir, G., Jourdain, A., Tergaonkar, V., Schmid, M. & Zubietta, C. (2017) A circRNA from SEPALLATA3 regulates splicing of its cognate mRNA through R-loop formation. *Nature plants*, 3(5), 17053.
- Corbo, M. & Hays, A. P. (1992) Peripherin and neurofilament protein coexist in spinal spheroids of motor neuron disease. *Journal of Neuropathology & Experimental Neurology*, 51(5), 531-537.
- Corcia, P., Pradat, P. F., Salachas, F., Bruneteau, G., Le Forestier, N., Seilhean, D., Hauw, J. J. & Meininger, V. (2008) Causes of death in a post-mortem series of ALS patients. *Amyotrophic Lateral Sclerosis*, 9(1), 59-62.
- Cornet, M., Ubl, J. & Kolb, H.-A. (1993) Cytoskeleton and ion movements during volume regulation in cultured PC12 cells. *The Journal of membrane biology*, 133(2), 161-170.
- Costa-Mattioli, M., Sossin, W. S., Klann, E. & Sonenberg, N. (2009) Translational control of long-lasting synaptic plasticity and memory. *Neuron*, 61(1), 10-26.
- Costa, F. F. (2010) Non-coding RNAs: meet thy masters. *Bioessays*, 32(7), 599-608.
- Couthouis, J., Hart, M. P., Erion, R., King, O. D., Diaz, Z., Nakaya, T., Ibrahim, F., Kim, H.-J., Mojsilovic-Petrovic, J. & Panossian, S. (2012) Evaluating the role of the FUS/TLS-related gene EWSR1 in amyotrophic lateral sclerosis. *Human molecular genetics*, 21(13), 2899-2911.
- Coyne, A. N., Zaepfel, B. L. & Zarnescu, D. C. (2017) Failure to deliver and translate—new insights into RNA dysregulation in ALS. *Frontiers in cellular neuroscience*, 11, 243.
- D'Ambrosi, N., Rossi, S., Gerbino, V. & Cozzolino, M. (2014) Rac1 at the crossroad of actin dynamics and neuroinflammation in Amyotrophic Lateral Sclerosis. *Frontiers in cellular neuroscience*, 8, 279.
- D'Erchia, A. M., Gallo, A., Manzari, C., Raho, S., Horner, D. S., Chiara, M., Valletti, A., Aiello, I., Mastropasqua, F. & Ciaccia, L. (2017) Massive transcriptome sequencing of human spinal cord tissues provides new insights into motor neuron degeneration in ALS. *Scientific reports*, 7(1), 1-20.
- Dahlberg, A. E. (1989) The functional role of ribosomal RNA in protein synthesis. *Cell*, 57(4), 525-529.
- Dangond, F., Hwang, D., Camelo, S., Pasinelli, P., Frosch, M. P., Stephanopoulos, G., Stephanopoulos, G., Brown Jr, R. H. & Gullans, S. R. (2004) Molecular signature of late-stage human ALS revealed by expression profiling of postmortem spinal cord gray matter. *Physiological genomics*, 16(2), 229-239.

- Davidson, Y., Robinson, A. C., Liu, X., Wu, D., Troakes, C., Rollinson, S., Masuda-Suzukake, M., Suzuki, G., Nonaka, T. & Shi, J. (2016) Neurodegeneration in frontotemporal lobar degeneration and motor neurone disease associated with expansions in C9orf72 is linked to TDP-43 pathology and not associated with aggregated forms of dipeptide repeat proteins. *Neuropathology and applied neurobiology*, 42(3), 242-254.
- Davis, G. M., Haas, M. A. & Pockock, R. (2015) MicroRNAs: not “fine-tuners” but key regulators of neuronal development and function. *Frontiers in neurology*, 6, 245.
- de Carvalho, M., Dengler, R., Eisen, A., England, J. D., Kaji, R., Kimura, J., Mills, K., Mitsumoto, H., Nodera, H. & Shefner, J. (2008) Electrodiagnostic criteria for diagnosis of ALS. *Clinical neurophysiology*, 119(3), 497-503.
- De Silva, D., Hsieh, S., Caga, J., Leslie, F. V., Kiernan, M. C., Hodges, J. R., Mioshi, E. & Burrell, J. R. (2016) Motor function and behaviour across the ALS-FTD spectrum. *Acta Neurologica Scandinavica*, 133(5), 367-372.
- Decker, C. J. & Parker, R. (1993) A turnover pathway for both stable and unstable mRNAs in yeast: evidence for a requirement for deadenylation. *Genes & development*, 7(8), 1632-1643.
- DeJesus-Hernandez, M., Mackenzie, I. R., Boeve, B. F., Boxer, A. L., Baker, M., Rutherford, N. J., Nicholson, A. M., Finch, N. A., Flynn, H. & Adamson, J. (2011) Expanded GGGGCC hexanucleotide repeat in noncoding region of C9ORF72 causes chromosome 9p-linked FTD and ALS. *Neuron*, 72(2), 245-256.
- Demandolx, D. & Davoust, J. (1996) Subcellular Cytofluorometry in Confocal Microscopy, *Fluorescence Microscopy and Fluorescent Probes* Springer, 279-283.
- Deng, H.-X., Chen, W., Hong, S.-T., Boycott, K. M., Gorrie, G. H., Siddique, N., Yang, Y., Fecto, F., Shi, Y. & Zhai, H. (2011) Mutations in UBQLN2 cause dominant X-linked juvenile and adult-onset ALS and ALS/dementia. *Nature*, 477(7363), 211-215.
- Deng, H. X., Zhai, H., Bigio, E. H., Yan, J., Fecto, F., Ajroud, K., Mishra, M., Ajroud-Driss, S., Heller, S. & Sufit, R. (2010) FUS-immunoreactive inclusions are a common feature in sporadic and non-SOD1 familial amyotrophic lateral sclerosis. *Annals of neurology*, 67(6), 739-748.
- Deshaies, J.-E., Shkreta, L., Moszczynski, A. J., Sidibé, H., Semmler, S., Fouillen, A., Bennett, E. R., Bekenstein, U., Destroismaisons, L. & Toutant, J. (2018) TDP-43 regulates the alternative splicing of hnRNP A1 to yield an aggregation-prone variant in amyotrophic lateral sclerosis. *Brain*, 141(5), 1320-1333.
- Devys, D., Lutz, Y., Rouyer, N., Bellocq, J.-P. & Mandel, J.-L. (1993) The FMR-1 protein is cytoplasmic, most abundant in neurons and appears normal in carriers of a fragile X premutation. *Nature genetics*, 4(4), 335-340.
- Di Ciano, C., Nie, Z., Szász, K., Lewis, A., Uruno, T., Zhan, X., Rotstein, O. D., Mak, A. & Kapus, A. (2002) Osmotic stress-induced remodeling of the cortical cytoskeleton. *American Journal of Physiology-Cell Physiology*, 283(3), C850-C865.

- Dihazi, H., Asif, A. R., Agarwal, N. K., Doncheva, Y. & Müller, G. A. (2005) Proteomic analysis of cellular response to osmotic stress in thick ascending limb of Henle's loop (TALH) cells. *Molecular & Cellular Proteomics*, 4(10), 1445-1458.
- Ding, L., Zhao, Y., Dang, S., Wang, Y., Li, X., Yu, X., Li, Z., Wei, J., Liu, M. & Li, G. (2019) Circular RNA circ-DONSON facilitates gastric cancer growth and invasion via NURF complex dependent activation of transcription factor SOX4. *Molecular cancer*, 18(1), 1-11.
- Ding, N., Wu, H., Tao, T. & Peng, E. (2017) NEAT1 regulates cell proliferation and apoptosis of ovarian cancer by miR-34a-5p/BCL2. *Oncotargets and therapy*, 10, 4905.
- Dolinar, A., Koritnik, B., Glavač, D. & Ravnik-Glavač, M. (2019) Circular RNAs as potential blood biomarkers in amyotrophic lateral sclerosis. *Molecular neurobiology*, 56(12), 8052-8062.
- Dong, R., Zhang, X.-O., Zhang, Y., Ma, X.-K., Chen, L.-L. & Yang, L. (2016) CircRNA-derived pseudogenes. *Cell research*, 26(6), 747-750.
- Dormann, D., Rodde, R., Edbauer, D., Bentmann, E., Fischer, I., Hruscha, A., Than, M. E., Mackenzie, I. R., Capell, A. & Schmid, B. (2010) ALS-associated fused in sarcoma (FUS) mutations disrupt Transportin-mediated nuclear import. *The EMBO journal*, 29(16), 2841-2857.
- Doxakis, E. (2010) Post-transcriptional regulation of α -synuclein expression by mir-7 and mir-153. *Journal of Biological Chemistry*, 285(17), 12726-12734.
- Droppelmann, C. A., Campos-Melo, D., Ishtiaq, M., Volkening, K. & Strong, M. J. (2014) RNA metabolism in ALS: when normal processes become pathological. *Amyotrophic Lateral Sclerosis and Frontotemporal Degeneration*, 15(5-6), 321-336.
- Droppelmann, C. A., Keller, B. A., Campos-Melo, D., Volkening, K. & Strong, M. J. (2013a) Rho guanine nucleotide exchange factor is an NFL mRNA destabilizing factor that forms cytoplasmic inclusions in amyotrophic lateral sclerosis. *Neurobiology of aging*, 34(1), 248-262.
- Droppelmann, C. A., Wang, J., Campos-Melo, D., Keller, B., Volkening, K., Hegele, R. A. & Strong, M. J. (2013b) Detection of a novel frameshift mutation and regions with homozygosity within ARHGAP28 gene in familial amyotrophic lateral sclerosis. *Amyotrophic Lateral Sclerosis and Frontotemporal Degeneration*, 14(5-6), 444-451.
- Du, W. W., Fang, L., Yang, W., Wu, N., Awan, F. M., Yang, Z. & Yang, B. B. (2017a) Induction of tumor apoptosis through a circular RNA enhancing Foxo3 activity. *Cell Death & Differentiation*, 24(2), 357-370.
- Du, W. W., Yang, W., Chen, Y., Wu, Z.-K., Foster, F. S., Yang, Z., Li, X. & Yang, B. B. (2017b) Foxo3 circular RNA promotes cardiac senescence by modulating multiple factors associated with stress and senescence responses. *European heart journal*, 38(18), 1402-1412.
- Du, W. W., Yang, W., Liu, E., Yang, Z., Dhaliwal, P. & Yang, B. B. (2016) Foxo3 circular RNA retards cell cycle progression via forming ternary complexes with p21 and CDK2. *Nucleic acids research*, 44(6), 2846-2858.

- Du, W. W., Zhang, C., Yang, W., Yong, T., Awan, F. M. & Yang, B. B. (2017c) Identifying and characterizing circRNA-protein interaction. *Theranostics*, 7(17), 4183.
- Dunn, K. W., Kamocka, M. M. & McDonald, J. H. (2011) A practical guide to evaluating colocalization in biological microscopy. *American Journal of Physiology-Cell Physiology*, 300(4), C723-C742.
- Eger, N., Schoppe, L., Schuster, S., Laufs, U. & Boeckel, J.-N. (2018) Circular RNA splicing, *Circular RNAs* Springer, 41-52.
- Eggermont, J. (2003) Rho's role in cell volume: sensing, strutting, or signaling? Focus on "Hyperosmotic stress activates Rho: differential involvement in Rho kinase-dependent MLC phosphorylation and NKCC activation". *American Journal of Physiology-Cell Physiology*, 285(3), C509-C511.
- Eisinger-Mathason, T. K., Andrade, J., Groehler, A. L., Clark, D. E., Muratore-Schroeder, T. L., Pasic, L., Smith, J. A., Shabanowitz, J., Hunt, D. F. & Macara, I. G. (2008) Codependent functions of RSK2 and the apoptosis-promoting factor TIA-1 in stress granule assembly and cell survival. *Molecular cell*, 31(5), 722-736.
- El Fatimy, R., Davidovic, L., Tremblay, S., Jaglin, X., Dury, A., Robert, C., De Koninck, P. & Khandjian, E. W. (2016) Tracking the fragile X mental retardation protein in a highly ordered neuronal ribonucleoparticles population: a link between stalled polyribosomes and RNA granules. *PLoS genetics*, 12(7).
- Elden, A. C., Kim, H.-J., Hart, M. P., Chen-Plotkin, A. S., Johnson, B. S., Fang, X., Armarkola, M., Geser, F., Greene, R. & Lu, M. M. (2010) Ataxin-2 intermediate-length polyglutamine expansions are associated with increased risk for ALS. *Nature*, 466(7310), 1069-1075.
- Elvira, G., Wasiak, S., Blandford, V., Tong, X.-K., Serrano, A., Fan, X., del Rayo Sanchez-Carbente, M., Servant, F., Bell, A. W. & Boismenu, D. (2006) Characterization of an RNA granule from developing brain. *Molecular & cellular proteomics*, 5(4), 635-651.
- Enuka, Y., Lauriola, M., Feldman, M. E., Sas-Chen, A., Ulitsky, I. & Yarden, Y. (2016) Circular RNAs are long-lived and display only minimal early alterations in response to a growth factor. *Nucleic acids research*, 44(3), 1370-1383.
- Ernst, C., Odom, D. T. & Kutter, C. (2017) The emergence of piRNAs against transposon invasion to preserve mammalian genome integrity. *Nature communications*, 8(1), 1-10.
- Errichelli, L., Modigliani, S. D., Laneve, P., Colantoni, A., Legnini, I., Capauto, D., Rosa, A., De Santis, R., Scarfo, R. & Peruzzi, G. (2017) FUS affects circular RNA expression in murine embryonic stem cell-derived motor neurons. *Nature communications*, 8(1), 1-11.
- Esue, O., Carson, A. A., Tseng, Y. & Wirtz, D. (2006) A direct interaction between actin and vimentin filaments mediated by the tail domain of vimentin. *Journal of Biological Chemistry*, 281(41), 30393-30399.

- Fabian, M. R., Sonenberg, N. & Filipowicz, W. (2010) Regulation of mRNA translation and stability by microRNAs. *Annual review of biochemistry*, 79, 351-379.
- Fang, L., Sun, J., Pan, Z., Song, Y., Zhong, L., Zhang, Y., Liu, Y., Zheng, X. & Huang, P. (2017) Long non-coding RNA NEAT1 promotes hepatocellular carcinoma cell proliferation through the regulation of miR-129-5p-VCP-I κ B. *American Journal of Physiology-Gastrointestinal and Liver Physiology*, 313(2), G150-G156.
- Fecto, F., Yan, J., Vemula, S. P., Liu, E., Yang, Y., Chen, W., Zheng, J. G., Shi, Y., Siddique, N. & Arrat, H. (2011) SQSTM1 mutations in familial and sporadic amyotrophic lateral sclerosis. *Archives of neurology*, 68(11), 1440-1446.
- Ferrari, S., Battini, R., Kaczmarek, L., Rittling, S., Calabretta, B., De Riel, J. K., Philiponis, V., Wei, J. & Baserga, R. (1986) Coding sequence and growth regulation of the human vimentin gene. *Molecular and cellular biology*, 6(11), 3614-3620.
- Figlewicz, D. A., Krizus, A., Martinoli, M. G., Meininger, V., Dib, M., Rouleau, G. A. & Julien, J.-P. (1994) Variants of the heavy neurofilament subunit are associated with the development of amyotrophic lateral sclerosis. *Human molecular genetics*, 3(10), 1757-1761.
- Fischer, J. W. & Leung, A. K. (2017) CircRNAs: a regulator of cellular stress. *Critical reviews in biochemistry and molecular biology*, 52(2), 220-233.
- Flory, P. J. (1941) Thermodynamics of high polymer solutions. *The Journal of chemical physics*, 9(8), 660-660.
- Fox, A. H. & Lamond, A. I. (2010) Paraspeckles. *Cold Spring Harbor perspectives in biology*, 2(7), a000687.
- Franke, W. W., Schmid, E., Osborn, M. & Weber, K. (1979a) Intermediate-sized filaments of human endothelial cells. *The Journal of cell biology*, 81(3), 570-580.
- Franke, W. W., Schmid, E., Winter, S., Osborn, M. & Weber, K. (1979b) Widespread occurrence of intermediate-sized filaments of the vimentin-type in cultured cells from diverse vertebrates. *Experimental cell research*, 123(1), 25-46.
- Freischmidt, A., Wieland, T., Richter, B., Ruf, W., Schaeffer, V., Müller, K., Marroquin, N., Nordin, F., Hübers, A. & Weydt, P. (2015) Haploinsufficiency of TBK1 causes familial ALS and fronto-temporal dementia. *Nature neuroscience*, 18(5), 631-636.
- Gal, J., Zhang, J., Kwinter, D. M., Zhai, J., Jia, H., Jia, J. & Zhu, H. (2011) Nuclear localization sequence of FUS and induction of stress granules by ALS mutants. *Neurobiology of aging*, 32(12), 2323. e27-2323. e40.
- Gallois-Montbrun, S., Kramer, B., Swanson, C. M., Byers, H., Lynham, S., Ward, M. & Malim, M. H. (2007) Antiviral protein APOBEC3G localizes to ribonucleoprotein complexes found in P bodies and stress granules. *Journal of virology*, 81(5), 2165-2178.

- Garruto, R. (1991) Pacific paradigms of environmentally-induced neurological disorders: clinical, epidemiological and molecular perspectives. *Neurotoxicology*, 12(3), 347-377.
- Gaudette, M. H., Teepu Siddique, Mara (2000) Current status of SOD1 mutations in familial amyotrophic lateral sclerosis. *Amyotrophic Lateral Sclerosis and Other Motor Neuron Disorders*, 1(2), 83-89.
- Ge, W.-w., Volkening, K., Leystra-Lantz, C., Jaffe, H. & Strong, M. J. (2007) 14-3-3 protein binds to the low molecular weight neurofilament (NFL) mRNA 3' UTR. *Molecular and Cellular Neuroscience*, 34(1), 80-87.
- Ge, W.-W., Wen, W., Strong, W., Leystra-Lantz, C. & Strong, M. J. (2005) Mutant copper-zinc superoxide dismutase binds to and destabilizes human low molecular weight neurofilament mRNA. *Journal of Biological Chemistry*, 280(1), 118-124.
- Genecode (2021) *Encyclopedia of DNA Elements Consortium (ENCODE)*, 2021. Available online: <https://www.genecodegenes.org/human/stats.html> [Accessed].
- Gerke, V. & Moss, S. E. (1997) Annexins and membrane dynamics. *Biochimica et Biophysica Acta (BBA)-Molecular Cell Research*, 1357(2), 129-154.
- Giaever, G., Chu, A. M., Ni, L., Connelly, C., Riles, L., Véronneau, S., Dow, S., Lucau-Danila, A., Anderson, K. & Andre, B. (2002) Functional profiling of the *Saccharomyces cerevisiae* genome. *nature*, 418(6896), 387-391.
- Gilks, N., Kedersha, N., Ayodele, M., Shen, L., Stoecklin, G., Dember, L. M. & Anderson, P. (2004) Stress granule assembly is mediated by prion-like aggregation of TIA-1. *Molecular biology of the cell*, 15(12), 5383-5398.
- Goodier, J. L., Zhang, L., Vetter, M. R. & Kazazian, H. H. (2007) LINE-1 ORF1 protein localizes in stress granules with other RNA-binding proteins, including components of RNA interference RNA-induced silencing complex. *Molecular and cellular biology*, 27(18), 6469-6483.
- Grassmann, R. & Jeang, K.-T. (2008) The roles of microRNAs in mammalian virus infection. *Biochimica et Biophysica Acta (BBA)-Gene Regulatory Mechanisms*, 1779(11), 706-711.
- Greenway, M. J., Andersen, P. M., Russ, C., Ennis, S., Cashman, S., Donaghy, C., Patterson, V., Swingler, R., Kieran, D. & Prehn, J. (2006) ANG mutations segregate with familial and sporadic amyotrophic lateral sclerosis. *Nature genetics*, 38(4), 411-413.
- Gros-Louis, F., Larivière, R., Gowing, G., Laurent, S., Camu, W., Bouchard, J.-P., Meininger, V., Rouleau, G. A. & Julien, J.-P. (2004) A frameshift deletion in peripherin gene associated with amyotrophic lateral sclerosis. *Journal of Biological Chemistry*, 279(44), 45951-45956.
- Gu, C., Yaddanapudi, S., Weins, A., Osborn, T., Reiser, J., Pollak, M., Hartwig, J. & Sever, S. (2010) Direct dynamin-actin interactions regulate the actin cytoskeleton. *The EMBO journal*, 29(21), 3593-3606.

- Guareschi, S., Cova, E., Cereda, C., Ceroni, M., Donetti, E., Bosco, D. A., Trotti, D. & Pasinelli, P. (2012) An over-oxidized form of superoxide dismutase found in sporadic amyotrophic lateral sclerosis with bulbar onset shares a toxic mechanism with mutant SOD1. *Proceedings of the National Academy of Sciences*, 109(13), 5074-5079.
- Guil, S., Long, J. C. & Cáceres, J. F. (2006) hnRNP A1 relocalization to the stress granules reflects a role in the stress response. *Molecular and cellular biology*, 26(15), 5744-5758.
- Guo, D., Ma, J., Yan, L., Li, T., Li, Z., Han, X. & Shui, S. (2017) Down-regulation of Lncrna MALAT1 attenuates neuronal cell death through suppressing Beclin1-dependent autophagy by regulating Mir-30a in cerebral ischemic stroke. *Cellular Physiology and Biochemistry*, 43(1), 182-194.
- Guo, J. U., Agarwal, V., Guo, H. & Bartel, D. P. (2014a) Expanded identification and characterization of mammalian circular RNAs. *Genome biology*, 15(7), 1-14.
- Guo, J. U., Agarwal, V., Guo, H. & Bartel, D. P. (2014b) Expanded identification and characterization of mammalian circular RNAs. *Genome biology*, 15(7), 409.
- Guo, X., Wu, X., Han, Y., Tian, E. & Cheng, J. (2019) LncRNA MALAT1 protects cardiomyocytes from isoproterenol-induced apoptosis through sponging miR-558 to enhance ULK1-mediated protective autophagy. *Journal of cellular physiology*, 234(7), 10842-10854.
- Guzikowski, A. R., Chen, Y. S. & Zid, B. M. (2019) Stress-induced mRNP granules: form and function of processing bodies and stress granules. *Wiley Interdisciplinary Reviews: RNA*, 10(3), e1524.
- Hadano, S., Yanagisawa, Y., Skaug, J., Fichter, K., Nasir, J., Martindale, D., Koop, B. F., Scherer, S. W., Nicholson, D. W. & Rouleau, G. A. (2001) Cloning and characterization of three novel genes, ALS2CR1, ALS2CR2, and ALS2CR3, in the juvenile amyotrophic lateral sclerosis (ALS2) critical region at chromosome 2q33–q34: candidate genes for ALS2. *Genomics*, 71(2), 200-213.
- Hafezparast, M., Klocke, R., Ruhrberg, C., Marquardt, A., Ahmad-Annuar, A., Bowen, S., Lalli, G., Witherden, A. S., Hummerich, H. & Nicholson, S. (2003) Mutations in dynein link motor neuron degeneration to defects in retrograde transport. *Science*, 300(5620), 808-812.
- Hanan, M., Simchovitz, A., Yayon, N., Vaknine, S., Cohen-Fultheim, R., Karmon, M., Madrer, N., Rohrllich, T. M., Maman, M. & Bennett, E. R. (2020) A Parkinson's disease Circ RNA s Resource reveals a link between circ SLC 8A1 and oxidative stress. *EMBO molecular medicine*, 12(9), e11942.
- Hanan, M., Soreq, H. & Kadener, S. (2017) CircRNAs in the brain. *RNA biology*, 14(8), 1028-1034.
- Hand, C. K., Khoris, J., Salachas, F., Gros-Louis, F., Lopes, A. A. S., Mayeux-Portas, V., Brown Jr, R. H., Meininger, V., Camu, W. & Rouleau, G. A. (2002) A novel locus for familial

- amyotrophic lateral sclerosis, on chromosome 18q. *The American Journal of Human Genetics*, 70(1), 251-256.
- Hansen, T. B., Jensen, T. I., Clausen, B. H., Bramsen, J. B., Finsen, B., Damgaard, C. K. & Kjems, J. (2013) Natural RNA circles function as efficient microRNA sponges. *Nature*, 495(7441), 384-388.
- Hargrove, J. L. & Schmidt, F. H. (1989) The role of mRNA and protein stability in gene expression. *The FASEB Journal*, 3(12), 2360-2370.
- Hawley, Z. C., Campos-Melo, D. & Strong, M. J. (2019) MiR-105 and miR-9 regulate the mRNA stability of neuronal intermediate filaments. Implications for the pathogenesis of amyotrophic lateral sclerosis (ALS). *Brain Research*, 1706, 93-100.
- Hayes, M. J., Rescher, U., Gerke, V. & Moss, S. E. (2004) Annexin–actin interactions. *Traffic*, 5(8), 571-576.
- Hennig, S., Kong, G., Mannen, T., Sadowska, A., Kobelke, S., Blythe, A., Knott, G. J., Iyer, K. S., Ho, D. & Newcombe, E. A. (2015) Prion-like domains in RNA binding proteins are essential for building subnuclear paraspeckles. *Journal of Cell Biology*, 210(4), 529-539.
- Hensel, N. & Claus, P. (2018) The actin cytoskeleton in SMA and ALS: how does it contribute to motoneuron degeneration? *The Neuroscientist*, 24(1), 54-72.
- Heo, J. B. & Sung, S. (2011) Vernalization-mediated epigenetic silencing by a long intronic noncoding RNA. *Science*, 331(6013), 76-79.
- Higgins, C. M., Jung, C. & Xu, Z. (2003) ALS-associated mutant SOD1 G93A causes mitochondrial vacuolation by expansion of the intermembrane space and by involvement of SOD1 aggregation and peroxisomes. *BMC neuroscience*, 4(1), 1-14.
- Hirano, A., Donnenfeld, H., Sasaki, S. & Nakano, I. (1984) Fine structural observations of neurofilamentous changes in amyotrophic lateral sclerosis. *Journal of Neuropathology & Experimental Neurology*, 43(5), 461-470.
- Hirose, T., Virnicchi, G., Tanigawa, A., Naganuma, T., Li, R., Kimura, H., Yokoi, T., Nakagawa, S., Bénard, M. & Fox, A. H. (2014) NEAT1 long noncoding RNA regulates transcription via protein sequestration within subnuclear bodies. *Molecular biology of the cell*, 25(1), 169-183.
- Hock, E.-M., Maniecka, Z., Hruska-Plochan, M., Reber, S., Laferriere, F., MK, S. S., Ederle, H., Gittings, L., Pelkmans, L. & Dupuis, L. (2018) Hypertonic stress causes cytoplasmic translocation of neuronal, but not astrocytic, FUS due to impaired transportin function. *Cell reports*, 24(4), 987-1000. e7.
- Holcik, M. & Sonenberg, N. (2005) Translational control in stress and apoptosis. *Nature reviews Molecular cell biology*, 6(4), 318-327.

- Holdt, L. M., Stahringer, A., Sass, K., Pichler, G., Kulak, N. A., Wilfert, W., Kohlmaier, A., Herbst, A., Northoff, B. H. & Nicolaou, A. (2016) Circular non-coding RNA ANRIL modulates ribosomal RNA maturation and atherosclerosis in humans. *Nature communications*, 7(1), 1-14.
- Holmes, K. D., Babwah, A. V., Dale, L. B., Poulter, M. O. & Ferguson, S. S. (2006) Differential regulation of corticotropin releasing factor 1 α receptor endocytosis and trafficking by β -arrestins and Rab GTPases. *Journal of neurochemistry*, 96(4), 934-949.
- Hon, K. W., Ab-Mutalib, N. S., Abdullah, N. M. A., Jamal, R. & Abu, N. (2019) Extracellular Vesicle-derived circular RNAs confers chemoresistance in Colorectal cancer. *Scientific reports*, 9(1), 1-13.
- Huang, C., Liang, D., Tatomer, D. C. & Wilusz, J. E. (2018) A length-dependent evolutionarily conserved pathway controls nuclear export of circular RNAs. *Genes & development*, 32(9-10), 639-644.
- Huang, Y., Shen, X. J., Zou, Q., Wang, S. P., Tang, S. M. & Zhang, G. Z. (2011) Biological functions of microRNAs: a review. *Journal of physiology and biochemistry*, 67(1), 129-139.
- Hubstenberger, A., Courel, M., Bénard, M., Souquere, S., Ernoult-Lange, M., Chouaib, R., Yi, Z., Morlot, J.-B., Munier, A. & Fradet, M. (2017) P-body purification reveals the condensation of repressed mRNA regulons. *Molecular cell*, 68(1), 144-157. e5.
- Hubstenberger, A., Noble, S. L., Cameron, C. & Evans, T. C. (2013) Translation repressors, an RNA helicase, and developmental cues control RNP phase transitions during early development. *Developmental cell*, 27(2), 161-173.
- Huggins, M. L. (1942) Some properties of solutions of long-chain compounds. *The Journal of Physical Chemistry*, 46(1), 151-158.
- Hutcheon, B., Brown, L. & Poulter, M. (2000) Digital analysis of light microscope immunofluorescence: high-resolution co-localization of synaptic proteins in cultured neurons. *Journal of neuroscience methods*, 96(1), 1-9.
- Hutcheon, B., Fritschy, J. & Poulter, M. (2004) Organization of GABAA receptor α -subunit clustering in the developing rat neocortex and hippocampus. *European Journal of Neuroscience*, 19(9), 2475-2487.
- Hwang, H. & Mendell, J. (2006) MicroRNAs in cell proliferation, cell death, and tumorigenesis. *British journal of cancer*, 94(6), 776-780.
- IDTDNA *oligo analyzer tool* Available online:
https://www.idtdna.com/pages/tools/oligoanalyzer?utm_source=google&utm_medium=cpc&utm_campaign=ga_oligoanalyzer&utm_content=ad_group_oligo_analyzer&gclid=CjwKCAiA1eKB BhBZEiwAX3gqlyBO4ztOyPnL0G-npZJYX-1oHWQJvojThoEyR7wcZhnK4W5-1GtAixoCsTYQAvD_BwE [Accessed.

Imbert, G., Feng, Y., Nelson, D., Warren, S. & Mandel, J. (1998) FMR1 and mutations in fragile X syndrome: molecular biology, biochemistry, and genetics. *Genetic instabilities and hereditary neurological diseases*, 27-53.

Ingelfinger, D., Arndt-Jovin, D. J., Lührmann, R. & Achsel, T. (2002) The human LSm1-7 proteins colocalize with the mRNA-degrading enzymes Dcp1/2 and Xrn1 in distinct cytoplasmic foci. *Rna*, 8(12), 1489-1501.

Ivanov, A., Memczak, S., Wyler, E., Torti, F., Porath, H. T., Orejuela, M. R., Piechotta, M., Levanon, E. Y., Landthaler, M. & Dieterich, C. (2015) Analysis of intron sequences reveals hallmarks of circular RNA biogenesis in animals. *Cell reports*, 10(2), 170-177.

Izmiryan, A., Franco, C. A., Paulin, D., Li, Z. & Xue, Z. (2009) Synemin isoforms during mouse development: multiplicity of partners in vascular and neuronal systems. *Experimental cell research*, 315(5), 769-783.

Jain, S., Wheeler, J. R., Walters, R. W., Agrawal, A., Barsic, A. & Parker, R. (2016) ATPase-modulated stress granules contain a diverse proteome and substructure. *Cell*, 164(3), 487-498.

Janmey, P. A. (1998) The cytoskeleton and cell signaling: component localization and mechanical coupling. *Physiological reviews*, 78(3), 763-781.

Jeck, W. R. & Sharpless, N. E. (2014) Detecting and characterizing circular RNAs. *Nature biotechnology*, 32(5), 453-461.

Jeck, W. R., Sorrentino, J. A., Wang, K., Slevin, M. K., Burd, C. E., Liu, J., Marzluff, W. F. & Sharpless, N. E. (2013) Circular RNAs are abundant, conserved, and associated with ALU repeats. *Rna*, 19(2), 141-157.

Jen, J., Tang, Y.-A., Lu, Y.-H., Lin, C.-C., Lai, W.-W. & Wang, Y.-C. (2017) Oct4 transcriptionally regulates the expression of long non-coding RNAs NEAT1 and MALAT1 to promote lung cancer progression. *Molecular cancer*, 16(1), 1-12.

Jiang, L., Shao, C., Wu, Q.-J., Chen, G., Zhou, J., Yang, B., Li, H., Gou, L.-T., Zhang, Y. & Wang, Y. (2017) NEAT1 scaffolds RNA-binding proteins and the Microprocessor to globally enhance pri-miRNA processing. *Nature structural & molecular biology*, 24(10), 816.

Jing, Q., Huang, S., Guth, S., Zarubin, T., Motoyama, A., Chen, J., Di Padova, F., Lin, S.-C., Gram, H. & Han, J. (2005) Involvement of microRNA in AU-rich element-mediated mRNA instability. *Cell*, 120(5), 623-634.

Johnson, J. O., Mandrioli, J., Benatar, M., Abramzon, Y., Van Deerlin, V. M., Trojanowski, J. Q., Gibbs, J. R., Brunetti, M., Gronka, S. & Wu, J. (2010) Exome sequencing reveals VCP mutations as a cause of familial ALS. *Neuron*, 68(5), 857-864.

Johnson, J. O., Pioro, E. P., Boehringer, A., Chia, R., Feit, H., Renton, A. E., Pliner, H. A., Abramzon, Y., Marangi, G. & Winborn, B. J. (2014) Mutations in the Matrin 3 gene cause familial amyotrophic lateral sclerosis. *Nature neuroscience*, 17(5), 664-666.

- Jolly, C., Usson, Y. & Morimoto, R. I. (1999) Rapid and reversible relocalization of heat shock factor 1 within seconds to nuclear stress granules. *Proceedings of the National Academy of Sciences*, 96(12), 6769-6774.
- Julien, J.-P., Millecamps, S. & Kriz, J. (2005) Cytoskeletal defects in amyotrophic lateral sclerosis (motor neuron disease), *Novartis Found Symp.* Wiley Online Library.
- Kamelgarn, M., Chen, J., Kuang, L., Arenas, A., Zhai, J., Zhu, H. & Gal, J. (2016) Proteomic analysis of FUS interacting proteins provides insights into FUS function and its role in ALS. *Biochimica et Biophysica Acta (BBA)-Molecular Basis of Disease*, 1862(10), 2004-2014.
- Kameyama, T., Suzuki, H. & Mayeda, A. (2012) Re-splicing of mature mRNA in cancer cells promotes activation of distant weak alternative splice sites. *Nucleic acids research*, 40(16), 7896-7906.
- Kanai, Y., Dohmae, N. & Hirokawa, N. (2004) Kinesin transports RNA: isolation and characterization of an RNA-transporting granule. *Neuron*, 43(4), 513-525.
- Karijolich, J. & Yu, Y.-T. (2010) Spliceosomal snRNA modifications and their function. *RNA biology*, 7(2), 192-204.
- Ke, H., Zhao, L., Feng, X., Xu, H., Zou, L., Yang, Q., Su, X., Peng, L. & Jiao, B. (2016) NEAT1 is required for survival of breast cancer cells through FUS and miR-548. *Gene regulation and systems biology*, 10, GRSB. S29414.
- Kedersha, N., Cho, M. R., Li, W., Yacono, P. W., Chen, S., Gilks, N., Golan, D. E. & Anderson, P. (2000) Dynamic shuttling of TIA-1 accompanies the recruitment of mRNA to mammalian stress granules. *The Journal of cell biology*, 151(6), 1257-1268.
- Kedersha, N., Ivanov, P. & Anderson, P. (2013) Stress granules and cell signaling: more than just a passing phase? *Trends in biochemical sciences*, 38(10), 494-506.
- Kedersha, N., Stoecklin, G., Ayodele, M., Yacono, P., Lykke-Andersen, J., Fritzler, M. J., Scheuner, D., Kaufman, R. J., Golan, D. E. & Anderson, P. (2005) Stress granules and processing bodies are dynamically linked sites of mRNP remodeling. *The Journal of cell biology*, 169(6), 871-884.
- Kelly, S., Greenman, C., Cook, P. R. & Papantonis, A. (2015) Exon skipping is correlated with exon circularization. *Journal of molecular biology*, 427(15), 2414-2417.
- Khong, A., Jain, S., Matheny, T., Wheeler, J. R. & Parker, R. (2018) Isolation of mammalian stress granule cores for RNA-Seq analysis. *Methods*, 137, 49-54.
- Khong, A., Matheny, T., Jain, S., Mitchell, S. F., Wheeler, J. R. & Parker, R. (2017) The stress granule transcriptome reveals principles of mRNA accumulation in stress granules. *Molecular cell*, 68(4), 808-820. e5.

- Kiebler, M. A. & Bassell, G. J. (2006) Neuronal RNA granules: movers and makers. *Neuron*, 51(6), 685-690.
- Kim, H. J., Kim, N. C., Wang, Y.-D., Scarborough, E. A., Moore, J., Diaz, Z., MacLea, K. S., Freibaum, B., Li, S. & Molliex, A. (2013) Mutations in prion-like domains in hnRNPA2B1 and hnRNPA1 cause multisystem proteinopathy and ALS. *Nature*, 495(7442), 467-473.
- King, O. D., Gitler, A. D. & Shorter, J. (2012) The tip of the iceberg: RNA-binding proteins with prion-like domains in neurodegenerative disease. *Brain research*, 1462, 61-80.
- Klim, J. R., Williams, L. A., Limone, F., San Juan, I. G., Davis-Dusenbery, B. N., Mordes, D. A., Burberry, A., Steinbaugh, M. J., Gamage, K. K. & Kirchner, R. (2019) ALS-implicated protein TDP-43 sustains levels of STMN2, a mediator of motor neuron growth and repair. *Nature neuroscience*, 22(2), 167-179.
- Knowles, R. B., Sabry, J. H., Martone, M. E., Deerinck, T. J., Ellisman, M. H., Bassell, G. J. & Kosik, K. S. (1996) Translocation of RNA granules in living neurons. *Journal of Neuroscience*, 16(24), 7812-7820.
- Koh, W., Pan, W., Gawad, C., Fan, H. C., Kerchner, G. A., Wyss-Coray, T., Blumenfeld, Y. J., El-Sayed, Y. Y. & Quake, S. R. (2014) Noninvasive in vivo monitoring of tissue-specific global gene expression in humans. *Proceedings of the National Academy of Sciences*, 111(20), 7361-7366.
- Kolb, S. J., Battle, D. J. & Dreyfuss, G. (2007) Molecular functions of the SMN complex. *Journal of child neurology*, 22(8), 990-994.
- Krichevsky, A. M. & Kosik, K. S. (2001) Neuronal RNA granules: a link between RNA localization and stimulation-dependent translation. *Neuron*, 32(4), 683-696.
- Kristensen, L., Hansen, T., Venø, M. & Kjems, J. (2018a) Circular RNAs in cancer: opportunities and challenges in the field. *Oncogene*, 37(5), 555-565.
- Kristensen, L. S., Okholm, T. L. H., Venø, M. T. & Kjems, J. (2018b) Circular RNAs are abundantly expressed and upregulated during human epidermal stem cell differentiation. *RNA biology*, 15(2), 280-291.
- Krol, J. (2017) Paraspeckles: nuclear nests helping to raise mature miRNAs. *Nature structural & molecular biology*, 24(10), 783.
- Kumar, L., Jadya, P., Haque, R., Shukla, S. & Nazir, A. (2018) Functional characterization of novel circular RNA molecule, circzip-2 and its synthesizing gene zip-2 in *C. elegans* model of Parkinson's disease. *Molecular neurobiology*, 55(8), 6914-6926.
- Landers, J. E., Melki, J., Meininger, V., Glass, J. D., Van Den Berg, L. H., Van Es, M. A., Sapp, P. C., Van Vught, P. W., McKenna-Yasek, D. M. & Blauw, H. M. (2009) Reduced expression of the Kinesin-Associated Protein 3 (KIFAP3) gene increases survival in sporadic amyotrophic lateral sclerosis. *Proceedings of the National Academy of Sciences*, 106(22), 9004-9009.

- Lasda, E. & Parker, R. (2014) Circular RNAs: diversity of form and function. *Rna*, 20(12), 1829-1842.
- Lee, C.-Y. S., Putnam, A., Lu, T., He, S., Ouyang, J. P. T. & Seydoux, G. (2020) Recruitment of mRNAs to P granules by condensation with intrinsically-disordered proteins. *Elife*, 9, e52896.
- Lee, C., Roberts, S. E. & Gladfelter, A. S. (2016) Quantitative spatial analysis of transcripts in multinucleate cells using single-molecule FISH. *Methods*, 98, 124-133.
- Lee, D. Y. & Brown, E. J. (2012) Ubiquilins in the crosstalk among proteolytic pathways. *Biological chemistry*, 393(6), 441-447.
- Legnini, I., Di Timoteo, G., Rossi, F., Morlando, M., Briganti, F., Sthandier, O., Fatica, A., Santini, T., Andronache, A. & Wade, M. (2017) Circ-ZNF609 is a circular RNA that can be translated and functions in myogenesis. *Molecular cell*, 66(1), 22-37. e9.
- Leigh, P., Anderton, B., Dodson, A., Gallo, J.-M., Swash, M. & Power, D. (1988) Ubiquitin deposits in anterior horn cells in motor neurone disease. *Neuroscience letters*, 93(2-3), 197-203.
- Levin, E. C., Acharya, N. K., Sedeyn, J. C., Venkataraman, V., D'Andrea, M. R., Wang, H.-Y. & Nagele, R. G. (2009) Neuronal expression of vimentin in the Alzheimer's disease brain may be part of a generalized dendritic damage-response mechanism. *Brain research*, 1298, 194-207.
- Li, D.-W., Liu, M., Cui, B., Fang, J., Guan, Y.-Z., Ding, Q., Li, X. & Cui, L. (2017a) The Awaji criteria increases the diagnostic sensitivity of the revised El Escorial criteria for amyotrophic lateral sclerosis diagnosis in a Chinese population. *PloS one*, 12(3), e0171522.
- Li, F., Xu, D., Wang, Y., Zhou, Z., Liu, J., Hu, S., Gong, Y., Yuan, J. & Pan, L. (2018a) Structural insights into the ubiquitin recognition by OPTN (optineurin) and its regulation by TBK1-mediated phosphorylation. *Autophagy*, 14(1), 66-79.
- Li, P., Banjade, S., Cheng, H.-C., Kim, S., Chen, B., Guo, L., Llaguno, M., Hollingsworth, J. V., King, D. S. & Banani, S. F. (2012) Phase transitions in the assembly of multivalent signalling proteins. *Nature*, 483(7389), 336-340.
- Li, P., Chen, S., Chen, H., Mo, X., Li, T., Shao, Y., Xiao, B. & Guo, J. (2015a) Using circular RNA as a novel type of biomarker in the screening of gastric cancer. *Clinica chimica acta*, 444, 132-136.
- Li, X.-H., Chavali, P. L., Pancsa, R., Chavali, S. & Babu, M. M. (2018b) Function and regulation of phase-separated biological condensates. *Biochemistry*, 57(17), 2452-2461.
- Li, X., Liu, C.-X., Xue, W., Zhang, Y., Jiang, S., Yin, Q.-F., Wei, J., Yao, R.-W., Yang, L. & Chen, L.-L. (2017b) Coordinated circRNA biogenesis and function with NF90/NF110 in viral infection. *Molecular cell*, 67(2), 214-227. e7.

- Li, X., Wang, X., Song, W., Xu, H., Huang, R., Wang, Y., Zhao, W., Xiao, Z. & Yang, X. (2018c) Oncogenic properties of NEAT1 in prostate cancer cells depend on the CDC5L–AGRN transcriptional regulation circuit. *Cancer research*, 78(15), 4138-4149.
- Li, Y., Zheng, Q., Bao, C., Li, S., Guo, W., Zhao, J., Chen, D., Gu, J., He, X. & Huang, S. (2015b) Circular RNA is enriched and stable in exosomes: a promising biomarker for cancer diagnosis. *Cell research*, 25(8), 981-984.
- Li, Y. R., King, O. D., Shorter, J. & Gitler, A. D. (2013) Stress granules as crucibles of ALS pathogenesis. *Journal of cell biology*, 201(3), 361-372.
- Li, Z., Huang, C., Bao, C., Chen, L., Lin, M., Wang, X., Zhong, G., Yu, B., Hu, W. & Dai, L. (2015c) Exon-intron circular RNAs regulate transcription in the nucleus. *Nature structural & molecular biology*, 22(3), 256.
- Lin, C.-L. G., Bristol, L. A., Jin, L., Dykes-Hoberg, M., Crawford, T., Clawson, L. & Rothstein, J. D. (1998) Aberrant RNA processing in a neurodegenerative disease: the cause for absent EAAT2, a glutamate transporter, in amyotrophic lateral sclerosis. *Neuron*, 20(3), 589-602.
- Lin, Y., Protter, D. S., Rosen, M. K. & Parker, R. (2015) Formation and maturation of phase-separated liquid droplets by RNA-binding proteins. *Molecular cell*, 60(2), 208-219.
- Lindquist, S. (1981) Regulation of protein synthesis during heat shock. *Nature*, 293(5830), 311-314.
- Ling, S.-C., Polymenidou, M. & Cleveland, D. W. (2013) Converging mechanisms in ALS and FTD: disrupted RNA and protein homeostasis. *Neuron*, 79(3), 416-438.
- Liu-Yesucevitz, L., Bilgutay, A., Zhang, Y.-J., Vanderwyde, T., Citro, A., Mehta, T., Zaarur, N., McKee, A., Bowser, R. & Sherman, M. (2010a) Tar DNA binding protein-43 (TDP-43) associates with stress granules: analysis of cultured cells and pathological brain tissue. *PloS one*, 5(10), e13250.
- Liu-Yesucevitz, L., Bilgutay, A., Zhang, Y.-J., Vanderwyde, T., Citro, A., Mehta, T., Zaarur, N., McKee, A., Bowser, R. & Sherman, M. (2010b) Tar DNA binding protein-43 (TDP-43) associates with stress granules: analysis of cultured cells and pathological brain tissue. *PloS one*, 5(10).
- Liu, Q., Shu, S., Wang, R. R., Liu, F., Cui, B., Guo, X. N., Lu, C. X., Li, X. G., Liu, M. S. & Peng, B. (2016) Whole-exome sequencing identifies a missense mutation in hnRNPA1 in a family with flail arm ALS. *Neurology*, 87(17), 1763-1769.
- Liu, Y. & Lu, Z. (2018) Long non-coding RNA NEAT 1 mediates the toxic of Parkinson's disease induced by MPTP/MPP+ via regulation of gene expression. *Clinical and Experimental Pharmacology and Physiology*, 45(8), 841-848.
- Livak, K. J. & Schmittgen, T. D. (2001) Analysis of relative gene expression data using real-time quantitative PCR and the 2⁻ΔΔCT method. *methods*, 25(4), 402-408.

- Lo, P.-K., Zhang, Y., Wolfson, B., Gernapudi, R., Yao, Y., Duru, N. & Zhou, Q. (2016) Dysregulation of the BRCA1/long non-coding RNA NEAT1 signaling axis contributes to breast tumorigenesis. *Oncotarget*, 7(40), 65067.
- Louro, R., Smirnova, A. S. & Verjovski-Almeida, S. (2009) Long intronic noncoding RNA transcription: expression noise or expression choice? *Genomics*, 93(4), 291-298.
- Luisier, R., Tyzack, G. E., Hall, C. E., Mitchell, J. S., Devine, H., Taha, D. M., Malik, B., Meyer, I., Greensmith, L. & Newcombe, J. (2018) Intron retention and nuclear loss of SFPQ are molecular hallmarks of ALS. *Nature communications*, 9(1), 1-15.
- Lukiw, W. (2013) Circular RNA (circRNA) in Alzheimer's disease (AD). *Frontiers in genetics*, 4, 307.
- Luo, H., Wang, J., Liu, D., Zang, S., Ma, N., Zhao, L., Zhang, L., Zhang, X. & Qiao, C. (2019) The lncRNA H19/miR-675 axis regulates myocardial ischemic and reperfusion injury by targeting PPAR α . *Molecular immunology*, 105, 46-54.
- Luty, A. A., Kwok, J. B., Dobson-Stone, C., Loy, C. T., Coupland, K. G., Karlström, H., Sobow, T., Tchorzewska, J., Maruszak, A. & Barcikowska, M. (2010) Sigma nonopioid intracellular receptor 1 mutations cause frontotemporal lobar degeneration–motor neuron disease. *Annals of neurology*, 68(5), 639-649.
- Ma, Y., Liu, Y. & Jiang, Z. (2020) CircRNAs: A new perspective of biomarkers in the nervous system. *Biomedicine & Pharmacotherapy*, 128, 110251.
- Mahadevan, K., Zhang, H., Akef, A., Cui, X. A., Gueroussov, S., Cenik, C., Roth, F. P. & Palazzo, A. F. (2013) RanBP2/Nup358 potentiates the translation of a subset of mRNAs encoding secretory proteins. *PLoS Biol*, 11(4), e1001545.
- Markmiller, S., Soltanieh, S., Server, K. L., Mak, R., Jin, W., Fang, M. Y., Luo, E.-C., Krach, F., Yang, D. & Sen, A. (2018) Context-dependent and disease-specific diversity in protein interactions within stress granules. *Cell*, 172(3), 590-604. e13.
- Martin, K. C. & Ephrussi, A. (2009) mRNA localization: gene expression in the spatial dimension. *Cell*, 136(4), 719-730.
- Maruyama, H., Morino, H., Ito, H., Izumi, Y., Kato, H., Watanabe, Y., Kinoshita, Y., Kamada, M., Nodera, H. & Suzuki, H. (2010) Mutations of optineurin in amyotrophic lateral sclerosis. *Nature*, 465(7295), 223-226.
- Matsuo, T. & Hayakawa, N. (2018) π -Electron systems containing Si=Si double bonds. *Science and Technology of advanced Materials*, 19(1), 108-129.
- Mattick, J. S. & Makunin, I. V. (2006) Non-coding RNA. *Human molecular genetics*, 15(suppl_1), R17-R29.

McGough, A., Way, M. & DeRosier, D. (1994) Determination of the alpha-actinin-binding site on actin filaments by cryoelectron microscopy and image analysis. *The Journal of Cell Biology*, 126(2), 433-443.

McGurk, L., Lee, V. M., Trojanowski, J. Q., Van Deerlin, V. M., Lee, E. B. & Bonini, N. M. (2014) Poly-A binding protein-1 localization to a subset of TDP-43 inclusions in amyotrophic lateral sclerosis occurs more frequently in patients harboring an expansion in C9orf72. *Journal of Neuropathology & Experimental Neurology*, 73(9), 837-845.

Memczak, S., Jens, M., Elefsinioti, A., Torti, F., Krueger, J., Rybak, A., Maier, L., Mackowiak, S. D., Gregersen, L. H. & Munschauer, M. (2013) Circular RNAs are a large class of animal RNAs with regulatory potency. *Nature*, 495(7441), 333-338.

Militello, G., Weirick, T., John, D., Döring, C., Dimmeler, S. & Uchida, S. (2017) Screening and validation of lncRNAs and circRNAs as miRNA sponges. *Briefings in bioinformatics*, 18(5), 780-788.

Miller, R., Mitchell, J., Lyon, M. & Moore, D. (2003) Riluzole for amyotrophic lateral sclerosis (ALS)/motor neuron disease (MND). *Amyotrophic lateral sclerosis and other motor neuron disorders: official publication of the World Federation of Neurology, Research Group on Motor Neuron Diseases*, 4(3), 191-206.

Miñones-Moyano, E., Porta, S., Escaramís, G., Rabionet, R., Iraola, S., Kagerbauer, B., Espinosa-Parrilla, Y., Ferrer, I., Estivill, X. & Martí, E. (2011) MicroRNA profiling of Parkinson's disease brains identifies early downregulation of miR-34b/c which modulate mitochondrial function. *Human molecular genetics*, 20(15), 3067-3078.

Mitchell, J., Paul, P., Chen, H.-J., Morris, A., Payling, M., Falchi, M., Habgood, J., Panoutsou, S., Winkler, S. & Tisato, V. (2010) Familial amyotrophic lateral sclerosis is associated with a mutation in D-amino acid oxidase. *Proceedings of the National Academy of Sciences*, 107(16), 7556-7561.

Mitreá, D. M. & Kriwacki, R. W. (2016) Phase separation in biology; functional organization of a higher order. *Cell Communication and Signaling*, 14(1), 1.

Mollet, S., Cougot, N., Wilczynska, A., Dautry, F., Kress, M., Bertrand, E. & Weil, D. (2008) Translationally repressed mRNA transiently cycles through stress granules during stress. *Molecular biology of the cell*, 19(10), 4469-4479.

Molliex, A., Temirov, J., Lee, J., Coughlin, M., Kanagaraj, A. P., Kim, H. J., Mittag, T. & Taylor, J. P. (2015) Phase separation by low complexity domains promotes stress granule assembly and drives pathological fibrillization. *Cell*, 163(1), 123-133.

Mourelatos, Z., Abel, L., Yong, J., Kataoka, N. & Dreyfuss, G. (2001) SMN interacts with a novel family of hnRNP and spliceosomal proteins. *The EMBO journal*, 20(19), 5443-5452.

Mu, X., He, J., Anderson, D. W., Springer, J. E. & Trojanowski, J. Q. (1996) Altered expression of bcl-2 and bax mRNA in amyotrophic lateral sclerosis spinal cord motor neurons. *Annals of*

Neurology: Official Journal of the American Neurological Association and the Child Neurology Society, 40(3), 379-386.

Münch, C., Rosenbohm, A., Sperfeld, A. D., Uttner, I., Reske, S., Krause, B. J., Sedlmeier, R., Meyer, T., Hanemann, C. O. & Stumm, G. (2005) Heterozygous R1101K mutation of the DCTN1 gene in a family with ALS and FTD. *Annals of Neurology: Official Journal of the American Neurological Association and the Child Neurology Society*, 58(5), 777-780.

Münch, C., Sedlmeier, R., Meyer, T., Homberg, V., Sperfeld, A., Kurt, A., Prudlo, J., Peraus, G., Hanemann, C. & Stumm, G. (2004) Point mutations of the p150 subunit of dynactin (DCTN1) gene in ALS. *Neurology*, 63(4), 724-726.

Nagai, M., Re, D. B., Nagata, T., Chalazonitis, A., Jessell, T. M., Wichterle, H. & Przedborski, S. (2007) Astrocytes expressing ALS-linked mutated SOD1 release factors selectively toxic to motor neurons. *Nature neuroscience*, 10(5), 615-622.

Nakagawa, S., Naganuma, T., Shioi, G. & Hirose, T. (2011) Paraspeckles are subpopulation-specific nuclear bodies that are not essential in mice. *Journal of Cell Biology*, 193(1), 31-39.

Namkoong, S., Ho, A., Woo, Y. M., Kwak, H. & Lee, J. H. (2018) Systematic characterization of stress-induced RNA granulation. *Molecular cell*, 70(1), 175-187. e8.

NCBI PRIMER BLAST. NCBI. Available online: https://www.ncbi.nlm.nih.gov/tools/primer-blast/index.cgi?ORGANISM=1235996&INPUT_SEQUENCE=JX869059.1&LINK_LOC=nucleore [Accessed

Ninomiya, K., Adachi, S., Natsume, T., Iwakiri, J., Terai, G., Asai, K. & Hirose, T. (2020) Lnc RNA-dependent nuclear stress bodies promote intron retention through SR protein phosphorylation. *The EMBO journal*, 39(3), e102729.

Nishimoto, Y., Nakagawa, S., Hirose, T., Okano, H. J., Takao, M., Shibata, S., Suyama, S., Kuwako, K.-i., Imai, T. & Murayama, S. (2013) The long non-coding RNA nuclear-enriched abundant transcript 1_2 induces paraspeckle formation in the motor neuron during the early phase of amyotrophic lateral sclerosis. *Molecular brain*, 6(1), 31.

Nishimura, S. (1972) Minor components in transfer RNA: their characterization, location, and function. *Progress in nucleic acid research and molecular biology*, 12, 49-85.

Nott, T. J., Craggs, T. D. & Baldwin, A. J. (2016) Membraneless organelles can melt nucleic acid duplexes and act as biomolecular filters. *Nature chemistry*, 8(6), 569-575.

Nott, T. J., Petsalaki, E., Farber, P., Jervis, D., Fussner, E., Plochowitz, A., Craggs, T. D., Bazett-Jones, D. P., Pawson, T. & Forman-Kay, J. D. (2015) Phase transition of a disordered nuage protein generates environmentally responsive membraneless organelles. *Molecular cell*, 57(5), 936-947.

O'Donnell, W. T. & Warren, S. T. (2002) A decade of molecular studies of fragile X syndrome. *Annual review of neuroscience*, 25(1), 315-338.

- Oakes, J. A., Davies, M. C. & Collins, M. O. (2017) TBK1: a new player in ALS linking autophagy and neuroinflammation. *Molecular brain*, 10(1), 1-10.
- Offen, D., Barhum, Y., Melamed, E., Embacher, N., Schindler, C. & Ransmayr, G. (2009) Spinal cord mRNA profile in patients with ALS: comparison with transgenic mice expressing the human SOD-1 mutant. *Journal of Molecular Neuroscience*, 38(2), 85-93.
- Orlacchio, A., Babalini, C., Borreca, A., Patrono, C., Massa, R., Basaran, S., Munhoz, R. P., Rogava, E. A., St George-Hyslop, P. H. & Bernardi, G. (2010) SPATACSIN mutations cause autosomal recessive juvenile amyotrophic lateral sclerosis. *Brain*, 133(2), 591-598.
- Orozco, D. & Edbauer, D. (2013) FUS-mediated alternative splicing in the nervous system: consequences for ALS and FTL. *Journal of Molecular Medicine*, 91(12), 1343-1354.
- Orozco, D., Tahirovic, S., Rentzsch, K., Schwenk, B. M., Haass, C. & Edbauer, D. (2012) Loss of fused in sarcoma (FUS) promotes pathological Tau splicing. *EMBO reports*, 13(8), 759-764.
- Pak, C. W., Kosno, M., Holehouse, A. S., Padrick, S. B., Mittal, A., Ali, R., Yunus, A. A., Liu, D. R., Pappu, R. V. & Rosen, M. K. (2016) Sequence determinants of intracellular phase separation by complex coacervation of a disordered protein. *Molecular cell*, 63(1), 72-85.
- Pamudurti, N. R., Bartok, O., Jens, M., Ashwal-Fluss, R., Stottmeister, C., Ruhe, L., Hanan, M., Wyler, E., Perez-Hernandez, D. & Ramberger, E. (2017) Translation of circRNAs. *Molecular cell*, 66(1), 9-21. e7.
- Pan, T., Sun, X., Liu, Y., Li, H., Deng, G., Lin, H. & Wang, S. (2018) Heat stress alters genome-wide profiles of circular RNAs in Arabidopsis. *Plant Molecular Biology*, 96(3), 217-229.
- Park, E. & Maquat, L. E. (2013) Staufen-mediated mRNA decay. *Wiley interdisciplinary reviews: RNA*, 4(4), 423-435.
- Parkinson, N., Ince, P., Smith, M., Highley, R., Skibinski, G., Andersen, P., Morrison, K., Pall, H., Hardiman, O. & Collinge, J. (2006) ALS phenotypes with mutations in CHMP2B (charged multivesicular body protein 2B). *Neurology*, 67(6), 1074-1077.
- Pasman, Z., Been, M. D. & Garcia-Blanco, M. A. (1996) Exon circularization in mammalian nuclear extracts. *Rna*, 2(6), 603.
- Pearce, A. K. & Humphrey, T. C. (2001) Integrating stress-response and cell-cycle checkpoint pathways. *Trends in cell biology*, 11(10), 426-433.
- Pelletier, J. & Sonenberg, N. (1988) Internal initiation of translation of eukaryotic mRNA directed by a sequence derived from poliovirus RNA. *Nature*, 334(6180), 320-325.
- Pickrell, A. M. & Youle, R. J. (2015) The roles of PINK1, parkin, and mitochondrial fidelity in Parkinson's disease. *Neuron*, 85(2), 257-273.

- Pisani, G. & Baron, B. (2019) Nuclear Paraspeckles function in mediating gene regulatory and apoptotic pathways. *Non-coding RNA Research*.
- Piwecka, M., Glažar, P., Hernandez-Miranda, L. R., Memczak, S., Wolf, S. A., Rybak-Wolf, A., Filipchuk, A., Klironomos, F., Jara, C. A. C. & Fenske, P. (2017) Loss of a mammalian circular RNA locus causes miRNA deregulation and affects brain function. *Science*, 357(6357).
- Pompey, S. N., Michaely, P. & Luby-Phelps, K. (2013) Quantitative fluorescence co-localization to study protein–receptor complexes, *Protein-Ligand Interactions* Springer, 439-453.
- Ponting, C. P., Oliver, P. L. & Reik, W. (2009) Evolution and functions of long noncoding RNAs. *Cell*, 136(4), 629-641.
- Prasanth, K. V., Prasanth, S. G., Xuan, Z., Hearn, S., Freier, S. M., Bennett, C. F., Zhang, M. Q. & Spector, D. L. (2005) Regulating gene expression through RNA nuclear retention. *Cell*, 123(2), 249-263.
- Protter, D. S. & Parker, R. (2016) Principles and properties of stress granules. *Trends in cell biology*, 26(9), 668-679.
- Prudencio, M., Belzil, V. V., Batra, R., Ross, C. A., Gendron, T. F., Pregent, L. J., Murray, M. E., Overstreet, K. K., Piazza-Johnston, A. E. & Desaro, P. (2015) Distinct brain transcriptome profiles in C9orf72-associated and sporadic ALS. *Nature neuroscience*, 18(8), 1175-1182.
- Puls, I., Jonnakuty, C., LaMonte, B. H., Holzbaur, E. L., Tokito, M., Mann, E., Floeter, M. K., Bidus, K., Drayna, D. & Oh, S. J. (2003) Mutant dynactin in motor neuron disease. *Nature genetics*, 33(4), 455-456.
- Qamar, S., Wang, G., Randle, S. J., Ruggeri, F. S., Varela, J. A., Lin, J. Q., Phillips, E. C., Miyashita, A., Williams, D. & Ströhl, F. (2018) FUS phase separation is modulated by a molecular chaperone and methylation of arginine cation- π interactions. *Cell*, 173(3), 720-734. e15.
- Rainier, S., Bui, M., Mark, E., Thomas, D., Tokarz, D., Ming, L., Delaney, C., Richardson, R. J., Albers, J. W. & Matsunami, N. (2008) Neuropathy target esterase gene mutations cause motor neuron disease. *The American Journal of Human Genetics*, 82(3), 780-785.
- Renton, A. E., Majounie, E., Waite, A., Simón-Sánchez, J., Rollinson, S., Gibbs, J. R., Schymick, J. C., Laaksovirta, H., Van Swieten, J. C. & Myllykangas, L. (2011) A hexanucleotide repeat expansion in C9ORF72 is the cause of chromosome 9p21-linked ALS-FTD. *Neuron*, 72(2), 257-268.
- Roberts, T. C., Morris, K. V. & Wood, M. J. (2014) The role of long non-coding RNAs in neurodevelopment, brain function and neurological disease. *Philosophical Transactions of the Royal Society B: Biological Sciences*, 369(1652), 20130507.
- Roegiers, F. & Jan, Y. N. (2000) Staufen: a common component of mRNA transport in oocytes and neurons? *Trends in cell biology*, 10(6), 220-224.

- Rosen, D. R., Siddique, T., Patterson, D., Figlewicz, D. A., Sapp, P., Hentati, A., Donaldson, D., Goto, J., O'Regan, J. P. & Deng, H.-X. (1993) Mutations in Cu/Zn superoxide dismutase gene are associated with familial amyotrophic lateral sclerosis. *Nature*, 362(6415), 59-62.
- Rossoll, W., Jablonka, S., Andreassi, C., Kröning, A.-K., Karle, K., Monani, U. R. & Sendtner, M. (2003) Smn, the spinal muscular atrophy–determining gene product, modulates axon growth and localization of β -actin mRNA in growth cones of motoneurons. *The Journal of cell biology*, 163(4), 801-812.
- Rothstein, J. D. (2009) Current hypotheses for the underlying biology of amyotrophic lateral sclerosis. *Annals of neurology*, 65(S1), S3-S9.
- Rothstein, J. D. (2017) Edaravone: a new drug approved for ALS. *Cell*, 171(4), 725.
- Rotunno, M. S. & Bosco, D. A. (2013) An emerging role for misfolded wild-type SOD1 in sporadic ALS pathogenesis. *Frontiers in cellular neuroscience*, 7, 253.
- Ruiz-Roig, C., Viéitez, C., Posas, F. & De Nadal, E. (2010) The Rpd3L HDAC complex is essential for the heat stress response in yeast. *Molecular microbiology*, 76(4), 1049-1062.
- Rybak-Wolf, A., Stottmeister, C., Glažar, P., Jens, M., Pino, N., Giusti, S., Hanan, M., Behm, M., Bartok, O. & Ashwal-Fluss, R. (2015) Circular RNAs in the mammalian brain are highly abundant, conserved, and dynamically expressed. *Molecular cell*, 58(5), 870-885.
- Sabatelli, M., Eusebi, F., Al-Chalabi, A., Conte, A., Madia, F., Luigetti, M., Mancuso, I., Limatola, C., Trettel, F. & Sobrero, F. (2009) Rare missense variants of neuronal nicotinic acetylcholine receptor altering receptor function are associated with sporadic amyotrophic lateral sclerosis. *Human molecular genetics*, 18(20), 3997-4006.
- Saberi, S., Stauffer, J. E., Schulte, D. J. & Ravits, J. (2015) Neuropathology of amyotrophic lateral sclerosis and its variants. *Neurologic clinics*, 33(4), 855-876.
- Saeed, M., Siddique, N., Hung, W., Usacheva, E., Liu, E., Sufit, R., Heller, S., Haines, J., Pericak-Vance, M. & Siddique, T. (2006) Paraoxonase cluster polymorphisms are associated with sporadic ALS. *Neurology*, 67(5), 771-776.
- Salzman, J. (2016) Circular RNA expression: its potential regulation and function. *Trends in genetics*, 32(5), 309-316.
- Salzman, J., Chen, R. E., Olsen, M. N., Wang, P. L. & Brown, P. O. (2013a) Cell-type specific features of circular RNA expression. *PLoS genetics*, 9(9).
- Salzman, J., Chen, R. E., Olsen, M. N., Wang, P. L. & Brown, P. O. (2013b) Cell-type specific features of circular RNA expression. *PLoS Genet*, 9(9), e1003777.
- Salzman, J., Gawad, C., Wang, P. L., Lacayo, N. & Brown, P. O. (2012) Circular RNAs are the predominant transcript isoform from hundreds of human genes in diverse cell types. *PLoS one*, 7(2), e30733.

- Sama, R. R. K., Ward, C. L., Kaushansky, L. J., Lemay, N., Ishigaki, S., Urano, F. & Bosco, D. A. (2013) FUS/TLS assembles into stress granules and is a prosurvival factor during hyperosmolar stress. *Journal of cellular physiology*, 228(11), 2222-2231.
- Sanger, H. L., Klotz, G., Riesner, D., Gross, H. J. & Kleinschmidt, A. K. (1976) Viroids are single-stranded covalently closed circular RNA molecules existing as highly base-paired rod-like structures. *Proceedings of the National Academy of Sciences*, 73(11), 3852-3856.
- Santoro, M., Nociti, V., Lucchini, M., De Fino, C., Losavio, F. A. & Mirabella, M. (2016) Expression profile of long non-coding RNAs in serum of patients with multiple sclerosis. *Journal of Molecular Neuroscience*, 59(1), 18-23.
- Satelli, A. & Li, S. (2011) Vimentin in cancer and its potential as a molecular target for cancer therapy. *Cellular and molecular life sciences*, 68(18), 3033-3046.
- Savino, T. M., Gébrane-Younès, J., De Mey, J., Sibarita, J.-B. & Hernandez-Verdun, D. (2001) Nucleolar assembly of the rRNA processing machinery in living cells. *The Journal of cell biology*, 153(5), 1097-1110.
- Schiffer, D., Cordera, S., Cavalla, P. & Migheli, A. (1996) Reactive astrogliosis of the spinal cord in amyotrophic lateral sclerosis. *Journal of the neurological sciences*, 139, 27-33.
- Schindelin, J., Arganda-Carreras, I., Frise, E., Kaynig, V., Longair, M., Pietzsch, T., Preibisch, S., Rueden, C., Saalfeld, S. & Schmid, B. (2012) Fiji: an open-source platform for biological-image analysis. *Nature methods*, 9(7), 676-682.
- Schwanhausser, B., Busse, D., Li, N., Dittmar, G., Schuchhardt, J., Wolf, J., Chen, W. & Selbach, M. (2013) Global quantification of mammalian gene expression control (vol 473, pg 337, 2011). *Nature*, 495(7439), 126-127.
- Shelkovanikova, T. A., Robinson, H. K., Troakes, C., Ninkina, N. & Buchman, V. L. (2014) Compromised paraspeckle formation as a pathogenic factor in FUSopathies. *Human molecular genetics*, 23(9), 2298-2312.
- Shiohama, A., Sasaki, T., Noda, S., Minoshima, S. & Shimizu, N. (2007) Nucleolar localization of DGCR8 and identification of eleven DGCR8-associated proteins. *Experimental cell research*, 313(20), 4196-4207.
- Simpson, C. L., Lemmens, R., Miskiewicz, K., Broom, W. J., Hansen, V. K., van Vught, P. W., Landers, J. E., Sapp, P., Van Den Bosch, L. & Knight, J. (2009) Variants of the elongator protein 3 (ELP3) gene are associated with motor neuron degeneration. *Human molecular genetics*, 18(3), 472-481.
- Sleeman, J. E. & Trinkle-Mulcahy, L. (2014) Nuclear bodies: new insights into assembly/dynamics and disease relevance. *Current opinion in cell biology*, 28, 76-83.

- Smith, B. N., Ticozzi, N., Fallini, C., Gkazi, A. S., Topp, S., Kenna, K. P., Scotter, E. L., Kost, J., Keagle, P. & Miller, J. W. (2014) Exome-wide rare variant analysis identifies TUBA4A mutations associated with familial ALS. *Neuron*, 84(2), 324-331.
- Sproviero, W., Shatunov, A., Stahl, D., Shoai, M., van Rheenen, W., Jones, A. R., Al-Sarraj, S., Andersen, P. M., Bonini, N. M. & Conforti, F. L. (2017) ATXN2 trinucleotide repeat length correlates with risk of ALS. *Neurobiology of aging*, 51, 178. e1-178. e9.
- Sreedharan, J., Blair, I. P., Tripathi, V. B., Hu, X., Vance, C., Rogelj, B., Ackerley, S., Durnall, J. C., Williams, K. L. & Buratti, E. (2008) TDP-43 mutations in familial and sporadic amyotrophic lateral sclerosis. *Science*, 319(5870), 1668-1672.
- Strong, M. J. (2010) The evidence for altered RNA metabolism in amyotrophic lateral sclerosis (ALS). *Journal of the neurological sciences*, 288(1-2), 1-12.
- Strong, M. J., Kesavapany, S. & Pant, H. C. (2005) The pathobiology of amyotrophic lateral sclerosis: a proteinopathy? *Journal of Neuropathology & Experimental Neurology*, 64(8), 649-664.
- Strong, M. J., Volkening, K., Hammond, R., Yang, W., Strong, W., Leystra-Lantz, C. & Shoesmith, C. (2007) TDP43 is a human low molecular weight neurofilament (hNFL) mRNA-binding protein. *Molecular and cellular neuroscience*, 35(2), 320-327.
- Sun, M. & Kraus, W. L. (2015) From discovery to function: the expanding roles of long noncoding RNAs in physiology and disease. *Endocrine reviews*, 36(1), 25-64.
- Sun, S., Lin, Q., Ma, J., Shi, W., Yang, B. & Li, F. (2017) Long non-coding RNA NEAT1 acts as oncogene in NSCLC by regulating the Wnt signaling pathway. *Eur Rev Med Pharmacol Sci*, 21(3), 504-510.
- Sunwoo, H., Dinger, M. E., Wilusz, J. E., Amaral, P. P., Mattick, J. S. & Spector, D. L. (2009) MEN ϵ/β nuclear-retained non-coding RNAs are up-regulated upon muscle differentiation and are essential components of paraspeckles. *Genome research*, 19(3), 347-359.
- Sunwoo, J.-S., Lee, S.-T., Im, W., Lee, M., Byun, J.-I., Jung, K.-H., Park, K.-I., Jung, K.-Y., Lee, S. K. & Chu, K. (2017) Altered expression of the long noncoding RNA NEAT1 in Huntington's disease. *Molecular neurobiology*, 54(2), 1577-1586.
- Suzuki, H., Zuo, Y., Wang, J., Zhang, M. Q., Malhotra, A. & Mayeda, A. (2006) Characterization of RNase R-digested cellular RNA source that consists of lariat and circular RNAs from pre-mRNA splicing. *Nucleic acids research*, 34(8), e63-e63.
- Tahira, A. C., Kubrusly, M. S., Faria, M. F., Dazzani, B., Fonseca, R. S., Maracaja-Coutinho, V., Verjovski-Almeida, S., Machado, M. C. & Reis, E. M. (2011) Long noncoding intronic RNAs are differentially expressed in primary and metastatic pancreatic cancer. *Molecular cancer*, 10(1), 1-19.

- Takahashi, Y., Fukuda, Y., Yoshimura, J., Toyoda, A., Kurppa, K., Moritoyo, H., Belzil, V. V., Dion, P. A., Higasa, K. & Doi, K. (2013) ERBB4 mutations that disrupt the neuregulin-ErbB4 pathway cause amyotrophic lateral sclerosis type 19. *The American Journal of Human Genetics*, 93(5), 900-905.
- Tang, Y., Jin, X., Xiang, Y., Chen, Y., Shen, C.-x., Zhang, Y.-c. & Li, Y.-g. (2015) The lncRNA MALAT1 protects the endothelium against ox-LDL-induced dysfunction via upregulating the expression of the miR-22-3p target genes CXCR2 and AKT. *FEBS letters*, 589(20), 3189-3196.
- Tauber, D., Tauber, G., Khong, A., Van Treeck, B., Pelletier, J. & Parker, R. (2020) Modulation of RNA condensation by the DEAD-box protein eIF4A. *Cell*, 180(3), 411-426. e16.
- Taylor, J. P., Brown, R. H. & Cleveland, D. W. (2016) Decoding ALS: from genes to mechanism. *Nature*, 539(7628), 197-206.
- Teyssou, E., Takeda, T., Lebon, V., Boillée, S., Doukouré, B., Bataillon, G., Sazdovitch, V., Cazeneuve, C., Meininger, V. & LeGuern, E. (2013) Mutations in SQSTM1 encoding p62 in amyotrophic lateral sclerosis: genetics and neuropathology. *Acta neuropathologica*, 125(4), 511-522.
- Teyssou, E., Vandenberghe, N., Moigneu, C., Boillée, S., Couratier, P., Meininger, V., Pradat, P.-F., Salachas, F., LeGuern, E. & Millecamps, S. (2014) Genetic analysis of SS18L1 in French amyotrophic lateral sclerosis. *Neurobiology of aging*, 35(5), 1213. e9-1213. e12.
- Tian, S., Curnutte, H. A. & Trecek, T. (2020) RNA Granules: A View from the RNA Perspective. *Molecules*, 25(14), 3130.
- Tosar, L. M., Thomas, M. G., Baez, M. V., Ibanez, I., Chernomoretz, A. & Boccaccio, G. L. (2012) Staufen: from embryo polarity to cellular stress and neurodegeneration. *Frontiers in Bioscience-Scholar*, 4(2), 432-452.
- Traynor, B. J., Codd, M. B., Corr, B., Forde, C., Frost, E. & Hardiman, O. M. (2000) Clinical features of amyotrophic lateral sclerosis according to the El Escorial and Airlie House diagnostic criteria: A population-based study. *Archives of neurology*, 57(8), 1171-1176.
- Trinkle-Mulcahy, L. & Sleeman, J. E. (2017) The Cajal body and the nucleolus: "In a relationship" or "It's complicated"? *RNA biology*, 14(6), 739-751.
- Turner, M., Galloway, A. & Vigorito, E. (2014) Noncoding RNA and its associated proteins as regulatory elements of the immune system. *Nature immunology*, 15(6), 484.
- Uversky, V. N. (2017) Intrinsically disordered proteins in overcrowded milieu: Membrane-less organelles, phase separation, and intrinsic disorder. *Current opinion in structural biology*, 44, 18-30.
- Uversky, V. N. (2019) Intrinsically disordered proteins and their "mysterious"(meta) physics. *Frontiers in Physics*, 7, 10.

Valadkhan, S. & Valencia-Hipólito, A. (2015) lncRNAs in stress response. *Long Non-coding RNAs in Human Disease*, 203-236.

Van Treeck, B., Protter, D. S., Matheny, T., Khong, A., Link, C. D. & Parker, R. (2018) RNA self-assembly contributes to stress granule formation and defining the stress granule transcriptome. *Proceedings of the National Academy of Sciences*, 115(11), 2734-2739.

Veldink, J., Kalmijn, S., Van der Hout, A., Lemmink, H., Groeneveld, G., Lummen, C., Scheffer, H., Wokke, J. & Van den Berg, L. (2005) SMN genotypes producing less SMN protein increase susceptibility to and severity of sporadic ALS. *Neurology*, 65(6), 820-825.

Venø, M. T., Hansen, T. B., Venø, S. T., Clausen, B. H., Grebing, M., Finsen, B., Holm, I. E. & Kjems, J. (2015a) Spatio-temporal regulation of circular RNA expression during porcine embryonic brain development. *Genome biology*, 16(1), 1-17.

Venø, M. T., Hansen, T. B., Venø, S. T., Clausen, B. H., Grebing, M., Finsen, B., Holm, I. E. & Kjems, J. (2015b) Spatio-temporal regulation of circular RNA expression during porcine embryonic brain development. *Genome biology*, 16(1), 245.

Vernon, R. M., Chong, P. A., Tsang, B., Kim, T. H., Bah, A., Farber, P., Lin, H. & Forman-Kay, J. D. (2018) Pi-Pi contacts are an overlooked protein feature relevant to phase separation. *Elife*, 7, e31486.

Vijayakumar, J. C. (2018) *Role of the Prion-like domain of Imp in neuronal RNP granule regulation* Université Côte d'Azur.

Vogler, T. O., Wheeler, J. R., Nguyen, E. D., Hughes, M. P., Britson, K. A., Lester, E., Rao, B., Dalla Betta, N., Whitney, O. N. & Ewachiw, T. E. (2018) TDP-43 and RNA form amyloid-like myo-granules in regenerating muscle. *Nature*, 563(7732), 508-513.

Volkening, K., Leystra-Lantz, C., Yang, W., Jaffee, H. & Strong, M. J. (2009) Tar DNA binding protein of 43 kDa (TDP-43), 14-3-3 proteins and copper/zinc superoxide dismutase (SOD1) interact to modulate NFL mRNA stability. Implications for altered RNA processing in amyotrophic lateral sclerosis (ALS). *Brain research*, 1305, 168-182.

Wächter, K., Köhn, M., Stöhr, N. & Hüttelmaier, S. (2013) Subcellular localization and RNP formation of IGF2BPs (IGF2 mRNA-binding proteins) is modulated by distinct RNA-binding domains. *Biological chemistry*, 394(8), 1077-1090.

Wang, G., Liu, W., Zou, Y., Wang, G., Deng, Y., Luo, J., Zhang, Y., Li, H., Zhang, Q. & Yang, Y. (2019a) Three isoforms of exosomal circPTGR1 promote hepatocellular carcinoma metastasis via the miR449a–MET pathway. *EBioMedicine*, 40, 432-445.

Wang, K.-W. & Dong, M. (2019) Role of circular RNAs in gastric cancer: recent advances and prospects. *World journal of gastrointestinal oncology*, 11(6), 459.

- Wang, L., Long, H., Zheng, Q., Bo, X., Xiao, X. & Li, B. (2019b) Circular RNA circRHOT1 promotes hepatocellular carcinoma progression by initiation of NR2F6 expression. *Molecular cancer*, 18(1), 1-12.
- Wang, W.-Z., Li, J., Liu, L., Zhang, Z.-D., Li, M.-X., Li, Q., Ma, H.-X., Yang, H. & Hou, X.-L. (2021) Role of circular RNA expression in the pathological progression after spinal cord injury. *Neural Regeneration Research*, 16(10), 2048.
- Wang, Y. & Wang, Z. (2015) Efficient backsplicing produces translatable circular mRNAs. *Rna*, 21(2), 172-179.
- Weingarten-Gabbay, S., Elias-Kirma, S., Nir, R., Gritsenko, A. A., Stern-Ginossar, N., Yakhini, Z., Weinberger, A. & Segal, E. (2016) Systematic discovery of cap-independent translation sequences in human and viral genomes. *Science*, 351(6270).
- Westholm, J. O., Miura, P., Olson, S., Shenker, S., Joseph, B., Sanfilippo, P., Celniker, S. E., Graveley, B. R. & Lai, E. C. (2014) Genome-wide analysis of drosophila circular RNAs reveals their structural and sequence properties and age-dependent neural accumulation. *Cell reports*, 9(5), 1966-1980.
- Wheeler, J. R., Matheny, T., Jain, S., Abrisch, R. & Parker, R. (2016) Distinct stages in stress granule assembly and disassembly. *Elife*, 5, e18413.
- Wilhelm, J. E. & Vale, R. D. (1993) RNA on the move: the mRNA localization pathway. *The Journal of cell biology*, 123(2), 269-274.
- Wilusz, J. E., Sunwoo, H. & Spector, D. L. (2009) Long noncoding RNAs: functional surprises from the RNA world. *Genes & development*, 23(13), 1494-1504.
- Wolozin, B. (2012a) Regulated protein aggregation: stress granules and neurodegeneration. *Molecular neurodegeneration*, 7(1), 56.
- Wolozin, B. (2012b) Regulated protein aggregation: stress granules and neurodegeneration. *Molecular neurodegeneration*, 7(1), 1-12.
- Wolozin, B. & Ivanov, P. (2019) Stress granules and neurodegeneration. *Nature Reviews Neuroscience*, 20(11), 649-666.
- Wong, N. K., He, B. P. & Strong, M. J. (2000) Characterization of neuronal intermediate filament protein expression in cervical spinal motor neurons in sporadic amyotrophic lateral sclerosis (ALS). *Journal of Neuropathology & Experimental Neurology*, 59(11), 972-982.
- Wu, C.-H., Fallini, C., Ticozzi, N., Keagle, P. J., Sapp, P. C., Piotrowska, K., Lowe, P., Koppers, M., McKenna-Yasek, D. & Baron, D. M. (2012) Mutations in the profilin 1 gene cause familial amyotrophic lateral sclerosis. *Nature*, 488(7412), 499-503.
- Xie, L., Mao, M., Xiong, K. & Jiang, B. (2017) Circular RNAs: a novel player in development and disease of the central nervous system. *Frontiers in cellular neuroscience*, 11, 354.

- Xiong, W., Huang, C., Deng, H., Jian, C., Zen, C., Ye, K., Zhong, Z., Zhao, X. & Zhu, L. (2018) Oncogenic non-coding RNA NEAT1 promotes the prostate cancer cell growth through the SRC3/IGF1R/AKT pathway. *The international journal of biochemistry & cell biology*, 94, 125-132.
- Yamamoto, M., Chen, M. Z., Wang, Y.-J., Sun, H.-Q., Wei, Y., Martinez, M. & Yin, H. L. (2006) Hypertonic stress increases phosphatidylinositol 4, 5-bisphosphate levels by activating PIP5K1 β . *Journal of Biological Chemistry*, 281(43), 32630-32638.
- Yamanaka, S., Siomi, M. C. & Siomi, H. (2014) piRNA clusters and open chromatin structure. *Mobile DNA*, 5(1), 1-12.
- Yamazaki, T. & Hirose, T. (2015) The building process of the functional paraspeckle with long non-coding RNAs. *Front Biosci (Elite Ed)*, 7(1), 1-41.
- Yamazaki, T., Nakagawa, S. & Hirose, T. (2019) Architectural RNAs for membraneless nuclear body formation, *Cold Spring Harbor symposia on quantitative biology*. Cold Spring Harbor Laboratory Press.
- Yang, P., Qiu, Z., Jiang, Y., Dong, L., Yang, W., Gu, C., Li, G. & Zhu, Y. (2016) Silencing of cZNF292 circular RNA suppresses human glioma tube formation via the Wnt/ β -catenin signaling pathway. *Oncotarget*, 7(39), 63449.
- Yang, Y., Gao, X., Zhang, M., Yan, S., Sun, C., Xiao, F., Huang, N., Yang, X., Zhao, K. & Zhou, H. (2018) Novel role of FBXW7 circular RNA in repressing glioma tumorigenesis. *JNCI: Journal of the National Cancer Institute*, 110(3), 304-315.
- Yasuda, K., Clatterbuck-Soper, S. F., Jackrel, M. E., Shorter, J. & Mili, S. (2017) FUS inclusions disrupt RNA localization by sequestering kinesin-1 and inhibiting microtubule detyrosination. *Journal of Cell Biology*, 216(4), 1015-1034.
- You, X., Vlatkovic, I., Babic, A., Will, T., Epstein, I., Tushev, G., Akbalik, G., Wang, M., Glock, C. & Quedenau, C. (2015) Neural circular RNAs are derived from synaptic genes and regulated by development and plasticity. *Nature neuroscience*, 18(4), 603-610.
- Yu, Z., Fan, D., Gui, B., Shi, L., Xuan, C., Shan, L., Wang, Q., Shang, Y. & Wang, Y. (2012) Neurodegeneration-associated TDP-43 interacts with fragile X mental retardation protein (FMRP)/Staufen (STAU1) and regulates SIRT1 expression in neuronal cells. *Journal of Biological Chemistry*, 287(27), 22560-22572.
- Zapater, M., Sohrmann, M., Peter, M., Posas, F. & de Nadal, E. (2007) Selective requirement for SAGA in Hog1-mediated gene expression depending on the severity of the external osmotic stress conditions. *Molecular and cellular biology*, 27(11), 3900-3910.
- Zarei, S., Carr, K., Reiley, L., Diaz, K., Guerra, O., Altamirano, P. F., Pagani, W., Lodin, D., Orozco, G. & Chinea, A. (2015) A comprehensive review of amyotrophic lateral sclerosis. *Surgical neurology international*, 6.

Zeng, W.-j., Lu, C., Shi, Y., Chen, X. & Yao, J. (2019) Osmotic stress-induced, rapid clustering of IGF2BP proteins nucleates stress granule assembly. *bioRxiv*, 846659.

Zhang, K., Donnelly, C. J., Haeusler, A. R., Grima, J. C., Machamer, J. B., Steinwald, P., Daley, E. L., Miller, S. J., Cunningham, K. M. & Vidensky, S. (2015) The C9orf72 repeat expansion disrupts nucleocytoplasmic transport. *Nature*, 525(7567), 56-61.

Zhang, L., Wang, L., Guo, E. & Qi, Y. (2019) Silence of lncRNA CHRFB protects H9c2 cells against lipopolysaccharide-induced injury via up-regulating microRNA-221. *Experimental and Molecular Pathology*, 107, 43-50.

Zhang, X.-O., Wang, H.-B., Zhang, Y., Lu, X., Chen, L.-L. & Yang, L. (2014) Complementary sequence-mediated exon circularization. *Cell*, 159(1), 134-147.

Zhang, Z., Carriero, N. & Gerstein, M. (2004) Comparative analysis of processed pseudogenes in the mouse and human genomes. *Trends in Genetics*, 20(2), 62-67.

Zheng, J., Liu, X., Xue, Y., Gong, W., Ma, J., Xi, Z., Que, Z. & Liu, Y. (2017) TTBK2 circular RNA promotes glioma malignancy by regulating miR-217/HNF1 β /Derlin-1 pathway. *Journal of hematology & oncology*, 10(1), 1-19.

Zhong, Q., Huang, J., Wei, J. & Wu, R. (2019) Circular RNA CDR1as sponges miR-7-5p to enhance E2F3 stability and promote the growth of nasopharyngeal carcinoma. *Cancer cell international*, 19(1), 252.

Zhou, H.-X., Nguemaha, V., Mazarakos, K. & Qin, S. (2018) Why do disordered and structured proteins behave differently in phase separation? *Trends in biochemical sciences*, 43(7), 499-516.

Zhu, X., Wang, X., Wei, S., Chen, Y., Chen, Y., Fan, X., Han, S. & Wu, G. (2017) hsa_circ_0013958: a circular RNA and potential novel biomarker for lung adenocarcinoma. *The FEBS journal*, 284(14), 2170-2182.

Zou, Z.-Y., Zhou, Z.-R., Che, C.-H., Liu, C.-Y., He, R.-L. & Huang, H.-P. (2017) Genetic epidemiology of amyotrophic lateral sclerosis: a systematic review and meta-analysis. *Journal of Neurology, Neurosurgery & Psychiatry*, 88(7), 540-549.

Curriculum Vitae

Asieh Alikhah

Education

- University of Western Ontario (UWO), London, Canada, **M.Sc.** in Pathology and Laboratory Medicine (**2019-present, in progress**). Thesis: Alteration of the expression and subcellular localization of circRNAs dysregulated in ALS in response to stress. Supervisor: Dr. Michael J. Strong.
- Tarbiat Modares University (TMU), Tehran, Iran, **M.Sc.** in Molecular Genetics (**2014-2016**). Thesis: expression profiling of *SOCS3*, *STAT3*, and *lnc-DC* in peripheral blood white cells in CAD+ and CAD- individuals. Supervisor: Dr. Mehrdad Behmanesh.
- Alzahra University, Tehran, Iran, **B.Sc.** in biotechnology (**2009-2013**).

Related research experience

- **2019-present:** Master of Science Candidate, University of Western Ontario (UWO), London, Canada
- **2018-2018:** Watson clinical genetics laboratory, Tehran, Iran
- **2016-2018:** Research technologist, Iranian Institute of Cell & Gene Therapy, Tehran Iran
- **2017-2018:** Research Assistant, Molecular Genetics Laboratory, Faculty of Medicine, University of North Khorasan Medical Sciences, Bojnourd, Iran.
- **2014-2016:** Research Assistant, Molecular Genetics Laboratory, Tarbiat Modares University, Tehran, Iran.
- **2013-2014:** Research technologist, Iranian Institute of Cell & Gene Therapy, Tehran Iran

Publications

- Reyhaneh Dehghanzad, Majid Pahlevan Kakhki, **Asieh Alikhah**, Mohammad Ali Sahraian & Mehrdad Behmanesh. The Putative Association of TOB1-AS1 Long Non-coding RNA with Immune Tolerance: A Study on Multiple Sclerosis Patients. *Journal of NeuroMolecular Medicine* (100–110(2020))
- Majid Pahlevan Kakhki, Nahid Rakhshi, Mohammad Sajad Emami Aleagha, Mahla Abdari, **Asieh Alikhah**, Ghazal Safarian, Mehrdad Behmanesh & Abbas Nikravesh. Differential expression of STAT3 gene and its regulatory long non-coding RNAs, namely lnc-DC and THRIL, in two eastern Iranian ethnicities with multiple sclerosis. *Journal of Neurological Sciences* (41, 561–568 (2020))
- Homa Hamledari, Seyedeh Fatemeh Sajjadi, **Asieh Alikhah**, Mohammad Ali Boroumand, Mehrdad Behmanesh. ASGR1 but not FOXM1 expression decreases in the peripheral blood mononuclear cells of diabetic atherosclerotic patients. *Journal of Diabetes and its Complications* (33, 539-546, 2019)
- **Asieh Alikhah**, Majid Pahlevan Kakhki, Amirhossein Ahmadi , Reyhaneh Dehghanzad, Mohammad Ali Boroumand, Mehrdad Behmanesh. The role of lnc-DC long non-coding RNA and SOCS1 in the regulation of *STAT3* in coronary artery disease and type 2 diabetes mellitus. *Journal of Diabetes and its Complications* (32, 258-265, 2017)

Poster Presentations

- **Asieh Alikhah**, Danae Campos-Melo and Michael J. Strong. Alteration of the expression and subcellular localization of circRNAs dysregulated in ALS in response to stress. 26th annual meeting of RNA society (2021)
- **Asieh Alikhah**, Danae Campos-Melo and Michael J. Strong. The expression and subcellular localization of circRNAs dysregulated in ALS in response to stress. ALS Canada Research Forum (2021)
- **Asieh Alikhah**, Danae Campos-Melo and Michael J. Strong. Dysregulated circRNAs in ALS colocalize with RNAGranules upon stress. 31 st international symposium of ALS/MND (2020)

- **Asieh Alikhah**, Danae Campos-Melo and Michael J. Strong. Mislocalization and aggregation of paraspeckle proteins under cellular stress. 31st international symposium of ALS/MND (2020)
- Asieh Alikhah, Danae Campos-Melo, and Michael J. Strong. Role of circRNAs in ALS. 25 th annual meeting of RNA society (2020)
- **Asieh Alikhah**, Danae Campos-Melo, Michael J. Strong. Upregulated circRNAs in ALS sponge/scaffold EIF4A3, AGO2, and FMRP andregulate cell survival. 15th symposium Andre-Delambre (2019)
- **Asieh Alikhah**, Danae Campos-Melo, Michael J. Strong. Upregulated circRNAs in ALS sponge/scaffold EIF4A3, AGO2, and FMRP andregulate cell survival. Riboclub 20th anniversary and Canada Gairdner International symposium (2019)
- **Asieh Alikhah**, Danae Campos-Melo and Michael J. Strong. Dysregulation of circRNAs in Amyotrophic Lateral Sclerosis. ALS Canada Research Forum (2019)
- **Asieh Alikhah**, Reyhaneh Dehghanzad, Majid Pahlevan Kakhki, Mohammad Ali Boroumand, Mehrdad Behmanesh. The role of lnc-DC long non-coding RNA and SOCS1 in the regulation of STAT3 in coronary artery disease and type 2 diabetes mellitus, 5th European Congress of Immunology, Amsterdam, the Netherlands, September 2018
- Rakhshi Nahid, Kakhki Majid Pahlevan, Abdarei Mahla, Ghazal Safarian, **Asieh Alikhah**, Mehrdad Behmanesh & Abbas Nikraves. Genetic background affects the inflammatory-related genes expression in Iranian multiple sclerosis patients, MSParis2017 - 7th Joint ECTRIMS-ACTRIMS Meeting.
- **Asieh Alikhah**, Reyhaneh Dehghanzad, Majid Pahlevan Kakhki, Mohammad Ali Boroumand, Mehrdad Behmanesh. Differential expression of Lnc-DC variants in CAD patients, Second International and 14th Iranian Genetic congress, Tehran, Iran, May 2016.
- **Asieh Alikhah**, Mohammad Ali Boroumand, Mehrdad Behmanesh. Study of *STAT3* gene expression in peripheral leukocytes of coronary artery disease patients, 5th international preventive cardiology congress, shiraz, iran, September 2016.
- **Asieh Alikhah**, Reyhaneh Dehghanzad, Majid Pahlevan Kakhki, Mehrdad Behmanesh. The ability of personalized medicine through gut microbiome signature in multiple sclerosis, 13th international MS congress of Iran, tehran, Iran, Nov. 2016.

- Reyhaneh Dehghanzad, Majid Pahlevan Kakhki, **Asieh Alikhah**, Behmanesh M. The importance role of expression profile based RNA-seq in discovering the etiology of multiple sclerosis. 12th international MS congress of Iran, Sari, Iran, Nov. 2015.
- Reyhaneh Dehghanzad, **Asieh Alikhah**, Behmanesh M. The roles of non-coding RNAs in maturation of human embryonic stem cell cardiomyocytes. International congress on Stem cells and regenerative medicine, Mashhad, Iran, May 2015.